The Results of a Borehole Infiltration Test with a Shallow Water Table

By
Richard R. Rabold

Submitted in Partial Fulfillment of
the Requirements for the Degree of
Master of Science in Hydrology

New Mexico Institute of Mining and Technology
Socorro, New Mexico
September 1984

ACKNOWLEDGMENTS

I would like to acknowledge the financial support for work performed for this paper provided by the United States Bureau of Reclaimation Office of Water Research and the Geoscience Department of New Mexico Institute of Mining and Technology. Also, I would like to thank Mr. and Mrs. Louis Baudoin for the use of their backyard as a field study area and the numerous times they allowed me to invade their privacy. They are really super people.

I am grateful to Dr. Daniel B. Stephens for his guidance and understanding throughout the course of this study and preparation of this report. His advice is an integral part of this paper although I assume complete responsibility for the accuracy of the work presented herein.

I am indebted to Mark Larsen, Greg Lewis, Chuck Spaulding, Ward Hurst, Chris Mikell, Steve Heermann, Tom Duval, Nancy Jannik, Amy Childers, and Jim Mc Cord for their technical assistance in the data collection during that awfully long borehole test. Also a special thanks to Bob Knowlton for his generous support and help that was always there to make my work easier.

Finally, my deepest thanks to my wife BJ for her boundless patience, encouragement, and support. Without her love, these college years would never have been. And to Megan and Melissa, I promise to repay you for your sacrifices.

ABSTRACT

Predicting the rate of water movement above a water table is a crucial problem in hazardous and radioactive waste disposal, in the design of dams, and in the irrigation and drainage of agricultural land. Hydraulic conductivity, the key soil characteristic governing the rate of water movement, was determined in the laboratory, using two different permeameter techniques, and in the field, using a constant head borehole infiltration test.

Hydraulic conductivity was measured in the lab on PF ring (100cc) soil samples and compared to hydraulic conductivity measurements of Shelby tube samples with the use of a newly designed multiple manometer Shelby tube permeameter. In this limited study, the PF ring samples gave generally higher hydraulic conductivity values, about 2.5x, than those obtained from the larger Shelby tube samples.

A long duration (8 day), shallow water table condition, constant head borehole infiltration test exhibited sensitivity to infiltration water temperature and chemistry. Infiltration rate from the borehole was also sensitive to water table position beneath the borehole. This water table elevation was controlled with the use of a 4-point well field centered on the borehole.

Measured hydraulic conductivity values from the borehole test were found to be in the range of vertical Ks values measured in the laboratory.

TABLE OF CONTENTS

PAGE

LIST OF FIGURES

LIST OF TABLES

NOMENCLATURE

D	Depth Below Landsurface (L)
H	Depth of Water in Borehole (L)
i	Hydraulic Gradient (Dimensionless)
Ks	Saturated Hydraulic Conductivity (L/T)
Q	Infiltration Rate (L^3 /T)
r	Radius of Borehole (L)
R	Radial Distance From the Borehole Axis (L)
Tu	Distance From the Water Level in the Borehole to the Water Table (L)
θ	Volumetric Moisture Content (Dimensionless)

INTRODUCTION

Within the last decade, hydrologists have realized the importance of the vadose zone for determining rates of recharge and pollutant migration from the land surface to an aquifer. There is considerable interest in developing methods to measure hydraulic properties of the unsaturated zone. One of the most important parameters describing the vadose zone is its saturated hydraulic conductivity, Ks, i.e., its ability to transmit fluids.

There are two approaches to quantifying this property. First is to obtain samples, preferably undisturbed, from the field and upon returning them to a soils lab, perform various permeameter experiments to determine saturated hydraulic conductivity. One commonly used method of sample acquisition is via the PF ring, a small 2.5 cm radius by 5.1 cm length cylindrical container. This unit is pushed into a soil zone and upon retrieval, removes an "undisturbed", 100 cc volume of soil, when full. This open ended container of soil can then be used in conjunction with an apparatus such as an Eijkelkamp multi-sample permeameter to determine saturated hydraulic conductivity.

Another technique to obtain an undisturbed soil sample for hydraulic conductivity measurements is with a shelby tube. A shelby tube is a long, 61 to 91 cm, thin-walled metal cylinder of radius 4.9 cm. This device is also used to retrieve undisturbed samples from a soil zone but its use

differs from a PF ring in that a drilling rig is usually required to push and retrieve it. Because of its larger size, when compared to a PF ring sample, a soil sample contained in a shelby tube might provide a more representative sample for determining Ks. One objective of this report, therefore, will be to provide a comparison of the standard PF ring method of measuring saturated hydraulic conductivity with a newly devised and constructed, multi-sample, shelby tube permeameter.

The second approach to quantifying saturated hydraulic conductivity is a direct measurement technique performed in-situ at a field site location. There are numerous field techniques to measure saturated conductivity (Bower, 1978; Hillel, 1980). One especially useful technique is called the constant head borehole infiltration test by Stephens (1979) and the well permeameter method by the USBR (1974). This technique has the advantage of being useful at any zone depth, a major drawback of most other methods. The method involves measuring the rate at which water flows outward from a cased or uncased well bore under constant head. Its popular use in the past has been for the estimation of canal seepage prior to construction for predetermining the need for canal lining. But now with the importance of vadose zone characterization in conjunction with hazardous waste disposal programs, the well permeameter method, or borehole method for short, is well suited for extensive field use.

Figure 1 depicts 3 possible borehole cases to measure

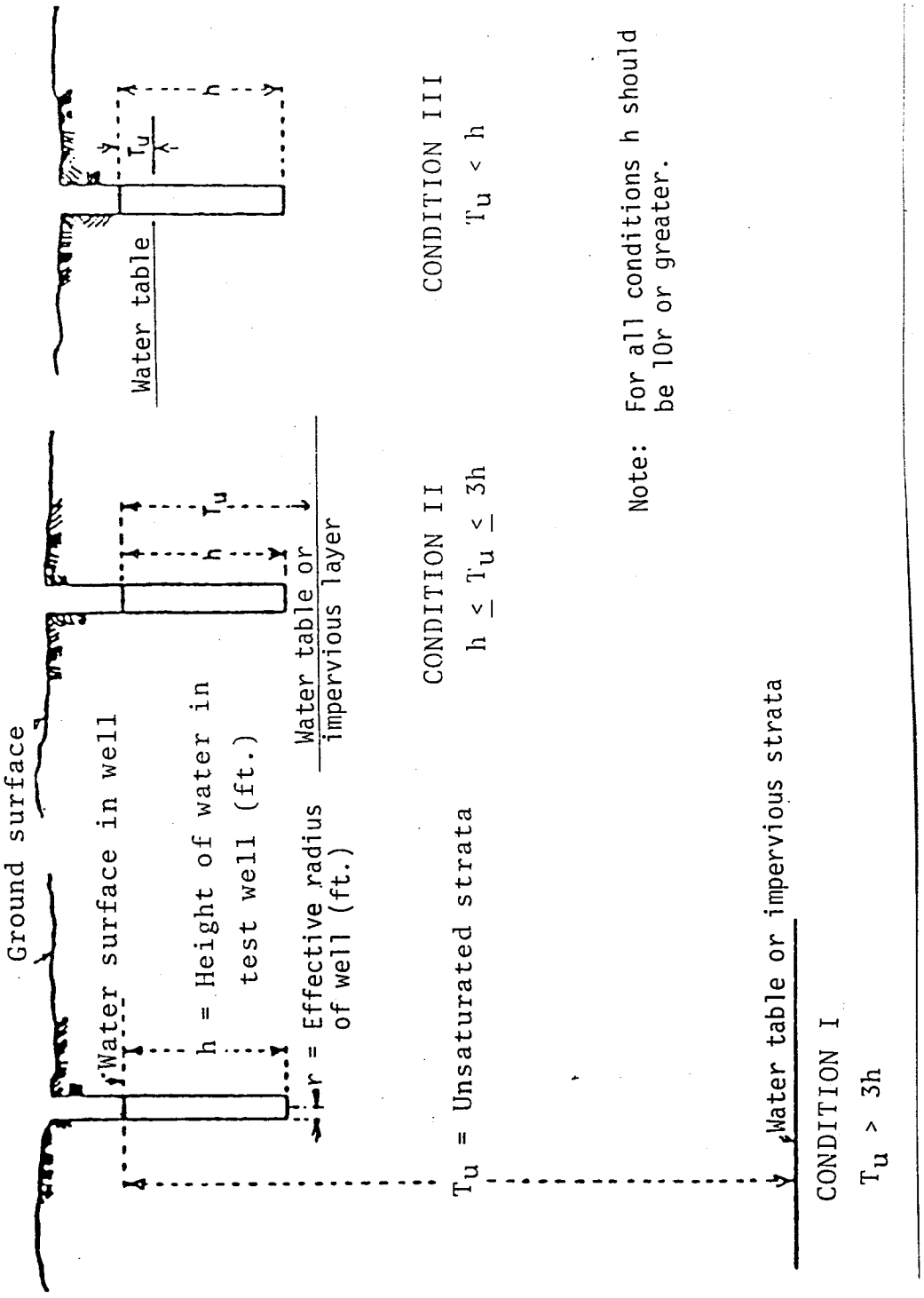

Figure 1. Criteria for Determining Appropriate Formula to be Used With the Well Permeameter Method (After USBR,1974)

saturated hydraulic conductivity, Ks, (USBR, 1974). All three cases shown involve a borehole of effective radius, r, in which a constant head of water, H, is maintained and outflow from this borehole, Q is measured by the amount of water necessary to maintain H constant. Please note here that in all cases, H should be 10r or greater, according to USBR (1974). The difference between the 3 boreholes shown is the parameter Tu, (L), which is the distance from the water level in the borehole to the first water table or impervious strata. The value of Tu designates 3 possible borehole conditions. Condition I is recognized when the value of Tu > 3H. This is referred to as a deep water table condition. Condition II, the shallow water table condition, applies when H < Tu < 3H. And condition III occurs when the value Tu < H. The present report is limited to condition II.

Figure 2 (USBR, 1974) shows 3 equations applicable to the solutions of Ks for a borehole test with the equation numbers pertaining to the borehole conditions just described. All three equations calculate Ks adjusted to 20^{o} C through a viscosity correction term (μ_T/μ_{20}). The value 525,600 is a conversion factor to compute Ks in units of feet per year.

The concept used to derive the steady state solutions is that water infiltrating from the borehole into the soil flows radially and downward in response to pressure and gravity gradients (figure 3). The flow region is fully saturated and is confined within an envelope known as "free surface". The

$$k_{20} = 525{,}600 \frac{\left[\sinh^{-1}\left(\frac{h}{r}\right) - 1\right] \frac{Q}{2\pi}}{h^2} \left(\frac{\mu_T}{\mu_{20}}\right) \qquad \text{(I)}$$

$$k_{20} = \frac{525{,}600 \log_e \left(\frac{h}{r}\right) \frac{Q}{2\pi}}{h^2 \left[\frac{1}{6} + \frac{1}{3}\left(\frac{h}{T_u}\right)^{-1}\right]} \left(\frac{\mu_T}{\mu_{20}}\right) \qquad \text{(II)}$$

$$k_{20} = \frac{525{,}600 \log_e \left(\frac{h}{r}\right) \frac{Q}{2\pi}}{h^2 \left[\left(\frac{h}{T_u}\right)^{-1} - \frac{1}{2}\left(\frac{h}{T_u}\right)^{-2}\right]} \left(\frac{\mu_T}{\mu_{20}}\right) \qquad \text{(III)}$$

WELL PERMEAMETER METHOD FORMULAS (AFTER USBR, 1974).

Figure 2. Formula to be Used With the Well Permeameter Method (After USBR,1974)

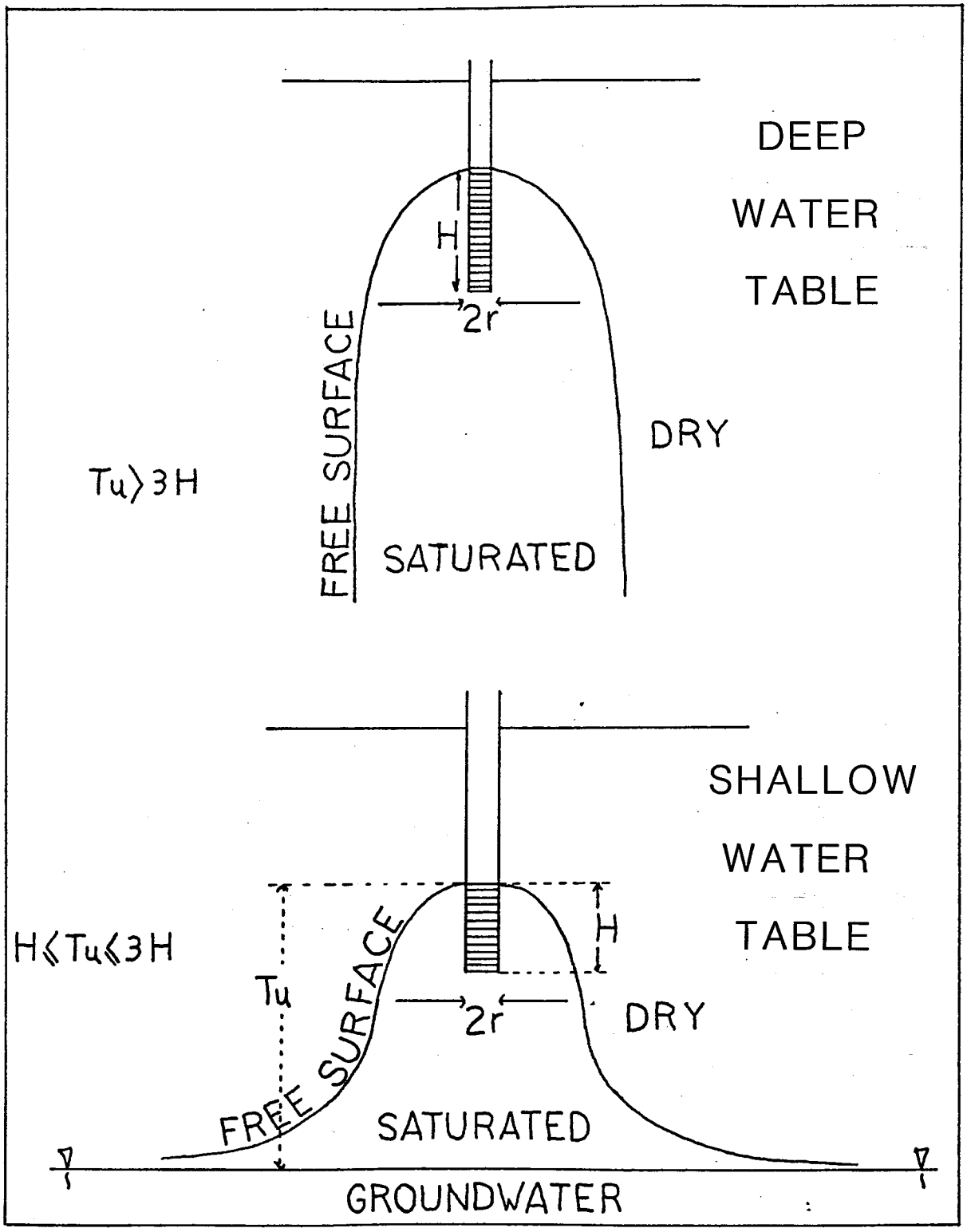

Figure 3. Free Surface Concept of Flow From a Borehole For Conditions I and II

latter is a streamline across which no flow can take place and an isobar along which the pressure is everywhere atmospheric. The soil outside the free surface envelope is dry and is not considered to be part of the flow region.

Within the last five years, extensive research has been carried out to better describe the flow processes occurring during a borehole test and more accurately measure Ks (Stephens, 1979; Stephens et al., 1982, Stephens and Neuman, 1982b; Stephens et al., 1983; Reynolds, Elrick and Topp, 1983; Lambert, 1983; Watson, 1983).

Stephens and Neuman (1982b) used numerical simulations of the constant head borehole infiltration problem which included both saturated and unsaturated flow. Their saturated-unsaturated simulations showed that at steady state, the zone of saturation is limited to a relatively small region surrounding the borehole, outside of which unsaturated flow occurred. This is in sharp contrast to the free surface flow concept in which the entire flow region is assumed to be saturated and bounded by a zero gauge pressure surface. The size of the flow region depends on the magnitude of the capillary effect which is usually large in fine textured soils and small in coarse textured soils. More important perhaps is the conclusion that for tests in homogeneous isotropic soils, existing analytical solutions may overestimate Ks by more than 160% in fine textured soils when the height of water in the borehole is small. When the height of water is large and the soil texture is coarse, existing analytical solutions may

underestimate Ks by more than 35%. The value of Ks was also found to by dependent on initial soil moisture conditions or recharge rate. Contrary to what is indicated by existing analytical solutions, Stephens (1979) and Stephens and Neuman (1982b) concluded that in homogeneous isotropic soils a unique relationship does not exist between Ks, borehole factors, and steady flow rate. They also showed that existing solutions may lead to errors of more than a few hundred percent from tests in heterogeneous and anisotropic soils.

Stephens et al. (1983) conducted extensive field and laboratory research. They executed 27 borehole infiltration tests of deep water table conditions, in a relatively homogeneous and isotropic sandy soil, using various H and r geometries. In these tests instrumentation was installed around the borehole to map out the flow field. They concluded that soil-water instrumentation surrounding a borehole indicated that the free surface concept of the flow field is inappropriate. Water flowing from the borehole passes through a saturated envelope which is fixed around the borehole and then through unsaturated soil. This same result was predicted by Stephens and Neuman (1982b) numerical solutions using saturated-unsaturated flow models.

Stephens et al. (1983) also found that entrapped air occurs in both field and laboratory permeameters. Carbon dioxide injection into soil prior to water infiltration is a practical means to reduce trapped air. Carbon dioxide treatment may increase calculated hydraulic conductivities by

about two to more than three-fold. They found that hydraulic conductivity from borehole infiltration tests is a dynamic characteristic of the soil which is sensitive to test procedures.

Stephens et al. (1983) concluded that soil-water temperature varied considerably due to changes in the temperature of the water supply. Diurnal temperature increases and decreases generally corresponded to respective decreases and increases in infiltration rate, even after correcting for viscosity.

Attempts thus far to develop new solutions for Ks from a borehole test, which account for capillarity, have been limited to deep water table conditions (Stephens et al. 1983). These have been found to give favorable results. On the other hand, there have been no field experiments pertaining to Condition II, although this condition was studied by Stephens (1979) using numerical simulation. He found that for fine textured soils, Ks computed using the USBR analytical solution for shallow water table cases will probably be 30 to 100% greater than the true value for a homogeneous, isotropic soil. The derivation of equation II, figure 2 is not locatable. Internal notes suggest (Warren, 1979, personal communication) that equation I, (figure 2) is a precise solution for the steady state flow from a well into an infinite unsaturated medium and equations II and III (figure 2) are empirical modifications of equation I to compensate for changes in boundary and flow conditions in the vicinity of the well.

In light of the uncertainties of equation II (figure 2), a second objective of this investigation is to evaluate the reliability of the shallow water table solution using field experiments. One parameter in equation II to be examined is the value Tu which can be controlled by lowering a water table during a borehole test. Secondly, the value of Ks determined through borehole testing can be compared to values of Ks obtained in a soils laboratory utilizing field obtained undisturbed samples.

In addition, the role of water chemistry as used for borehole testing has been ignored in previous investigations.

In summary then, the objectives of this paper are to:

1) Compare values of Ks obtained from both PF ring and shelby tube sampling techniques.

2) Compare laboratory determined values of Ks with values measured insitu using recently developed procedures for the borehole method.

3) Evaluate the role of water chemistry used for Ks measurements in a soil media in both laboratory and field conditions.

SITE DESCRIPTION

Field work for this report was completed on the domestic property of Mr. and Mrs. L. Baudoin located on the eastern edge of the city of Socorro, Socorro County, New Mexico (figure 4). The property is situated on the Rio Grande floodplain approximately 1 km west of the main river channel. This site was chosen primarily because of its shallow depth to groundwater, about 2 m, its close proximity to New Mexico Tech and its high security afforded by the property owners living on site.

Figure 5 shows the relation of the borehole site to the northeast property line.

HYDRAULIC PROPERTIES

Because this site had not been previously investigated, a preliminary site characterization was required. The characterization included analyses to determine particle size distribution, soil moisture characteristic properties and saturated hydraulic conductivities. Twelve PF ring soil samples for laboratory analysis were taken from the field site. The radial distance, R, of the sample was measured from the center axis of the borehole reference location and sample depth, D, was measured below landsurface. This landsurface datum was established early in the field investigation and then made permanent by marking a reference point on the borehole casing. Nine of the PF samples were taken from R= 30 cm in a 2.5 cm radius hole, used subsequently for a neutron

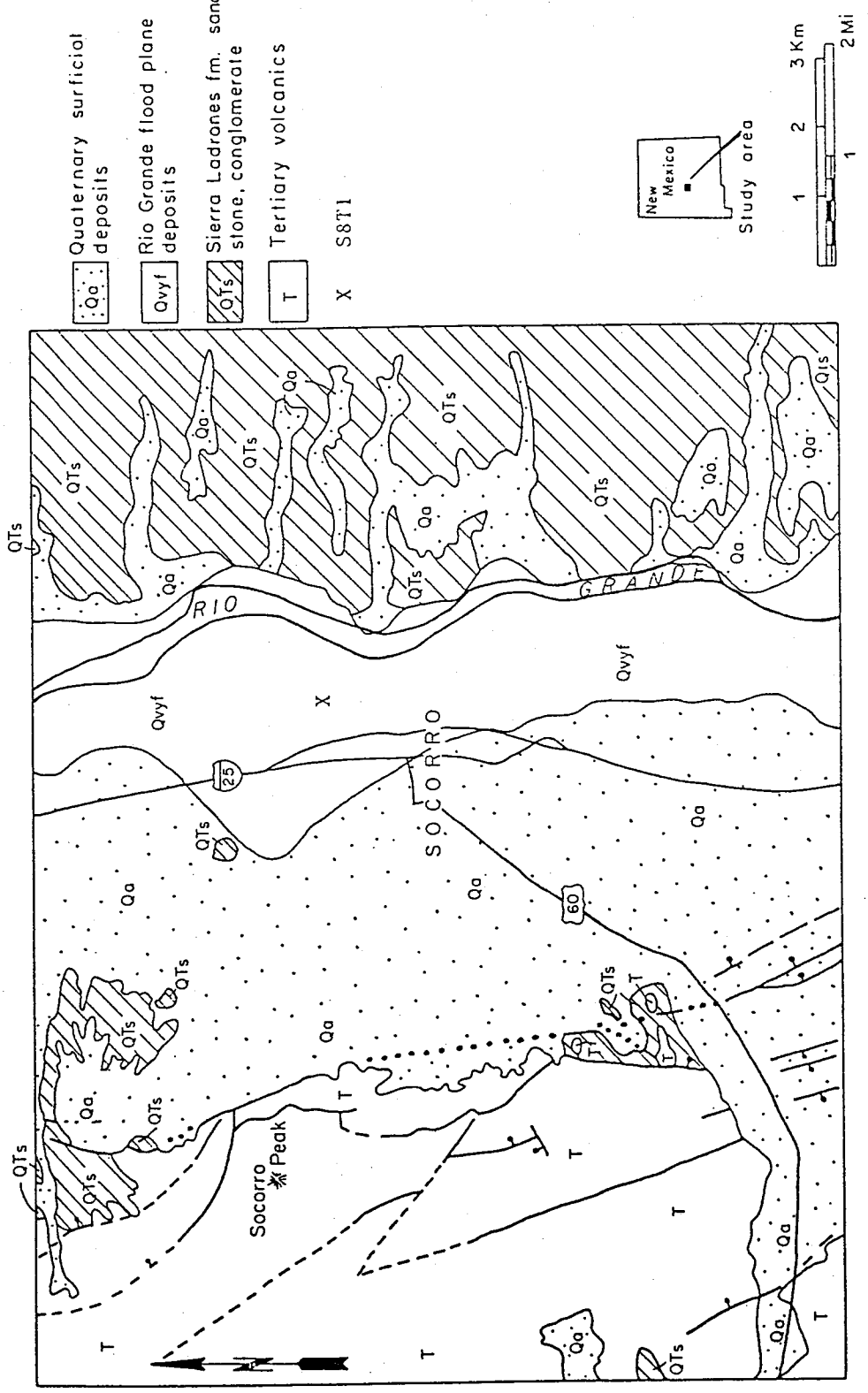

Figure 4. Field Site Location Map

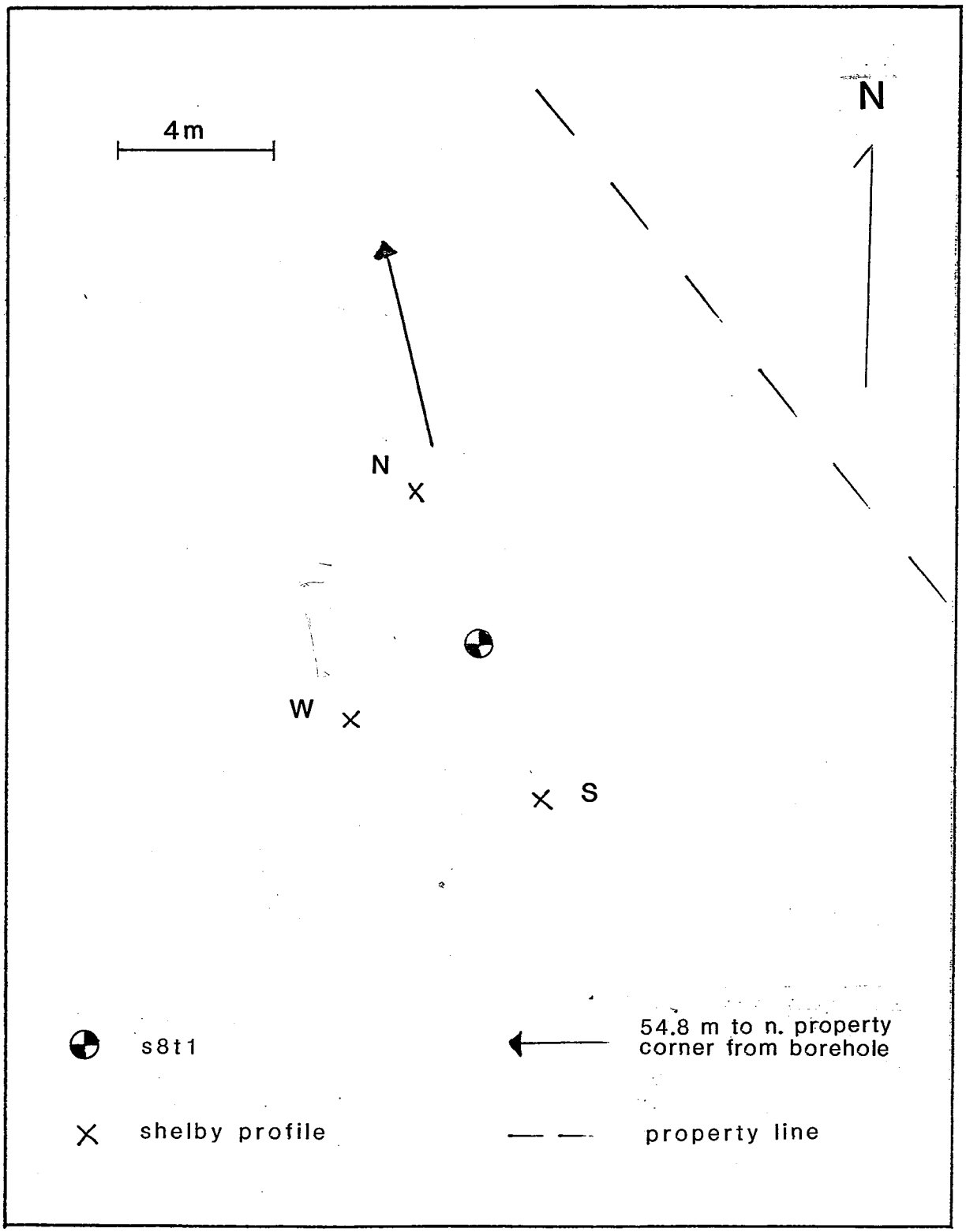

Figure 5. Test Site on the Baudoins' Property

access tube. Three additional samples were taken from R= 60 cm in another hole to be used for a neutron access tube.

Particle Size Distribution

Stainless steel 100 cc PF rings were used to extract the samples that were analyzed for grain size distribution and soil classification.

Upon returning to the lab the ring samples were immediately weighed. After the samples were utilized for other saturated analysis, the specimens were oven dried to determine dry bulk density and field moisture contents. The procedures used to carry out the complete mechanical analysis are described by Black et al.(1965). Specifically, after oven drying each sample for a minimum time of 48 hours at 105^{o} C samples were removed from the rings and gently disaggregated with mortar and pestle. Inasmuch as the soil was suspected of containing soluble material as cement and matrix, a procedure as outlined by Day (1965) was implemented to attempt to remove this material. The procedure utilized approximately 125 grams of soil sample that was placed in a beaker and weighed. Then enough distilled water was added to provide about 600 ml of solution. To this first flushing, approximately 4 ml of 0.1 N HCl was added. The contents were stirred and left to settle; excess water with salts in solution were then drawn off using a vacuum pump and filter candle apparatus as depicted in Black (1965 p. 551). Successive additions of water, settling and drawing off of materials in solution was carried out without

the addition of the small amount of 0.1 N HCl. This initial acid treatment was executed in the hope of speeding up the dissolution process. At least 350 ml of water with dissolved material was removed from all samples. As much as 950 ml of water was added and removed from samples whose settling times were the quickest, on the order of 8 hours. After a couple of days of this procedure, as much water was removed as possible using vacuum and filtering. The samples were then oven dried and weighed to measure relative amounts of materials removed in solution. After this process, it was necessary to remove organics, such as roots, that were evident in all samples. An initial screening and physical removal with tweezers was implemented where possible, followed by an addition of 35% H_2O_2 to the dried soil in a beaker. Individual dry sample weights used in this process averaged 68 grams. Due to the violent reactions of the individual samples to the H_2O_2, it was felt the treatment was important, but due to the extreme cost of the treatment, sample weights treated were minimized. Approximately 250 ml of H_2O_2 was reacted with each soil sample. Table 1 indicates the relative effects of both the salt dissolution treatment and the hydrogen peroxide application. As seen in Table 1, the distilled water had the greatest effects when used in the largest quantities and the percent loss seems nearly proportional to volumes of H_2O The samples most affected also turned out to have the smallest average grain size. This may indicate that the greater reaction occurred due to the larger specific surface or

TABLE 1
EFFECTS OF SALT DISSOLUTION AND H_2O_2 TREATMENT ON SOIL SAMPLES FOR HYDROMETER ANALYSIS

Sample Radius (cm)	Sample Depth (cm)	Distilled H2O Flushed (ml)	Wt. Loss to dissolution (% of dry wt)	H2O2 Applied (ml)	Wt. Loss to dissolution (% of dry wt
60	112.5	900	2.5	250	6.8
60	121.0	900	3.0	250	0.0
60	129.5	900	3.1	250	-8.1
30	143.5	350	1.2	250	1.5
30	159.5	350	1.5	250	0.1
30	166.5	350	1.5	250	0.9
30	175.5	950	1.7	250	1.4
30	182.5	350	1.6	250	0.2
30	189.5	350	2.0	250	0.1
30	197.5	350	1.9	250	3.2
30	203.5	350	1.8	250	0.2
30	218.5	0	0.0	250	na

na: not available

different mineralogy of the finer materials. The correct, most precise method to reach total salt dissolution would be to dry the soil sample after each beaker volume flushed until which time no additional weight loss is recorded. But it is believed that a procedure of this extent is not practical within the scope of this project.

The H_2O_2 treatment in Table 1 produced varied results. The calculated loss to the sample from 129.51 cm depth is possibly in error as no other samples show increases in weight. Possibly an error in a scale reading is to blame. Losses on the order of one or two percent are believed to be insignificant for characterizing particle size; and due to the high cost, H_2O_2 treatment is not recommended for other analyses at this site. The approximate H_2O_2 treatment cost per sample was $6.50.

Following extensive pretreatments, the samples were analyzed for the fine fraction using hydrometer techniques and the coarse fraction using standard sieves. Table 2 provides the results of the complete mechanical analysis on the PF ring soil samples. Parameters in Table 2 include mean grain size (d_{50}), Curvature Coefficient (Cc), Uniformity Coefficient (Cu), porosity (n), dry bulk density (ρ_b), sample particle density (ρ_s), field moisture content (θ_F), and soil description from the USDA soil texture triangle. Particle densities were carried out on pretreated samples (flushing and H_2O_2) using the pycnometer technique. Porosity was calculated using the bulk density/particle density relationship.

TABLE 2
RESULTS OF MECHANICAL ANALYSIS

Radius (cm)	Depth (cm)	d50 (mm)	Cc	Cu	n (%)	ρ_b g/cc	ρ_s g/cc	θ_f (%)	Description (**)
60	112.5	0.004	na	na	41	1.43	2.42	na	silty clay loam
60	121.0	0.001	na	na	45	1.33	2.40	na	silty clay
60	129.5	0.001	na	na	42	1.36	2.36	na	silty clay
30	143.5	0.145	1.4	4.8	35	1.58	2.42	20.4	loamy sand
30	159.5	0.096	1.9	7.1	35	1.51	2.32	24.9	sandy loam
30	166.5	0.080	3.0	11.1	37	1.50	2.39	28.9	sandy loam
30	175.5	0.064	3.7	15.6	40	1.43	2.38	36.9	sandy loam
30	182.5	0.048	3.8	15.0	39	1.40	2.31	41.7	loam
30	189.5	0.054	2.1	11.7	39	1.42	2.31	42.0	sandy loam
30	197.5	0.023	4.3	28.0	42	1.37	2.37	45.9	silt loam
30	203.5	0.043	2.5	20.0	44	1.36	2.45	42.7	loam
30	218.5	0.175	1.1	1.9	36	1.51	2.37	41.4	sand

d50: mean grain size
Cc : curvature coefficient = $(d30)^2$ / (d10 * d60)
Cu : uniformity coefficient = d60 / d10
n : porosity from dry bulk density
ρ_b : dry bulk density
ρ_s : particle density from pycnometer
θ_f : field moisture content
** : USDA Soil Texture Triangle (Hillel, 1980)
na : not available

And field moisture content was calculated using the difference between field sample weight and dry sample weight over the measured field sample volume.

Comparing the values of porosity and volumetric field moisture contents for samples from depths 182.5, 189.5, 197.5 and 218.5 cm a discrepancy appears evident. This point will be addressed more thoroughly in the next section.

Soil Moisture Characteristics

The volumetric water content-pressure head relationship, $\Psi-\theta$, for the PF ring samples was determined in the laboratory. The wide range of pressure head values covered necessitated using hanging column methods, 2-bar volumetric pressure plate extractors and a 15-bar ceramic plate extractor. The precise detailed procedures followed for the soil-moisture characteristics are acutely detailed by Larson (1984), with the only change being that the hanging column annulus dewatering was executed with the gentle use of a vacuum pump and suction flask.

Figures 6 through 9 illustrate the soil moisture characteristics for the 12 PF ring samples. Figure 6 illustrates the large water holding capacity of an approximately 31 cm thick clay layer from 99 cm to 130 cm in depth. Upon drying from zero to 15 bars, a minimum amount of sample shrinkage occurred: 2% for the 112.5 cm depth sample, 2% for the 121.0 cm depth, and 4% for the 129.5 cm depth. By

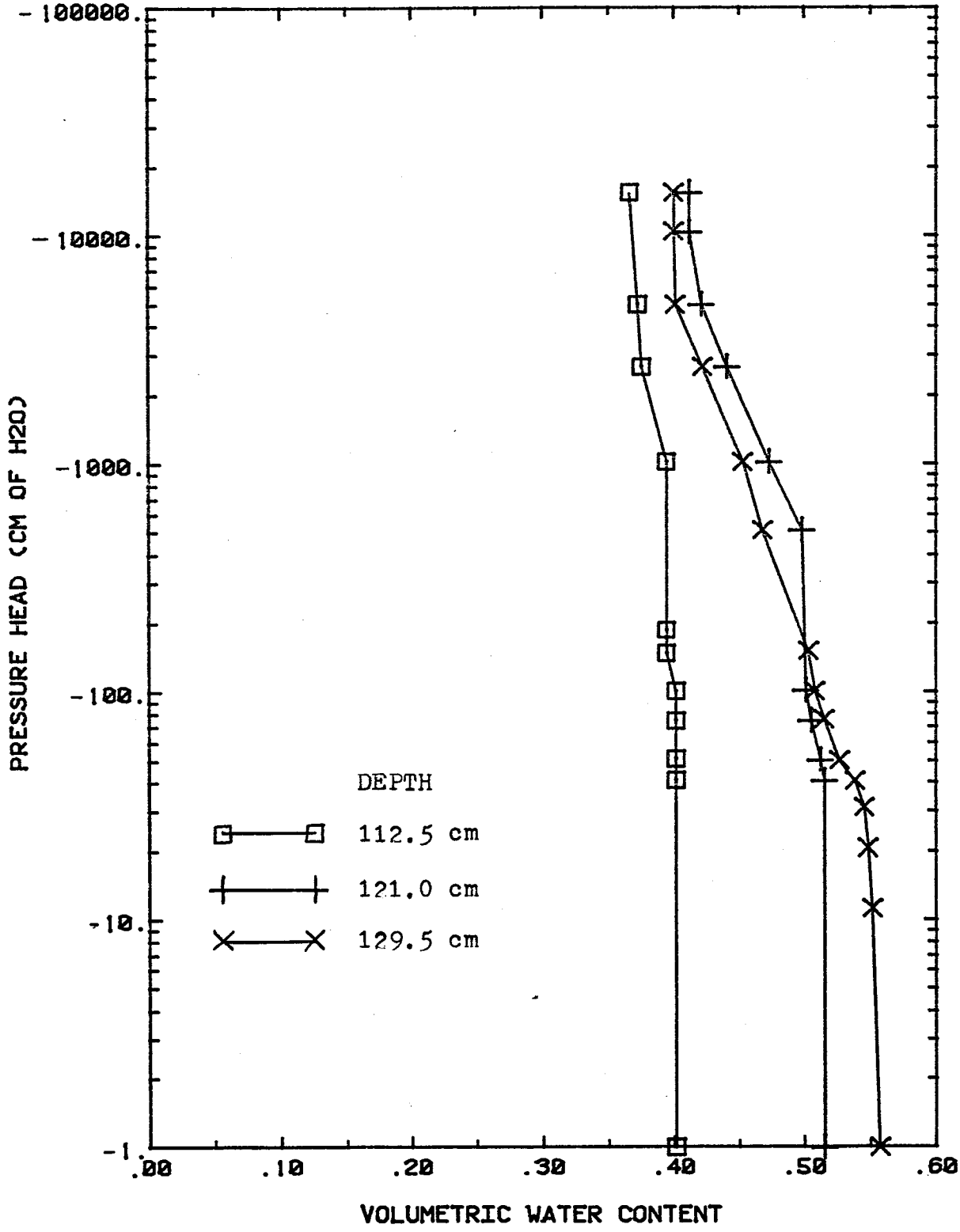

Figure 6. Soil-Water Characteristic Curves of the Clay Zone from R= 60 cm

comparison, after oven drying the samples subjected to the 15 bars of pressure, shrinkages of 9%, 14% and 10% respectively were recorded at the 112.5, 121, and the 129.5 cm depths respectively. Only the 112.5 cm sample agrees in porosity with that reported in Table 2. The clay sample from 121.0 cm shows a higher saturated moisture content using the hanging column and pressure plate apparatuses than reported in Table 2. The increase is about 0.06 cm^3/cm^3. The sample from 129.5 cm depth shows a difference of about 0.14 cm^3/cm^3 between the desorption methods and Table 2. The reason for this is not clearly understood but it is believed to be possibly due to the shrinking/swelling nature of these clays. The saturated moisture contents calculated from the desorption techniques occur under saturated conditions when the sample had the largest volume and possibly the largest void space. Another possibility is the low values of particle density used in Table 2. It is felt that additional research would be called for to gain a better understanding of this zone's characteristics. Figures 7 and 8 show drying curves for samples 30 cm adjacent to the zone to be examined in the borehole test. From figures 7 and 8, the more gradual slopes of the Ψ-θ curves with depth indicate that the soil texture may become finer with depth.

Figure 9 shows the hysteresis involved between the drying and wetting processes using the hanging column apparatus. This relationship was obtained for only 1 of the 12 PF ring samples, as the nature of the sand sample permitted maximum

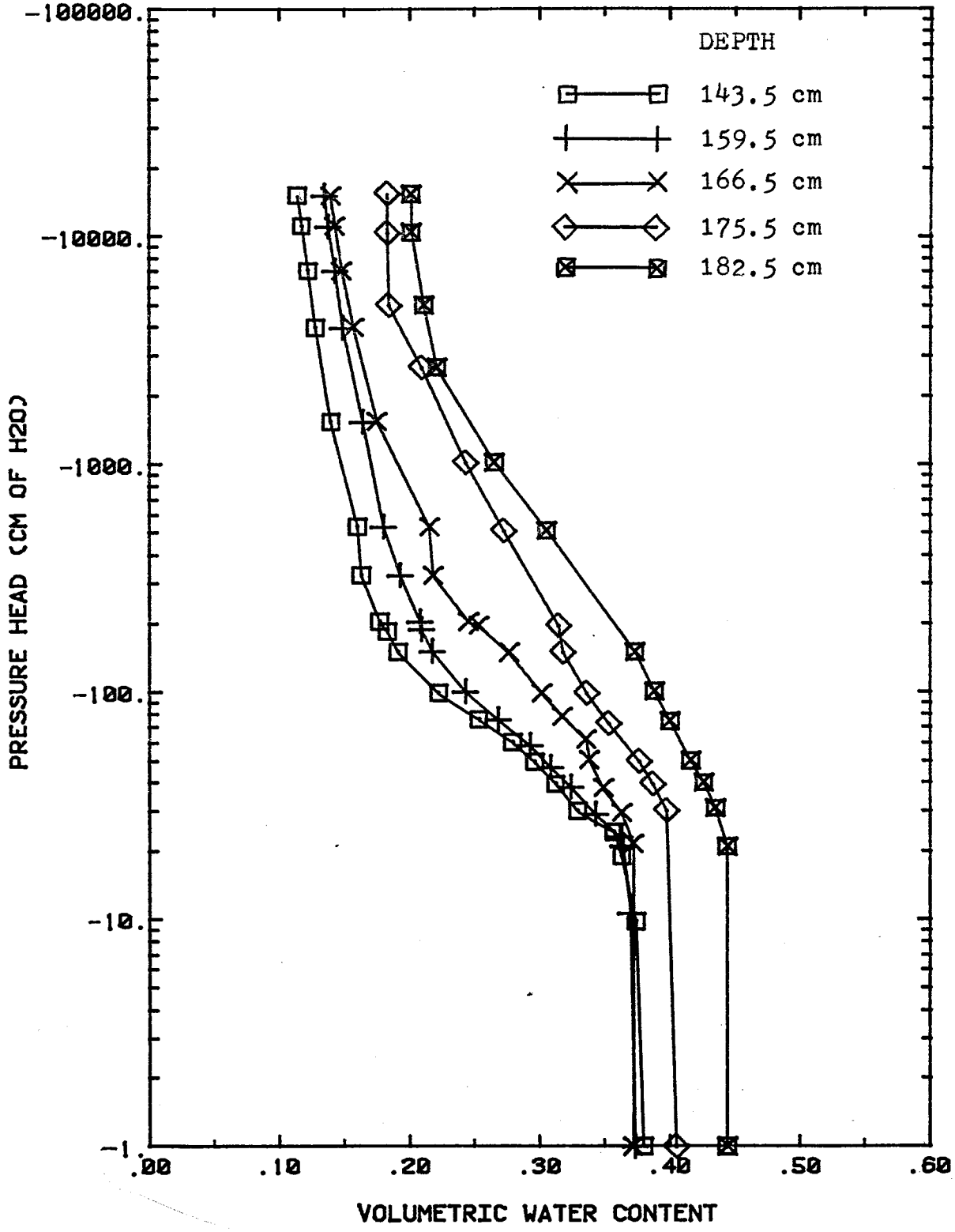

Figure 7. Soil-Water Characteristic Curves from R= 30 cm

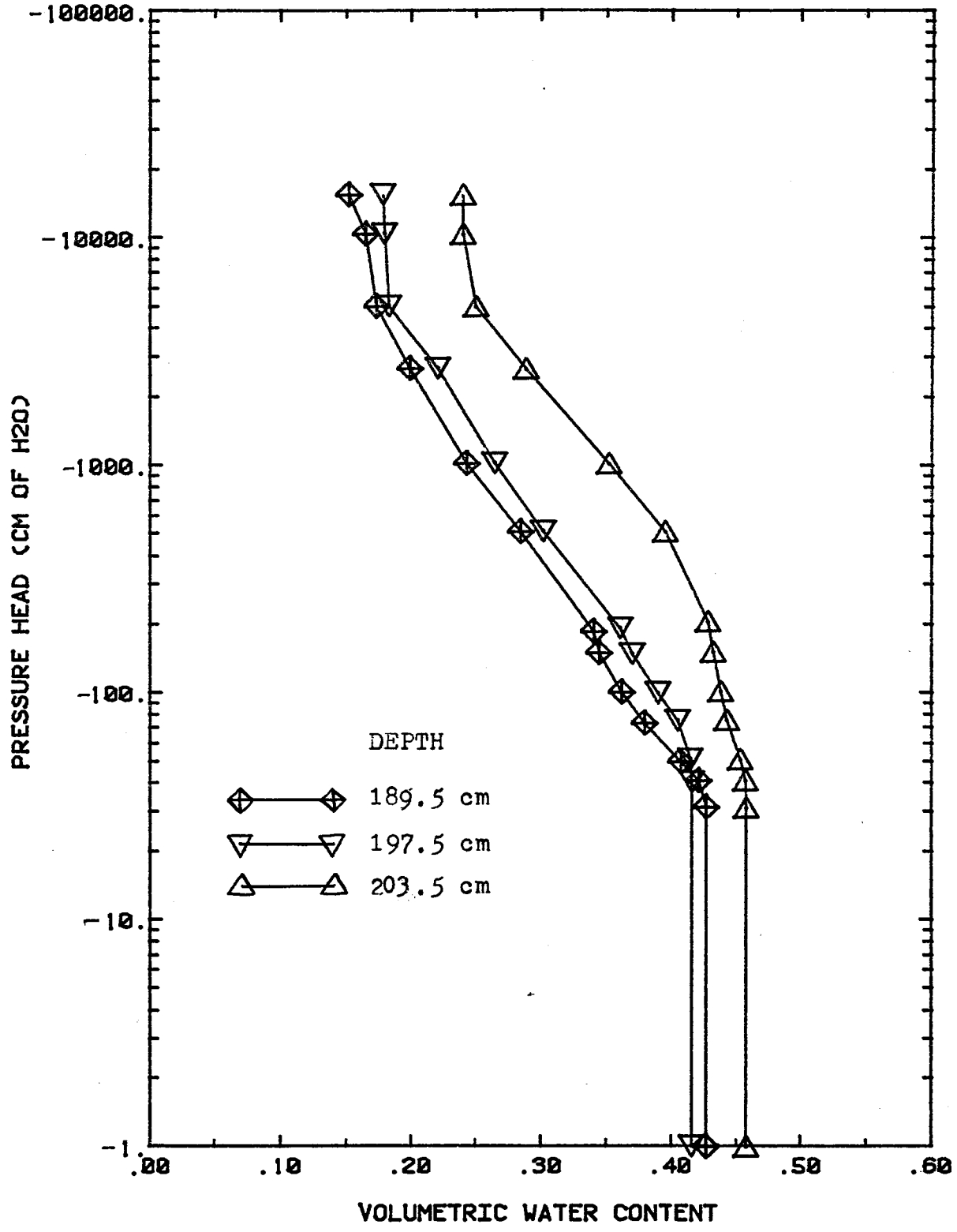

Figure 8. Soil-Water Characteristic Curves from R= 30 cm

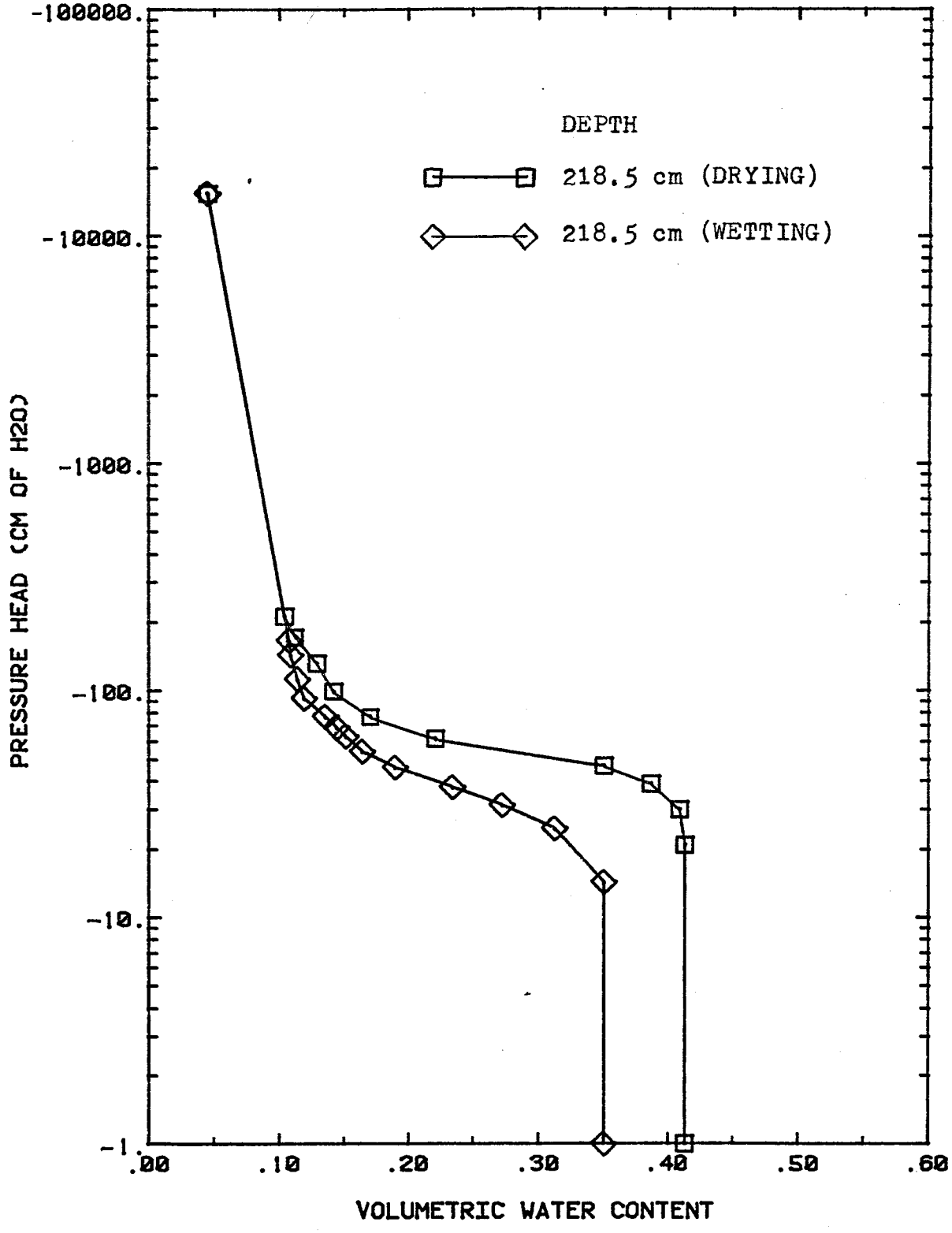

Figure 9. Soil-Water Characteristic Curve from R= 30 cm

dewatering within the -200 cm pressure head range of the hanging column device.

Table 3 was compiled for comparative purposes of porosity n, field volumetric moisture content θ_F ,calculated saturated moisture content,θ_S , and percent saturation, S. Field weights of the three clay zone samples (60 cm radius) were lost, unfortunately. A comparison of field volumetric water contents,θ_F , to calculated saturated moisture contents,θ_S , shows that with increasing depth, the saturation value of θ_F/θ_S approximates 100%, as would be expected as the sample depth approaches the water table. But when a comparison is made between porosity (from bulk density) and saturated moisture contents, 8 out of 12 values of porosity are low with 3 samples in agreement and one value of 44.5 (203.5 cm) is greater than θ_S. Due to the reasonable agreement between θ_F and θ_S values, a high confidence level is placed on the values of θ_S. The values of porosity n were calculated from the difference of 1 minus the ratio of bulk density to particle density. The porosity values would be lessened for values of bulk density that are too high and/or values of particle density that are too low. Although it is felt that a good pretreatment procedure was performed, and pycnometer methods were strictly adhered to, the values of sample particle density are possibily in error. A commonly used particle density for soils of this type would be 2.6 g/cc which suggests that the pycnometer values are too low. As the samples involved are loams with high moisture contents,

TABLE 3
COMPARISON OF POROSITY, FIELD MOISTURE CONTENT, SATURATED MOISTURE CONTENT, AND PERCENT SATURATION

Radius (cm)	Depth (cm)	n (%)	θ_F (%)	θ_S (%)	S (θ_F/θ_S)
60	112.5	40.9	na	40.1	na
60	121.0	44.6	na	51.5	na
60	129.5	42.4	na	55.7	na
30	143.5	34.7	20.4	38.0	0.54
30	159.5	34.9	24.9	37.3	0.67
30	166.5	37.2	28.9	37.2	0.78
30	175.5	39.9	36.9	40.5	0.91
30	182.5	39.4	41.7	44.4	0.94
30	189.5	38.5	42.0	42.7	0.98
30	197.5	42.2	45.9	45.8	1.00
30	203.5	44.5	42.7	41.6	1.03
30	218.5	36.3	41.4	41.3	1.00

n : porosity from dry bulk density

θ_F: field moisture content

θ_S: maximum water content from θ-Ψ curve

na: not available

another possibility might be that the bulk densities measured from the field are too high. This effect could have resulted from the PF ring sampling technique. The friction encountered when pushing the sampling device into the wet sticky soil could cause compaction that would provide higher bulk densities than field conditions. Therefore wet up values of saturated volumetric moisture contents are believed to be closer to the actual porosity values.

Saturated Hydraulic Conductivity

Saturated hydraulic conductivities were measured at five radial distances from the borehole and at depths ranging from 16 cm to 275 cm. Two modes of sampling were utilized: PF ring samples and shelby tube samples. Two separate sampling techniques were used to test the hypothesis that, relatively small samples which have larger ratios of ring wall circumference to sample area (e.g., PF rings), tend to produce comparatively 'greater' values of saturated hydraulic conductivities than larger samples, such as those in shelby tubes, due to wall effects (piping).

Shelby Tube Method

The first experiments for determining saturated hydraulic conductivities were carried out using samples collected from three locations relative to the borehole (figure 5). These three positions were chosen to quantify saturated hydraulic conductivity profiles with depth to delineate possible

layering which would be taken into consideration in analyzing the borehole test results. From figure 5, the profile locations are designated N (north), W (west), and S (south). Three shelby tube samples from each location were recovered utilizing the Mobile Drill B-30 drill rig of New Mexico Tech. For reference purposes, shelby tube samples analyzed will be numbered 1 through 9; samples 1, 2, 3 were collected from increasing depths in the north hole, samples 4, 5, 6 were taken from increasing depths in the south hole and samples 7, 8, and 9 were collected from increasing depths from the west hole.

Figure 10 shows the constant head permeameter, constructed specifically for this project, which utilizes shelby tube samples to provide up to six hydraulic conductivity values from each tube sample. The permeameter has a capability of handling six shelby tube samples at a time with a maximum head of water of about 2 meters at the top of each shelby tube and a minimum head of about 0.1 meter.

Figure 11 illustrates a multiple manometered shelby tube sample for acquiring six values of K_s from segments of sample within the tube.

Calculations follow Darcy's law:

$$Q = - KA \, dH/dL \tag{4}$$

$$Ki = (Q/A) \, (dLi/-dHi) \qquad i=1,6 \tag{5}$$

where Ki is the interval saturated hydraulic conductivity in cm/sec; Q is the discharge from the bottom of the sample in cm^3/sec; A is the cross-sectional sample area which was

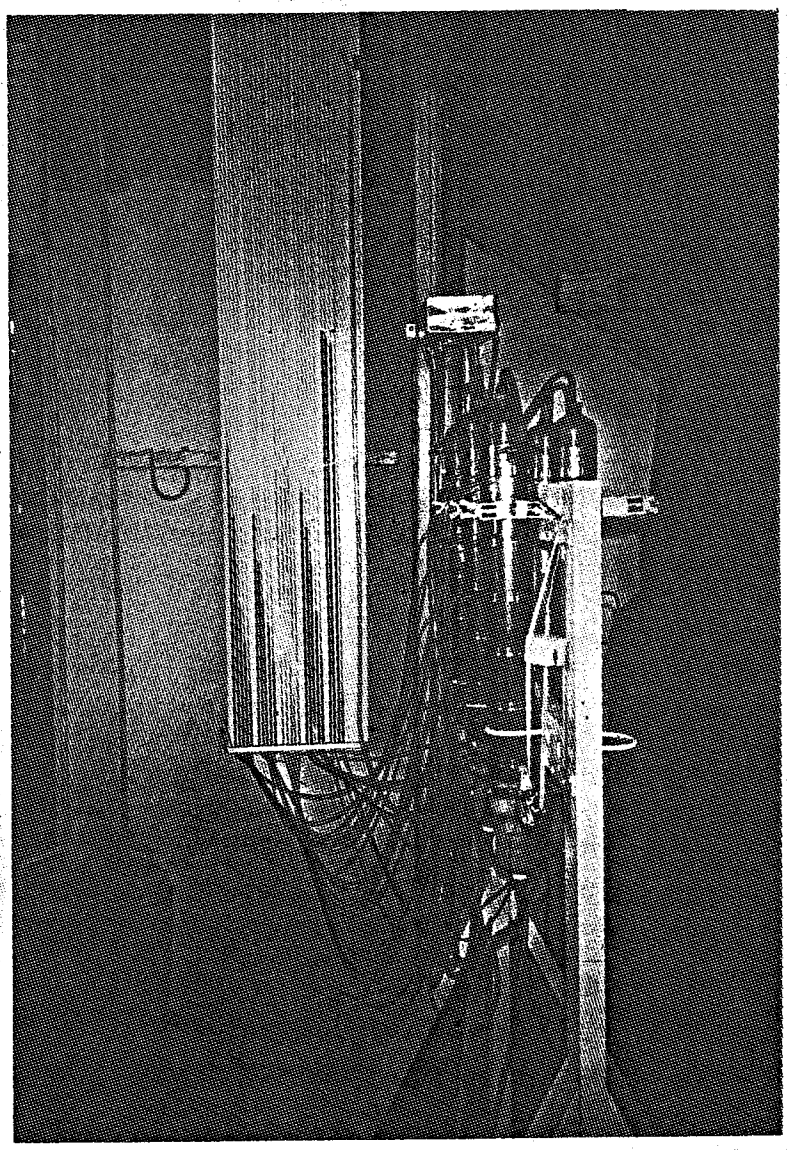

Figure 10. Multiple Manometer Shelby Tube Permeameter

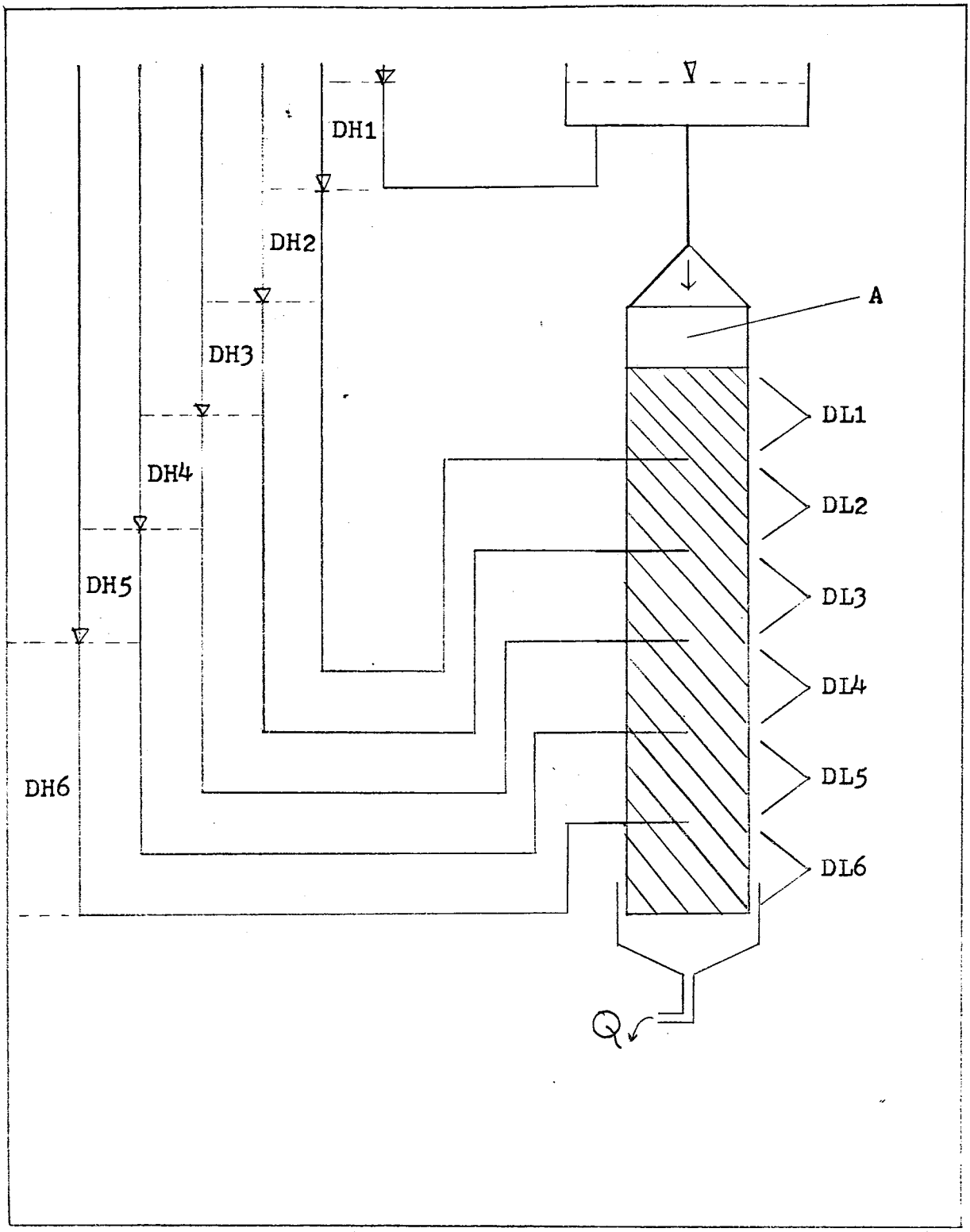

Figure 11. Shelby Tube Permeameter Schematic

constant at 41.88 cm^2 for these tube samples; dLi is the sample length in cm between the top of sample and first manometer, successive manometers, and the last manometer and sample bottom; -dHi is the difference in elevation between fluid levels measured on the manometer tube board between the applied head level and the first manometer water level, successive manometer water levels, and the last manometer water level and the elevation of the sample bottom.

An analysis of measurement error in Ks reveals that Ks values shown in figures 12-20 may vary by +/- 10%.

Shelby tube samples obtained in the field were logged for length of sample retrieved and length of void space (hole) left after retraction, to look at possible sample compaction (Riggs, 1983). Seven of nine samples taken gave near 100% sample-length to length-pushed ratios. Only the eighth sample retrieved from the west profile, between 135-187 cm depth proved not obtainable using standard shelby tube sampling methods. For this sample the strength of the soil was greater than the skin friction between the soil and sampler; thus the sample could not be retrieved by pulling. Finally, after 12 attempts at this zone, a hand dug pit was excavated next to and below the shelby tube, and the bottom of the sample was cut off with a spatula so that the full sample length could be retrieved.

The end of each sample was then taped and the samples were carefully transported to the soils lab. At the lab, shelby tube samples were equipped with manometers and given

special inflow and outflow fittings. Complete details of the shelby tube preparations for the permeameter are listed in appendix A. With the shelby tubes ready for inflow, an initial CO_2 flooding was applied in order to minimize the effect of entrapped air by displacing soil air with the more water soluble CO_2 (Lambert, 1983). Table 4 provides volumes of CO_2 used to flood each shelby tube sample. Flooding rates varied with the gas permeability of the sample. Pressures were kept below about 2 psi and flooding rates varied from 100 ml/min to 2 l/m. After CO_2 application, water was slowly applied to the top of the sample until ponding in the inflow fitting occurred; at this time a head of about 30-40 cm was applied.

As with any water permeameter system there is concern over changes in the water quality with time. Factors affecting water quality include bacteria growth, precipitation, or ion exchange reactions. To best simulate field permeabilities, all water used in the shelby tube permeameter was recirculated groundwater, pumped from the shallow aquifer at the site; this water was used for borehole tests in the field.

Table 5 gives the chemistry of the field ground water. Past permeameter experience and the anticipation of long measurement periods with the new permeameter apparatus, dictated the addition of a minute amount (20-30 cc) of Chlorox bleach to the 42 liter recirculating water system. After a short period of circulating time, an accumulation of tan and

TABLE 4
VOLUMES OF CO_2 APPLIED TO SHELBY TUBE SAMPLES BEFORE PERMEABILITY MEASUREMENTS

Shelby Tube Sample	CO_2 Applied (liters)
1	112
2	59
3	316
4	130
5	126
6	54
7	120
8	80
9	67

TABLE 5
CHEMICAL ANALYSIS OF FIELD GROUNDWATER AND FIELD TAP WATER

	Site Groundwater 2/20/84	Site Tap Water 6 /22/84
pH	7.39	7.60
CO_3 (ppm)	0.0	0.0
HCO_3 (ppm)	700.	205.
Cl (ppm)	120.	19.
SO_4 (ppm)	360.	108.
NO_3 (ppm)	2.2	2.3
F (ppm)	<0.2	0.5
Na (ppm)	185.	44.
K (ppm)	15.0	2.6
Mg (ppm)	30.	7.8
Ca (ppm)	215.	55.
Mn (ppm)	* 3.2	* <0.5
Fe (ppm)	* 1.74	* <0.5
Conductivity (μmhos)	1780.	460.
TDS (ppm)	1286.	342.
Hardness (ppm $CaCO_3$)	661.	169.

*: These values determined on 5/21/84

Analysis performed by the New Mexico Bureau of Mines and Mineral Resources.

white material accumulated on some metallic fittings within the water system. Dr. Tom Lynch, N.M.T. Biology Department, suggested that the tan material could possibly be a fungus growth, due to the extensive use of tygon plastic tubing in the system. At his suggestion, a 0.05% solution benzalkonium chloride was added to the permeating water to minimize fungus growth. During this water treatment, shelby tubes 1 and 2 were being measured for Ks.

When shelby tubes 3 through 6 were measured, it was realized that the Chlorox produced a chemical reaction which caused an oxidation and precipitation of an apparent iron oxide; so, this treatment was stopped. Upon visual examination of samples 1 and 2 it was also apparent that the insides of the steel shelby tubes were oxidizing profusely, due to the metal contact to the field water. Precautions taken on samples 3-6 to prevent this shelby tube rusting were as follows: the permeameter system was shut down and the inflow fittings from tubes 3-6 were removed. The inside of the shelby tubes, above the contained samples, were cleaned of rust and coated with a clear polyurethane coating that was obtained from a local hardware store. Also all metallic parts having water contact in the permeameter were coated. The permeameter was put back into service with samples 3 through 6 and it was observed that the polyurethane coated inside tops of the shelby tubes resisted rusting during the water contact. Also there was no use of the 0.05% benzalkonium chloride solution, because it was believed that the tan accretions were

not organic and the treatment was costly. A benzalkonium chloride treatment for the 42 liter shelby tube permeameter reservoir costs about $7.50.

Before shelby tube samples 7-9 were collected, the insides of the shelby tubes, as received from the factory, were washed in regular grade gasoline to remove residual machine oil and then thoroughly washed with Alconox detergent to remove the gas residue. The used tubes were also washed in this manner, but tubes 7-9 were given a thorough inside coating of the clear polyurethane. No benzalkonium chloride or Chlorox was used in the water reservoir for samples 7-9 and the precipitation was lessened. From this experience , it is recommended procedure that the insides of the shelby tubes be thoroughly cleaned and treated with a hard coating, such as a polyurethane, to prohibit rusting during water contact. Shelby tubes to be reused for sampling and in the permeameter should be thoroughly cleaned inside by a drill-powered wire brush on a long extension and a new coating of rust inhibitor applied.

The results of the shelby tube permeameter samples will be presented, then a discussion will follow. Figures 12 through 20 show the change in hydraulic conductivity, Ks, with time for the nine shelby tube samples. Shown in each figure are measured Ks values for different segments within the shelby tube sample. In all shelby tube samples, segment 1 pertains to the sample segment starting at the inflow surface. The largest sample segment number for any figure will always

be the segment containing the outflow surface. Also shown in figures 12 through 20 are the pressure heads applied to the number 1 sample segment.

Shelby tube 1 (figure 12) contains a clean medium-fine sand. In this figure, the decreasing Ks with time from 0-76 hours of sample segment 1 suggests that the iron oxide precipitation plugged only pores in the upper (inflow) part of the shelby tube sample. This clogging reduced the flow rate through the sample which resulted in a decrease in manometer heads of the lower segments. At a time of 76 hours, the constant head level was raised from 31 to 55 cm above the sample top. The effect of this head increase was an increase in Ks in the first sample segment. One possible explanation for the increased Ks might be a redistribution of the fine fraction due to greater flow velocities within sample segment 1. Sample segments 2 through 6 are apparently unaffected by the increase in head at the inflow boundary and values of measured Ks with time are relatively constant. The clogging of the pore space at the inflow end of the sample in the shelby tube constant head permeameter may have no effect on values of Ks in the lower portions of the shelby tube sample.

Shelby tube sample 2 (figure 13) contains a sandy loam soil. A head of 31 cm of water was applied at the inflow end of the sample during the first 4 hours; thereafter the head was maintained constant at 55 cm. However, increases in Ks for sample segments 4, 5, and 6 at early time is attributed to manometer equilibration time. The long manometer tubing

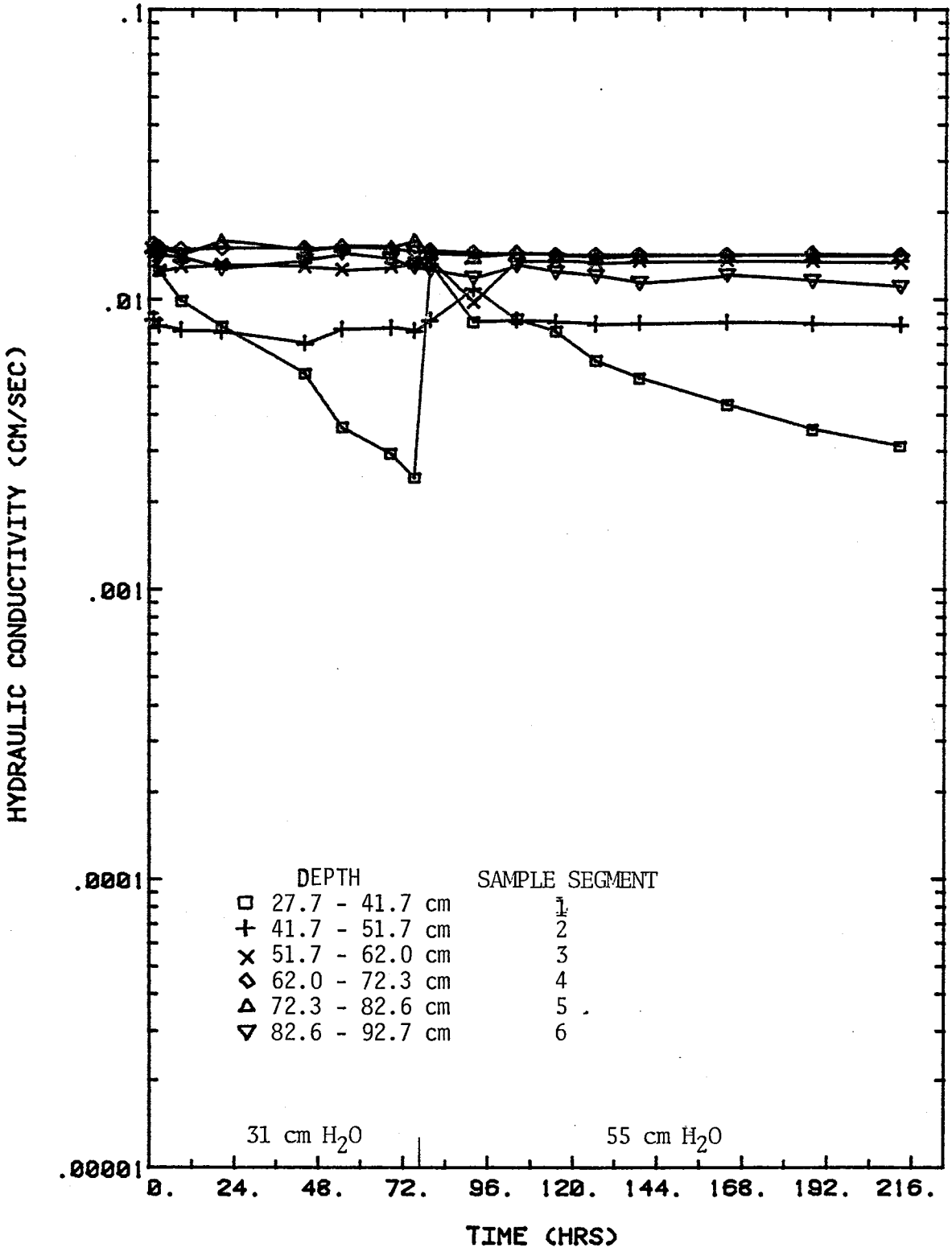

Figure 12. Shelby Tube Hydraulic Conductivities: North Profile, Sample 1

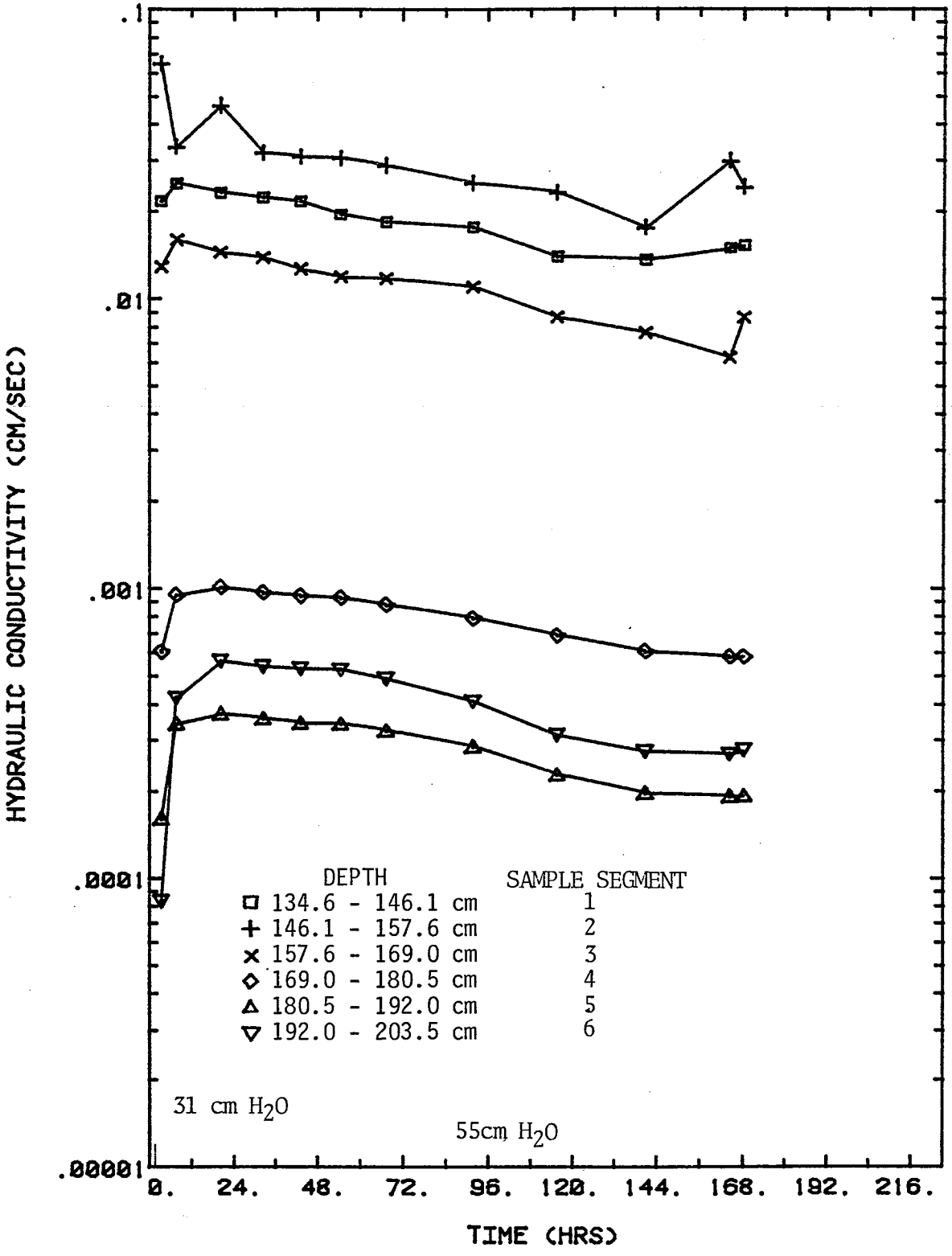

Figure 13. Shelby Tube Hydraulic Conductivities: North Profile, Sample 2

attached to shelby tube samples 1 and 2 were left to fill with water from within the sample after infiltration began; and shelby sample 2 with the lower composite vertical Ks required longer for the manometers to equilibrate, owing to a lower flow rate through the system. The upper sample, segment 1, shows no greater decline with time than the underlying segments, even though clogging of the inflow face was visually observed. Possibly because of the lower flow rate through the sample, less of the iron oxide precipitation was transported to the inflow sample face. Figure 13 indicates that all Ks values in shelby tube sample 2 decrease with time in contrast to shelby tube sample 1, however the reduction in Ks is only about 44% of that after 148 hours.

Shelby tube samples 3 (figure 14), 4 (figure 15), 5 (figure 16), and 6 (figure 17) were wetted simultaneously in the permeameter; therefore a change in elevation of the constant head applied to the top of one sample affected all four samples simultaneously. Before infiltration began, all the manometer tubes from each sample were clamped shut where the tubes enter the shelby. Then the tubes were filled with water to a height on the manometer board of a fraction of the pressure head that was to be applied to the sample top from the constant head reservoir. After infiltration through the sample was begun, the clamps were removed from the manometer tubes. Water from the manometer tubes then flowed into and through the shelby tube sample until the pressure head inside the shelby tube manometer was equal to that on the manometer

tube board. This filling of the manometer tubes or "priming" before infiltration was to prevent the soil sample from washing into the manometer tubes when flow was allowed to fill the manometer tubes from within the shelby tube system. The time used for manometer equilibration in figures 14-20 is when the Ks curve appears to take a steady trend.

In figure 14, the manometers equilibrated within 12 hours. Sample segments 1 and 2 both show similar decreases in Ks from 12 to 76 hours time that appear to be resultant from clogging. Sample segments 3, 4, and 5 show relatively stable measured Ks values. Of interesting note here is that from 12 to 76 hours time, the bottom manometer (top of the lowest sample segment) indicated negative pressure head, i.e. the level in the manometer was several centimeters below the point where the manometer enters the shelby tube. Because this "suction" is still believed to be within the capillary fringe zone, the soil is saturated and Ks should still be valid. To test this hypothesis, the head was raised at 76 hours from 92 cm to 203 cm to try to put a positive pressure on the bottom manometer. This head change affected the entire shelby tube sample, as can be seen in figure 14. The number 1 sample segment appears to show a step-like increase in measured Ks after the increase in applied head; while simultaneously, sample segments 2 and 3 appear to show step-like decreases in Ks. Sample segment 4 appears to show a step-like increase in Ks. The possible explanation for these changes in Ks is the same as mentioned for shelby tube sample 1. The increase in

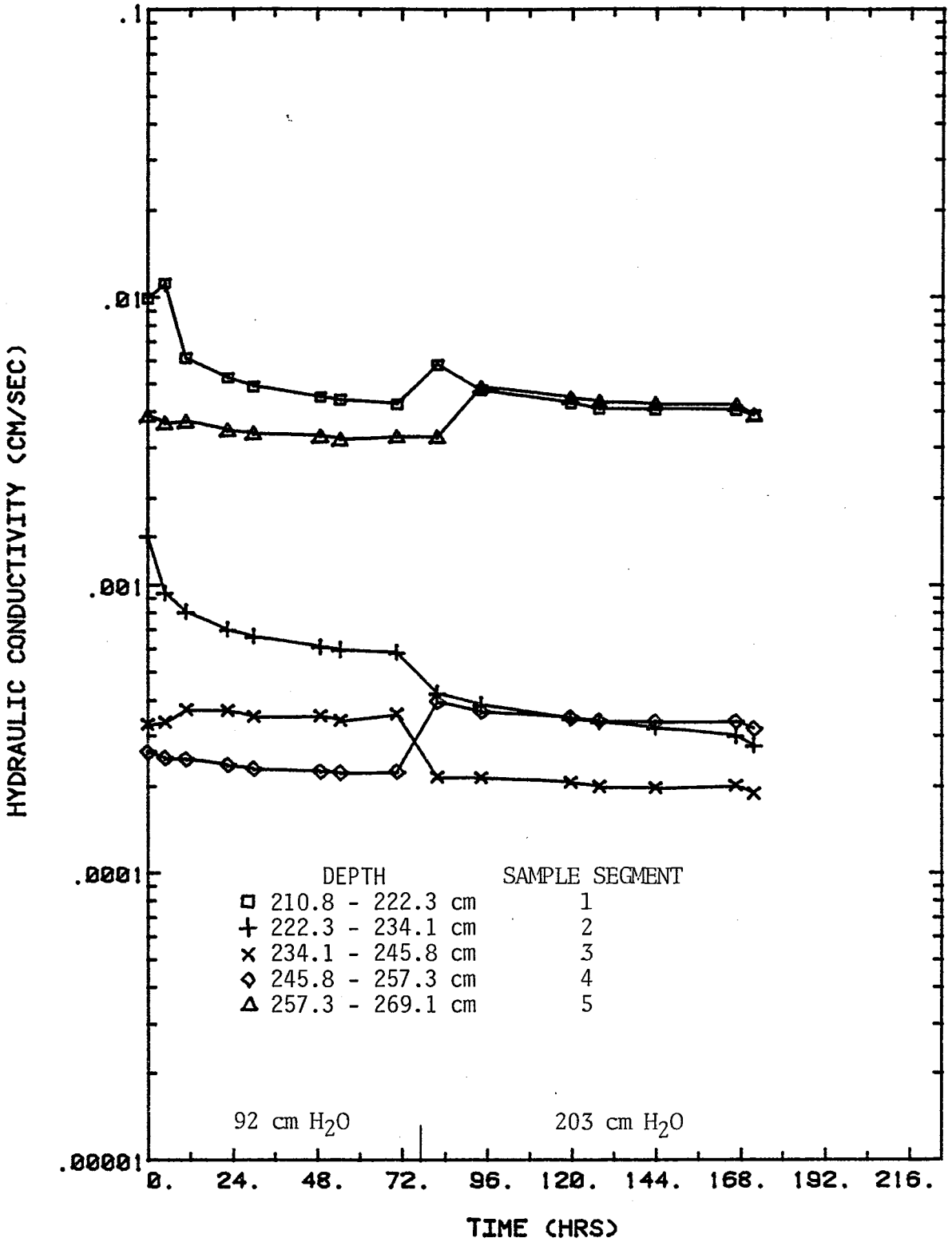

Figure 14. Shelby Tube Hydraulic Conductivities: North Profile, Sample 3

head to the top or first sample segment causes a redistribution of the fine fraction within the sample segment. When a decrease in Ks is seen in successive segments, then the fine fraction may be deposited beneath the successive manometer positions. Sample segment 5 in figure 14 shows an apparent increase in Ks that occurs 7 hours after the increase in head. This increase in Ks is still believed to be resultant from the redistribution of soil within the entire sample. A further analysis in which rapid measurements of manometer elevations and flow are collected after a change in the reservoir head is made, might resolve whether this step-like increase in Ks really occurs.

Shelby tube 4 (figure 15) contains a medium-fine sand, similar to shelby tube 1. The manometers of shelby tube sample 4 equilibrated after 12 hours. During early times, 12-75 hours, due to a decrease in outflow caused by clogging of the inflow surface, pressure heads at the last two manometers were several centimeters below where the manometers entered the shelby tube. The change in head mentioned for shelby tube sample 3 corresponded to 75 hours of infiltration time for shelby tube sample 4. From figure 15, sample segment 1 decreases in Ks between 12 hours and 75 hours. After an increase in head to segment 1, Ks increases and then shows continued effects of clogging until 171 hours. Sample segment 2 is at a steady Ks from 12 to 75 hours after which a decrease in Ks again possibly due to a redistribution of the fine

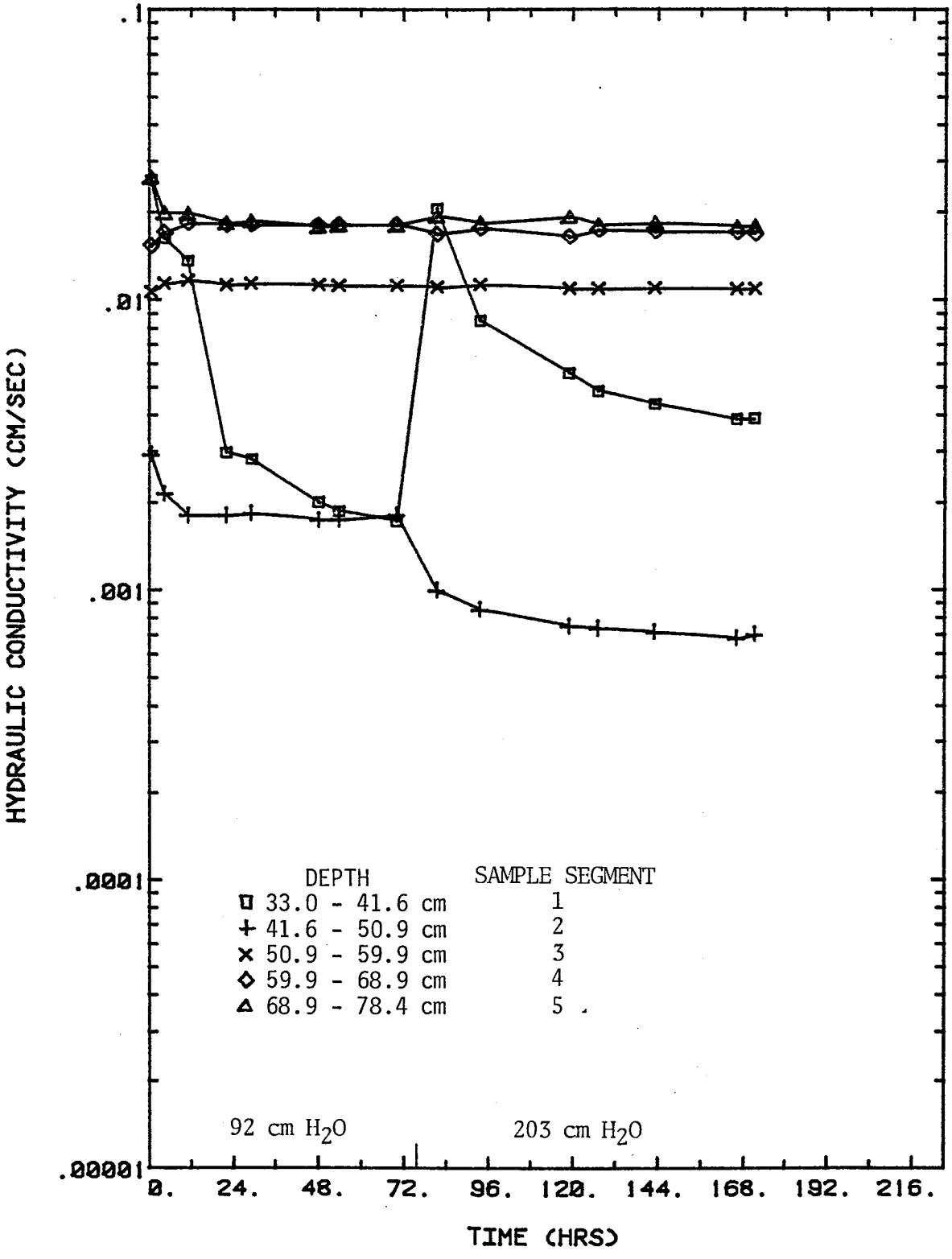

Figure 15. Shelby Tube Hydraulic Conductivities: South Profile, Sample 4

fraction that may have been transported to sample segment 2 from segment 1. From 12 to 171 hours, sample segments 3, 4, and 5 are unaffected in Ks values by the change in head. An interesting result of the head change to shelby sample 4 was recorded. The bottom two manometers now registered positive pressures with negligible changes in Ks; this indicates that saturated hydraulic conductivity holds within the capillary fringe zone under negative pressure heads.

Shelby tube sample 5 (figure 16) contains a sandy loam soil similar to shelby tube 2 (figure 13). Because of the fine textured material and lower flow through the system, the manometers take approximately 24 hours to equilibrate. The effects of clogging are again evident in sample segment 1. Sample segment 2 shows a decreasing trend but Ks is only decreased by 33% in 140 hours. Sample segment 4 in figure 16 never registered a positive pressure at its top manometer. After manometer equilibration, Ks decreased 60% in 136 hours. There are no apparent effects of the head change at 74 hours.

Shelby tube sample 6 (figure 17), like shelby tube 3, extends below the water table and contains a loam in the upper sample segments. Manometers in this sample have equilibrated after about 6 hours. From figure 17, all sample segments are decreasing from 6 to 70 hours. This decrease in Ks, unlike shelby sample 3 (figure 14), may possibly be due to an ion exchange leading to the flocculation of sample colloids. Response to the change in head is similar to other shelby tube samples.

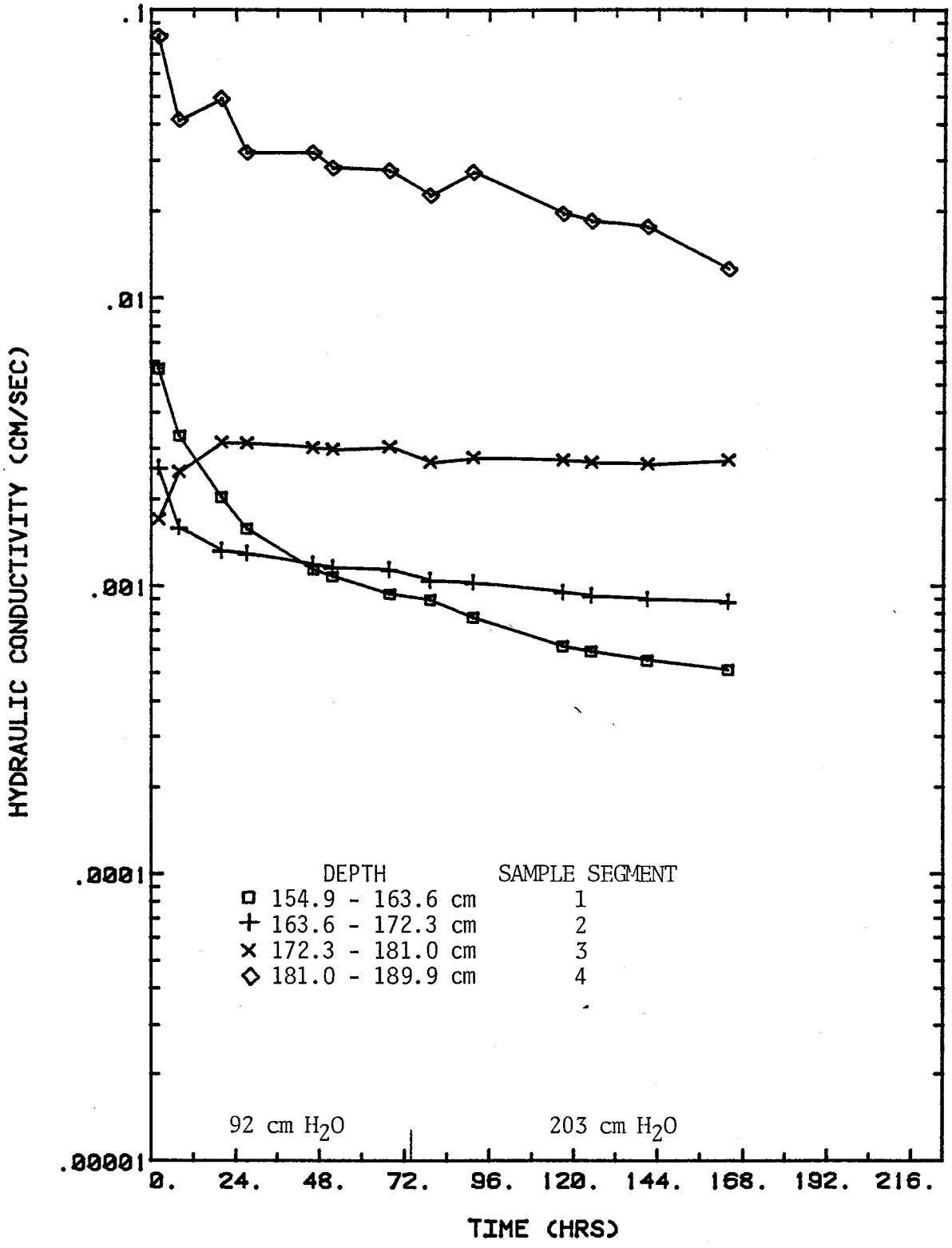

Figure 16. Shelby Tube Hydraulic Conductivities: South Profile, Sample 5

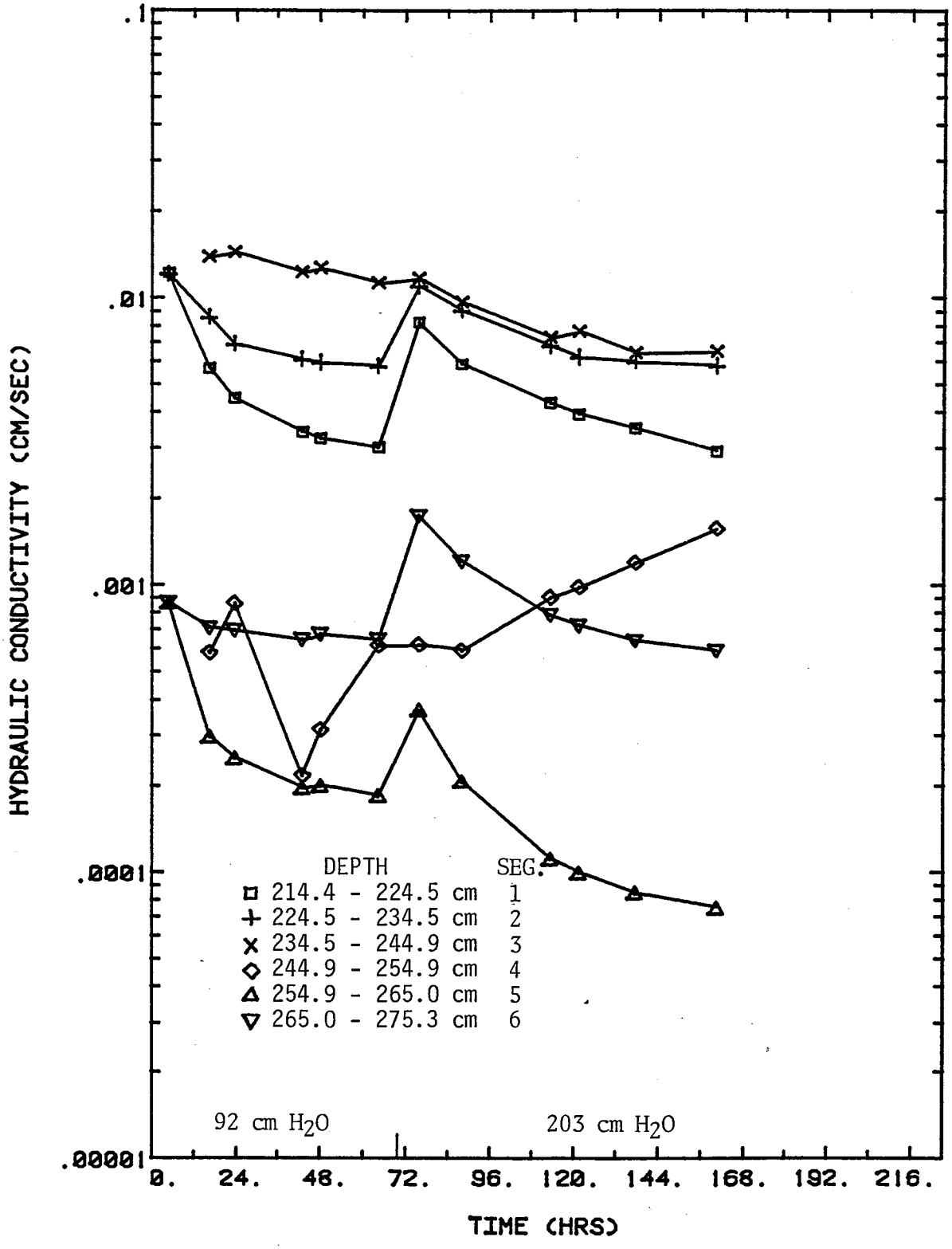

Figure 17. Shelby Tube Hydraulic Conductivities: South Profile, Sample 6

The last group of shelby tube samples to be wetted together are shelby tube sample 7 (figure 18), shelby tube sample 8 (figure 19), and shelby tube sample 9 (figure 20). All three of these shelby tubes were pretreated with a clear polyurethane in order to minimize the precipitation of iron-oxide and the clogging of the top sample segment. Even with this treatment, Ks in the upper-most segment still decreased with time due to clogging.

Similar to samples from shelby tubes 1 and 4, shelby tube sample 7, figure 18, contains a medium-fine sand. The manometers in this shelby tube have equilibrated after 6 hours.

Shelby tube sample 8 (figure 19) is a loam similar to shelby tube samples 2 and 5. The manometers in this shelby tube equilibrate after about 20 hours.

Shelby tube sample 9 (figure 20) contains loam in the upper segments and sand in the bottom segments similar to shelby tube samples 3 and 6. Manometer equilibration times are about 3 hours.

The constant head reservoir was increased twice while samples 7, 8, and 9 were in the permeameter to increase pressure heads in the manometer tubes. The pressure heads in the manometer tubes were decreasing with time due to the clogging of the top sample segments. Figure 18, 19, and 20 show similar trends with the other shelby samples of similar soils.

On 5/21/84 after the shelby tube investigation was

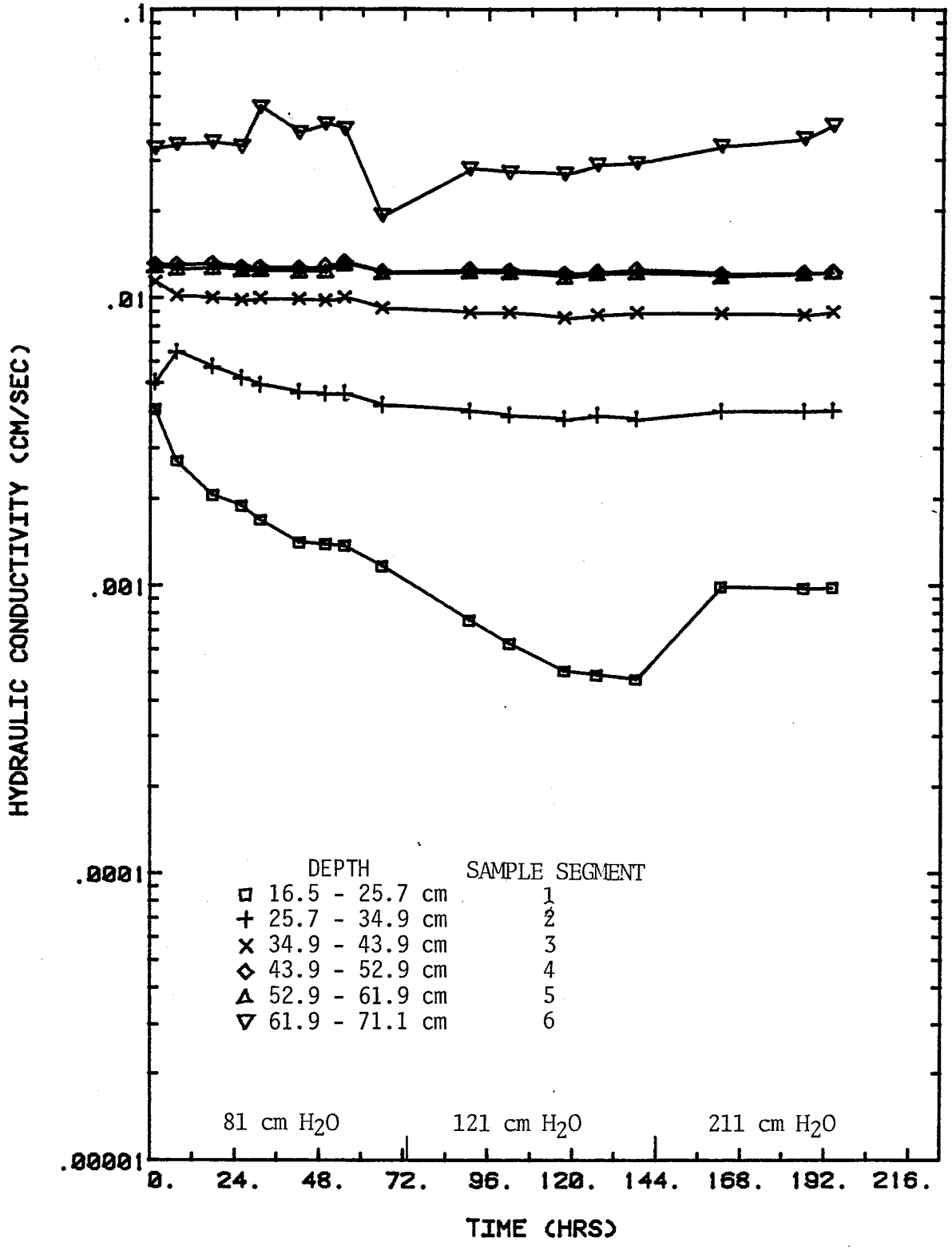

Figure 18. Shelby Tube Hydraulic Conductivities: West Profile, Sample 7

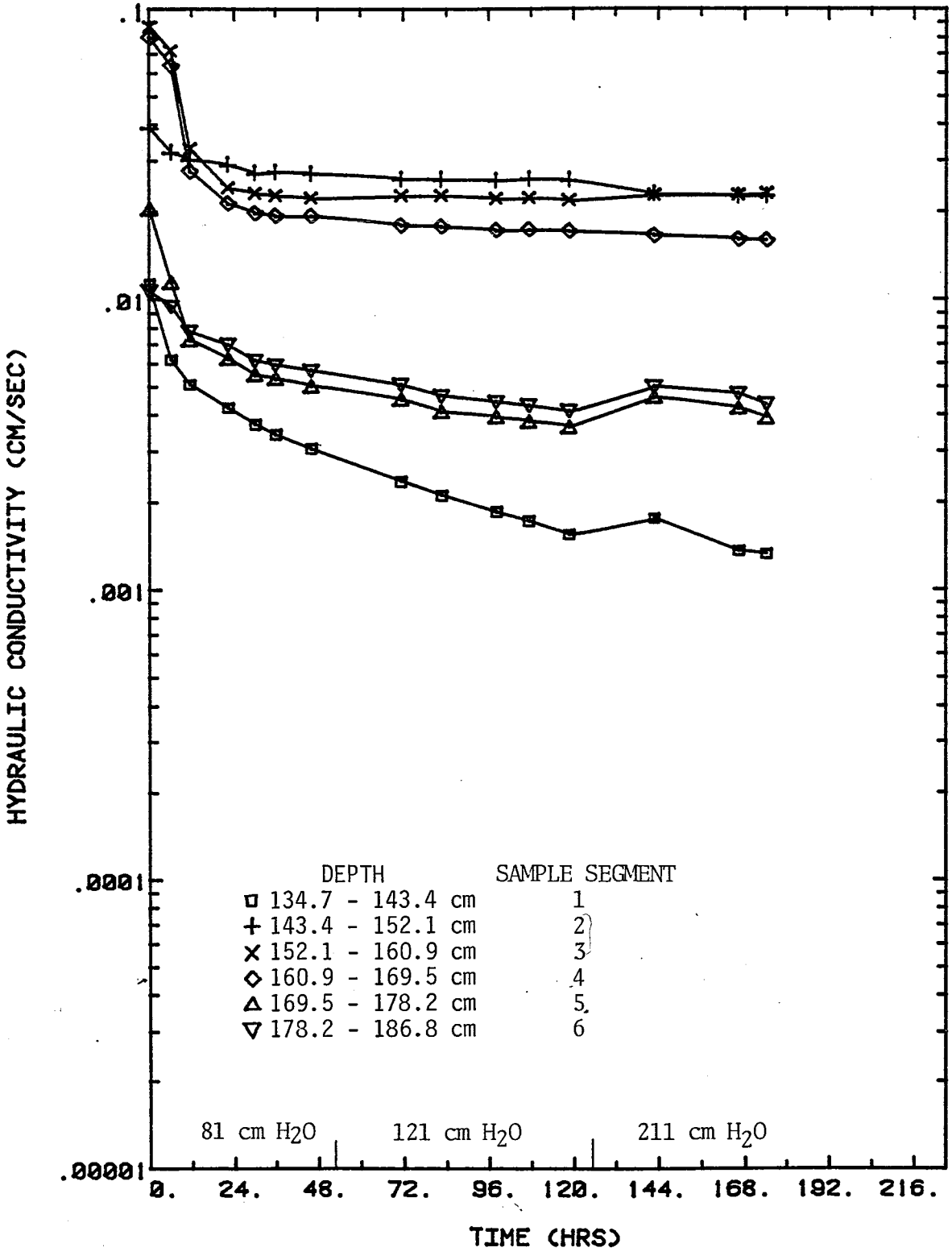

Figure 19. Shelby Tube Hydraulic Conductivities: West Profile, Sample 8

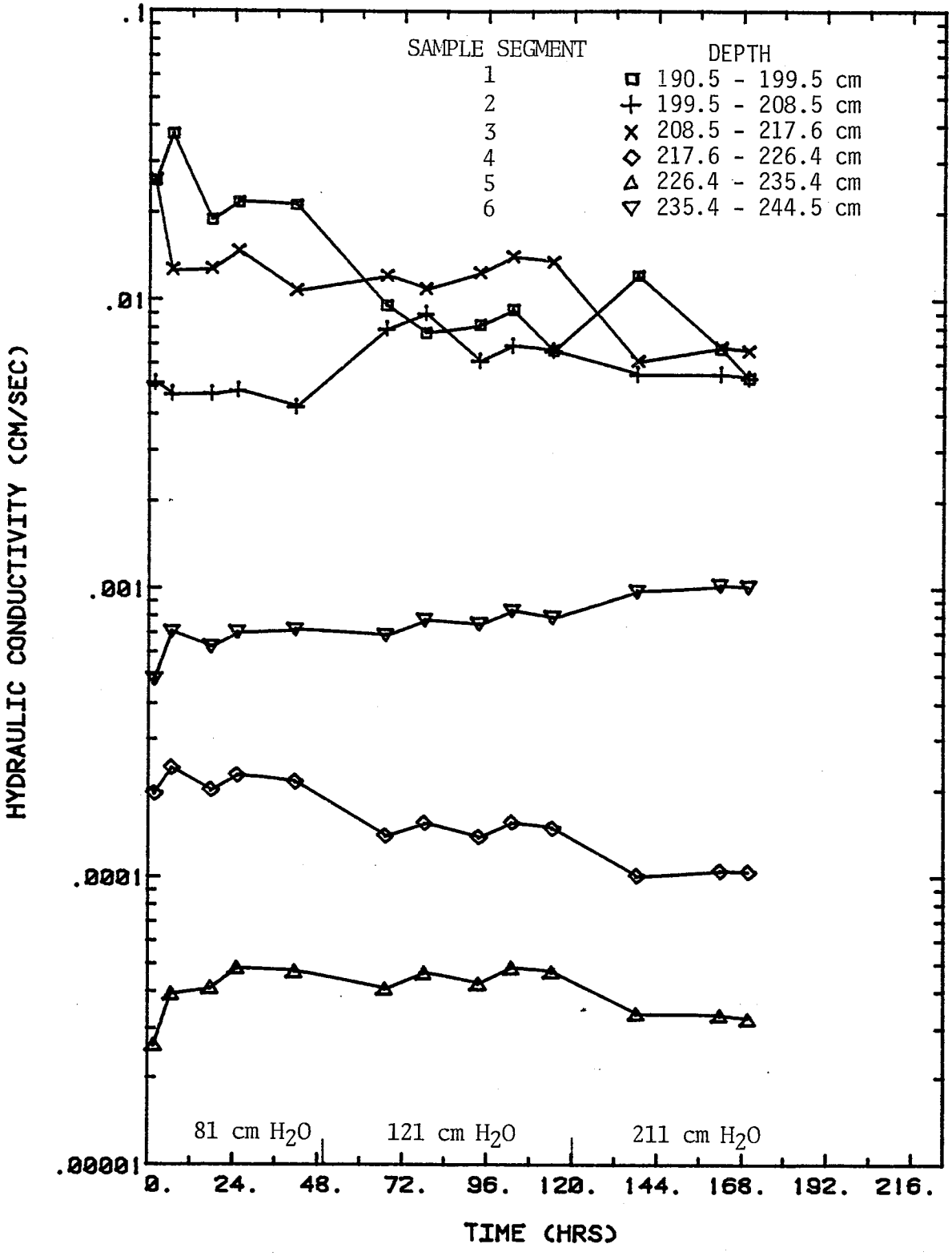

Figure 20. Shelby Tube Hydraulic Conductivities: West Profile, Sample 9

completed, a chemical analysis of the field site shallow ground water used in the shelby tube permeameter showed very high levels of Fe (1.74 ppm) and Mn (3.2 ppm). It is now believed that some of the precipitation in the recirculated shelby tube permeameter water system occurred from oxidation of these elements due to system water aeration. An interesting further study would be replicate profile samples run with tap water to observe clogging trends.

A minimum value of pressure head applied to the top of the shelby tube sample is recommended. That head value which will allow the manometers to function properly should be used. Increases in applied pressure head to the sample top after infiltration has begun is not recommended as step-like changes in measured Ks may result.

Additional conclusions from figures 12-20 are that CO_2 flooding effectively displaces soil air and allows for a steady measured value of Ks with time; this is in agreement with Watson (1983). Although temperature values of recirculated permeameter water ranged diurnally between 11 and 24 degrees Celcius, no apparent cyclic trends of Ks with time are evident. This temperature independence appears to denote that shelby tube samples which were rid of soil air by CO_2 remained free of accumulated air bubbles which might have come out of solution with time.

Figure 21 is a cross-section of saturated hydraulic conductivities from the shelby tube permeameter. These Ks values were determined from the most steady part of the Ks vs

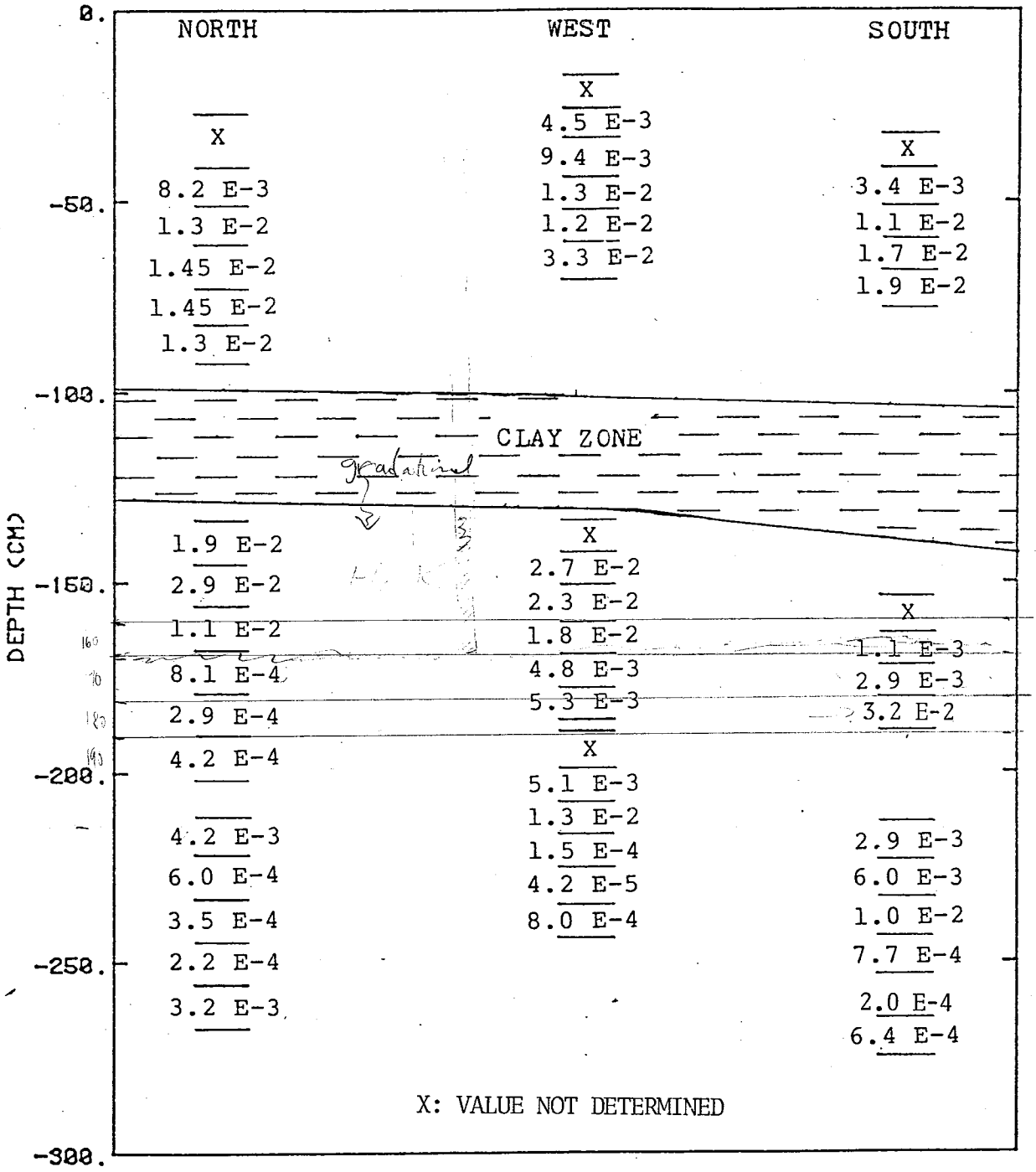

Figure 21. Shelby Tube Saturated Hydraulic Conductivity Profile

time curves before any sample disruption might have occurred as a result of increased reservoir elevation.

Actual layering trends from figure 21 are not easily discernible but values below the clay zone vary by three orders of magnitude with the highest Ks values usually closest to the overlying clay zone. In general, a decrease in Ks with depth below the clay zone is shown in figure 21. This decrease in Ks with depth was also inferred from the $\theta - \Psi$ curves.

PF Ring Method

The twelve PF ring samples that were analyzed for particle size analyses and soil moisture characteristics were first subject to measurements of saturated hydraulic conductivity using a fifteen sample PF ring permeameter (Eijkelkamp-Giesbeek, the Netherlands). The permeameter provides the option of utilizing constant head and falling head techniques on different samples simultaneously. Both methods were utilized, as will be shown later.

On the date that the samples were acquired from the field and returned to the soils laboratory, the PF ring permeameter was in use for other research. To make use of the lag time of 5 days, the samples were prepared for the permeameter by the installation of the bottom screen attachment to the ring bottom and placed into about 2 cm of field ground water within a 23 cm by 23 cm square aluminum pie pan that had been plastic

lined to prevent leaks. A small amount of water was added each day until the level in the pan was at the midpoint of the samples. The samples were presumed to be saturated by capillary rise of water. When the permeameter was ready, samples were carefully emplaced and re-wet up for 16 hours (overnight) before flow measurements were taken.

Figure 22 shows values of hydraulic conductivity with time for the twelve samples. On samples 197.5 cm, 112.5 cm. 121.0 cm, and 129.5 cm, the falling head method of measuring Ks was employed, inasmuch as these samples had the lowest conductivities. In the falling head method, the flow rate is determined by measuring changes in head with time in a reservoir above the sample having a known cross-sectional area.

The remaining 8 samples were measured with a constant head difference across the sample on the order of 2 centimeters.

The twelve samples measured showed saturated hydraulic conductivity values ranging over six orders of magnitude. All values plotted are corrected to 20 degrees Celcius.

The trends of the Ks with time curves in figure 22 appear to be related to the relative magnitude of the samples hydraulic conductivity. The three samples with the highest Ks values, approximately 2×10^{-2} cm/sec, showed similar trends of decreasing Ks for approximately 113 hours, and then, an increase in Ks that becomes steady after about 245 hours. The near steady value after 245 hours is equal to or greater

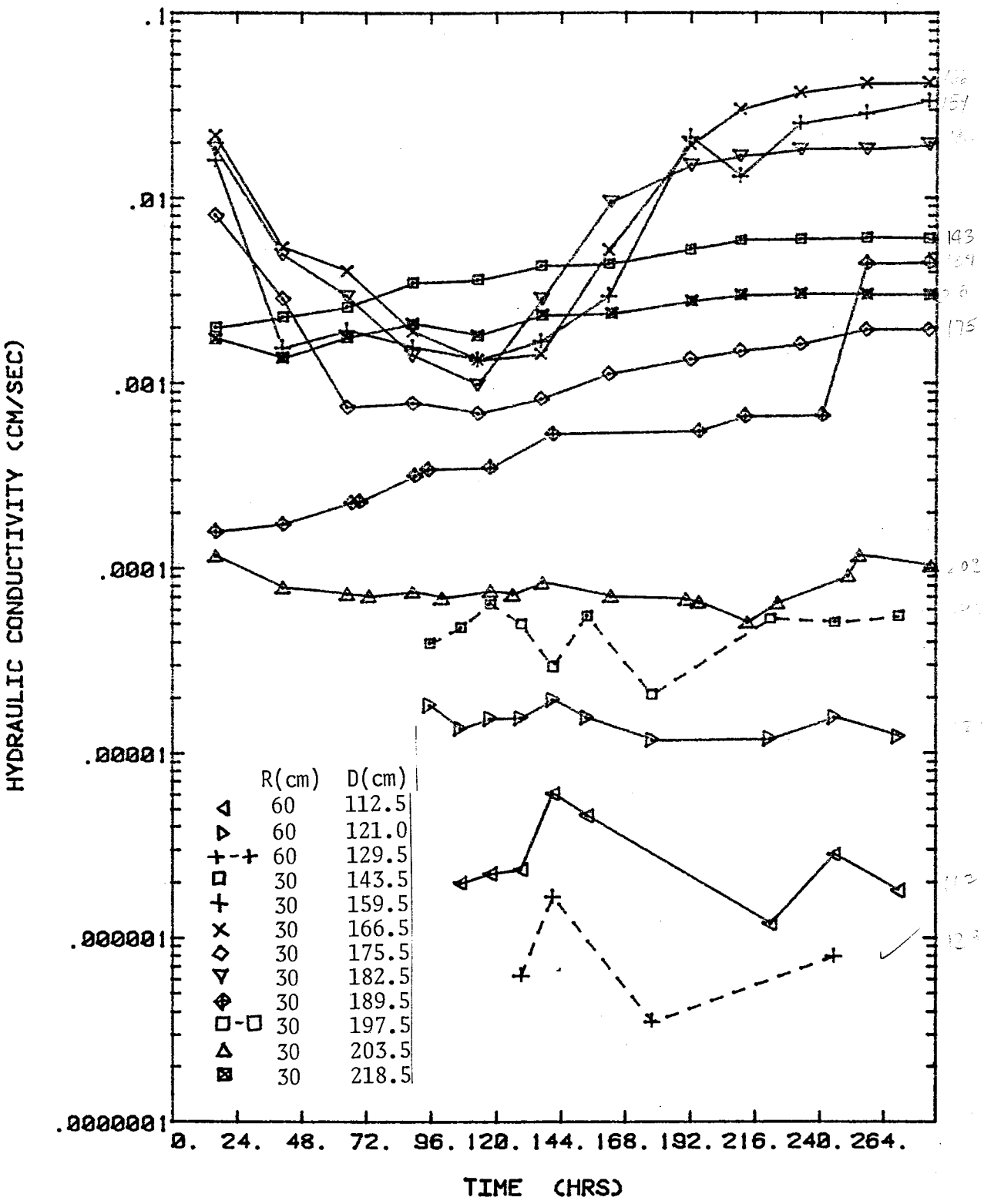

Figure 22. Saturated Hydraulic Conductivities from Pf Ring Samples

than that which was first measured (after about 12 hours). Decreases in hydraulic conductivity with time have in the past been attributed to bacterial growth within the sample (Gupta and Swartzendruber, 1962; Andrews, 1982; Watson, 1983), whereas increases in Ks at early time have in the past been attributed to the decreases in the amount of entrapped air in the pore space (Andrews, 1982; Watson, 1983).

It is believed that microorganisms, rather than the purging of entrapped air, play a significant part in the observed trends for Ks to decrease and then increase with time. During the measurement period with the PF ring permeameter, a change in the water chemistry of the recirculating water system was observed. During the first 96 hours, the water system appeared clear and clean. After 96 hours of water circulation through the permeameter, an opaque scale floated to the water surface; a few drops of hydrochloric acid added to the precipitate indicated a calcium carbonate composition. A possible explanation for the decrease and then an increase in the largest Ks values, in figure 22, is as follows: those samples with the highest initial Ks values might have contained a form of microorganism. The growth of the bacteria may have continued for about 96 hours; during this time, the pores plugged and Ks decreased. If the recirculating water system were then depleted of oxygen, the dead organisms could have been removed from the pores through flushing; hence, Ks would increase.

The sample from 175.5 cm depth shows an initial decrease

in Ks similar to the three higher conductivity samples but apparently Ks becomes steady before the sample returns to its initial value.

Figure 22 also indicates that the two samples from 143.5 cm depth and 218.5 cm depth start at about 2×10^{-3} cm/sec and show nearly identical (parallel) increasing trends of Ks with time, from times 12 hours to 210 hours, after which time a steady state is reached. If this increase is due to the gradual removal of entrapped air, then the long term capillary wet-up was not completely effective at saturating the samples. The fine textured sample, in figure 22, from the 189.5 cm depth also increases in Ks with time, presumably owing to the removal of entrapped air. The last two data points of this sample which reflect a sharp increase in Ks may reflect changes in pore structure associated with a chemical process such as ion exchange.

The fine textured sample from the 203.5 cm depth in figure 22 indicates a relatively constant Ks with time. This sample may have been saturated at the time of field acquisition and remained so until put in the permeameter; therefore entrapped air was not a factor.

The three samples with the lowest Ks values do not appear to have increasing or decreasing trends with time but appear to fluctuate around a fairly constant mean. This measurement variability of as much as 66% might be reduced with higher heads or use of a pressurized consolidometer/permeameter unit.

Table 6 lists saturated hydraulic conductivity values

TABLE 6
SATURATED VALUES OF HYDRAULIC CONDUCTIVITY MEASURED IN THE PF RING PERMEAMETER

Radius (cm)	Depth (cm)	Ks (PF Ring) (cm/sec)
60	112.5	2.86 E-6
60	121.0	1.49 E-5
60	129.5	8.56 E-7
30	143.5	6.00 E-3
30	159.5	3.35 E-2
30	166.5	4.15 E-2
30	175.5	8.00 E-3
30	182.5	1.90 E-2
30	189.5	6.60 E-4
30	197.5	5.50 E-5
30	203.5	1.15 E-4
30	218.5	3.00 E-3

with respect to distance from the borehole and land surface. The 30 cm radius values are steady state values from figure 22, with the exception of the sample from 175.5 cm depth which is a maximum recorded value. Steady state values for the 60 cm radius samples were determined from the arithmetic means of the measured points (figure 22) due to the measurement variability.

Values of saturated hydraulic conductivity from both the shelby tube profiles and the PF ring samples are compared for depths of 140 cm to 218 cm . Ks values in the clay zone were not obtained from the shelby tube permeameter, because a very high pressure head was required to promote flow through the system. This high head coupled with the long equilibration time for the manometers (greater than 5 days) was not compatible with the testing conditions used for the other shelby tube samples. For the purpose of this study, the extended research of the clay zone with the shelby tube permeameter was not pursued.

Table 7 shows average shelby tube sample Ks values calculated from the arithmetic average of shelby tube measured values at depths equal to the PF ring sample depths. This type of average gives more weight to the larger values, and it may produce a result which exceeds the true mean of the population, especially if Ks is log-normally distributed. In spite of this fact, Ks from the PF rings exceeds that from the Shelby tube permeameter in 6 of 9 samples by about 2.5 times (Table 7). Summary data in Table 7 suggest that PF ring

TABLE 7
COMPARISON OF Ks VALUES BETWEEN SHELBY TUBE SAMPLES AND PF RING SAMPLES

Sample Depth (cm)	Ks (Shelby) (cm/sec) N	W	S	Ks (Shelby) (cm/sec)	Ks (PF Ring) (cm/sec)	Ks PF>She
143.5	1.9E-2	2.7E-2	na	2.3E-2	6.0E-3	
159.5	1.1E-2	2.3E-2	na	1.7E-2	3.4E-2	X
166.5	1.1E-2	1.8E-2	1.1E-3	1.0E-2	4.2E-2	X
175.5	8.1E-4	4.8E-3	2.9E-3	2.8E-3	8.0E-3	X
182.5	2.9E-4	5.3E-3	3.2E-2	1.3E-2	1.9E-2	X
189.5	2.9E-4	na	na	2.9E-4	6.6E-4	X
197.5	4.2E-4	na	na	4.2E-4	5.5E-5	
203.5	na	5.1E-3	na	5.1E-3	1.2E-4	
218.5	4.2E-3	1.5E-4	2.9E-3	2.4E-3	3.0E-3	X

na: not available

samples have given higher saturated conductivity values than a comparative method when the ratio of ring-wall-circumference to sample area is reduced.

FIELD PROCEDURES

A long duration borehole infiltration test of a shallow water table condition was conducted at a new field site (figures 4, 5). This test shall be designated S8T1 as the first test conducted at field site number 8. The objectives of the test were to study the effects of a changing water table level on the calculated value of Ks using equation 2. Also the effects of a changing infiltrating water chemistry were addressed.

Procedures of this borehole test follow the USBR (1974) well-permeameter method with exception of the increase in soil instrumentation to better research the flow processes; also, a new constant head device is introduced.

Figure 23 is a map view of the instrumentation of S8T1.

Borehole Construction

A well screen was constructed using a 201 cm length of 3.81 cm radius PVC plastic. Outside diameter of the casing measured 8.9 cm. The PVC was slotted, using a band saw, with 1 mm wide cuts over a length of 38.1 cm. The density of the slots provided an open area of approximately 4.7 cm^2 / cm length of casing. This open area is equivalent to about a 30 slot commercial well screen. The borehole was first dug using a 10.2 cm diameter hand auger to a depth of 170 cm. The slotted casing was set into position so that the slotted interval ranged in depth from 132 cm to 170 cm below land surface. The minimal amount of open annulus around the

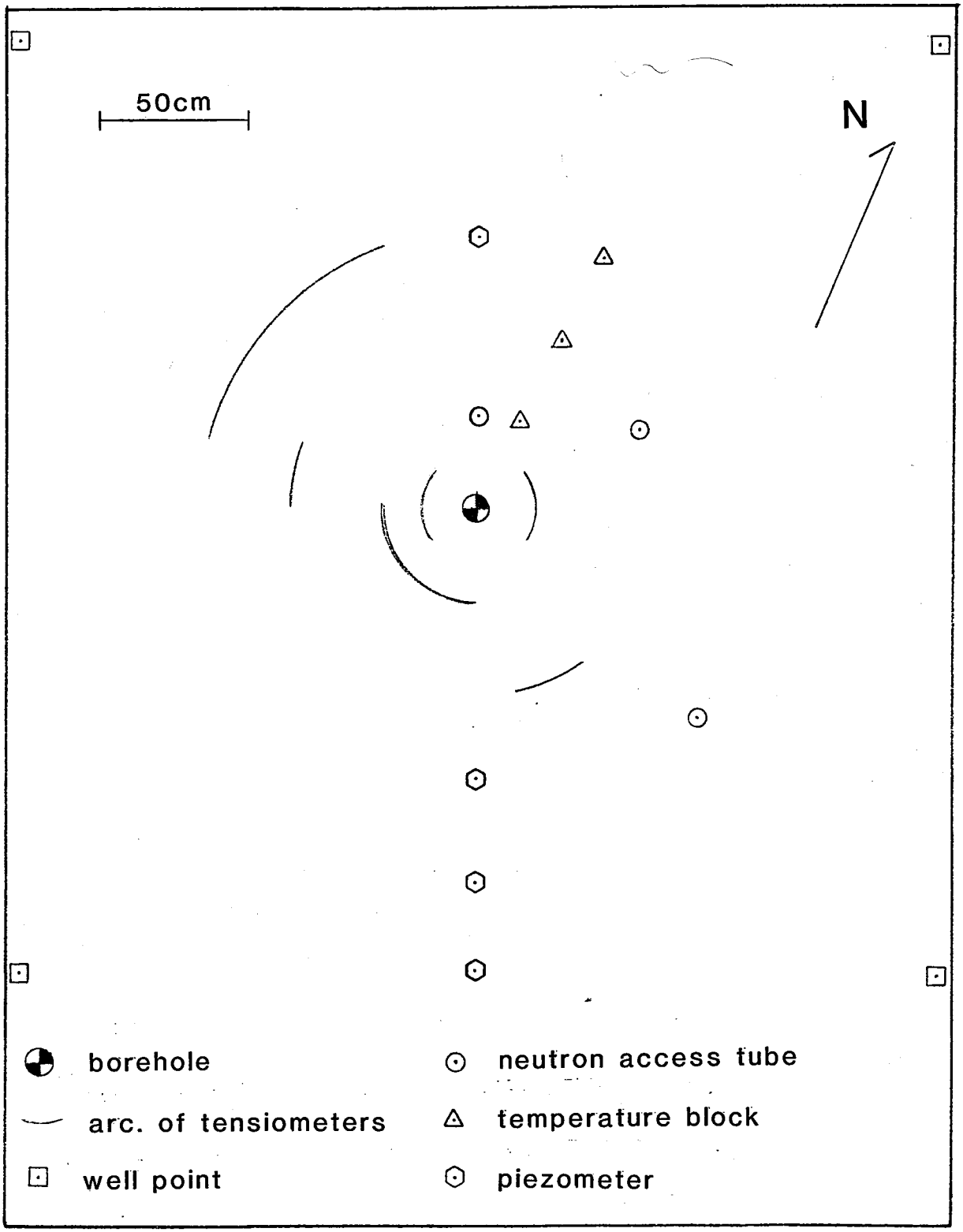

Figure 23. Instrumentation at S8T1

borehole was backfilled with clean dry medium-fine sand from above the clay layer that was vibrated down alongside the casing. The overall length of casing allowed 30.5 cm of stick-up above the established land surface datum. This borehole casing was then used as the benchmark to which all other instrumentation was leveled. The bottom of the borehole was fitted with a fine mesh brass screen.

Carbon Dioxide

The equipment used to inject CO_2 into the borehole and the screened formation consisted of a commercial CO_2 tank, a Victor number VTS400D pressure regulator fitted with a Victor 4000 psi inflow gauge and a Marsh Safecase discharge gauge of 0-15 psi range calibrated in 0.1 psi increments. This pressure tank regulator was coupled via tygon tubing to a Sho-Rate Flometer (Model 1355, Brooks Instrument Division, Emerson Electric Company, Hatfield, PA). Gas flow rate is determined from the rise of a steel ball in a graduated glass cylinder of the flowmeter using the calibration equation 6.

$$Q(LPM) = (GAUGE - 0.04) / 0.51 \qquad (6)$$

Elapsed time and flow rate is used to compute volumes of injected CO_2. A discharge hose from the gas flowmeter is coupled to the borehole casing using a circular rubber gasket through which the injection hose extends. This rubber gasket is affixed to the borehole casing using duct tape. Sealing of

the injection line in the borehole allows the borehole casing to be pressurized and the formation to be flooded with CO_2.

A noteworthy characteristic of the CO_2 injection system was discovered in that the maximum rate of flow through the pressure regulator was 3.84 lpm, corresponding to a gas flow meter gauge reading of 2. Any discharge greater than this produced rapid freezing and malfunctioning of the pressure regulator.

Water Supply

Two sources of water were utilized for S8T1. The chemistries of the water, designated field groundwater and field tap water, are given in Table 5. Field groundwater was obtained from an 11 meter deep sandpoint well located approximately 15 meters southwest of the borehole site. Water was pumped from the well with an electric shallow well suction pump and to the site via a 2 cm garden hose. Field tap water was provided by the property owner at a distance from the borehole site of about 25 meters, and again, garden hose was used to convey water to the borehole site.

Water storage was provided by a newly constructed, 400 liter capacity, 2 barrel holding system. The barrels were acquired new and, after a thorough cleaning to remove trace chemicals, they were internally coated with a waterproof coating to inhibit rust and corrosion. Both barrels were fitted with new manometers. The discharge outlet was positioned 15 cm above barrel bottom to provide a sediment

trap in the barrel bottom. The manifold used to provide water from the drums to the borehole was built around a 3.2 cm cross-coupling (4 female ports). To this cross-coupling were connected 2 brass gate valves (1 per reservoir barrel), one discharge spigot (for additional reservoir water use) and a 2 m length of galvanized pipe to position water at the borehole. The valving system was such that either a 1 or a 2 barrel reservoir system could be used. Flow from a single barrel system was measured using the following relationship:

$$\text{Vol.} = 2.55 \text{ liters } H_2O \text{ / cm barrel manometer} \qquad (7)$$

which says that 2.55 liters of water have been released from the barrel when a 1 cm decline of water is measured in the barrel manometer. When both barrels are discharging simultaneously, the calibration is doubled. The nice quality of this manifold was that through the use of a universal coupling at each barrel, at any time during flow, one barrel could be removed from the system for cleaning, for example, before enacting a water chemistry change, without disrupting the flow system.

The constant head of water necessary for the borehole test was achieved using 2 different types of float valves. Figure 24 illustrates a 1.9 cm diameter stock tank valve with a float arm connected to a counter weighted lever. This unit follows USBR design (USBR, 1974). The stock tank valve assembly was used during early time when flow rates would be

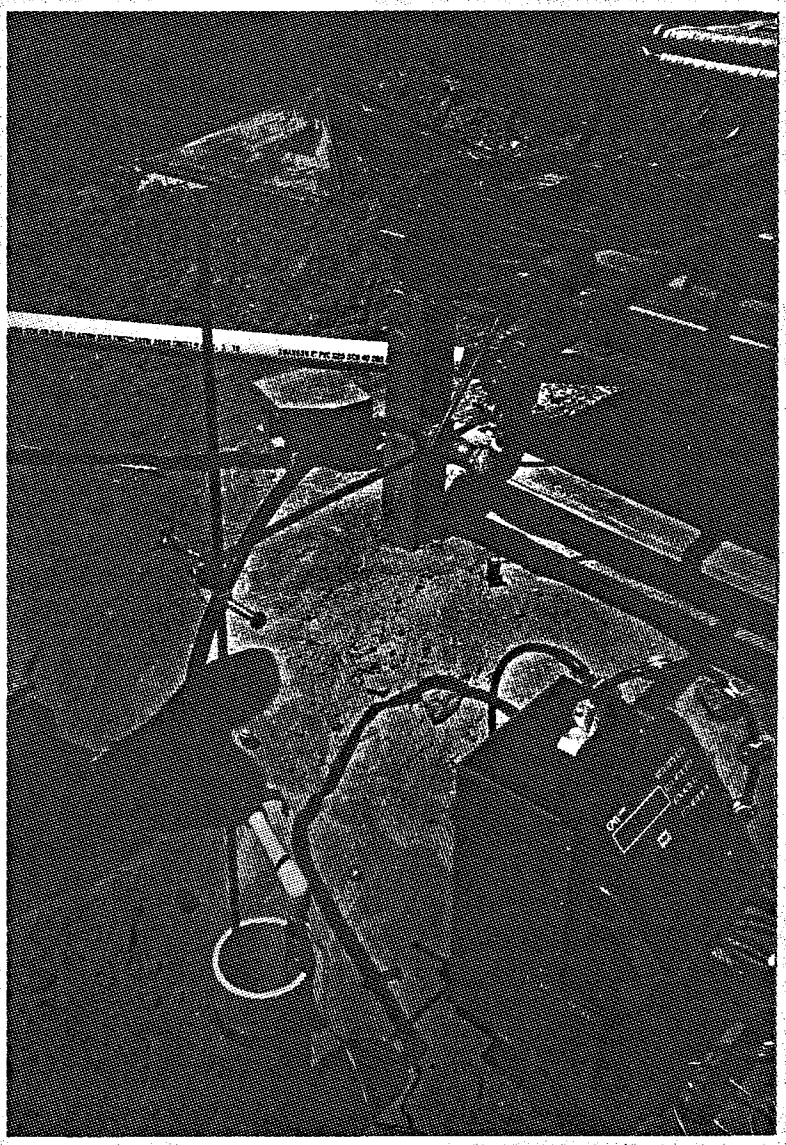

Figure 24. Stock Tank Valve Constant Head Device

greatest. But when flow rates dropped below 1 lpm, this valve assembly was not sensitive enough to maintain a constant head in the borehole without operator intervention.

Figure 25 shows a newly constructed carburetor float valve specifically designed to provide a constant head under low flow conditions. The carburetor float valve (herein termed CFV) is a simple unit without arms or counterweighted levers. A principal advantage of the CFV is that the actual flow valve is submerged below the water level in the borehole. When used in the hot sun, the internal seals in the stock tank valve assembly had a tendency to dry out and either stick in one position or leak water. The CFV unit was calibrated in the lab to determine valve position in the borehole for a desired head level as a function of water pressure to the valve. It was found that changes in water pressure to the valve, dictated by changing water levels in the reservoir barrels, changed water levels in the borehole by only 2 mm. Maximum flow from the CFV valve was 4 lpm when lab tested with an applied head of water to the valve of 2.8 meters which simulated full barrels in the field. Minimum flow for the valve was recorded in the field as low as 0.1 lpm but the valve has lower flow capabilities.

Due to the simplicity of design of the CFV, a larger unit could eaily be constructed which would pass sufficient quantities of water to eliminate need for the stock tank lever valve assembly. More information and CFV details are provided in Appendix B.

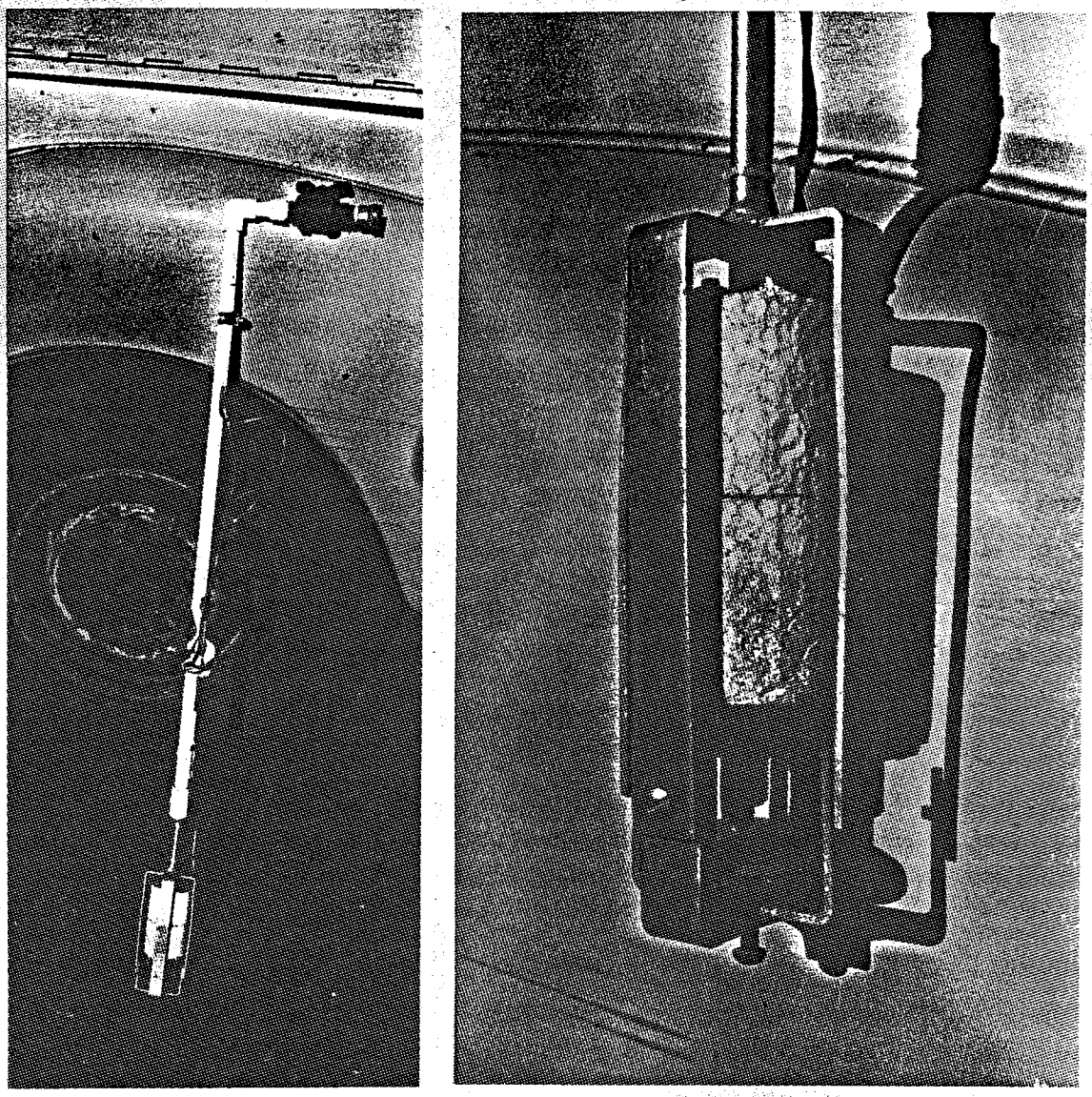

Figure 25. Carburetor Float Valve Constant Head Device

As shown in figure 24, water from the stock tank valve was passed through a garden hose and then through PVC pipe in the borehole. The latter was plugged at the lower end and perforated on the sides to disperse inflow water energy and minimize erosion of the formation during initial wet-up.

The CFV assembly, due to its geometry, projects inflowing water downward toward a deflecting plate thus dispersing energy.

Water levels in the borehole were measured with a steel tape.

Instrumentation

Total Head and Pressure Head

Total head and pressure head were measured in the flow field around the borehole with the use of 1.9 cm OD mercury manometer tensiometers (Soil Moisture Equipment Corporation, Santa Barbara, CA). Individual tensiometers were installed using an insertion tool available from the manufacturer. Locations of the tensiometers are depicted in figure 23 as arcs of tensiometers at radii from the borehole axis of 17.8 cm, 30.5 cm, 61 cm and 91.4 cm. Depths of the tensiometers ranged from 122 cm to 240 cm below land surface datum. Table 8 lists exact radius and depth for each unit.

The tensiometer manometer scales were positioned to read total hydraulic head in centimeters rise above a zero total head reference position mark on the manometer scale; the zero total head reference mark (cm) above land surface is

TABLE 8
LOCATION OF TENSIOMETER UNITS FOR S8T1

Radius (cm)	Depth (cm)
17.8	137.2
17.8	172.7
17.8	199.1
30.5	122.0
30.5	134.6
30.5	148.9
30.5	170.2
30.5	209.6
30.5	240.0
61.0	122.0
61.0	134.6
61.0	170.2
61.0	209.6
61.0	240.0
91.0	122.0
91.0	134.6
91.0	170.2
91.0	177.0
91.0	209.5
91.0	238.8

calculated according to:

$$b = c * (\rho w) / (\rho Hg - \rho w) \qquad (8)$$

where "b" is the height (cm) above the mercury reservoir surface to the zero on the manometer scale and "c" is the elevation (cm) of the mercury reservoir surface above the landsurface datum. Values used for ρHg and ρw are 13.55 g/cc and 1.0 g/cc, respectively. Density variations with temperature were not considered in establishing the zero marks for the tensiometers. More will be said about temperature effects on tensiometers in the future research section.

Values of total head were calculated from the manometer scale readings using equation 9:

$$TH = a * (1- \rho Hg/\rho w) \qquad (9)$$

where TH is total head in cm of water, a is mercury rise (cm) above the zero mark. Pressure head was calculated from equation 10:

$$PH = TH - d \qquad (10)$$

where d is the distance (cm) from landsurface datum to the center of the tensiometer cup. The value of d is negative below landsurface.

Soil Moisture Contents

Volumetric moisture contents were measured as a function of depth around the borehole using a neutron moisture meter device. The neutron probe (Model 3222, Troxler Electronic Laboratories, Inc., Research Triangle Park, NC) was calibrated against gravimetric water contents. Previously, in similar studies at NM Tech, calibration against gravimetric techniques involved small (100 cc) samples taken alongside neutron access tubes and calibrated to the neutron probe readings; in these studies access tubes were installed in slightly oversized holes and the annulus was backfilled. Since it is known that the area around the neutron probe that is measured for moisture content may vary from a 10 to 25 cm sphere radius (Hillel, 1980), a better means to sample for gravimetric comparison was envisioned.

In the present study, gravimetric samples were collected by driving the neutron probe aluminum access tubes (5cm OD) into the soil, at desired radii from the borehole. The access tubes were withdrawn and the soil filled portions were hacksawed off, taped, and returned to the soils lab for gravimetric measurements. As the soils sampled appeared very wet, sample lengths cut were about 15 cm in length. The resultant holes using this technique provided a snug fit to install clean tubes for immediate background measurement with the neutron probe. This technique for gravimetric correlation to neutron probe readings proved quite efficient with

gravimetric samples being closer in size to that measured with the neutron probe. The resultant calibration equation for the Troxler unit agreed very well with the previous equations acquired in a homogeneous medium fine sand.

Unfortunately, after the installation and correlation of the three neutron access tubes located in figure 23, the Troxler neutron probe malfunctioned and was replaced with a different brand (CPN) which had a 50 millicurie instead of a 10 millicurie Amerecum-Beryllium source (Campbell Pacific Nuclear Corp. model 503, 130 South Buchanan Circle, Pachero, CA).

All data using this CPN unit was acquired using 16 second counts.

A correlation equation for the CPN unit was not developed at site 8 for this report but was determined with the CPN unit at the Sevilleta Wildlife Refuge. As past correlations of the Sevilleta sand with the site 8 soils provided very similar correlation equations for the Troxler unit, the correlation equation acquired for the CPN unit at the Sevilleta site was felt to be accurate for the site 8 soils.

Equation 10 was used to correct field acquired volumetric moisture contents (CPN READING) to actual volumetric moisture contents from gravimetric techniques:

$$\underset{\text{(decimal)}}{\text{Act. Vol. Water Content}} = .9069\ (\text{CPN Reading}) - \underset{\text{(decimal)}}{0.0352} \qquad (10)$$

This equation produced an R^2 value of 0.974.

Aluminum access tubes were inserted to depths of 191 cm with 19.5 cm of above landsurface stickup. This "standard" stickup allows the depth markers on the probe cable to be utilized at various research sites without being moved. The lower 5 cm of access tube was sealed with a rubber stopper and a cement slurry to prevent water intrusion into the access tube due to a rising water table. The cement slurry was emplaced using a small plastic bag to contain the cement as it dropped down the tube. Afterwards, a 0.5 cm diameter pointed steel rod was used to perforate the plastic bag and release the cement to plug the tube bottom.

Access tube radii from the borehole axis in figure 23 are 30, 60, and 100 cm.

Soil-Water Temperatures

Soil-water temperatures were measured using model MC-312 thermistors (Soiltest, Inc., Evanston, IL). Accuracy of these units is approximately $\pm 1^{\circ}$ C. Three units were emplaced in the borehole flow field at r = 30.5, d = 152.4, r = 61.0, d = 162.5, and at r = 91.4, d = 170.2 cm. An additional unit was placed in the borehole to measure infiltrating water temperature.

Dissolved Oxygen

D. O. was measured from the barrel reservoirs with a Bausch and Lomb dissolved Oxygen Spectrokit (Bausch and Lomb,

Analytical Systems Division, Rochester, NY).

Well Point Field

Four well points were constructed at the corners of a 3.05 m square, centered on the well bore axis. The radial distance from the well bore axis to any one of the 4 wells was 2.15 m. Three of the well screens used were newly purchased 3.18 cm diameter by 91.5 cm length, stainless wire-wrapped, 20 slot well points. The fourth screen used was a 5.08 cm diameter by 152.4 cm length galvanized wire-wrapped 20 slot screen. Galvanized pipe was used exclusively for well casings to 30 cm above land surface. The top of each well screen was positioned 2.13 meters below the water table surface to provide this much maximum draw down at any well-point.

The well points were manifolded together using 5.08 cm diameter PVC plastic. A gas driven, 7.62 cm, suction pump, borrowed from the Socorro Fire Department, was connected to the manifold to control pumping rate, and hence control the water table level beneath the borehole.

Four 1.3 cm diameter PVC piezometers were installed at locations shown in figure 23. These piezometers were perforated, using a hand drill, over an approximate 76 cm interval. Depths of the perforated regions are listed in table 9, with piezometer number 1 being the north unit (figure 23) and increasing numbers toward the south.

Two preliminary tests were conducted to determine the well field's capability to lower the water table. The first

TABLE 9
PERFORATED PIEZOMETER INTERVALS

Piezometer	Perforated Interval Below Land Surface
1	2.46 - 3.21 m
2	2.44 - 3.21 m
3	2.59 - 3.35 m
4	2.70 - 3.45 m

pump test utilized a 2 H.P. gas-driven suction pump which delivered 85 lpm from the well field. Drawdown beneath the well bore in the center of the well field was calculated to be only 15 cm below the static water level of -223 cm.

A larger 5 H.P. pump (Socorro Fire Department) was used in a second pump test. A discharge of 104 lpm provided 30 cm of drawdown that was desired for the borehole test. Static water level before the second pump test was 217 cm below land surface.

FIELD RESULTS OF S8T1

A time log of S8T1 is first described as a test procedure overview, after which the field data is presented.

CO_2 injection commenced at 06:44 on 5/5/84. Injection at a rate of 3.84 lpm proceeded for 66 minutes for a total injection volume of 253 liters of CO_2. It is inferred from Bouwer and Jackson (1974) that the volume of the soil tested using the borehole method is 0.4 H^3, where H is 38.1 cm. Thus one pore volume would be the volume of soil tested multiplied by the porosity. The porosity n is conservatively estimated at 0.40. Therefore, one pore volume is 8.85 liters. The volume of the borehole casing is 7.8 l. According to Stephens (1984, personal communication), on the basis of previous borehole tests in fine sand, a minimum of 20 soil porevolumes CO_2 is desired to maximize effectiveness. Therefore, if 245 liters flowed into the soil, then 27.7 pore volumes were passed.

After CO_2 flooding, a background Tu value of 61.7 cm was calculated from the 210 cm and 240 cm depth tensiometers located below the water table. Infiltration into the borehole started at 8:05 Saturday morning, 5/5/84. The borehole filled to a depth of 38.1 cm in approximately 10 seconds. All measurement instrumentation functioned well. At a test time of 713 minutes, the stock tank valve assembly was by-passed in favor of the carburetor float valve. This switch took about 2 minutes. The CFV unit functioned well, except for one instance where it needed to be set about 1 cm deeper into the borehole. It is believed that mineral encrustation of the valve made this adjustment necessary. At about 3000 test minutes (Monday morning), it was observed that the field groundwater stored in the barrels since the test began, had accumulated an orange precipitation; it was feared this sediment would clog the formation and affect the test results. Therefore, at 11:10 on Monday (3065 test minutes) a switch in water chemistry was made from field groundwater to field tap water (Table 5, Chemistries). Because the tap water is much less mineralized, problems of precipitation were expected to be minimal. Because of the change in operational procedure, a stage concept is introduced. Stage 1 will refer to test times from 0 to 3500 minutes.

On Wednesday, 5/9/84, at 12:00, 6000 minutes into the test, a steady rate of infiltration had been verified, and the well field was put into service by starting the suction pump. Stage 2 will be refered to when discussing events of 3500 to

6000 test minutes. Instrumentation measurements and pumping were continued until Saturday, 5/12/84, at 09:41 (10,176 test minutes) when infiltration stabilized at a different rate. Stage 3 will refer to 6000 to 10,300 test minutes. Subsequently, the water supply was changed back to field groundwater. Measurements and pumping continued until Sunday, 5/13/84, at 14:40 (11,915 minutes), when a crack in the well field collector manifold caused a decrease in discharge and termination of the test. Stage 4 will be referred to when discussing events from 10,300 minutes to test end.

The field operational procedures of S8T1 are summarized in Table 10.

Figure 26 illustrates the height of water in the borehole. This height of water was controlled by the stock tank valve assembly from time 0 to 713 minutes. From 713 minutes until test end, water depth in the borehole was controlled by the new carburetor float valve assembly.

Figure 27 presents infiltration rate from the borehole versus time in minutes. Infiltration values have been corrected to 20^{o} C to account for the dependence of flow rate on temperature induced viscosity fluctuations.

Figure 28 illustrates cumulative infiltration out of the borehole with time. According to the USBR (1974), "the (well-permeameter) test should be run long enough to develop a saturated envelope in the soil but not long enough to build up the water table or produce an excessively large saturated envelope which will cause erroneous results". The concepts of

TABLE 10
SUMMARY OF FIELD OPERATIONAL PROCEDURES: S8T1

H (cm)	38.10
A (cm)	38.10
R (cm)	3.81
H/R	10.00
Duration (min)	11,915.

Const. Head Device:	Stock Tank Valve	Carb. Float Valve
Time (min)	0-713	713-test end

	Stage 1	Stage 2	Stage 3	Stage 4
Time (min)	0-3500	3500-6000	6000-10,300	10,300-end
Well Field	Off	Off	On	On
Water Source	Gw	Tap	Tap	Gw

Gw: groundwater

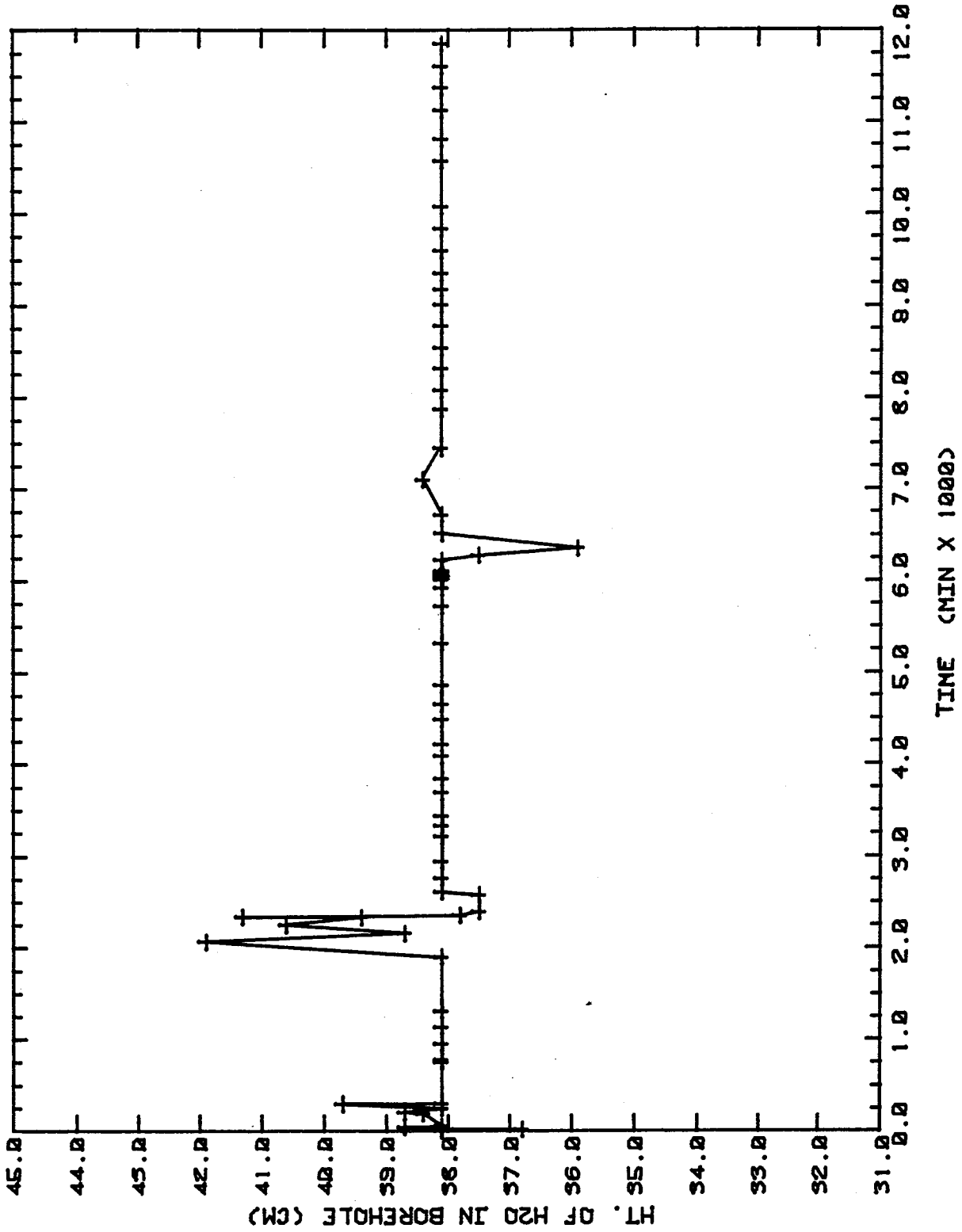

Figure 26. Height of Water in the Borehole for S8T1

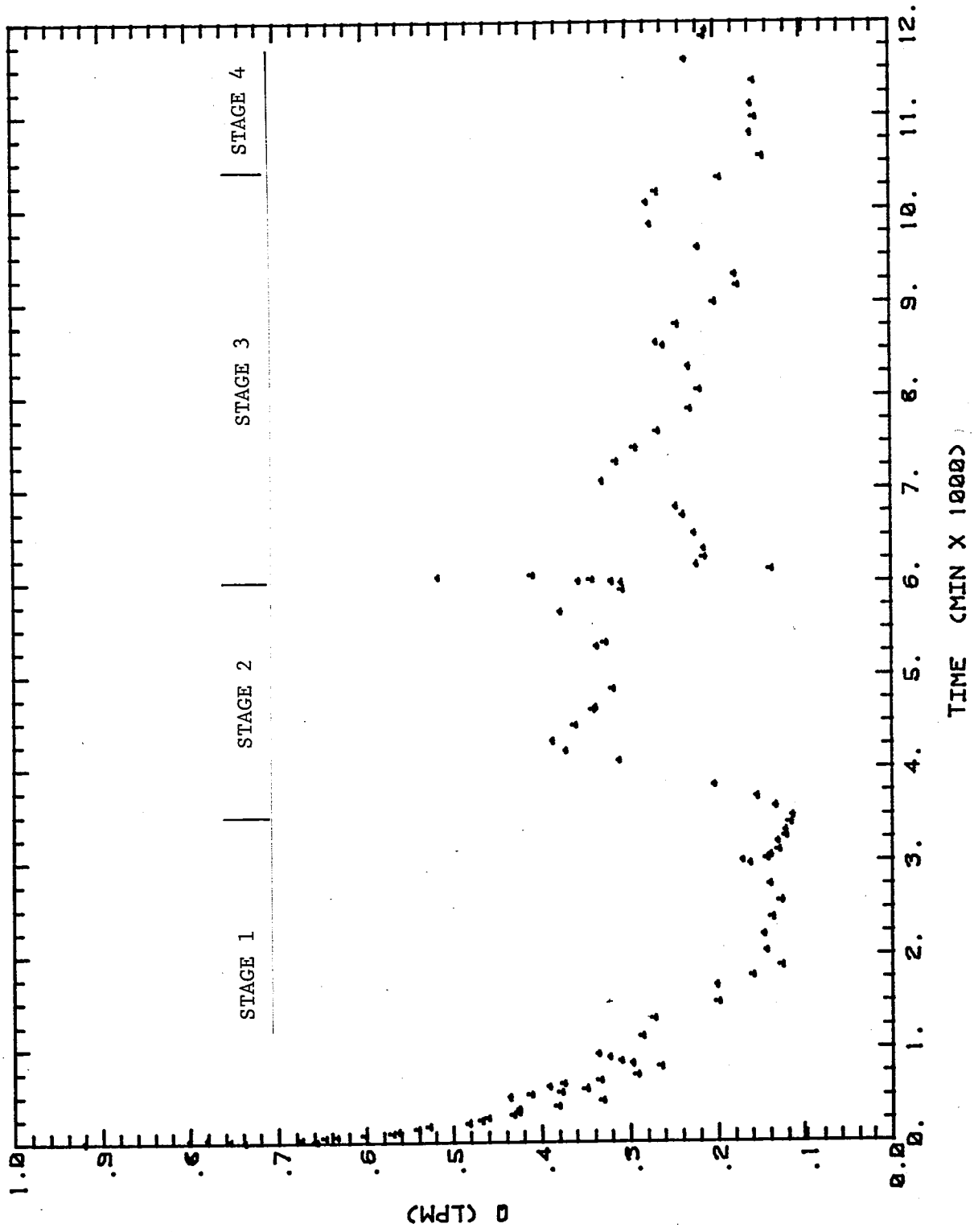

Figure 27. Infiltration Rate for S8T1

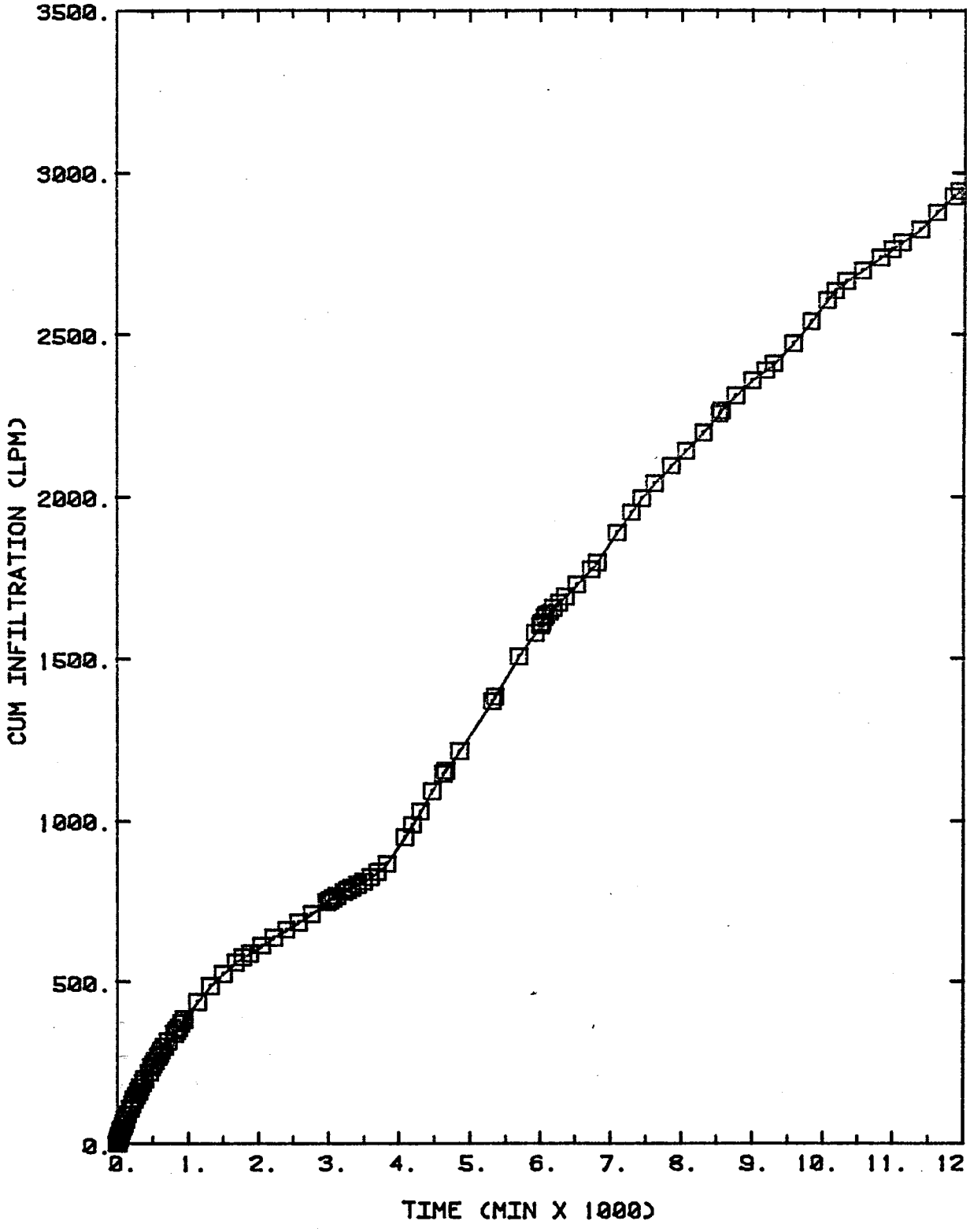

Figure 28. Cumulative Infiltration for S8T1

"minimum test duration time" are described by the USBR (1974) as the times at which specific volumes of water have infiltrated into the soil under deep water table conditions. The minimum volume of test water, V_{min}, is calculated as follows:

$$V_{min} = 2.09\ Ys \left[H \sqrt{\frac{2}{\sinh^{-1}\left(\frac{H}{r}\right) - 1}} \right]^3 \qquad (11)$$

where Ys is the specific yield of the soil tested, H is the depth of water in the borehole (L), and r is the radius of the borehole (L).

The value of Ys can be calculated as the soil porosity or saturated water content, θs, minus the specific retention at 15 bars. Using table 3 for an average θs value of 0.37 between 132 cm and 170 cm depth and figure 7 for an average specific retention of 0.12 over these depths, a value of 0.25 is used for the specific yield.

Using values of 38.1 cm for H and 3.81 cm for R, a minimum volume is determined to be 28.9 liters. This volume of water is reached at 37 minutes into the test.

According to USBR 1974, the maximum water volume infiltrated should not exceed 2.05 V_{min} or 59.3 liters in this test; this volume is reached after 84 minutes.

According to USBR (1974), "...to avoid discontinuing a test prematurely, it shall be continued for at least 6 hours .. " then the first appearance of steady infiltration "... after a period of 2 to 3 hours should be utilized".

It can be seen in figure 28 that the first steady state portion of the cumulative infiltration curve occurs after about 2215 minutes; at this time 638 liters of water had infiltrated.

Figures 29 through 32 show the diurnal fluctuations in temperature in the borehole and in the surrounding soil within the flow field. Temperature in the borehole ranged from 11 C to 35 C whereas at R = 91.4 cm and D = 170.2 cm, temperature ranged from 14 to 18 C.

Figures 33 through 36 show values of pressure head (Ψ) in cm H_2O versus time at four increasing radii from the borehole axis.

Figures 37 through 39 show values of volumetric moisture content versus time at three increasing radii from the borehole axis.

ANALYSIS

Temperature

The effects of water temperature fluctuations on infiltration rate (Q), pressure head (Ψ), and volumetric moisture content (θ) are evident in figures 27, and 33-39, respectively.

Figure 40 shows infiltration rate and borehole water temperature plotted together. Steady state infiltration is inferred when Q, in figure 40, fluctuates in a sine wave pattern with a regular period about some average value. It

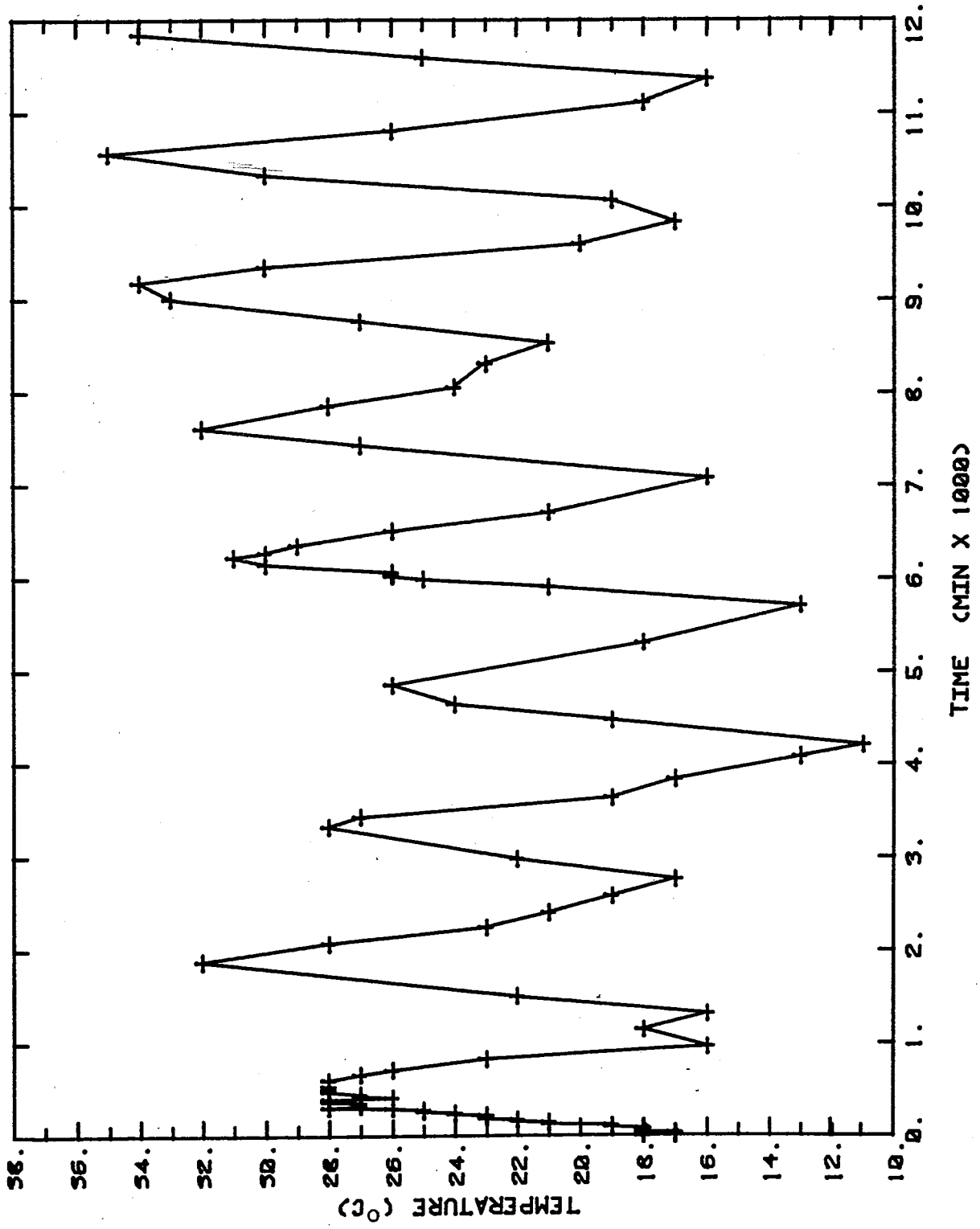

Figure 29. Borehole Water Temperature for S8T1

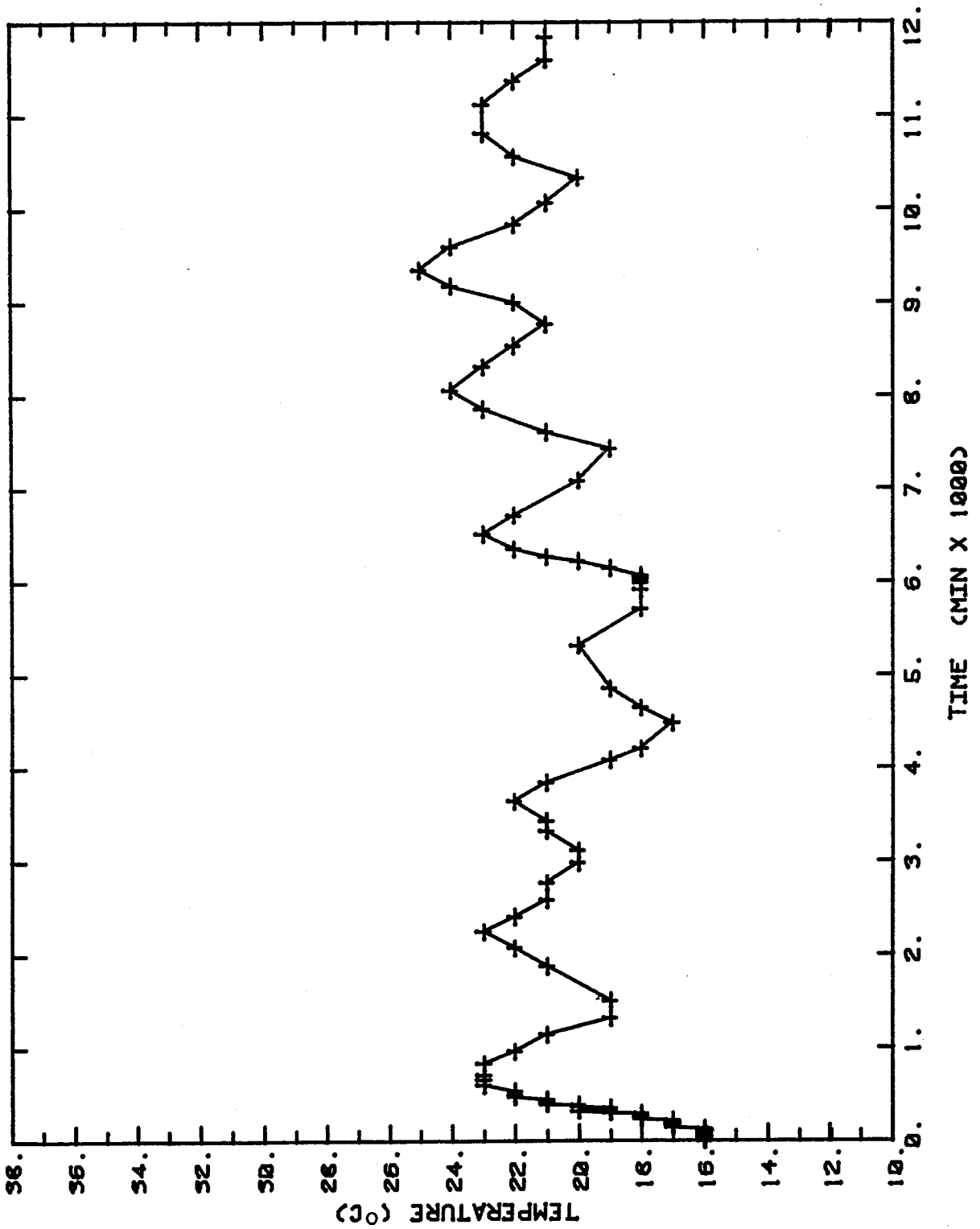

Figure 30. Change in Temperature with Time at R= 30.5 cm, D= 152.4 cm

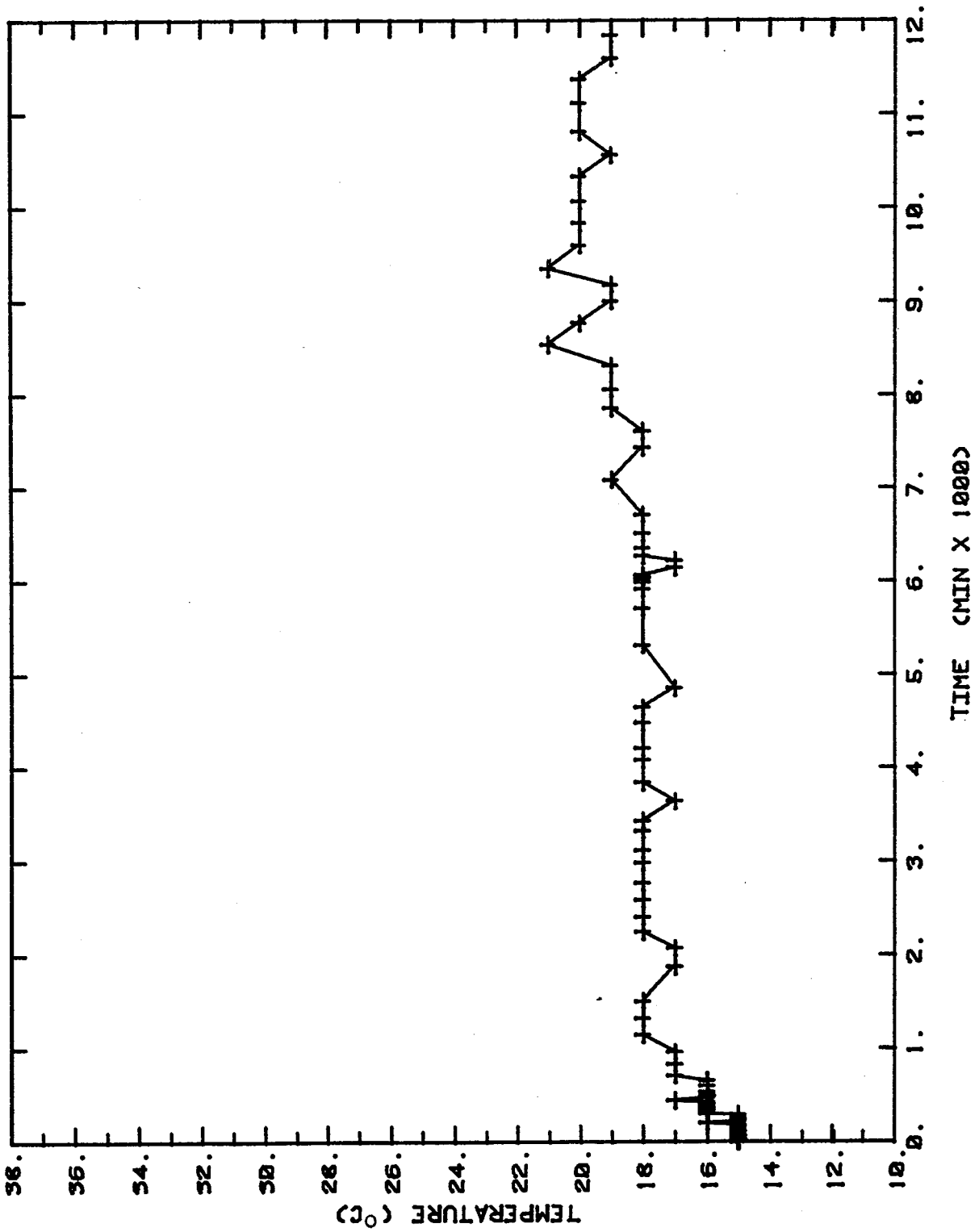

Figure 31. Change in Temperature with Time at R= 61. cm, D= 162.5 cm

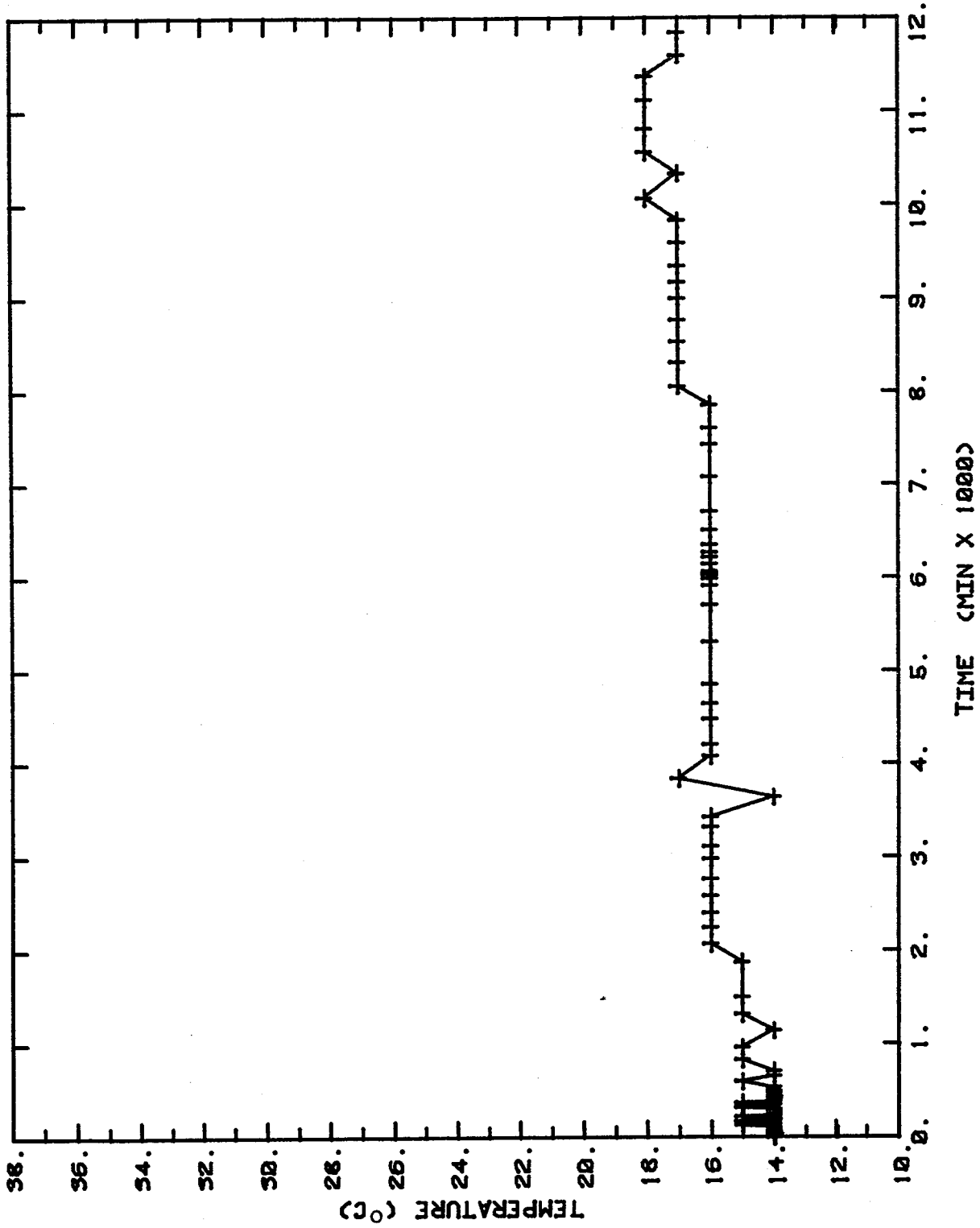

Figure 32. Change in Temperature with Time at R= 91.4 cm, D= 170.2 cm

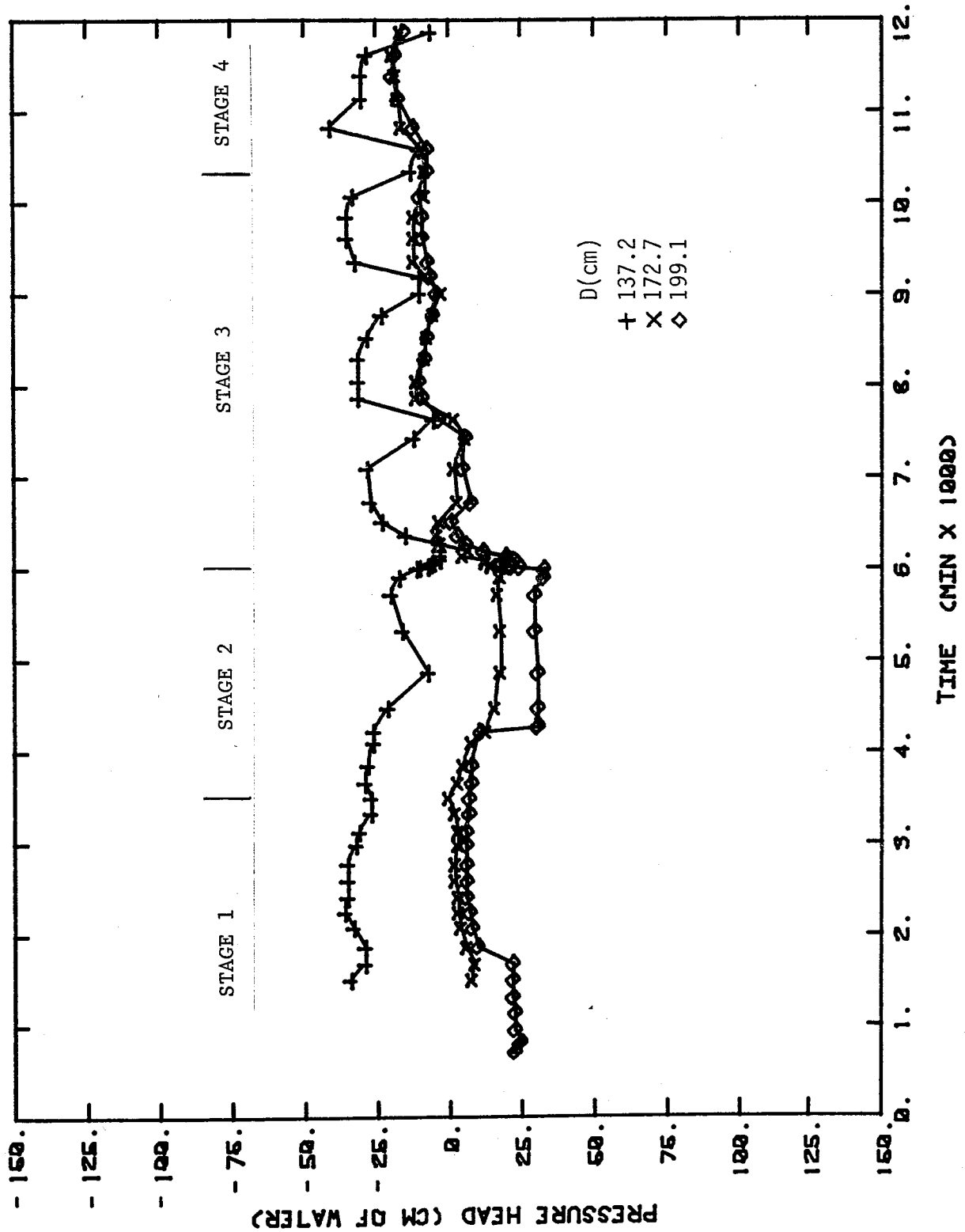

Figure 33. Change in Pressure Heads with Time at R= 17.8

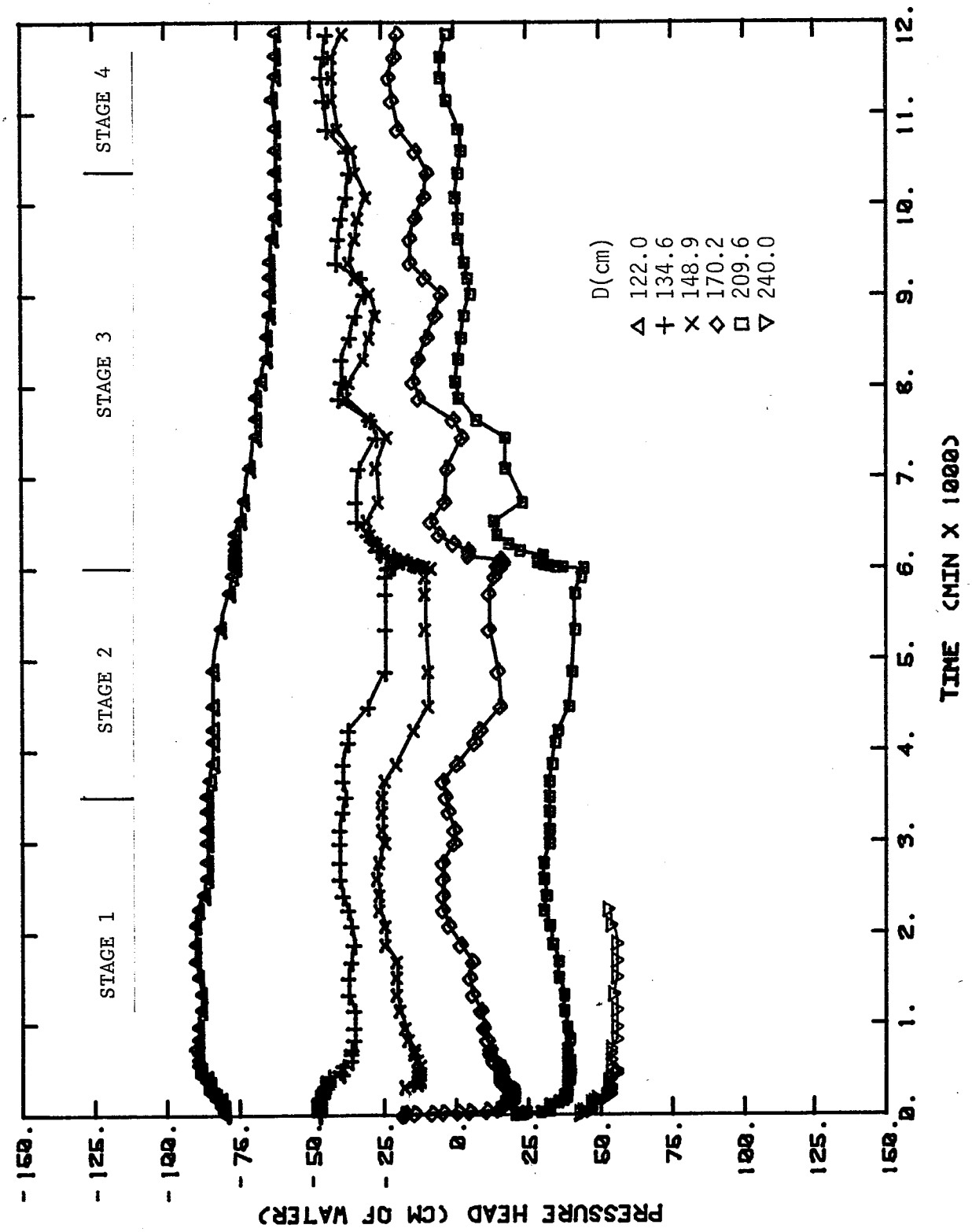

Figure 34. Change in Pressure Heads with Time at R= 30.5 cm

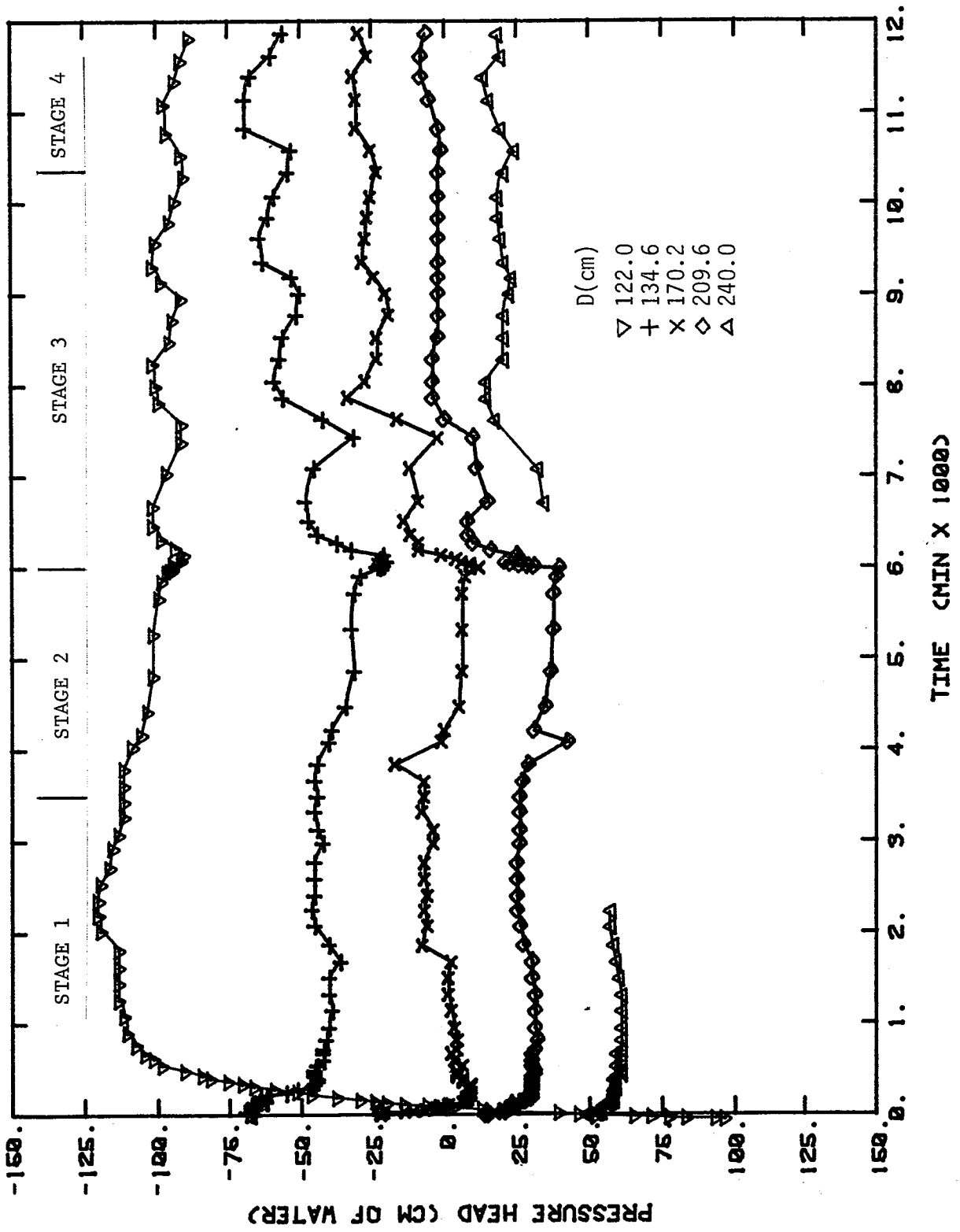

Figure 35. Change in Pressure Heads with Time at R= 61.0 cm

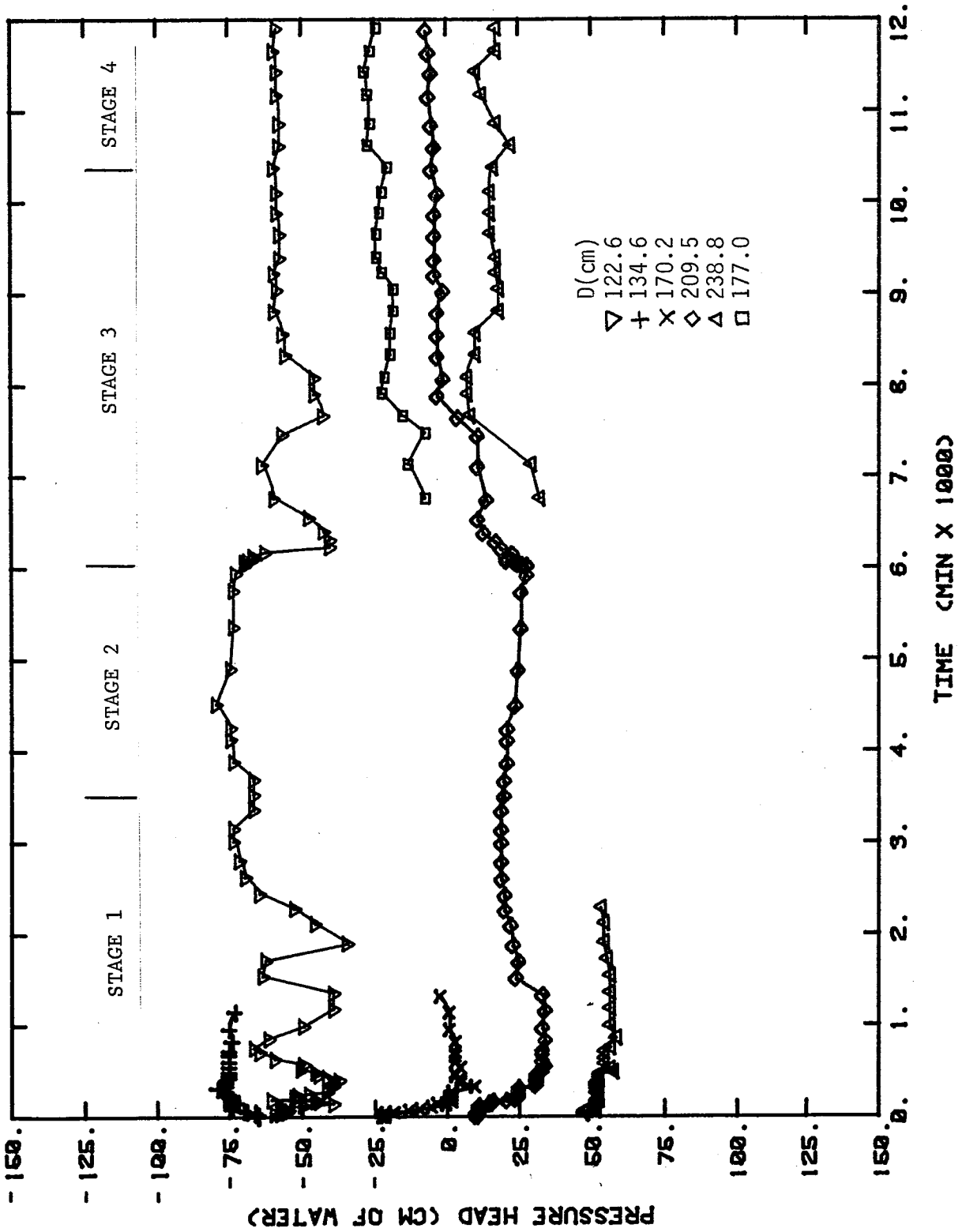

Figure 36. Change in Pressure Heads with Time at R= 91.0 cm

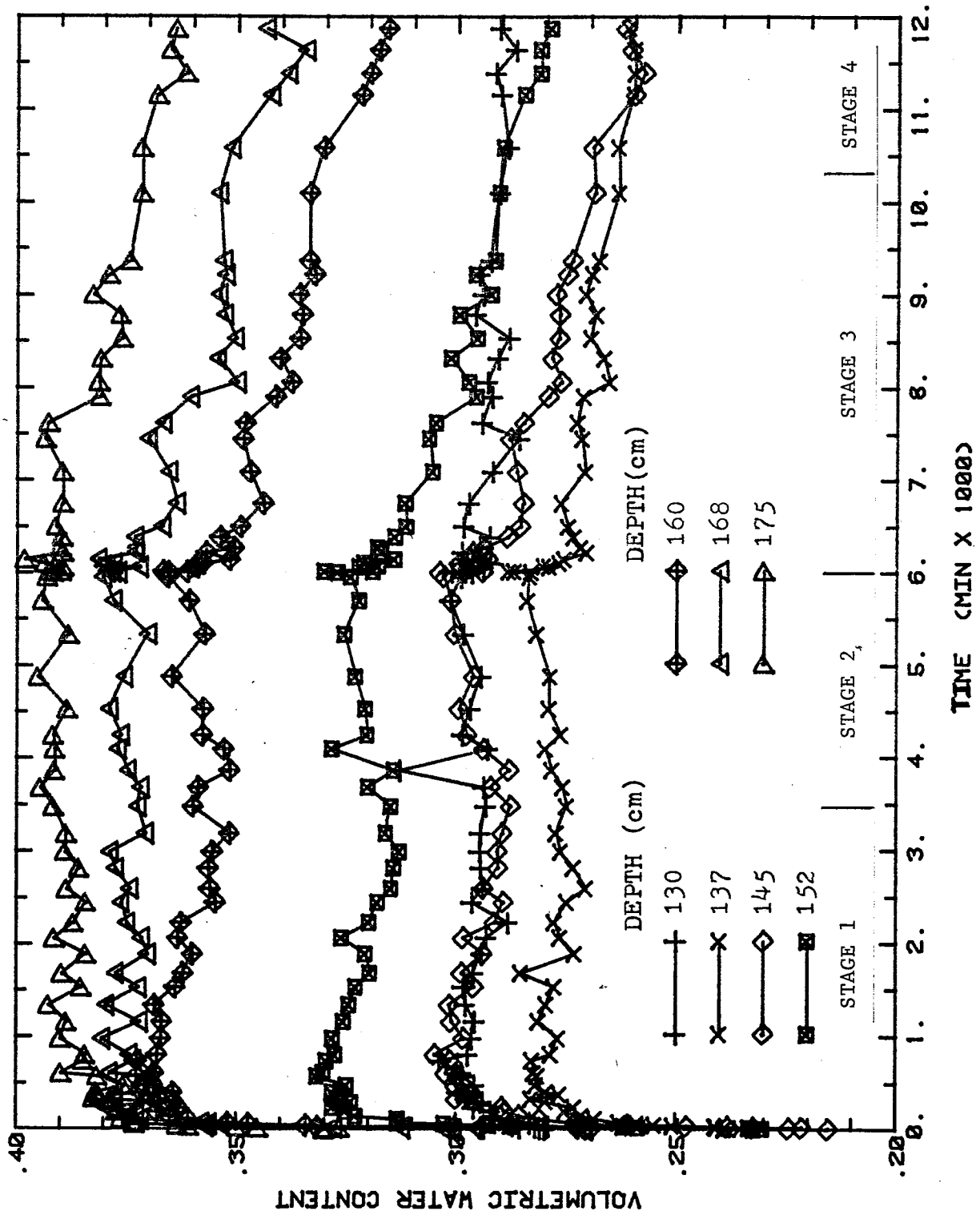

Figure 37. Change in Moisture Contents with Time at R= 30.0 cm

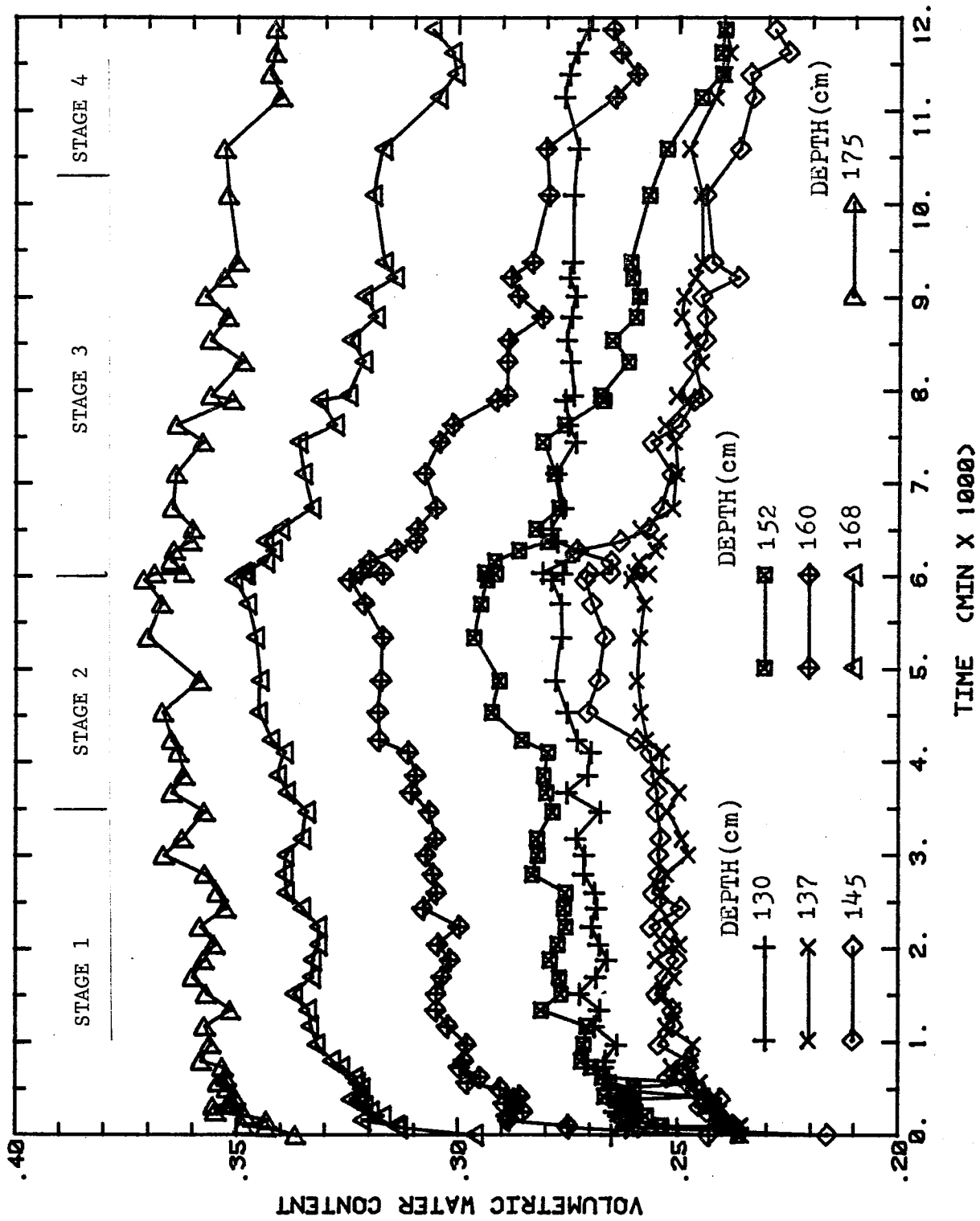

Figure 38. Change in Moisture Contents with Time at R= 60.0 cm

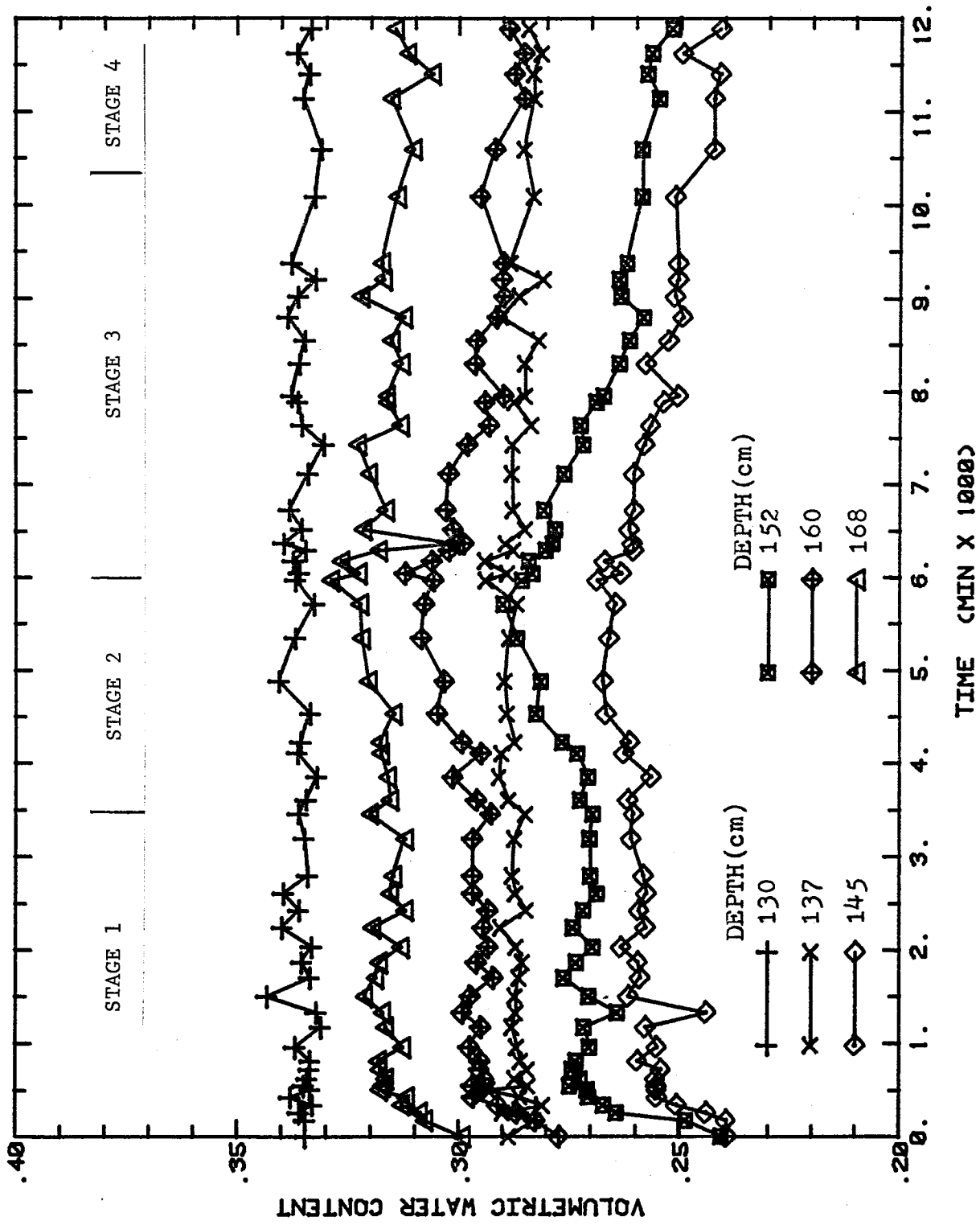

Figure 39. Change in Moisture Contents with Time at R=100.0 cm

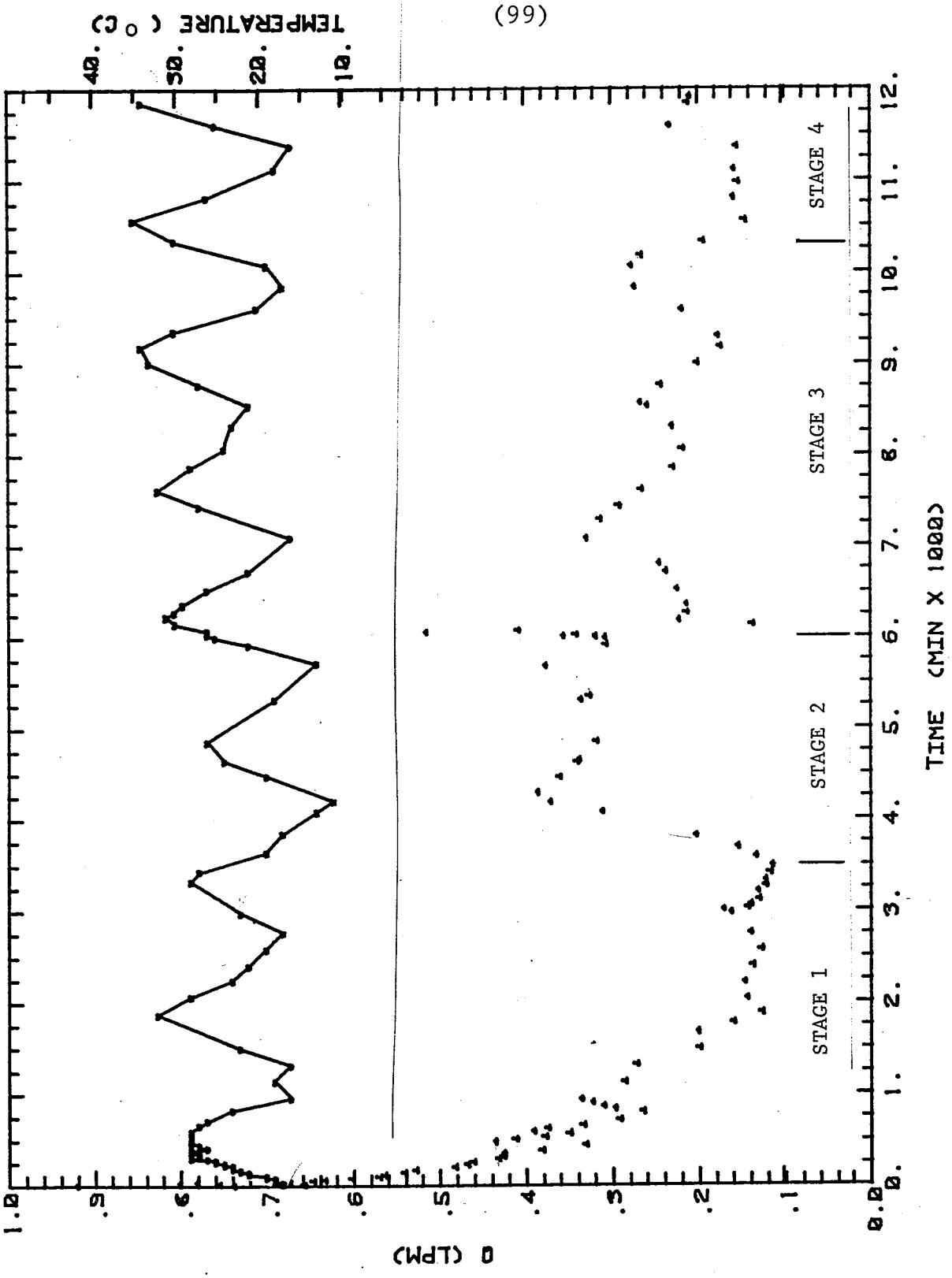

Figure 40. Infiltration Rate and Borehole Water Temperature for S8T1

appears clear that maximum temperatures occur simultaneously with minimums in flow rate. The correlation first becomes evident at about 2000 minutes where Q fluctuates by $\pm$0.01 lpm between 2000 and 3500 minutes. During stage 2, steady state Q varies by $\pm$ 0.035 lpm between 4000 and 6000 minutes. During steady state in stage 3, diurnal fluctuation in Q are $\pm$0.5 lpm. The effects of temperature at the very beginning of the test may be masked by the sharp decline in Q. It is unlikely that temperature affects the measuring system from the barrel reservoir. Changes in Q, from fluctuating temperatures in the soil-water outside the borehole may be due to changes in effective porosity caused by changes in volume of entrapped air bubbles. Increases in Q with decreasing temperature have been previously recognized by Stephens et al. (1983).

There are two possibilities that may explain the presence of entrapped air. The CO_2 flooding before test start may not have been effective in removing soil air in the same region that infiltration is taking place. From the site characterization, it is known that adjacent to the borehole screened interval a higher Ks material exists than below the borehole. It is possible that the CO_2 flowed laterally through this gas-permeable zone from the screened interval and did not exchange with the soil air beneath the screened zone where infiltration is taking place. Other possibilities may be that gas is being released from the infiltrating water as temperature increases and decreases; also, a low solubility gas may be released due to chemical reaction. Dissolved

oxygen (D.O.) measurements made during the test with the Hach Kit at high and low temperatures of both site groundwater and tap water indicate that D.O. levels are about 2 mg/l. Other measurements of dissolved oxygen content were made after the test period by the N. M. Bureau of Mines. Ranges in dissolved oxygen were obtained from multiple water samples that were left exposed to the atmosphere for different lengths of time; thus simulating borehole test conditions. A dissolved oxygen content range of 0-0.8 mg/l was measured for the groundwater; and, it is possible that this low a value was not obtained during S8T1 with the use of the Hach Kit due to poor resolution. A range of dissolved oxygen content of 1.4 - 2.2 mg/l was measured for the tap water; which agrees well with measurements made during S8T1. At field temperatures of 20° C, the concentration of dissolved oxygen at saturation should be about 9 mg/l (Bausch and Lomb Spectrokit, catalog number 33 09 08, Bausch and Lomb Analytical Systems Division, Rochester, New York). The increase in the magnitude of the Q fluctuations with time (figure 40), suggests that the volume of entrapped air is increasing during each diurnal cycle; also, there is a general trend of increasing temperature in the borehole with time.

Comparing pressure head data in figures 33-36 with temperature data in figures 30-32, it is also apparent that temperature changes correlate with small changes in pressure head. Temperature peaks can be matched to minimums in pressure heads. Two possibilities exist for the pressure head

fluctuations. The first may be a temperature effect on the above ground tensiometer apparatus that is exposed to daily fluctuations in temperature; such as expansion and contraction of tubing and the possible changes in fluid densities in the manometer tubes. A calibration equation to correct for temperature effects on the fluid densities in the manometers was not determined. Secondly, entrapped air bubbles that increase in volume could be expected to cause a more negative pressure head if moisture contents decreased accordingly (figure 7). Work by Chahal (1965) showed that when entrapped air is involved in a soil sample, an increase in soil-water temperature tends to shift the soil moisture characteristic curve to the right. Chahals' work showed that the resultant pressure head may increase or decrease if soil-water temperature increases and moisture content is allowed to decrease.

Pressure head fluctuations caused by changes in the volume of water held in the soil should correspond with water content fluctuations. Figures 37-39 indicate moisture content does vary with temperature in the same manner as Ψ, although these fluctuations do not seem to be as great as and Q, possibly due to measurement error and graph scale. It is also possible that the neutron probe electronics are affected by temperature and give only apparent changes in soil-water content; this has not been evaluated.

If entrapped air is causing the temperature fluctuations on Q, Ψ, and Θ, then calculated values of Ks are not at

saturated conditions. Furthermore, if the magnitude of these fluctuations increase with time, suggesting increases in entrapped air volume with time, then hydraulic conductivities calculated will be increasingly smaller than Ks.

Infiltration Rate

Referring to figure 40, infiltration rate (Q) decreases almost exponentially during stage 1 until about 2000 minutes. From 2000 to 3500 minutes, Q is steady at a value of about 0.135 lpm. The time for Q to reach steady state in stage 1 is 2000 minutes. From figure 28, approximately 600 liters of water have flowed from the borehole at 2000 minutes test time. This cumulative infiltration value of 600 liters is about 10 times the maximum water volume to be used according to the USBR (1974). Experiments by Stephens et al.(1983) found that volumes of water necessary to reach Qs were also greater than V_{max} USBR (1974). These field results suggest that either the USBR method to estimate the time or water requirement for Qs is in error, or that hydraulic properties are possibly changing which might prevent steady state from being achieved with less water. One possibility might be the decrease in Ks in the formation around the borehole, inasmuch as Stephens 1979 showed that the time to reach steady state is inversely proportional to Ks.

During stage 2 (figure 40), Q increases 2.6 times (260%) from 3500 minutes to 6000 minutes. The average steady state Q during stage 2 is 0.35 lpm. Recall that the test procedure

difference from stage 1 to stage 2 is a switch from site groundwater to site tap water. This increase in Q resulting from a chemistry change in stage 2 is a significant change. The long duration decrease in Q over early time stage 1 and the sharp increase in Q during stage 2 could be related to the observation of cloudiness and an orange precipitate in the water barrel reservoirs during stage 1. A possible hypothesis for the stage 1/stage 2 increase is a physical clogging around the borehole by a precipitate or colloidal fraction which is flushed out by using the stage 2 tap water. Another hypothesis for the change in Qs is related to the different Sodium Adsorption Ratio (SAR) values of the two infiltrating waters; a high SAR and low TDS (Todd 1980) tend to disperse clay particles and reduce permeability. When using values from Table 5, of Ca, Na, and Mg for both waters, site groundwater has a SAR of 3.4 while site tap water has a SAR of 1.5. The relatively high TDS of the groundwater of 1286 ppm when compared to the 342 ppm TDS of the tap water would tend to counter the effect of th lower SAR of tap water on increasing permeability and infiltration rate. The time involved to increase Q from the end of stage 1 steady state to stage 2 steady state is about 500 minutes with about 150 liters of tap water passing through the borehole.

During stage 3, with steady pumping of the shallow aquifer to lower the water table, a steady state Q value of 0.22 lpm is reached at about 7750 test minutes. Recall that site tap water is still being used for infiltration. This

steady state Q of 0.22 lpm is a 37% decrease in infiltration rate from the steady state value of 0.35 lpm in stage 2. With the pumping of groundwater from beneath the borehole, an increase in infiltration rate was expected if the gradient beneath the borehole increased and other factors remained constant.

During stage 4 (10,300 minutes to test end), when the water source was switched from groundwater to tap water, Q remains steady at a value of 0.15 lpm until about 11,300 minutes when it shows an increase to 0.23 lpm. A steady state infiltration of 0.15 lpm will be used for stage 4. Stage 4 infiltration, using site groundwater and pumping, is only 13% larger than stage 1 infiltration without pumping. A more certain steady state infiltration might have occurred had the test not terminated at 12,000 minutes due to a crack in the well field manifold.

Pressure Head and Total Head

Figures 34, 35, and 36 show that pressure head increases rapidly within the first 500 minutes of the test. This increase is due to the advance of the wetting front. This increase is followed by a gradual decrease and then a steady state which continues to the end of stage 1 at 3500 minutes. Stage 2 is characterized by a increase in most pressure heads in figures 33-36. Stage 3 exhibits rapid decreases in pressure head which typically continue to rise throughout the stage without stabilizing. The exception to stage 3 behavior

occurs at the R=91 cm (figure 36) where a rapid decrease is followed by steady state. Stage 4 pressure head response is difficult to separate from the non-steady state trends shown in stage 3. During the period of water table lowering at 6000 minutes until test end, stages 3 and 4 pressure heads show the most correlation with diurnal temperature changes.

Figures 41 and 42 show total head and pressure head profiles at 3300 minutes when pressure heads and flow rate were steady at the end of stage 1.

Figure 43 and 44 show Total Head and Pressure head profiles at 5500 minutes at the end of stage 2 when pressure heads and flow rate were steady after the water chemistry change from groundwater to tap water.

Comparing figures 41 and 42, also 43 and 44, indicates that water flowing from the borehole along any path will pass from a saturated to an unsaturated region. This observation contradicts the free surface approach (figure 3), and supports the results of saturated-unsaturated numerical simulations conducted by Stephens (1979), and the field results of Stephens et al. (1983) for deep water table conditions. However, for this shallow water table case, there is a mound in the zero pressure isobar which appears to intercept the free water surface in the borehole.

Figure 45 and 46 show Total Head and Pressure Head profiles at 9600 minutes during stage 3 steady state. From figure 45, we can see that flow from the borehole would approach a more vertical downward orientation and more flow

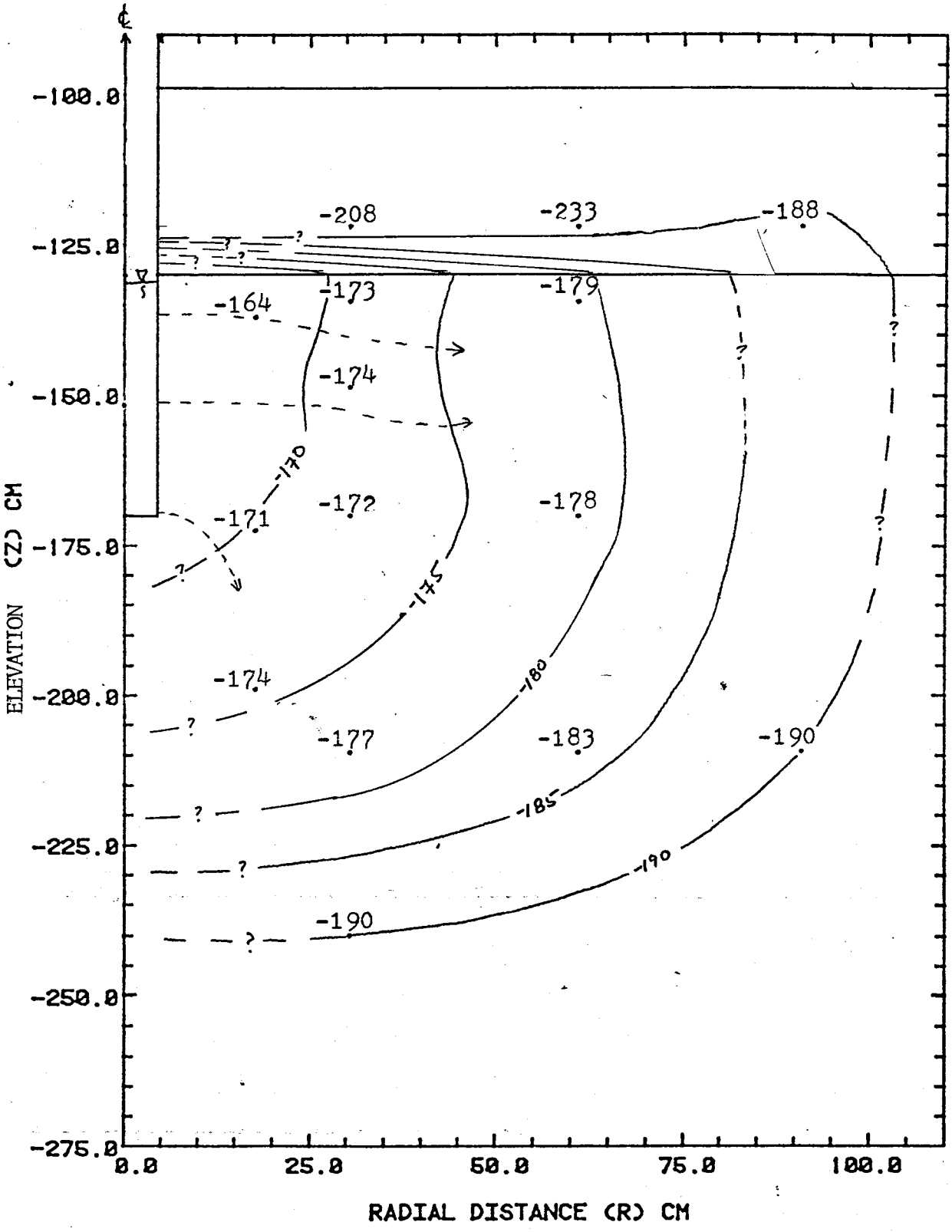

Figure 41. Total Hydraulic Head after 3300 Minutes

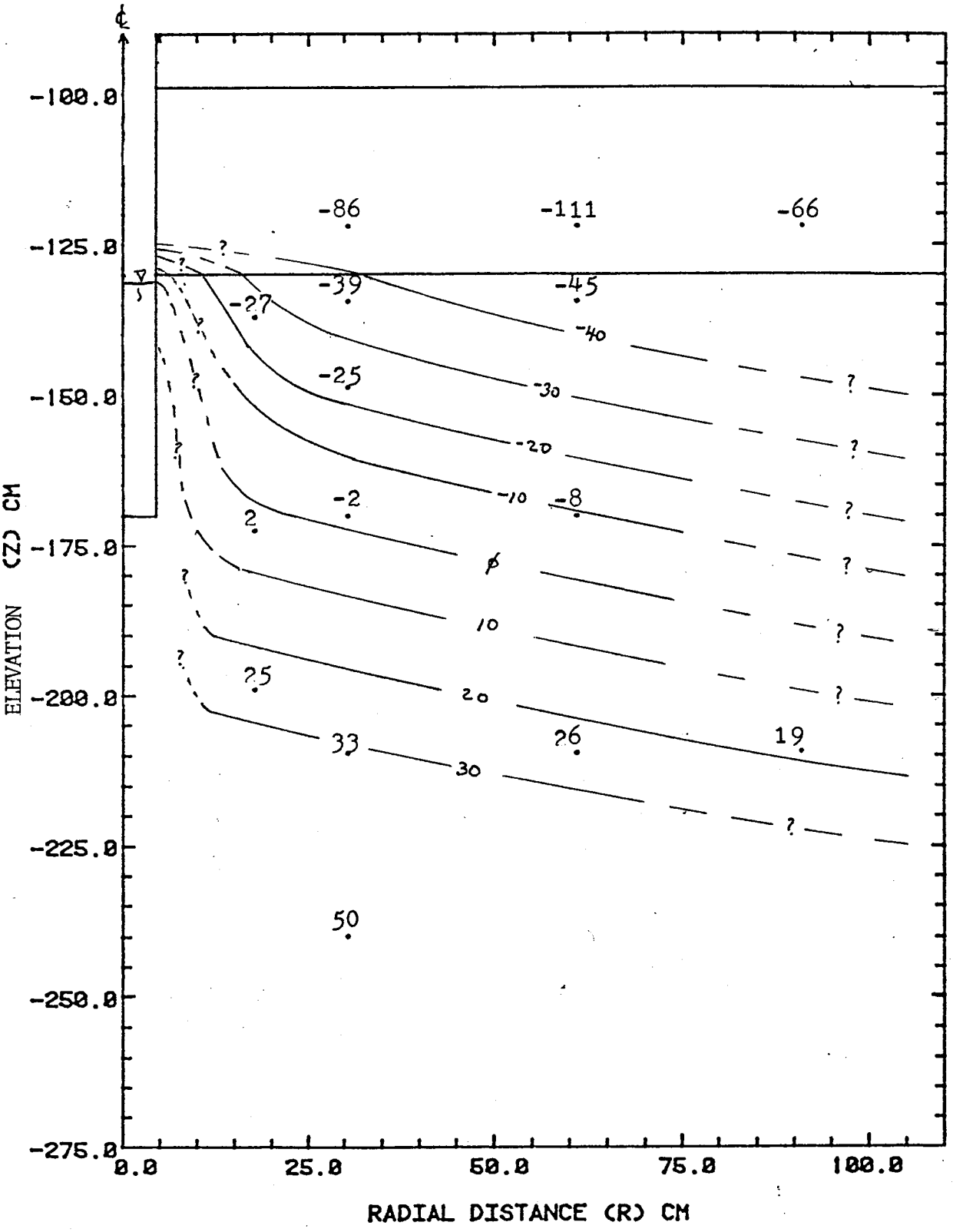

Figure 42. Pressure Head after 3300 Minutes

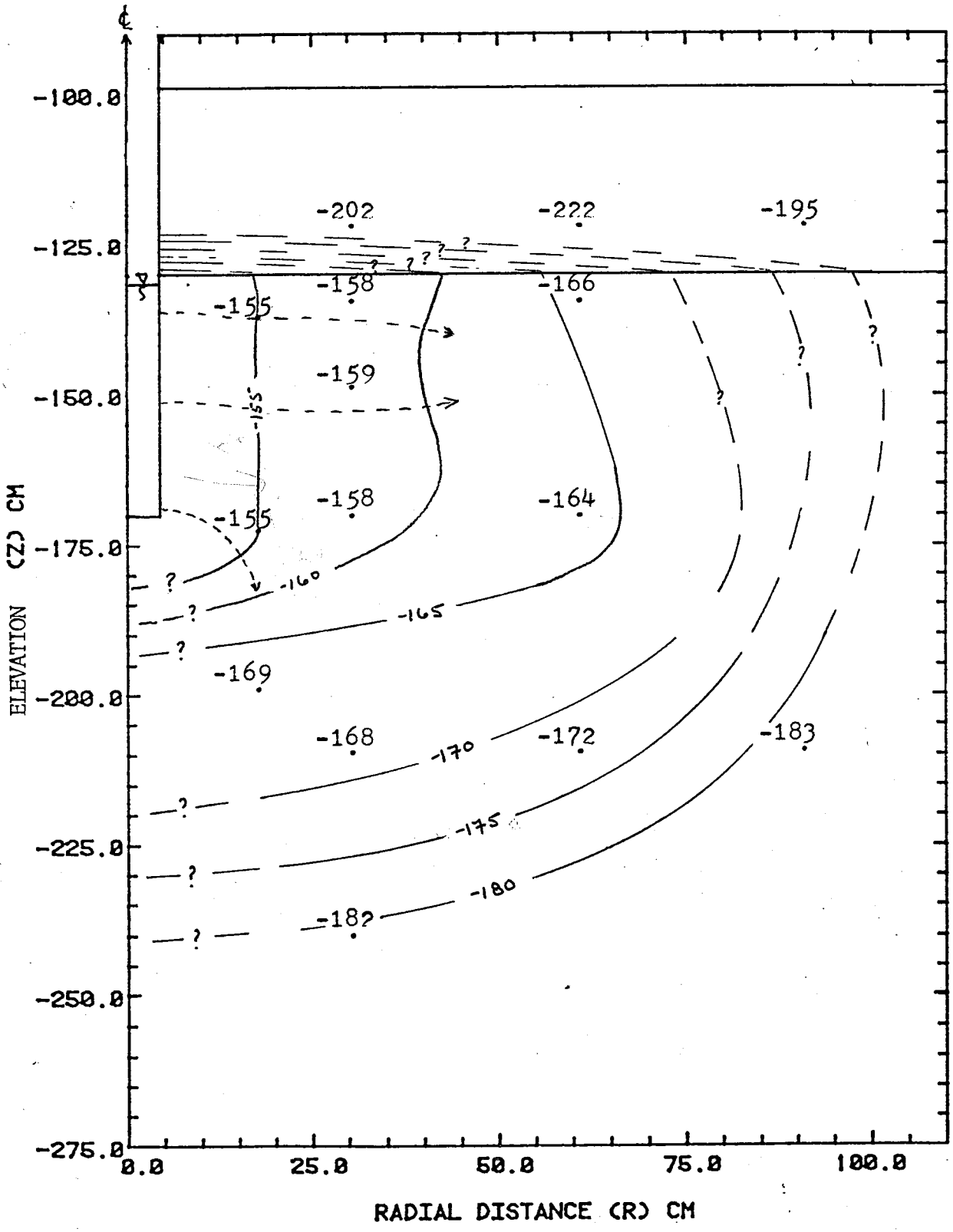

Figure 43. Total Hydraulic Head after 5500 Minutes

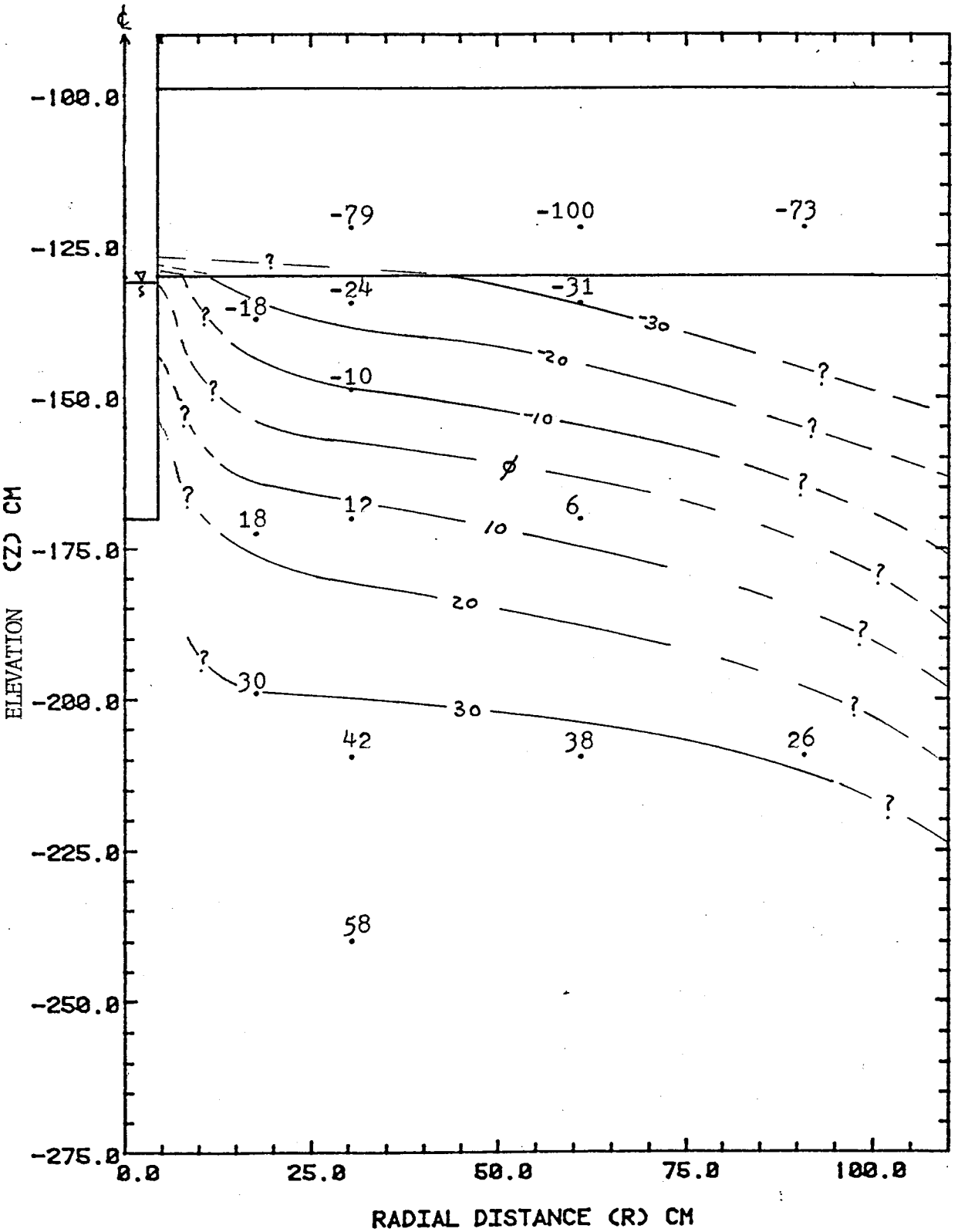

Figure 44. Pressure Head after 5500 minutes

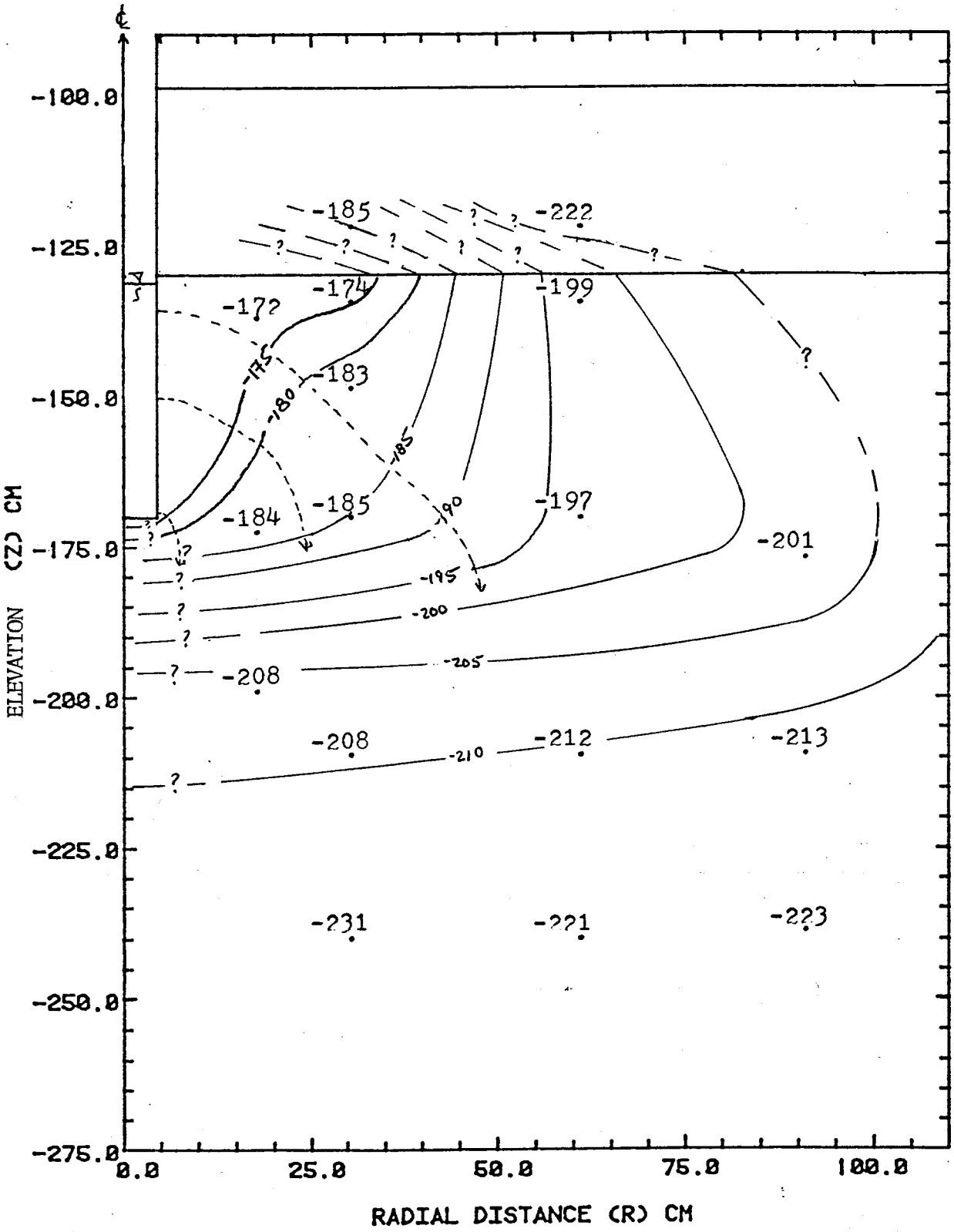

Figure 45. Total Hydraulic Head after 9600 minutes

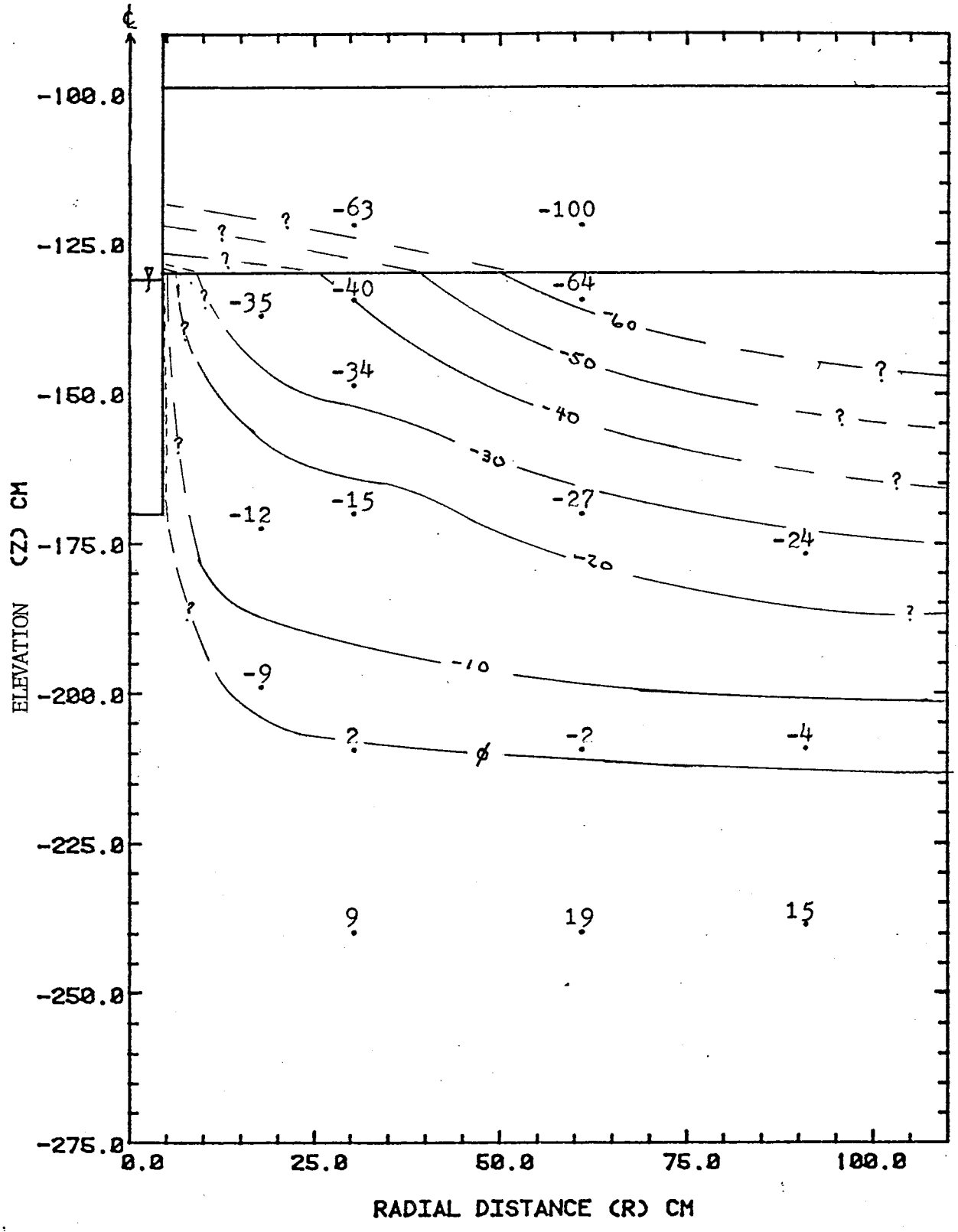

Figure 46. Pressure Head after 9600 Minutes

from the borehole occurs within a smaller radial distance from the borehole compared to stage 2 (figure 43). This more vertical orientation of flow paths during pumping would show itself as smaller values of Ks measured from borehole infiltration due to the layering that was observed during site characterization (table 7).

Hydraulic Gradient

From the analysis of infiltration rate, changes in Q might be attributed to changes in Ks. But from Darcy's Law, Q is also proportional to the hydraulic gradient. Figures 47 and 48 show the S8T1 average negative hydraulic gradient as a function of time. The average gradient over a distance is determined by averaging the difference in the total head between the borehole and the tensiometers at that distance divided by the distance between the borehole wall and the tensiometers. (The negative of hydraulic gradient is used so that infiltration rate as calculated by Darcy's Law, is positive; thus Q is proportional to the negative of i as well as Ks.)

In figure 48, tensiometers at 30.5 cm are used since early time data were acquired. The gradient decreases very quickly in figure 48 at the beginning of stage 1 from time 0 to about 250 minutes. This is due to the soil getting wetter. From 250 minutes to about 2000 minutes there is an increase in hydraulic gradient which then remains steady until about 3500 test minutes. A similar gradient with time response was

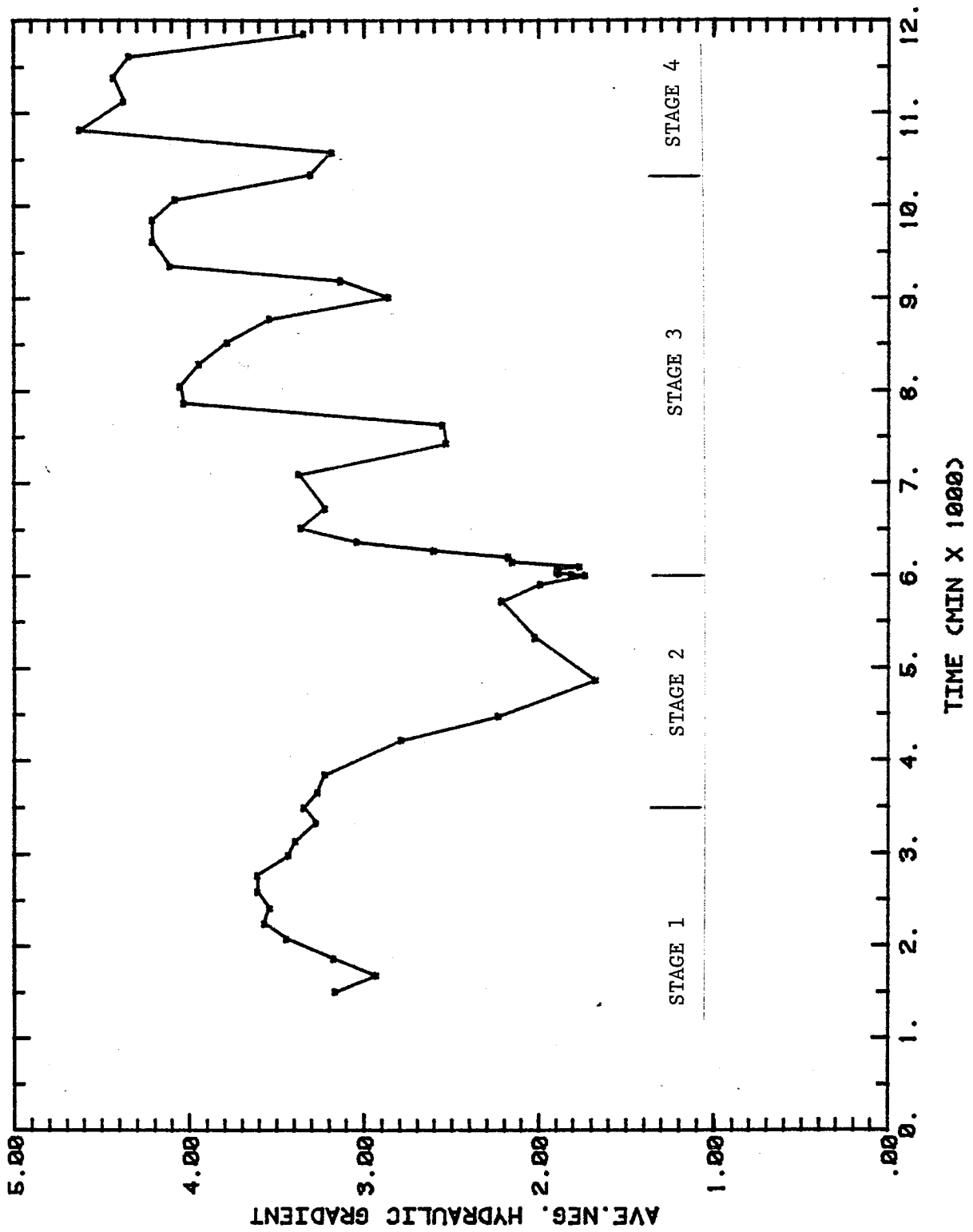

Figure 47. Change in Average Negative Hydraulic Gradient With Time at R= 17.8 cm

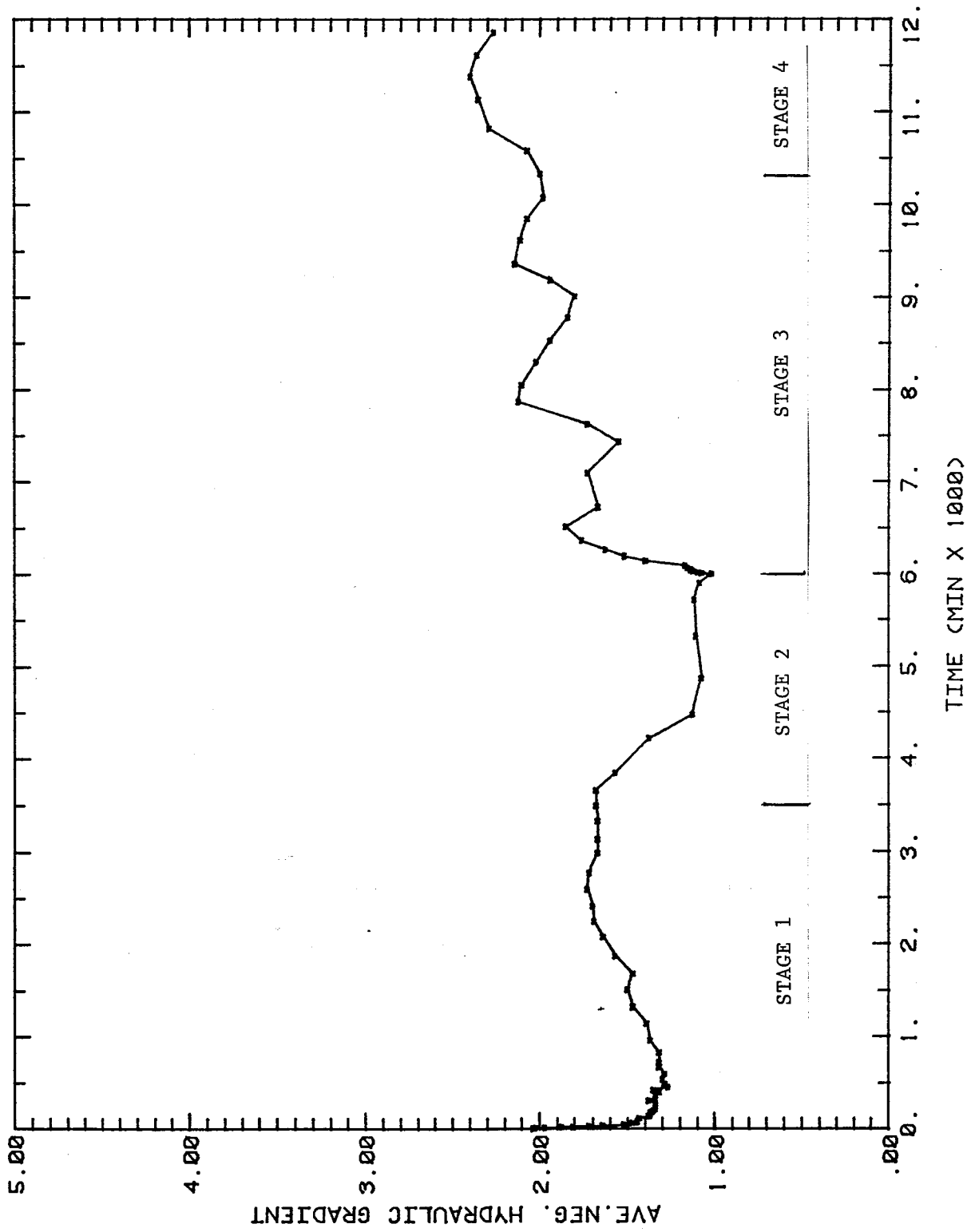

Figure 48. Change in Average Negative Hydraulic Gradient With Time at R= 30.5 cm

reported by Stephens et al.(1983). Early time data was not obtained at R = 17.8 cm; but from figure 47, stage 1 behavior is similar to that at 30.5 cm in figure 48. The decrease in infiltration from test start to 2000 minutes while gradients decrease and then increase can be explained if Ks is changing with time. Figures 49 and 50 show the ratios of Q to average negative hydraulic gradient ($Q/-i \propto Ks$) versus time at R = 17.8 cm and 30.5 cm respectively. Only early time calculations could be made for R = 30.5 cm. From the ratio in figure 50, it is inferred that Ks decreases by 49% between 0 and 250 minutes; for comparison, Q (figure 40) decreases by 66% and the gradient decreases by 34% (figure 48). From 250 to 2000 minutes, a 75% net decrease in Ks (figure 50) is calculated; during this same time, Q decreases by 69% (figure 40) and gradient increases by 18% (figure 48). From 2000 minutes to the end of stage 1 at 3500 minutes, a steady state Q and stable gradient could signify a constant Ks.

During the first 1000 minutes of stage 2, from 3500 to 4500 minutes, the gradient decreases by 42% (figure 47). During this time, Q (figure 40) increases by 260% (2.6x). These changes in Q and i signify an increase in Ks of 450% (4.5x). Recall that the only test procedure change in stage 2 was the use of site tap water instead of groundwater. From 4500 minutes to the end of stage 2 at 6000 minutes, both the gradient (i) and Q have stabilized, signifying a constant Ks. For purposes of calculations, average values of Q and i are used when fluctuations appear to be diurnal.

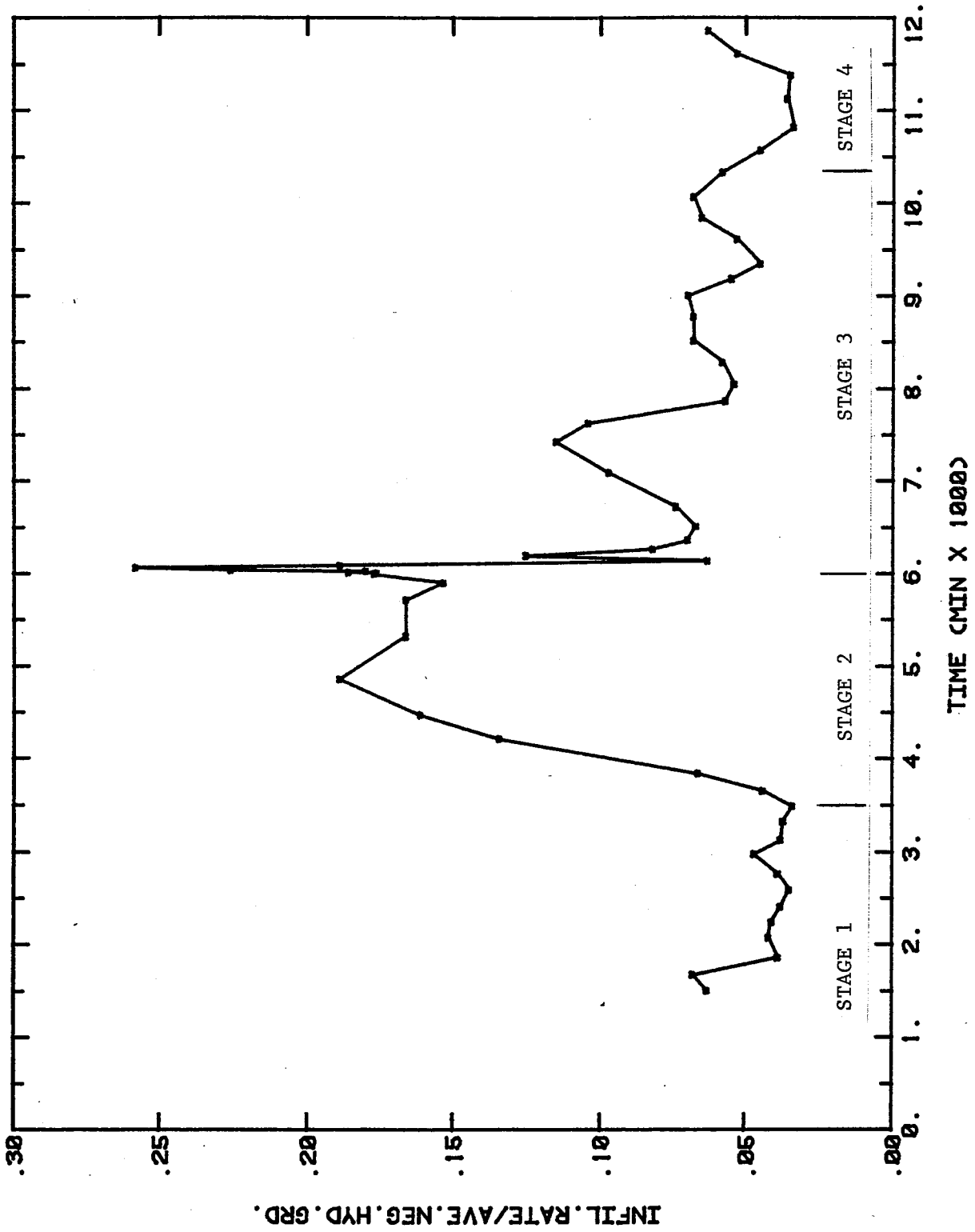

Figure 49. Ratio of Infiltration Rate to Average Negative Hydraulic Gradient at R= 17.8 cm

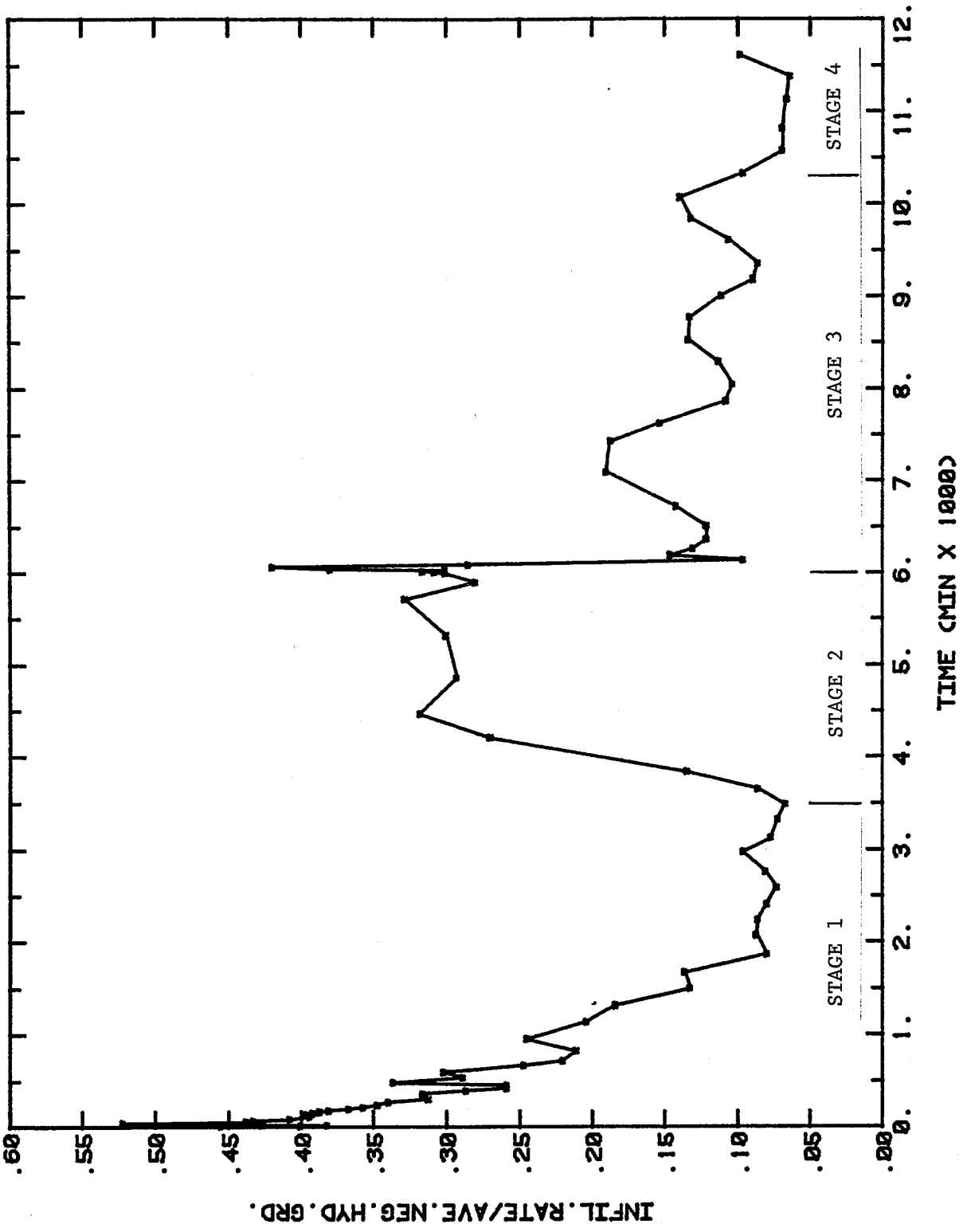

Figure 50. Ratio of Infiltration Rate to Average Negative Hydraulic Gradient at R= 30.5 cm

During stage 3, from 6000 to 10,300 minutes, with lowering of the water table by approximately 18 cm with groundwater pumping, figure 40 shows a decrease in steady state Q by 37% from stage 2 without pumping. Figure 47 indicates an increase in gradient by 190% (1.9x) during stage 3 from 6000 to 10,300 minutes. As infiltration rate becomes steady during stage 3, the gradient in figure 47 continues to increase throughout stage 3. These changes, when viewed together in figure 49, result in a decrease in Ks of 67% with the advent of pumping. Yet with the advent of pumping, both Q and i were intuitively expected to increase. In fact equation II in figure 2 shows that Q increases with increasing Tu for a constant Ks. Since i does not reach steady state, Ks might continue to decrease if stage 3 had been run longer. Because there is no water chemistry change between stages 2 and 3, the possible cause for the decrease in Ks with pumping might be the change in flow path (orientation of stream tubes) around the borehole due to pumping. From the site characterization, it is known that horizontal layering of different Ks soils occurs beneath the borehole. The effective Ks of these soils, when the soils are viewed as one unit, is directionally dependent, with the minimum Ks in the vertical direction. From the analyses of the total head profiles in figures 43 and 45, it is shown that flow does become more vertical outside the borehole with the advent of groundwater pumping.

The analysis of stage 4 from 10,300 minutes to test end, shows that coupled with the limited flow data (figure 40) and

the increasing gradient which continues through stage 4 (figure 47), an effect of water chemistry change from tap water to groundwater, can still be deduced from the stage 4 data. In figure 40, a continuation of the sine wave pattern of flow after 10,300 minutes would be expected if a change in water chemistry had not taken place; therefore, the steady state Q, after 10,300 minutes, could denote a decrease in Q from the expected trend due to the water chemistry change.

Volumetric Moisture Content

Figures 37-39 indicate moisture content versus time at radii 30, 60, and 100 cm, respectively.

Moisture content data at depths greater than 175 cm was limited by the practice of keeping the neutron probe access tubes above the water table. This practice was to prevent any moisture intrusion into the access tube by leakage through the tube bottom.

Figure 37 of moisture contents at R = 30 cm, shows an early stage 1 wet-up that is followed by a decrease in moisture content until a time of 3500 minutes. This cycle of wetting and drying is supported by the 30 cm pressure head data (figure 34). In contrast, during stage 1, moisture content at 60 cm increases more gradually over the entire 3500 minute interval. Stage 1 moisture content at the 100 cm radius shows an initial increase between 0 and 750 minutes and then a steady state condition from 750 to 3500 minutes.

Stage 2 is characterized by increased moisture contents

at all radii. This increase compares well with the increased stage 2 values in figures 33-36. At R = 30 cm, the increased moisture contents of stage 2 return to the maximum values that are achieved during early time in stage 1. Those moisture contents achieved by the end of stage 2 at radii 60 and 100 cm are, for most cases, the maximum water contents achieved throughout the test duration.

Stages 3 and 4 are both characterized by decreasing moisture contents at all radii from 6000 minutes to test end. The decrease in moisture content is due to the groundwater pumping and figures 37-39 show that moisture contents are not at steady state even after approximately 6000 minutes of pumping to lower the water table.

Figures 37-39 show general decreases in moisture content for increasing radius for any given depth. Maximum moisture contents at R = 30 cm, agree well with Θs values recorded in the hanging column apparatus (table 3); this suggests that porosity values (table 3) calculated from ρ_b and ρ_s may be low.

Figures 51, 52 and 53 exhibit water content profiles after 3300, 5500, and 9600 minutes; these times reflect the 'steady state' conditions near the end of stages 1, 2 and 3. Maximum wetness in the profile is observed during stage 2 (figure 52). The moisture content distribution for stage 3 (figure 53) is similar to that observed near the end of stage 1; however equilibrium moisture contents were never reached in stage 3 or 4.

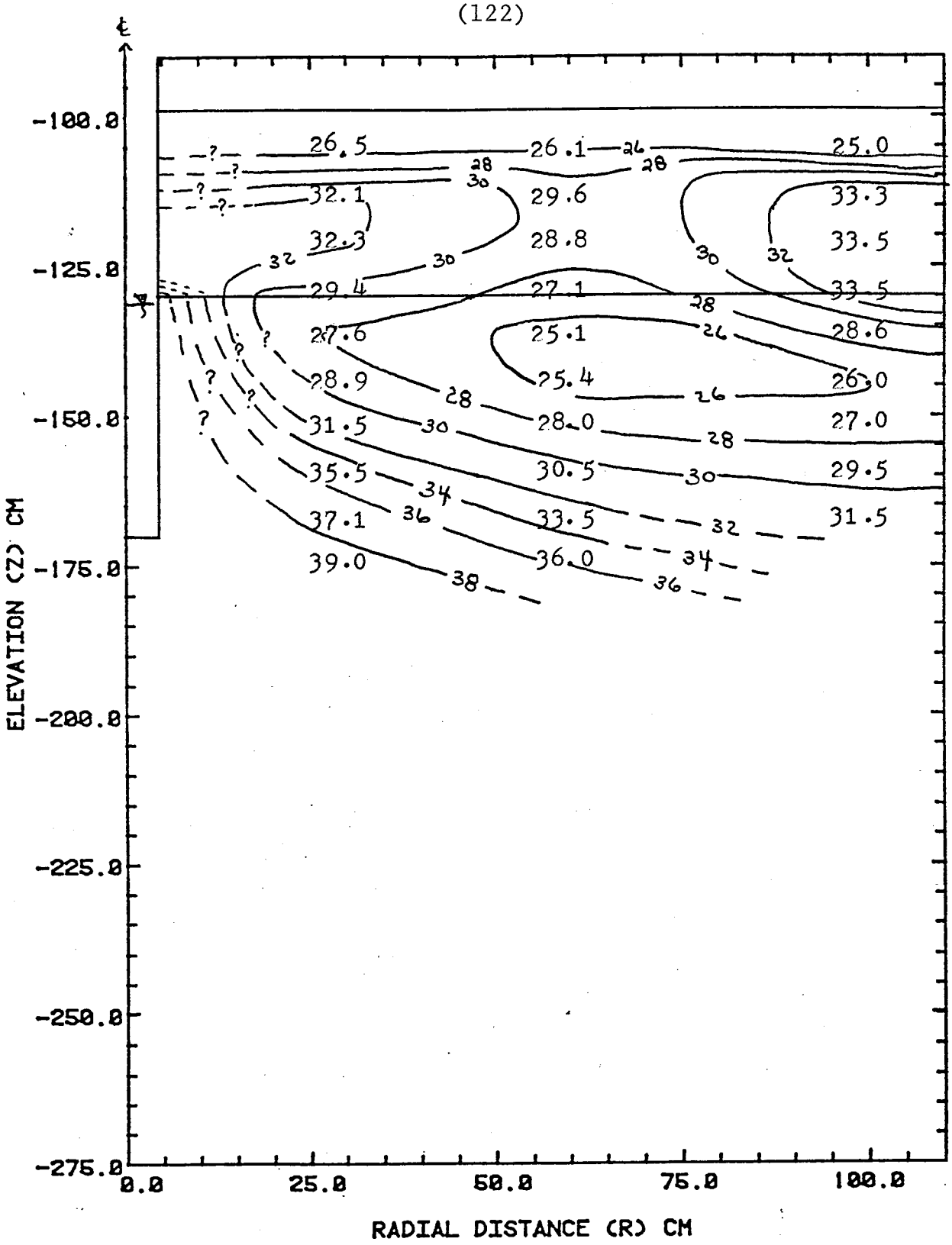

Figure 51. Water Content after 3300 Minutes

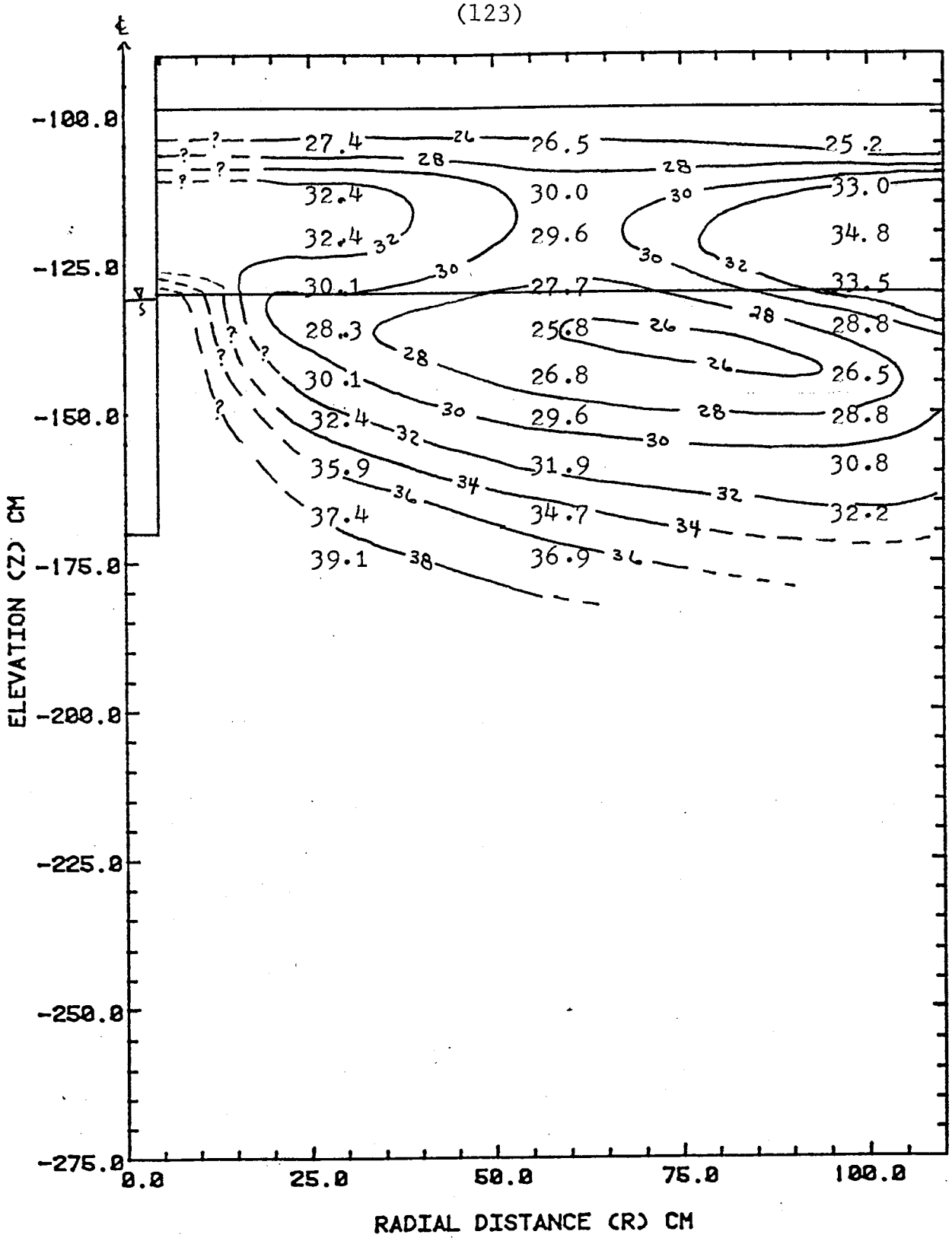

Figure 52. Water Content after 5500 Minutes

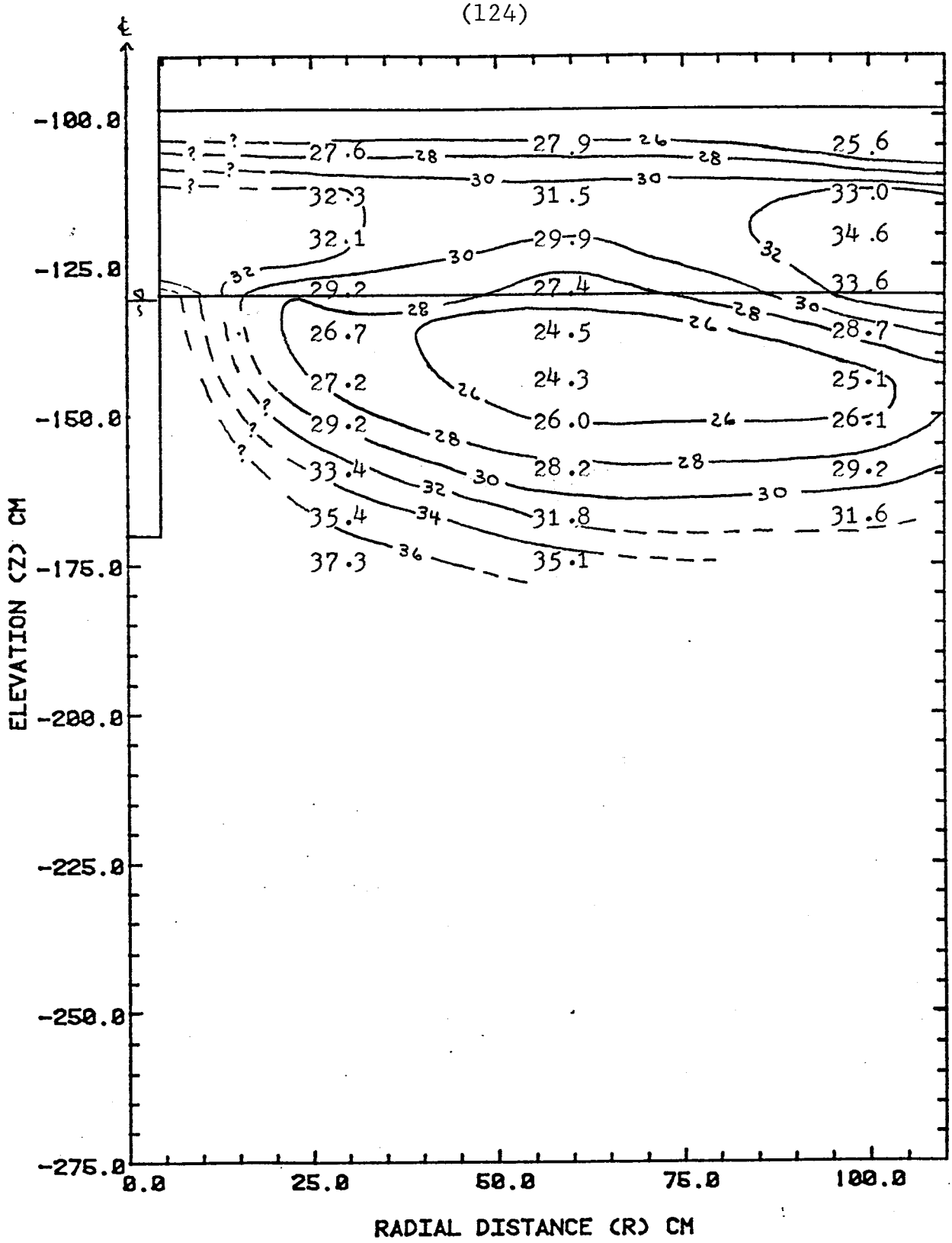

Figure 53. Water Content after 9600 Minutes

Saturated Hydraulic Conductivity

The calculation of saturated hydraulic conductivity using equation 2 requires knowing the length parameter Tu, to differentiate between shallow and deep water table conditions. Recall that Tu is the absolute distance from water level in the borehole (132.1 cm below datum) to the static water table free surface prior to testing (193.8 cm below datum). Tu for S8T1 stages 1 and 2 is constant at 61.7 cm even though some mounding occurs. At the start of stage 3 at 6000 minutes, the free water surface below the borehole is lowered by the aquifer pumping to increase the value of Tu. Due to downward flow gradients during pumping, the elevation of the free surface was difficult to measure with the piezometers. The four piezometers installed to monitor the pumped water table level did not correlate in readings with the six deepest tensiometers. The reason for the discrepancy was that the piezometers were measuring pressure head over an integrated interval of approximately 75 cm whereas, the tensiometers were near point measurements. The perforated interval of the piezometers was located beneath the water table elevation and therefore could not be used to extrapolate the distance to the free surface. During stabilized infiltration during stage 3, the 210 cm-depth tensiometers were located at the free surface. For the calculation of Tu, the tensiometers at R = 61, D = 209.6 cm and R = 91, D = 209.5 cm were used. Figure 54 shows the average value of Tu during pumping through stages 3 and 4.

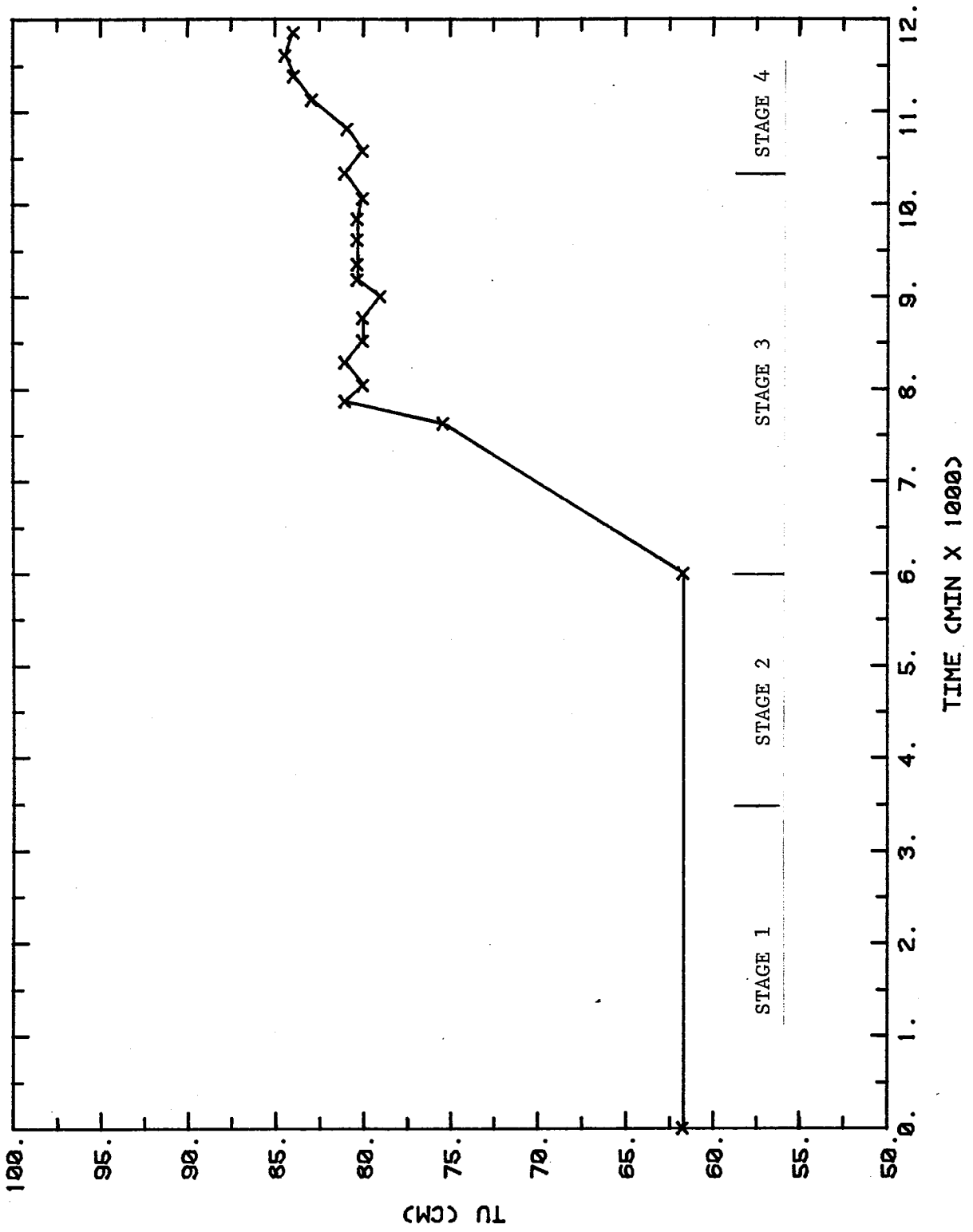

Figure 54. Change in Tu With Time

Equation 2 also utilizes the steady state infiltration rate. Since it is observed in figure 40 that infiltration rates fluctuate with time, average values of Q are used for calculations of saturated hydraulic conductivity. Table 11 lists saturated hydraulic conductivities calculated from equation 2.

Table 11 indicates that all stages of the test are at shallow water table conditions as Tu < 3H. The original plan of the test was to lower the water table enough that Tu would be greater than 3H and deep water table test conditions would exist.

According to equation II, in stages 1 and 2, Ks is directly proportional to Qs, inasmuch as Tu is considered a constant. Therefore, since Qs increases 2.6 times, Ks should also increase the same amount. Of interesting note is that hydraulic gradient is not tken into account in equation II. The time to reach steady state during stage 1 seemed very long (2000 minutes) when compared to other borehole tests carried out by our group (Stephens et al. 1983). The analysis of average negative hydraulic gradient (figures 47 and 48) showed that during very early time, 0-250 minutes, Q and i both decreased as expected, due to the soil becoming wetter and the reduction in capillary forces that takes place. But when gradients around the borehole increased during 250 minutes to 2000 minutes, Q continued to decrease. This continued decrease in Q is believed to be from borehole clogging, possibly resulting from a colloidal fraction that is present

TABLE 11
SATURATED HYDRAULIC CONDUCTIVITIES

STAGE	Qs (LPM)	Tu (cm)	Tu/H	Ks (cm/sec)
1	.135	61.7	1.6	8.04 x 10-4
2	.350	61.7	1.6	2.08 x 10-3
3	.229	80.3	2.1	1.06 x 10-3
4	.150	82.4	2.2	7.11 x 10-4

H = 38.1 cm

in the infiltrating groundwater.

With the stage 2 switch to site tap water, it appears that increases in Ks occurred due to the unclogging around the borehole. Stage 2 showed increases in moisture content, increases in gradients, and increases in Q; therefore increases in Ks.

If stage 2 Ks is closer to a "true" value of saturated hydraulic conductivity (in the absence of borehole clogging) then the Ks value of 2.08 $x10^{-3}$ cm/sec (Table 10, stage 2) may have been measured before borehole clogging took place.

Figure 33 shows that near the base of the borehole a maximum pressure head was recorded at about 240 test minutes; after which time, pressure head decreases decreases. A similar response, termed Phase 2, was reported by Stephens et al.(1983). This time of 240 minutes corresponds to maximum water contents around the base of the borehole as well. At 240 test minutes, cumulative infiltration was 140 liters ; this should have been sufficient to reach steady state, according to USBR equation 11. The infiltration rate at 240 minutes test time is 0.465 lpm. Using equation 2, Ks would equal 2.77 x 10^{-3} cm/sec. During stage 2, while temperature correlations are easily evident (figure 40), it was observed that the infiltration fluctuation magnitude is greater than observed in stage 1. If the increases in fluctuations are attributed to increases in entrapped air in the formation, then the maximum Q value during these fluctuations should be used to calculate a saturated hydraulic conductivity. If a

maximum Q, from a peak in the oscillation about steady state, during stage 2 (figure 40) of 0.373 lpm is used in equation 2, then Ks = 2.22×10^{-3} cm/sec for stage 2. This stage 2 Ks is only 20% less than stage 1 Ks at t = 240 minutes . Both values of 2.77×10^{-3} cm/sec (stage 1) and 2.22×10^{-3} cm/sec (stage 2) would fall within the range of vertical Ks measurements between 132 and 170 cm depths obtained in the lab (Table 7). The range of lab Ks values for these depths is from 6.0×10^{-3} to 4.2×10^{-2} cm/sec. Unfortunately, no horizontal Ks measurements are available at this time for comparative purposes.

The only operational change from stage 2 to stage 3 was the lowering of the water table in an area below the borehole. The calculated Ks of 1.06×10^{-3} cm/sec from an average steady state Q for stage 3 (Table 10) is 49% less than the stage 2 Ks value of 2.08×10^{-3} cm/sec (Table 10) from average steady state Q. If the maximum Q encountered (peak) during stage 3 steady state of 0.267 lpm is used to calculate Ks, then Ks = 1.29×10^{-3} cm/sec for stage 3. The decrease from stage 2 to stage 3 using peak Q values is 42% which is about the same as the percent reduction calculated in Ks from average steady state Q values during each stage.

A hypothesis for the decrease in Ks from stage 2 to stage 3 may be the directional change in flow paths to a more vertical orientation, as evidenced by the tendency for equipotential lines to become more horizontal (figures 43 and 45). Since the vertical Ks values, obtained in the lab, span

4 orders of magnitude from 10^{-2} to 10^{-5} cm/sec, a shift in flow path orientation to a more vertical direction outside the borehole would tend to decrease the Ks measured.

During stage 4, an increased Tu is observed in figure 54. This was due to an increase in the depth of the water table caused by pumping. During both stage 3 and stage 4, the suction pump was operating at maximum capacity to maximize Tu. The value of Ks during stage 4 is open to interpretation, because the Qs value used may not represent a true steady state value. In figure 40, Qs appears to stabilize during 10,500 to 11,500 minutes, however this may be attributed to the switch from tap water to groundwater. Q increases at the end of stage 4 (11,400 minutes to test end), while Tu only varies slightly. It is of interest to note that Ks values calculated from the apparent steady state Q during stages 1 and 4 (Table 10) are quite similar: 8.04×10^{-4} and 7.11×10^{-4} cm/sec respectively; tap water was used during both of these stages, although depth to groundwater differed.

A summary of the factors influencing steady infiltration from the borehole should be considered. The hypothesis of the changing water chemistry causing a clogging then unclogging of the borehole between stage 1 and stage 2 is supported by two observations. First, potential oxide clogging agents occur in the groundwater used during parts of the experiment: iron and manganese oxides (Table 5). These metallic oxides apparently precipitated in the water storage reservoir and clouded the water. They were also observed in the flow system of the

shelby tube permeameter, however their presence could not be linked solely to the water because some metallic parts of the system that were in water contact were observed to be rusting. Metallic oxides were not recognized in the flow system of the PF ring permeameter where most of the components of the permeameter are plastic, but the precipitate may have settled to the bottom of the permeameter, out of view.

Secondly, precipitation of calcium carbonate crystal flakes (another potential clogging agent) was observed floating on top of the water reservoir in the PF ring permeameter; groundwater from the site was used as the permeating fluid. The same crystals were observed in the storage barrels in the field test. Calcium carbonate was not evident in the shelby tube permeameter.

On the other hand, both the metallic oxides and the calcium carbonate precipitates are unlikely clogging agents, in light of the fact that the reaction of the soil to a change from groundwater to tap water seemed so rapid; only 500 minutes and 150 liters of tap water were necessary to increase Q 2.6 times to a new steady state value between stages 1 and 2. The dissolution of the metallic oxides in the tap water would have required an oxygen-free environment which, from dissolved oxygen measurements, was not the case.

Further field experimentation, where an actual clogged soil, obtained after the infiltration of groundwater, is removed and examined, could be the only means to quantify the clogging mechanism. A complete analysis might include: Eh,

Ph, D.O., Temp, and bacteria in the water and soil.

The hypothesis of increased fluctuation magnitude of Q being due to increased entrapped air that came out of solution from the infiltrating water needs further investigation to be conclusive. Measurements of the waters for different compounds that might gasify when subjected to temperature increases could add support to the observations.

ESTIMATING FINAL INFILTRATION RATE FROM EARLY TIME DATA

Stephens (1979) recognized, on the basis of computer simulations and a few field experiments, a reasonably linear relationship between infiltration rate and inverse square root of time. A further evaluation of this relationship was conducted by Stephens et al. (1983). They found that calculating steady infiltration rate, by extrapolating to $t^{-0.5} = 0$ using simple linear regression, produced estimated Qs values within 13 to 179% of actual field measured Qs values.

Infiltration data of S8T1 from the time the borehole filled completely until the time when V_{max} (= 2.05 V_{min}) occurred was used to test this method. This limit was selected because V_{max} is easy to calculate, the corresponding time is simple to measure in the field, and it usually is reached before flow rate stabilizes. The steady flow calculated by this extrapolation method, Q_{sc}, the infiltration rate at V_{max}, QV_{max}, and the infiltration rate at t=240 minutes when the area around the borehole was the wettest, Qs_1, are listed

in Table 12. A linear regression between Q and $t^{-0.5}$ indicates a reasonable straight line fit (Figure 55). The percent error in Q_{sc} with respect to Qs_1 is 9.7: this is less than the smallest error reported by Stephens et al. (1983) by 23%.

It is apparent that more work is necessary before the Q versus $t^{-0.5}$ extrapolation procedure can be recommended with predictable results. For the loamy soil at site 8, the flow rate calculated is a fair estimate of what flow rate might have been had clogging not occurred; although it does over estimate it (Table 12).

CONCLUSIONS

The shelby tube permeameter was found to be an efficient means of measuring multiple values of Ks within each shelby tube sample. Sediment accumulations on the top of the sample, due to precipitation in the recirculating water, did not affect the Ks calculated near the center portion of the shelby tube sample. Ks measurements on CO_2 treated, unclogged shelby tube sample segments reached stabilization within 24 hours. A minimum head of water should be applied to the top of the shelby tube sample to prevent sample disturbance. And finally, all shelby tubes to be used in the shelby tube permeameter should be internally coated with a hard, waterproof coating such as a polyurethane.

Measured Ks in the PF ring permeameter reached maximum values after about 12 days for 7 of 8 samples in the 10^{-4} to

TABLE 12
STEADY INFILTRATION RATE PREDICTED FROM EARLY TIME DATA

Data Points	Q_{sc} (lpm)	R^2	Q_{vmx} (lpm)	t_{vmx} (min)	Q_{sl} (lpm)	t_{sl} (min)
12	0.51	0.76	0.60	80	0.465	240

$$\frac{Q_{sc} - Q_{sl}}{Q_{sl}} \times 100 = 10\% \qquad \frac{Q_{vmx} - Q_{sl}}{Q_{sl}} \times 100 = 29\%$$

Q_{sc} = Calculated flow rate

Q_{vmx} = Measured flow rate when V_{max} infiltrated

t_{vmx} = Time when V_{max} infiltrated

Q_{sl} = Flow rate at t = 240 minutes

t_{sl} = Time of wettest conditions

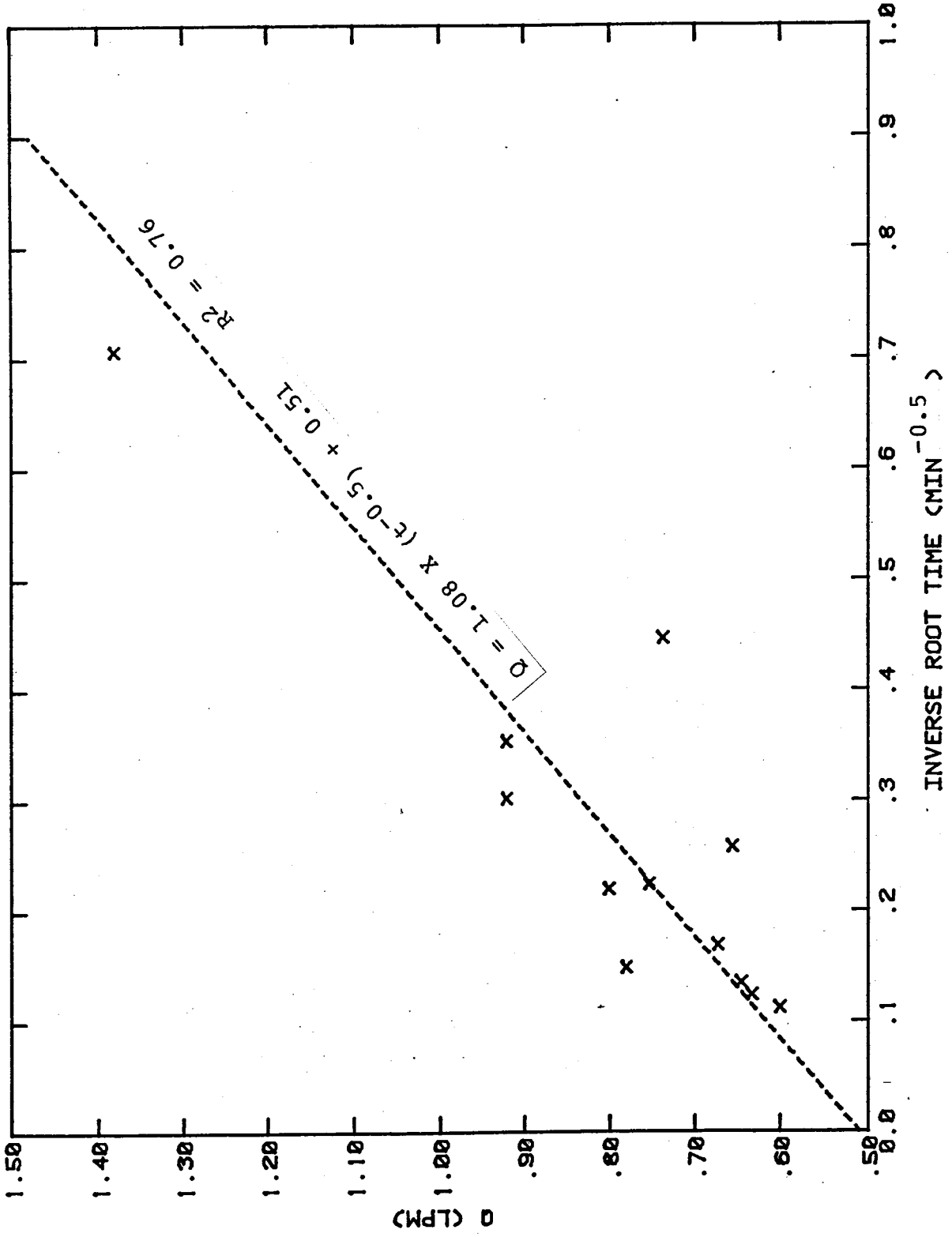

Figure 55. Change In Q With Inverse Square Root of Time

10^{-1} cm/sec Ks range. Four samples in the 10^{-7} to 10^{-5} cm/sec range showed fluctuation with time, but showed no signs of increasing or decreasing trends.

Measurements of Ks made with the PF ring permeameter appear to be slightly higher (about 2.5 X) than those obtained in the shelby tube permeameter but further comparisons need to be carried out.

A long-duration borehole test of 8 days in shallow water table conditions exhibited infiltration sensitivity to water chemistry, water temperature, and pumpage of the shallow water table.

Changes in infiltrating water from groundwater to tap water sources resulted in increased Q values of 260% with the borehole infiltration method. The precipitation of metallic oxides and calcium carbonate when observed in laboratory Ks analyses might be viewed as an early warning as to the suitability of the water for borehole infiltration methods.

Soil-water temperature varied due to changes in the temperature of the water supply. Diurnal temperature increases and decreases corresponded to respective decreases and increases in infiltration rate, even after correcting for viscosity. Correlation of minimum borehole water temperature with maximum infiltration rate appeared most evident when tap water was used for infiltration. Infiltration fluctuation was observed to increase with test duration. This increase might be associated with an increased mean daily temperature of the infiltration water. While it is suggested that increase

fluctuations might be attributed to increased entrapped gases around the borehole, there are no conclusive measurements to support this.

Measurement of Ks during stage 2 steady state (tap water) compared favorably with the stage 1 (groundwater) early time Ks measurement made when pressure heads close to the borehole indicated the wettest conditions. Future borehole tests, where clogging of the formation appears evident with time, might use the infiltration rate when pressure heads are maximum as a value of steady state for calculation purposes.

While laboratory investigations indicated that Ks decreased with depth below the borehole, Ks measurements during stage 2 calculated from the USBR shallow water table equation were within the range of laboratory measured vertical Ks values of that material adjacent to the screened interval of the borehole.

Pumping of the shallow water table during infiltration did not increase the value of Tu enough to convert the flow field from shallow to deep water table conditions, as defined by the USBR(1974). Lowering of the water table increased gradients around the borehole, but Qs decreased; the net result was a decrease in Ks. The reduction in flow rate may be due to changes in flow direction outside the borehole and soil anisotropy. Flow paths from the borehole became more vertical (perpendicular to bedding) after pumping began. As a several order of magnitude range of Ks at various depths outside the borehole was indicated in laboratory experiments,

a vertical Ks would be considerably lower than a horizontal Ks because of sedimentary layering.

RECOMMENDATIONS FOR FUTURE RESEARCH

A small experiment to better compare the shelby tube and PF ring permeameters might be to sample 2 soil profiles that are very close to each other. Two sampling locations could be used at the Sevilleta National Wildlife Refuge investigation site where soils have been shown to be relatively homogeneous and isotropic (Andrews, 1983). If the sampling locations were within 30 cm of each other and one site utilized PF samples and the other used shelby tubes, a minimization of spatial variability effects might be realized. The shelby tube samples should be manometer equipped such that the center of each sample within the shelby tube would correlate in depth with the center of each PF ring sample. Also, distilled or 0.01N $CaCl_2$ water would be recommended for the system to eliminate any possible interfering effects that might be encountered when using groundwater.

Future tests to evaluate the USBR solutions for deep and shallow water table conditions should by made with different initial Tu values rather then by pumping, unless increased pump capacity becomes available. These tests could be carried out at site 8 during different times of the year when depth to water varies with the agricultural season.

During future borehole tests, the infiltrating water should be analyzed for any compounds that may come out of

solution as a gas when temperature fluctuations are encountered.

Additional work might be done on the temperature sensitivity of the tensiometer apparatus. A small test might be to construct a "null" tensiometer unit. This would differ from a regular unit in that it would contain no porous cup and need only extend below ground about one foot. If a vacuum was first applied to this unit, then the vacuum should remain constant; barring leaks and temperature effects. This unit could be read during a borehole test along with the other units at no extra effort.

Another interesting test would be a temperature calibration of the neutron probe device. This would be carried out using a 55 gal. drum of a homogeneous sand with a neutron access tube in the center. The tube must be sealed on the bottom. The drum would be filled with water to cause saturated conditions. Measurements of saturated moisture contents could be made at different ambient temperatures to determine instrumentation sensitivity.

REFERENCES CITED

Andrews, E. 1982. Geologic predictors of saturated hydraulic conductivity in the fluvial sand of the Sevilleta Wildlife Refuge. Independent Study, New Mexico Institute of Mining and Technology.

Bouwer, H. 1978. Groundwater Hydrology. McGraw-Hill Inc., New York, 480pp.

Bouwer, H., and R.D. Jackson. 1974. Determining soil properties, in Drainage for Agriculture. J. van Schilfgaarde (ed.). American Society Agronomy, Monograph 17: 611-672.

Chahal, R.S. 1965. Effect of Temperature and Trapped Air on Matric Suction. Soil Sci., V.100: 262-266.

Day, P.R. 1956. "Particle Fractionation and Particle-Size Analysis." in Methods of Soil Analysis, Black, et al. (eds.), Amer. Soc. Agron., Monograph No.9: 545-567.

Gupta, R.P., and D. Swartzendruber. 1962. Flow-associated reduction in the hydraulic conductivity of quartz sand. Soil Sci. Soc. Amer. Proc., V.26: 6-10.

Hillel, D. 1980. Fundamentals of Soil Physics. Academic Press, New York, 413pp.

Lambert, K.A. 1982. The Effects of Carbon Dioxide Flooding on Constant Head Borehole Infiltration tests. Independent Study, New Mexico Institute of Mining and Technology.

Larson, M.B. A Comparison of Empirical/Theoretical, Laboratory, anf Field Techniques in Evaluating Unsaturated Hydraulic Properties of Mill Tailings. Independent Study, New Mexico Institute of Mining and Technology.

Reynolds, W.D., Elrick, D.E., Topp, G.C., 1983, A Re-examination of the Constant Head Well Permeameter Method for Measuring Saturated Hydraulic Conductivity Above the Water Table, Soil Sci., 136(4):250-268.

Riggs, C.O., Soil Sampling in the Vadose Zone. Conference on Characterization and Monitoring of the Vadose (Unsaturated) Zone. Las Vegas, Nevada, December 8, 1983.

Stephens, D.B. 1979. Analysis of constant head borehole infiltration tests in the vadose zone. Ph.D. dissertation, University of Arizona, Tucson, Arizona.

Stephens, D.B. and Neuman, S.P. 1982b. Vadose zone permeability tests: steady state. Amer. Soc. Civ. Engrs. Proc., J. Hyd. Div. 108(HY5):640-659.

Stephens, D.B., Neuman, S.P., Tyler, S., Lambert, K., Watson, D., Rabold, R., Knowlton, R., Byers, E., and Yates, S., 1983, Insitu Determination of Hydraulic Conductivity in the Vadose Zone Using Borehole Infiltration Tests, Technical Completion Report, Project B-073-NMEX, Water Resources Research Institute, Las Cruces, New Mexico, 165pp.

Stephens, D.B., S. Tyler, K. Lambert, and S. Yates. 1982. Field experiments to determine saturated hydraulic conductivity in the vadose zone, in Role of the Unsaturated Zone in Radioactive and Hazardous Waste Disposal, Mercer, et al. (eds.), Ann Arbor Science Publishers, Ann Arbor, Michigan, 339pp.

Todd, D.K. 1980. Groundwater Hydrology. second edition, John Wiley and Sons, New York, 535pp.

Watson, D.B., 1983 The Effect of Head on Constant Head Borehole Infiltration Tests and Other Related Flow Phenomenon, New Mexico Institute of Mining and Technology.

U.S. Bureau of Reclamation. 1974. Earth Manual, second edition, U.S. Government Printing Office, Washington, D.C., 310pp.

APPENDICES

Appendix A

Shelby Tube Sample Preparation and Permeameter Operation.

1. Before Sampling

Old shelby tubes (reused) are to be clean inside and free of rust and debris. This is accomplished using a circular wire brush on an extension and powered by a portable drill. New tubes are shipped with a residual machine oil coating, to prevent rust, which must be removed either with a solvent and then detergent or just detergent. It is important that if a solvent is used, that all traces of this are removed.

After the tubes are cleaned and dried, an immediate inner coating of a durable rust preventive is applied before oxidation sets in. A polyurethane wood coating worked successfully in these experiments, but any material designed to prevent rust might work if immune to water contact.

2. During Sampling

Assurance of a good sample retrieval depends on several factors:

a) a good vacuum within the sampling apparatus at retrieval,

b) careful shelby tube handling during retrieval, and

c) the ability of the sampled zone to lend itself to shelby tube sampling techniques.

A good vacuum in the sapling device is achieved by a thorough cleaning of the check valve in the shelby tube head prior to sampling. Careful handling necessitates not jarring

the shelby tube in the hole or banging it against the hole walls. After removal from the hole, the shelby tube and head are removed from the drill string and the bottom of the shelby tube is taped (masking tape works good) to prevent sample loss. The shelby tube is kept in an upright vertical orientation and the sample head is removed. At this time, the length of sample is calculated and it is determined if the sample is a good one. If the sample is acceptable, the top of the shelby tube is taped and the sample and tube are transported to the lab in this upright position to prevent sample dislodging.

3. Lab Preparation

Back in the lab, the tape is first removed from the top of the tube (end with holes) keeping the tube in the upright position. The condition of the top of the sample is observed and if heavily cracked or compacted, the top few centimeters may be shaved off. The sample length is divided into the desired number of dL values. The shelby tube is drilled at sample segment centers and manometers consisting of a 7 or 8 cm length of small diameter copper tubing are inserted to the sample segment center. A number 44 (minimum) hose clamp, and 2 rubber gaskets (inner tube material) are inserted over the copper tubing and tightened. A number 13.5 rubber stopper (with some means of retrieval attached) is now pushed into the top of the shelby tube to secure the sample and the tube is laid on its' side. The tape is now removed from the bottom of

the sample. If the sample exposed is a dry non-cohesive sand, a small amount of water is squirted on the sample to provide cohesion. Next a circular, fine mesh stainless or brass screen of are equal to the shelby tube is pushed against the sample and a 15 cm by 15 cm square of fiberglass window screen material is centered over the first screen and pulled up around the shelby tube. These two screens are held in place by double wrapping a gasket of 1 cm by 23 cm innertube material around the screen and taping it in place. Next the outflow collector (cut off vinegar bottle) is placed over the gasket and secured with a hose clamp (number 44). The sample, when positioned upright with top stopper removed, is now ready to be clamped into the permeameter rack. This procedure involves a 3" U-bolt lower clamp and a 3" sandwich clamp on top (these clamps are just 3" muffler clamps from the local automotive store). After the manometered sample is tightened into the rack, a triple wrapping of duct tape around the tube top covers the 4 holes and provides a gasket for the inflow connection. A one liter round plastic bottle with the bottom cut out will slide over the tube and duct tape and when clamped into place, will provide a water-tight seal. Tygon hose from the CO2 flooding regulator is connected to the bottle as follows: a small rubber stopper, with a copper tube inserted through the center, is inverted and placed in the plastic bottle before the bottle is clamped to the shelby tube. The tygon tubing is connected to the copper tubing in the stopper through the bottle top. With the bottle clamped

into place, an attempt to pull the rubber stopper via the tygon tubing through the bottle top will provide a water/gas tight seal that will get tighter with increased internal system pressure.

The appropriate number of plastic manometer tubes are primed with water, clamped shut near the shelby ends, and placed over the copper tubes. A small amount of water is allowed to flow from the plastic tubes to fill the copper tubing lengths. The reason for this initial manometer priming is due to the long nature of the plastic manometer tubes to and up the manometer board. If these are allowed to fill from inflow to the sample, sample loss through the manometer and manometer clogging will occur. With the manometer tubes primed and clamped and in place, the sample is now ready for CO2 flooding at the minimum pressure to provide acceptable flow rates.

4. Shelby Tube Permeameter Procedure

While the sample is being purged with CO2, the constant head device and water reservoir are made ready. Depending on the amount of lift required to the constant head device, water can be pumped using either a swamp-cooler pump (good for about 2.5 meters lift) or one of the (inhouse) Masterflex tubing pump systems. The Masterflex pump was opted for during this study because of its good lift capabilities (4 m). Using the Masterflex requires special long life tubing in the pump head; recommended material here is the silicone

tubing.

The six discharge hoses from the constant head tank are clamped shut, the over-flow tube is positioned into the collector reservoir and the pump is turned on to establish a constant head in the tank which is now available to the shelby samples.

A float-valved water supply from a 45 l carboy was also positioned in the collector reservoir (sitting on the floor) to maintain a constant amount of water in the recirculating water systems.

After CO2 flooding, a water supply line is connected to the stopper at the top of the shelby. The stopper is loosened and the tube and stopper is advanced into the shelby close to the sample top. By opening the clamped water supply line, water is allowed to drip slowly on the sample until ponding when the plastic bottle fills to overflowing. Now the stopper is pulled tightly into place and the desired head is applied. When the sample produces a value of Q from the drip bottle, the manometer clamps can be removed and the water levels left to equilibrate. This inflow of water from the manometers into the sample provided soil-free manometer lines.

Time zero was noted when an initial value of Q is produced. Thereafter, values of dLi, dHi and Q are recorded as a function of time to be used in equation 5.

Disassembly and removal of sample from the shelby is easiest soon after stopping inflow.

Appendix B

This appendix contains the materials list and plans for the construction of the USBR Carburetor Float Valve.

CARBURETOR FLOAT VALVE MATERIALS LIST

Quantity	Description
42 inches	1/8 - by 3/4-inch brass or aluminum strap
8-1/4 inches	3/8-inch outside-diameter tubing, brass o aluminum
1 set	John Deere Model "D" tractor meedle valve and seat, Part No. AR10113R
4 each	3/8-inch flat-head 8-32 bolt, stainless steel
1 each	1-inch round-head 10-32 bolt, stainless steel
5 each	10-32 hex mut, stainless steel
4 inches	2-1/2-inch-diameter styrofoam cylinder (seal of not closed cell material
2 each	6-inch - 3/16-inch-diameter aluminum rod (spec. 20-24-T4)
1 each	2-1/2-inch-diameter - 1/8-inch thick aluminum base plate (spec. 20-24-T4)
4 each	3/16-inch washer, stainless steel or brass

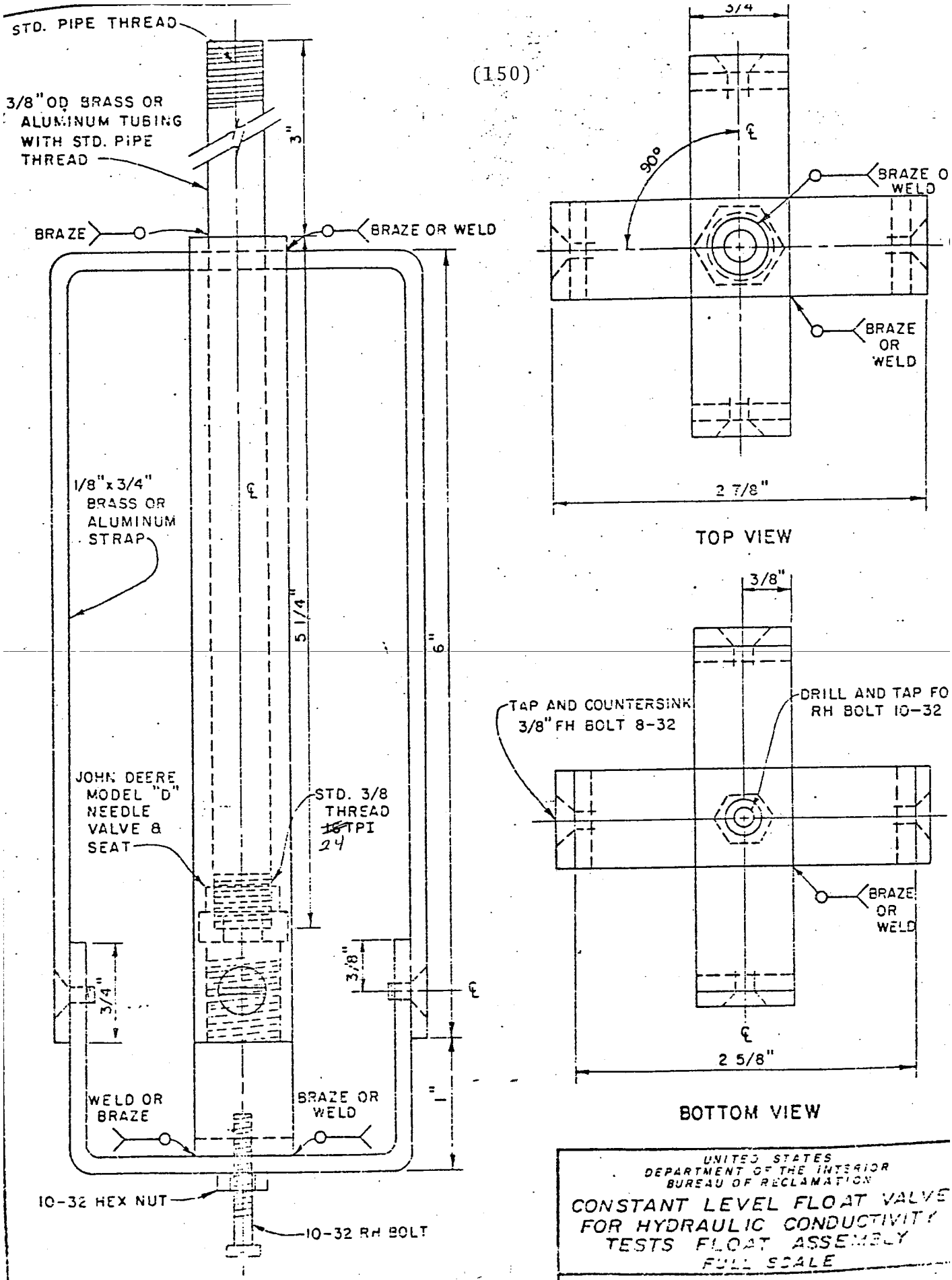

UNITED STATES
DEPARTMENT OF THE INTERIOR
BUREAU OF RECLAMATION

CONSTANT LEVEL FLOAT VALVE FOR HYDRAULIC CONDUCTIVITY TESTS FLOAT ASSEMBLY

FULL SCALE

DRAWN
TRACED
CHECKED

DATE: 2-7-67

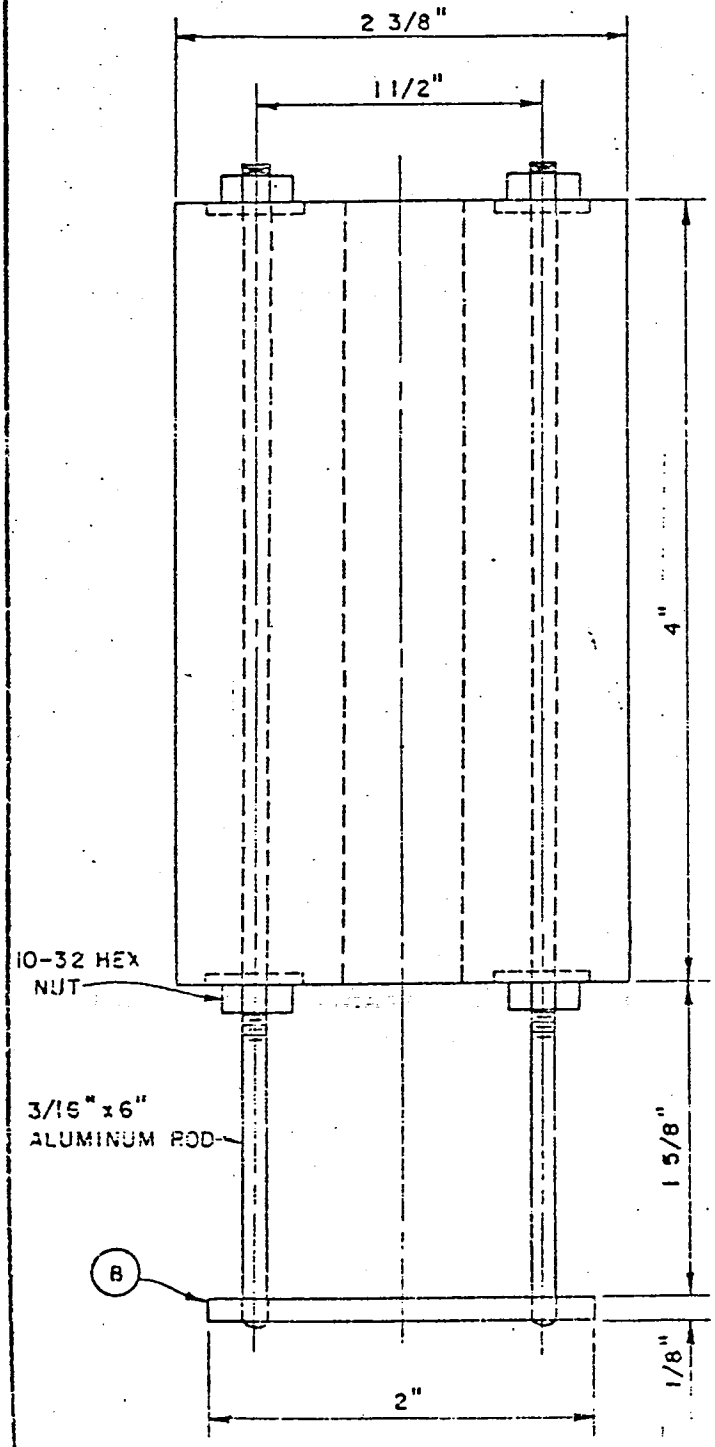

FLOAT ASSEMBLY

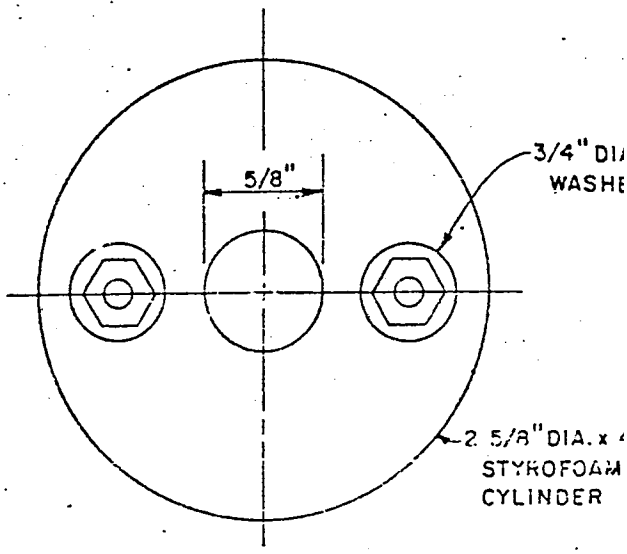

TOP VIEW

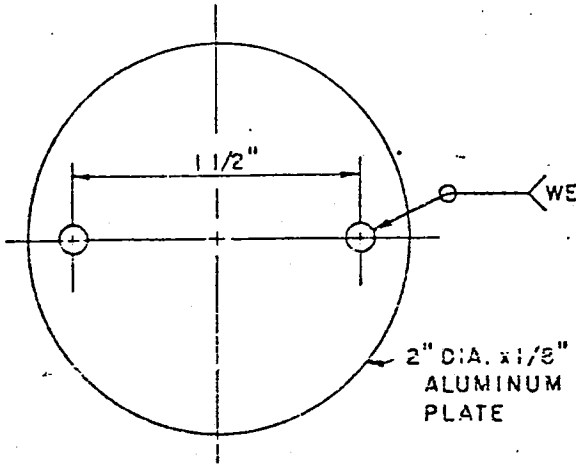

DETAIL B BASE PLATE

UNITED STATES
DEPARTMENT OF THE INTERIOR
BUREAU OF RECLAMATION

CONSTANT LEVEL FLOAT VALVE FOR HYDRAULIC CONDUCTIVITY TESTS FLOAT ASSEMBLY
FULL SCALE

DRAWN
TRACED
CHECKED
DATE: 2-7-67
SHEET 2 OF

Appendix C

SOIL-WATER CHARACTERISTIC DATA
DEPTH = 112.5 cm Radius = 60 cm

THETA	PSI(cm H_2O)
0.401	0.0
0.401	40.6
0.401	50.4
0.401	73.9
0.401	99.7
0.394	147.0
0.394	186.0
0.394	1017.0
0.375	2644.0
0.372	4963.0
0.366	15357.0

SOIL-WATER CHARACTERISTIC DATA
D = 121.0 cm R = 60 cm

THETA	PSI (cm H_2O)
0.515	0.0
0.515	40.5
0.512	50.0
0.505	74.2
0.501	101.0
0.498	509.0
0.473	1017.0
0.441	2644.0
0.421	4963.0
0.412	10323.0
0.412	15357.0

VG2.DAT

SOIL-WATER CHARACTERISTIC DATA
D = 129.5 cm R = 60 cm

THETA	PSI (cm H_2O)
0.557	0.0
0.551	11.1
0.548	20.4
0.545	30.7
0.538	40.2
0.526	49.7
0.515	75.0
0.508	100.0
0.503	150.0
0.468	509.0
0.453	1017.0
0.422	2644.0
0.401	4963.0
0.400	10323.0
0.400	15357.0

SOIL-WATER CHARACTERISTIC DATA
D=143.5 cm R=30 cm

THETA	PSI(cm H_2O)
0.380	0.0
0.374	9.7
0.363	18.8
0.357	24.0
0.329	29.8
0.312	39.1
0.296	49.0
0.279	59.9
0.253	75.6
0.222	98.2
0.191	149.0
0.183	184.0
0.177	203.0
0.163	324.0
0.160	528.0
0.140	1526.0
0.128	3966.0
0.122	7017.0
0.117	10984.0
0.114	15031.0

SOIL-WATER CHARACTERISTIC DATA
D=159.5 cm R=30 cm

THETA	PSI(cm H_2O)
0.373	0.0
0.370	10.5
0.364	20.8
0.362	22.9
0.343	28.9
0.324	38.1
0.308	46.4
0.292	58.3
0.208	75.0
0.243	99.7
0.217	150.0
0.209	188.0
0.208	203.0
0.193	324.0
0.180	528.0
0.164	1526.0
0.149	3966.0
0.143	7017.0
0.138	10984.0
0.135	15031.0

V61.DAT

SOIL-WATER CHARACTERISTIC DATA
D=166.5 cm R=30 cm

THETA	PSI(cm H_2O)
0.372	0.0
0.372	21.2
0.363	29.2
0.349	37.5
0.338	49.9
0.336	61.4
0.317	77.5
0.301	98.2
0.276	148.0
0.253	194.0
0.245	203.0
0.218	324.0
0.215	528.0
0.175	1526.0
0.157	3966.0
0.148	7017.0
0.143	10984.0
0.140	15031.0

SOIL-WATER CHARACTERISTIC DATA
D=175.5 cm R=30 cm

THETA	PSI(cm H_2O)
0.405	0.0
0.397	30.0
0.387	39.3
0.376	49.2
0.353	72.7
0.336	98.5
0.317	149.0
0.314	196.0
0.272	509.0
0.243	1017.0
0.209	2644.0
0.184	4963.0
0.183	10323.0
0.183	15357.0

V64.DAT

SOIL-WATER CHARACTERISTIC DATA
D=182.5 cm R=30 cm

THETA	PSI(cm H_2O)
0.444	0.0
0.444	20.7
0.435	30.5
0.426	39.6
0.416	49.5
0.400	73.5
0.388	99.7
0.373	149.0
0.305	509.0
0.265	1017.0
0.221	2644.0
0.211	4963.0
0.201	10323.0
0.201	15255.0

SOIL-WATER CHARACTERISTIC DATA
D=189.5 cm R=30 cm

THETA	PSI(cm H_2O)
0.427	0.0
0.427	31.1
0.421	40.6
0.407	49.2
0.379	72.8
0.362	99.8
0.344	149.0
0.340	186.0
0.284	509.0
0.243	1017.0
0.199	2644.0
0.173	4963.0
0.165	10323.0
0.152	15357.0

SOIL-WATER CHARACTERISTIC CURVE
D=197.5 cm R=30 cm

THETA	PSI(cm H_2O)
0.458	0.0
0.456	30.9
0.457	40.8
0.453	50.6
0.443	75.4
0.438	101.0
0.432	150.0
0.428	205.0
0.395	509.0
0.352	1017.0
0.288	2644.0
0.250	4963.0
0.240	10323.0
0.240	15357.0

SOIL-WATER CHARACTERISTIC DATA
D=203.5 cm R=30 cm

THETA	PSI(cm H_2O)
0.416	0.0
0.416	40.2
0.415	50.7
0.405	74.6
0.390	99.0
0.370	147.0
0.361	191.0
0.302	509.0
0.264	1017.0
0.221	2644.0
0.183	4963.0
0.179	10323.0
0.178	15357.0

SOIL-WATER CHARACTERISTIC DATA
D=218.5 cm R=30 cm

THETA	PSI(cm H_2O)
0.413	0.0
0.413	20.7
0.409	29.9
0.387	38.7
0.350	46.5
0.221	61.4
0.170	76.4
0.142	98.7
0.129	131.0
0.112	171.0
0.104	211.0
0.045	15255.0
0.108	165.0
0.109	142.0
0.114	112.0
0.119	92.1
0.130	76.3
0.144	68.4
0.151	62.7
0.164	53.7
0.190	45.8
0.234	37.5
0.272	31.2
0.312	24.6
0.350	14.2
0.350	0.0

SHELBY TUBE PERMEAMETER
HYDRAULIC CONDUCTIVITY DATA
VISCOSITY CORRECTED TO 20° C

SHELBY TUBE SAMPLE 1, NORTH PROFILE

DEPTH (cm)	27.7 to 41.7	41.7 to 51.7	51.7 to 62.0	62.0 to 72.3	72.3 to 82.6	82.6 to 92.7
TIME (hrs)	**********		K (cm /sec)	**********		
1.33	1.34E-02	8.49E-03	1.45E-02	1.54E-02	1.51E-02	
3.00	1.24E-02	8.08E-03	1.25E-02	1.49E-02	1.48E-02	1.40E-02
9.03	9.79E-03	7.79E-03	1.29E-02	1.48E-02	1.42E-02	1.39E-02
20.42	8.02E-03	7.70E-03	1.31E-02	1.50E-02	1.58E-02	1.27E-02
44.05	5.51E-03	7.00E-03	1.29E-02	1.49E-02	1.46E-02	1.36E-02
54.58	3.60E-03	7.87E-03	1.26E-02	1.51E-02	1.53E-02	1.43E-02
68.42	2.92E-03	7.95E-03	1.29E-02	1.48E-02	1.51E-02	1.37E-02
75.08	2.41E-03	7.75E-03	1.33E-02	1.45E-02	1.59E-02	1.28E-02
79.58	1.32E-02	8.44E-03	1.36E-02	1.47E-02	1.44E-02	1.25E-02
91.75	8.29E-03	1.08E-02	9.71E-03	1.44E-02	1.40E-02	1.18E-02
103.90	8.49E-03	8.42E-03	1.35E-02	1.44E-02	1.44E-02	1.30E-02
114.90	7.72E-03	8.30E-03	1.35E-02	1.42E-02	1.41E-02	1.23E-02
126.20	6.08E-03	8.16E-03	1.33E-02	1.42E-02	1.39E-02	1.19E-02
138.70	5.30E-03	8.25E-03	1.34E-02	1.42E-02	1.41E-02	1.13E-02
163.40	4.30E-03	8.29E-03	1.35E-02	1.42E-02	1.42E-02	1.20E-02
187.40	3.54E-03	8.20E-03	1.34E-02	1.43E-02	1.41E-02	1.15E-02
212.20	3.10E-03	8.13E-03	1.33E-02	1.41E-02	1.41E-02	1.10E-02

SHELBY TUBE SAMPLE 2, NORTH PROFILE

DEPTH (cm)	134.6 to 146.1	146.1 to 157.6	157.6 to 169.0	169.0 to 180.5	180.5 to 192.0	192.0 to 203.5
TIME (hrs)	**********		K (cm /sec)	**********		
3.47	2.16E-02	6.47E-02	1.28E-02	6.04E-04	1.61E-04	8.28E-05
7.78	2.50E-02	3.34E-02	1.59E-02	9.49E-04	3.42E-04	4.19E-04
20.30	2.32E-02	4.64E-02	1.44E-02	1.01E-03	3.71E-04	5.60E-04
32.38	2.23E-02	3.18E-02	1.38E-02	9.69E-04	3.57E-04	5.36E-04
43.13	2.16E-02	3.09E-02	1.20E-02	9.40E-04	3.44E-04	5.26E-04
54.38	1.94E-02	3.05E-02	1.16E-02	9.25E-04	3.41E-04	5.21E-04
67.13	1.83E-02	2.88E-02	1.17E-02	8.75E-04	3.23E-04	4.87E-04
91.63	1.75E-02	2.50E-02	1.09E-02	7.85E-04	2.85E-04	4.00E-04
115.63	1.39E-02	2.32E-02	8.62E-03	6.88E-04	2.28E-04	3.10E-04
140.63	1.30E-02	1.75E-02	7.59E-03	6.00E-04	1.97E-04	2.73E-04
164.30	1.49E-02	2.99E-02	6.24E-03	5.80E-04	1.92E-04	2.67E-04
168.13	1.52E-02	2.43E-02	8.59E-03	5.83E-04	1.93E-04	2.76E-04

SHELBY TUBE SAMPLE 3, NORTH PROFILE

DEPTH (cm)	210.8 to 222.3	222.3 to 234.1	234.1 to 245.8	245.8 to 257.3	257.3 to 269.1
TIME (hrs)	**********	**********	K (cm /sec)	**********	**********
0.20	9.89E-03	1.47E-03	3.28E-04	2.62E-04	3.86E-03
5.07	1.11E-02	9.32E-04	3.33E-04	2.50E-04	3.65E-03
10.90	6.08E-03	8.04E-04	3.67E-04	2.48E-04	3.69E-03
22.73	5.23E-03	6.98E-04	3.65E-04	2.37E-04	3.44E-03
29.93	4.86E-03	6.61E-04	3.48E-04	2.29E-04	3.36E-03
48.85	4.48E-03	6.07E-04	3.50E-04	2.25E-04	3.28E-03
54.40	4.37E-03	5.93E-04	3.37E-04	2.22E-04	3.21E-03
70.57	4.23E-03	5.81E-04	3.53E-04	2.24E-04	3.27E-03
81.90	5.78E-03	4.18E-04	2.14E-04	3.91E-04	3.26E-03
94.24	4.72E-03	3.83E-04	2.13E-04	3.62E-04	4.84E-03
119.57	4.20E-03	3.42E-04	2.05E-04	3.44E-04	4.45E-03
127.65	4.06E-03	3.33E-04	1.98E-04	3.36E-04	4.33E-03
143.57	4.05E-03	3.18E-04	1.90E-04	3.35E-04	4.24E-03
166.57	4.03E-03	2.98E-04	2.01E-04	3.34E-04	4.21E-03
171.65	3.84E-03	2.75E-04	1.88E-04	3.15E-04	3.87E-03

SHELBY TUBE SAMPLE 4, SOUTH PROFILE

DEPTH (cm)	33.0 to 41.6	41.6 to 50.9	50.9 to 59.9	59.9 to 68.9	68.9 to 78.4
TIME (hrs)	**********	**********	K (cm /sec)	**********	**********
0.03	2.58E-02	2.92E-03	1.06E-02	1.53E-02	2.63E-02
4.42	1.62E-02	2.14E-03	1.13E-02	1.70E-02	1.99E-02
11.25	1.35E-02	1.80E-03	1.16E-02	1.83E-02	1.97E-02
22.17	2.96E-03	1.80E-03	1.12E-02	1.80E-02	1.83E-02
29.29	2.81E-03	1.83E-03	1.13E-02	1.81E-02	1.86E-02
48.20	1.99E-03	1.74E-03	1.12E-02	1.80E-02	1.77E-02
53.75	1.86E-03	1.74E-03	1.11E-02	1.81E-02	1.80E-02
69.92	1.72E-03	1.80E-03	1.11E-02	1.81E-02	1.80E-02
81.25	2.04E-02	9.91E-04	1.10E-02	1.67E-02	1.93E-02
93.59	8.40E-03	8.48E-04	1.12E-02	1.75E-02	1.83E-02
118.92	5.54E-03	7.44E-04	1.08E-02	1.64E-02	1.92E-02
127.00	4.80E-03	7.32E-04	1.08E-02	1.73E-02	1.80E-02
142.92	4.35E-03	7.11E-04	1.09E-02	1.71E-02	1.83E-02
165.92	3.85E-03	6.76E-04	1.08E-02	1.70E-02	1.76E-02
171.09	3.87E-03	6.98E-04	1.08E-02	1.66E-02	1.79E-02

SHELBY TUBE SAMPLE 5, SOUTH PROFILE

DEPTH (cm)	154.9 to 163.6	163.6 to 172.3	172.3 to 181.0	181.0 to 189.9
TIME (hrs)	**********	K (cm /sec)	**********	
2.17	5.66E-03	2.56E-03	1.70E-03	8.04E-02
8.00	3.31E-03	1.59E-03	2.48E-03	4.15E-02
19.93	2.02E-03	1.32E-03	3.13E-03	4.91E-02
27.08	1.57E-03	1.29E-03	3.11E-03	3.19E-02
46.08	1.13E-03	1.18E-03	3.01E-03	3.19E-02
51.58	1.07E-03	1.15E-03	2.96E-03	2.82E-02
67.66	9.30E-04	1.13E-03	3.02E-03	2.75E-02
79.16	8.86E-04	1.04E-03	2.68E-03	2.26E-02
91.33	7.70E-04	1.02E-03	2.77E-03	2.72E-02
116.66	6.12E-04	9.45E-04	2.72E-03	1.95E-02
124.83	5.86E-04	9.16E-04	2.68E-03	1.84E-02
140.75	5.47E-04	8.95E-04	2.65E-03	1.75E-02
163.75	5.07E-04	8.75E-04	2.73E-03	1.25E-02

SHELBY TUBE SAMPLE 6, SOUTH PROFILE

DEPTH (cm)	214.4 to 224.5	224.5 to 234.5	234.5 to 244.9	244.9 to 254.9	254.9 to 265.0	265.0 to 275.3
TIME (hrs)	**********	**********	K (cm /sec)	**********	**********	**********
4.83	1.21E-02	1.20E-02			8.62E-04	8.62E-04
16.42	5.64E-03	8.49E-03	1.38E-02	5.77E-04	2.96E-04	7.03E-04
23.58	4.42E-03	6.86E-03	1.43E-02	8.61E-04	2.49E-04	6.89E-04
43.00	3.39E-03	6.00E-03	1.22E-02	2.10E-04	1.90E-04	6.39E-04
48.08	3.22E-03	5.89E-03	1.20E-02	3.13E-04	2.00E-04	6.69E-04
64.16	2.99E-03	5.74E-03	1.12E-02	6.13E-04	1.84E-04	6.39E-04
75.66	3.15E-03	1.09E-02	1.10E-02	6.17E-04	3.56E-04	1.73E-03
87.83	5.84E-03	8.97E-03	9.58E-03	5.89E-04	2.06E-04	1.20E-03
113.16	4.28E-03	6.75E-03	7.25E-03	9.00E-04	1.11E-04	7.78E-04
121.33	3.90E-03	6.15E-03	7.59E-03	9.80E-04	9.95E-05	7.17E-04
137.25	3.48E-03	5.94E-03	6.39E-03	1.19E-03	8.44E-05	6.30E-04
160.25	2.91E-03	5.77E-03	6.46E-03	1.57E-03	7.47E-05	5.88E-04

SHELBY TUBE SAMPLE 7, WEST PROFILE

DEPTH (cm)	16.5 to 25.7	25.7 to 34.9	34.9 to 43.9	43.9 to 52.9	52.9 to 61.9	61.9 to 71.1
TIME (hrs)	**********	**********	**********	K (cm /sec)	**********	**********
1.42	4.08E-03	5.00E-03	1.13E-02	1.30E-02	1.28E-02	3.30E-02
7.58	2.69E-03	6.45E-03	1.01E-02	1.30E-02	1.20E-02	3.39E-02
17.67	2.05E-03	5.73E-03	9.96E-03	1.31E-02	1.27E-02	3.45E-02
25.92	1.88E-03	5.25E-03	9.74E-03	1.27E-02	1.24E-02	3.33E-02
31.17	1.66E-03	4.97E-03	9.91E-03	1.27E-02	1.24E-02	4.56E-02
42.08	1.40E-03	4.67E-03	9.84E-03	1.26E-02	1.23E-02	3.71E-02
49.58	1.38E-03	4.61E-03	9.67E-03	1.26E-02	1.23E-02	3.99E-02
55.00	1.36E-03	4.63E-03	9.97E-03	1.32E-02	1.30E-02	3.83E-02
65.75	1.16E-03	4.21E-03	9.11E-03	1.22E-02	1.21E-02	1.91E-02
90.67	7.48E-04	3.99E-03	8.78E-03	1.24E-02	1.22E-02	2.78E-02
102.00	6.22E-04	3.87E-03	8.79E-03	1.23E-02	1.21E-02	2.70E-02
117.00	5.00E-04	3.76E-03	8.44E-03	1.20E-02	1.17E-02	2.66E-02
126.80	4.64E-04	3.87E-03	8.63E-03	1.22E-02	1.20E-02	2.86E-02
138.00	4.67E-04	3.76E-03	8.76E-03	1.24E-02	1.21E-02	2.91E-02
162.20	9.77E-04	3.99E-03	8.73E-03	1.20E-02	1.18E-02	3.34E-02
185.80	9.69E-04	4.00E-03	8.65E-03	1.21E-02	1.20E-02	3.56E-02
193.90	9.76E-04	4.03E-03	8.83E-03	1.22E-02	1.22E-02	3.95E-02

SHELBY TUBE SAMPLE 8, WEST PROFILE

DEPTH (cm)	134.7 to 143.4	143.4 to 152.1	152.1 to 160.9	160.9 to 169.5	169.5 to 178.2	178.2 to 186.8
TIME (hrs)	**********	**********	K (cm /sec)	**********	**********	**********
0.33	1.12E-02	3.89E-02	8.60E-02	7.92E-02	2.04E-02	1.06E-02
6.33	6.17E-03	3.20E-02	7.13E-02	6.33E-02	1.14E-02	9.41E-03
11.67	5.07E-03	3.02E-02	3.29E-02	2.75E-02	7.23E-03	7.71E-03
22.42	4.20E-03	2.90E-02	2.41E-02	2.13E-02	6.24E-03	6.93E-03
30.02	3.69E-03	2.71E-02	2.31E-02	1.97E-02	5.50E-03	6.10E-03
36.00	3.40E-03	2.73E-02	2.20E-02	1.93E-02	5.32E-03	5.91E-03
46.00	3.05E-03	2.70E-02	2.22E-02	1.93E-02	5.02E-03	5.65E-03
71.25	2.34E-03	2.59E-02	2.26E-02	1.79E-02	4.51E-03	5.05E-03
82.50	2.10E-03	2.58E-02	2.26E-02	1.77E-02	4.10E-03	4.60E-03
98.08	1.84E-03	2.56E-02	2.21E-02	1.72E-02	3.92E-03	4.39E-03
107.30	1.71E-03	2.59E-02	2.22E-02	1.73E-02	3.79E-03	4.27E-03
118.70	1.54E-03	2.57E-02	2.18E-02	1.71E-02	3.62E-03	4.09E-03
142.60	1.75E-03	2.30E-02	2.28E-02	1.65E-02	4.59E-03	4.97E-03
166.20	1.35E-03	2.20E-02	2.28E-02	1.60E-02	4.20E-03	4.70E-03
174.20	1.32E-03	2.26E-02	2.31E-02	1.59E-02	3.89E-03	4.33E-03

SHELBY TUBE SAMPLE 9, WEST PROFILE

DEPTH (cm)	190.5 to 199.5	199.5 to 208.5	208.5 to 217.6	217.6 to 226.4	226.4 to 235.4	235.4 to 244.5
TIME (hrs)	**********	**********	K (cm /sec)	**********	**********	**********
1.83	2.57E-02	5.13E-03	2.59E-02	1.94E-04	2.61E-05	4.80E-04
6.75	3.74E-02	4.68E-03	1.20E-02	2.39E-04	3.92E-05	7.01E-04
17.83	1.80E-02	4.70E-03	1.27E-02	1.99E-04	4.12E-05	6.23E-04
25.17	2.17E-02	4.83E-03	1.47E-02	2.25E-04	4.81E-05	6.38E-04
41.33	2.12E-02	4.23E-03	1.07E-02	2.13E-04	4.69E-05	7.14E-04
66.83	9.48E-03	7.90E-03	1.20E-02	1.36E-04	4.08E-05	6.84E-04
78.08	7.63E-03	8.90E-03	1.06E-02	1.53E-04	4.63E-05	7.71E-04
93.58	8.13E-03	6.10E-03	1.23E-02	1.37E-04	4.25E-05	7.47E-04
102.80	9.21E-03	6.91E-03	1.40E-02	1.54E-04	4.83E-05	8.34E-04
114.20	6.64E-03	6.64E-03	1.34E-02	1.47E-04	4.60E-05	7.69E-04
136.10	1.21E-02	5.52E-03	6.14E-03	1.01E-04	3.30E-05	9.75E-04
161.70	6.73E-03	5.51E-03	6.81E-03	1.05E-04	3.32E-05	1.02E-03
169.70	5.35E-03	5.35E-03	6.61E-03	1.04E-04	3.21E-05	1.01E-03

PF RING PERMEAMETER
HYDRAULIC CONDUCTIVITY DATA
VISCOSITY CORRECTED TO 20°C

D=112.5 cm TIME(min)	R=60 cm K(cm/sec)
6398	1.97E-6
7063	2.21E-6
7744	2.33E-6
8444	6.01E-6
9207	4.56E-6
13281	1.19E-6
14706	2.83E-6
16158	1.79E-6

D=121.0 cm TIME(min)	R=60 cm K(cm/sec)
5720	1.80E-5
6398	1.35E-5
7064	1.53E-5
7745	1.54E-5
8445	1.94E-5
9208	1.55E-5
10673	1.17E-5
13281	1.19E-5
14708	1.56E-5
16159	1.22E-5

D=129.5 cm TIME(min)	R=60 cm) K(cm/sec)
7746	6.22E-7
8446	1.06E-6
10673	3.51E-7
14709	7.92E-7

D=143.5 cm TIME(min)	R=30 cm K(cm/sec)
960	1.98E-3
2460	2.20E-3
3900	2.56E-3
5340	3.44E-3
6780	3.57E-3
8180	4.27E-3
9707	4.36E-3
11515	5.24E-3
12615	5.38E-3
13935	5.92E-3
15425	6.03E-3
16810	6.02E-3

D=159.5 cm TIME(min)	R=30 cm K(cm/sec)
960	1.69E-2
2460	1.55E-3
3900	1.91E-3
5340	1.55E-3
6780	1.32E-3
8180	1.67E-3
9707	2.95E-3
11515	2.13E-2
12615	1.31E-2
13935	2.53E-2
15425	2.66E-2
16810	3.33E-2

D=166.5 cm TIME(min)	R=30 cm K(cm/sec)
960	2.17E-2
2460	5.36E-3
3900	3.99E-3
5340	1.89E-3
6780	1.32E-3
8180	1.42E-3
9707	5.18E-3
11515	1.92E-2
12615	2.94E-2
13935	3.69E-2
15425	4.16E-2
16810	4.17E-2

D=175.5 cm TIME(min)	R=30 cm K(cm/sec)
960	8.02E-3
2460	2.04E-3
3900	7.35E-4
5340	7.71E-4
6780	6.32E-4
8180	8.19E-4
9707	1.12E-3
11515	1.34E-3
12615	1.49E-3
13935	1.62E-3
15425	1.93E-3
16810	1.93E-3

D=182.5 cm TIME(min)	R=30 cm K(cm?sec)
960	1.85E-4
2460	4.89E-3
3900	2.91E-3
5340	1.39E-3
6780	9.68E-4
8205	2.82E-3
9750	9.43E-3
11535	1.50E-2
12620	1.68E-2
13945	1.82E-2
15435	1.82E-2
16820	1.93E-2

D=189.5 cm TIME(min)	R=30 cm K(cm/sec)
960	1.57E-4
2460	1.72E-4
3990	2.25E-4
4170	2.27E-4
5400	3.14E-4
5685	3.39E-4
7050	3.48E-4
8445	5.28E-4
11700	5.49E-4
12720	6.62E-4
14440	6.66E-4
15438	4.43E-3
16820	4.48E-3

D=197.5 cm TIME(min)	R=30 cm K(cm/sec)
5719	3.90E-5
6398	4.71E-5
7062	6.36E-5
7743	4.95E-5
8443	2.90E-5
9204	5.51E-5
10669	2.05E-5
13280	5.31E-5
14716	5.97E-5
16157	5.48E-5

D=203.5 cm TIME(min)	R=30 cm K(cm/sec)
960	1.1[illegible]E-4
2460	7.85E-5
3900	7.20E-5
4387	7.00E-5
5340	7.37E-5
5984	6.82E-5
7060	7.45E-5
7547	7.17E-5
8207	8.32E-5
9744	7.0[illegible]E-5
11415	6.76E-5
11700	6.54E-5
12780	5.07E-5
13440	6.50E-5
15030	9.08E-5
15270	1.17E-4
16870	1.02E-4

D=218.5 cm TIME(min)	R=30 cm K(cm/sec)
960	1.72E-3
2460	1.36E-3
3900	1.75E-3
5340	2.07E-3
6780	1.73E-3
8207	2.31E-3
9755	2.37E-3
11545	2.75E-3
12630	2.97E-3
13950	3.01E-3
15435	2.99E-3
16830	2.98E-3

Appendix D

HEIGHT OF WATER IN THE BOREHOLE: S8T1

TIME (min)	H (cm)
0.17	38.1
4.00	38.1
8.00	38.1
15.00	38.8
19.00	38.1
41.00	38.1
45.00	38.7
49.00	38.1
55.00	38.1
191.00	38.4
208.00	38.7
250.00	38.1
295.00	39.7
296.00	38.1
750.00	38.1
775.00	38.1
955.00	38.1
1135.00	38.1
1309.00	38.1
1896.00	38.1
2065.00	41.9
2155.00	38.7
2245.00	40.6
2330.00	39.4
2339.00	41.3
2352.00	37.8
2398.00	37.5
2578.00	37.5
2608.00	38.1
2757.00	38.1
2943.00	38.1
3207.00	38.1
3325.00	38.1
3437.00	38.1
3688.00	38.1
3845.00	38.1
4088.00	38.1
4212.00	38.1
4483.00	38.1
4647.00	38.1
4856.00	38.1
5314.00	38.1
5717.00	38.1
5915.00	38.1
6006.00	38.1
6012.00	38.1
6013.00	38.1
6015.00	38.1
6021.00	38.1
6024.00	38.1
6028.00	38.1
6033.00	38.1
6038.00	38.1
6042.00	38.1
6050.00	38.1
6055.00	38.1
6060.00	38.1
6065.00	38.1
6072.00	38.1
6075.00	38.1
6080.00	38.1
6085.00	38.1
6093.00	38.1
6099.00	38.1
6221.00	38.1
6276.00	37.5
6356.00	35.9
6513.00	38.1
6715.00	38.1
7098.00	38.4
7443.00	38.1
7860.00	38.1
8067.00	38.1
8310.00	38.1
8535.00	38.1
8772.00	38.1
9007.00	38.1
9175.00	38.1
9346.00	38.1
9595.00	38.1
9832.00	38.1
10069.00	38.1
10568.00	38.1
10808.00	38.1
11127.00	38.1
11377.00	38.1
11605.00	38.1
11854.00	38.1

$Q_1 = .135$ 0-3500
$Q_2 = .35$ 3500-6000
$Q_3 = .22$ 6000-10,
$Q_4 = .15$

INFILTRATION RATE: S8T1
VISCOSITY CORRECTED TO 20° C

TIME (min)	Q (lpm)	TIME (min)	Q (lpm)	TIME (min)	Q (lpm)
2.0	1.380	1318.0	0.271	6026.0	0.340
5.0	0.736	1497.0	0.198	6056.0	0.514
8.0	0.920	1576.0	0.200	6076.0	0.406
11.0	0.920	1777.0	0.153	6132.0	0.135
15.0	0.655	1880.0	0.125	6185.0	0.222
20.0	0.753	2042.0	0.143	6267.0	0.212
25.0	0.800	2215.0	0.146	6354.0	0.213
35.0	0.672	2395.0	0.136	6520.0	0.224
45.0	0.780	2575.0	0.126	6717.0	0.237
55.0	0.645	2755.0	0.139	6807.0	0.245
65.0	0.632	2981.0	0.161	7083.0	0.328
80.0	0.600	3009.0	0.170	7288.0	0.311
95.0	0.568	3025.0	0.141	7435.0	0.290
116.0	0.562	3063.0	0.138	7616.0	0.264
145.0	0.539	3115.0	0.128	7853.0	0.228
175.0	0.525	3211.0	0.139	8061.0	0.217
206.0	0.480	3269.0	0.120	8306.0	0.230
235.0	0.466	3328.0	0.121	8535.0	0.258
265.0	0.459	3412.0	0.115	8566.0	0.266
295.0	0.430	3490.0	0.113	8763.0	0.242
325.0	0.424	3595.0	0.132	8998.0	0.199
355.0	0.424	3692.0	0.153	9179.0	0.172
385.0	0.379	3821.0	0.202	9298.0	0.176
446.0	0.329	4084.0	0.310	9581.0	0.213
483.0	0.434	4190.0	0.370	9830.0	0.272
511.0	0.410	4299.0	0.385	10068.0	0.276
535.0	0.376	4469.0	0.359	10175.0	0.264
575.0	0.348	4633.0	0.338	10328.0	0.192
596.0	0.390	4661.0	0.336	10559.0	0.143
624.0	0.373	4853.0	0.316	10810.0	0.157
659.0	0.332	5312.0	0.335	10979.0	0.151
713.0	0.290	5355.0	0.324	11115.0	0.156
804.0	0.263	5686.0	0.375	11366.0	0.153
837.0	0.296	5919.0	0.305	11599.0	0.232
865.0	0.309	5995.0	0.307	11844.0	0.210
909.0	0.322	6000.0	0.318	11915.0	0.208
942.0	0.335	6005.0	0.315		
1133.0	0.284	6010.0	0.355		

CUMULATIVE INFILTRATION: S8T1

TIME (min)	CUMQ (l)	TIME (min)	CUMQ (l)	TIME (min)	CUMQ (l)
2.0	2.3	1318.0	489.2	6026.0	1610.8
5.0	5.0	1497.0	524.5	6056.7	1626.2
8.0	7.7	1676.0	560.1	6076.0	1634.4
11.0	10.5	1777.0	576.4	6132.0	1641.9
15.0	13.1	1880.0	589.2	6185.0	1653.7
20.0	16.9	2042.0	612.4	6267.0	1671.1
25.0	20.9	2215.0	637.7	6354.0	1689.6
35.0	27.6	2395.0	662.1	6520.0	1726.8
45.0	35.4	2575.0	684.0	6717.0	1773.5
55.0	41.8	2755.0	709.8	6807.0	1795.5
65.0	48.2	2981.0	746.2	7083.0	1866.1
80.0	57.2	3009.0	751.0	7288.0	1949.8
95.0	65.7	3025.0	753.2	7435.0	1992.4
116.0	77.5	3063.0	758.5	7616.0	2040.2
145.0	93.1	3115.0	765.1	7853.0	2094.3
175.0	108.9	3211.0	777.6	8061.0	2139.4
206.0	123.7	3269.0	784.5	8306.0	2195.7
235.0	137.3	3328.0	791.7	8535.0	2254.8
265.0	151.0	3412.0	801.4	8566.0	2263.1
295.0	163.9	3490.0	810.2	8763.0	2310.7
325.0	176.6	3595.0	824.1	8998.0	2357.5
355.0	189.4	3692.0	838.9	9179.0	2388.6
385.0	200.7	3821.0	865.0	9298.0	2409.6
446.0	220.8	4084.0	946.5	9581.0	2471.3
483.0	236.9	4190.0	985.7	9830.0	2539.0
511.0	248.3	4299.0	1027.7	10068.0	2604.7
535.0	257.4	4469.0	1088.7	10175.0	2632.9
575.0	271.3	4633.0	1144.1	10328.0	2662.3
596.0	279.5	4661.0	1153.5	10559.0	2695.4
624.0	289.9	4853.0	1214.2	10810.0	2734.8
659.0	301.5	5312.0	1369.0	10979.0	2760.3
713.0	317.2	5355.0	1381.9	11115.0	2781.5
804.0	341.1	5686.0	1506.0	11366.0	2819.9
837.0	350.9	5919.0	1577.1	11599.0	2874.0
865.0	359.6	5995.0	1600.4	11644.0	2925.4
909.0	373.7	6000.0	1602.0	11915.0	2940.2
942.0	384.8	6005.0	1603.6		
1133.0	439.0	6010.0	1605.4		

BOREHOLE WATER TEMPERATURE

TIME (min)	TEMP. (°C)
0.	18.
5.	17.
10.	17.
15.	17.
20.	18.
25.	17.
30.	17.
40.	18.
50.	18.
60.	18.
70.	18.
80.	18.
95.	19.
110.	19.
131.	21.
148.	21.
162.	22.
176.	22.
190.	23.
205.	23.
220.	23.
235.	24.
250.	24.
265.	25.
280.	25.
295.	26.
310.	28.
325.	27.
340.	27.
355.	27.
370.	28.
385.	28.
400.	28.
415.	26.
430.	27.
445.	27.
475.	28.
490.	28.
505.	28.
536.	28.
597.	28.
665.	27.
711.	25.
833.	23.
963.	16.
1147.	18.
1319.	16.
1506.	22.
1874.	32.
2070.	28.
2245.	23.
2400.	21.
2588.	19.
2766.	17.
2983.	22.
3329.	28.
3435.	27.
3648.	19.
3847.	17.
4089.	13.
4209.	11.
4482.	19.
4648.	24.
4853.	26.
5314.	18.
5715.	13.
5916.	21.
5995.	25.
6025.	26.
6035.	26.
6045.	26.
6060.	26.
6079.	26.
6146.	30.
6220.	31.
6271.	30.
6355.	29.
6514.	26.
6717.	21.
7086.	16.
7432.	27.
7604.	32.
7854.	28.
8059.	24.
8308.	23.
8535.	21.
8764.	27.
9000.	33.
9175.	34.
9345.	30.
9594.	20.
9831.	17.
10068.	19.
10328.	30.
10560.	35.
10808.	26.
11116.	18.
11367.	16.
11599.	25.
11845.	34.

SOIL-WATER TEMPERATURE
R=30.5 cm D=152.4 cm

TIME (min)	TEMP. (°C)
0.	16.
5.	16.
10.	16.
15.	16.
20.	16.
25.	16.
30.	16.
40.	16.
50.	16.
60.	16.
70.	16.
80.	16.
95.	16.
110.	16.
131.	16.
148.	17.
162.	17.
176.	17.
190.	17.
205.	17.
220.	17.
235.	18.
250.	18.
265.	18.
280.	18.
295.	18.
310.	19.
325.	20.
340.	19.
355.	19.
370.	20.
385.	20.
400.	21.
415.	21.
430.	21.
445.	21.
475.	22.
490.	22.
505.	22.
536.	22.
597.	23.
665.	23.
711.	23.
833.	23.
963.	22.
1147.	21.
1319.	19.
1506.	19.
1874.	21.
2070.	22.
2245.	23.
2466.	22.
2588.	21.
2766.	21.
2983.	20.
3116.	20.
3329.	21.
3435.	21.
3648.	22.
3847.	21.
4089.	19.
4209.	18.
4482.	17.
4648.	18.
4853.	19.
5314.	20.
5715.	18.
5916.	18.
5995.	18.
6025.	18.
6035.	18.
6045.	18.
6060.	18.
6079.	18.
6146.	19.
6220.	20.
6271.	21.
6355.	22.
6514.	23.
6717.	22.
7086.	20.
7432.	19.
7604.	21.
7854.	23.
8059.	24.
8308.	23.
8535.	22.
8764.	21.
9000.	22.
9175.	24.
9345.	25.
9594.	24.
9831.	22.
10068.	21.
10328.	20.
10560.	22.
10808.	23.
11116.	23.
11367.	22.
11599.	21.
11845.	21.

SOIL-WATER TEMPERATURE
R=61.0 cm D=162.5 cm

TIME (min)	TEMP. (°C)	TIME (min)	TEMP. (°C)	TIME (min)	TEMP. (°C)
0.	15.	430.	16.	5998.	18.
5.	15.	445.	17.	6025.	18.
10.	15.	475.	16.	6035.	18.
15.	15.	490.	16.	6045.	18.
20.	15.	505.	16.	6060.	18.
25.	15.	536.	16.	6070.	18.
30.	15.	597.	16.	6145.	17.
40.	15.	665.	16.	6220.	17.
50.	15.	711.	17.	6271.	18.
60.	15.	833.	17.	6355.	18.
70.	15.	963.	17.	6514.	18.
80.	15.	1147.	16.	6717.	18.
95.	15.	1319.	16.	7086.	19.
110.	15.	1506.	18.	7432.	18.
131.	15.	1874.	17.	7604.	18.
148.	15.	2070.	17.	7854.	19.
162.	15.	2245.	18.	8059.	19.
176.	15.	2400.	18.	8308.	19.
190.	15.	2588.	18.	8535.	21.
205.	16.	2760.	18.	8704.	20.
220.	15.	2983.	18.	9000.	19.
235.	15.	3116.	16.	9175.	19.
250.	15.	3329.	18.	9345.	21.
265.	15.	3435.	18.	9594.	20.
280.	15.	3648.	17.	9831.	20.
295.	15.	3847.	18.	10068.	20.
310.	16.	4089.	18.	10328.	20.
325.	16.	4209.	18.	10560.	19.
340.	16.	4482.	18.	10808.	20.
355.	16.	4648.	18.	11110.	20.
370.	16.	4853.	17.	11367.	20.
385.	16.	5314.	18.	11599.	19.
400.	16.	5715.	19.	11645.	19.
415.	16.	5916.	18.		

SOIL-WATER TEMPERATURE
R=91.4 cm D=170.2 cm

TIME (min)	TEMP. (°C)	TIME (min)	TEMP. (°C)	TIME (min)	TEMP. (°C)
0.	14.	430.	14.	5995.	16.
5.	14.	445.	14.	6025.	16.
10.	14.	475.	14.	6035.	16.
15.	14.	490.	14.	6045.	16.
20.	14.	505.	14.	6060.	16.
25.	14.	536.	14.	6070.	16.
30.	14.	597.	15.	6146.	16.
40.	14.	665.	14.	6220.	16.
50.	14.	711.	14.	6271.	16.
60.	14.	833.	15.	6355.	16.
70.	14.	963.	15.	6514.	16.
80.	14.	1147.	14.	6717.	16.
95.	14.	1319.	15.	7086.	16.
110.	14.	1506.	15.	7432.	16.
131.	15.	1874.	15.	7604.	16.
148.	14.	2070.	16.	7854.	16.
162.	15.	2245.	16.	8059.	17.
176.	15.	2406.	16.	8308.	17.
190.	14.	2586.	16.	8535.	17.
205.	14.	2766.	15.	8764.	17.
220.	15.	2983.	16.	9000.	17.
235.	14.	3116.	16.	9175.	17.
250.	14.	3329.	16.	9345.	17.
265.	14.	3435.	16.	9594.	17.
280.	14.	3648.	14.	9831.	17.
295.	14.	3847.	17.	10068.	18.
310.	14.	4089.	16.	10328.	17.
325.	15.	4209.	16.	10560.	18.
340.	15.	4482.	16.	10808.	18.
355.	14.	4648.	16.	11116.	18.
370.	15.	4853.	16.	11367.	18.
385.	14.	5314.	16.	11599.	17.
400.	14.	5715.	16.	11645.	17.
415.	14.	5916.	16.		

PRESSURE HEAD DATA: S8T1
R=17.8 cm D=137.2 cm

TIME (min)	PH (cmH_2O)	TIME (min)	PH (cmH_2O)
1500.	-34.	6135.	-3.
1675.	-29.	6191.	-3.
1857.	-29.	6265.	-3.
2075.	-33.	6359.	-15.
2239.	-36.	6509.	-23.
2399.	-35.	6719.	-27.
2583.	-35.	7088.	-28.
2762.	-35.	7420.	-12.
2974.	-32.	7620.	-5.
3119.	-31.	7861.	-31.
3322.	-27.	8038.	-31.
3483.	-27.	8283.	-31.
3653.	-29.	8518.	-28.
3841.	-28.	8765.	-23.
4084.	-26.	9001.	-10.
4212.	-26.	9180.	-10.
4474.	-21.	9346.	-32.
4858.	-7.	9606.	-35.
5318.	-16.	9835.	-35.
5713.	-20.	10051.	-33.
5898.	-17.	10330.	-13.
5995.	-11.	10570.	-10.
6005.	-10.	10811.	-41.
6015.	-7.	11127.	-30.
6025.	-7.	11378.	-30.
6040.	-6.	11608.	-28.
6060.	-5.	11857.	-6.
6090.	-3.		

PRESSURE HEAD DATA: S8T1
R=17.8 cm D=172.7 cm

TIME (min)	PH (cmH_2O)	TIME (min)	PH (cmH_2O)
1500.	8.	6135.	5.
1675.	9.	6191.	7.
1857.	6.	6265.	-3.
2075.	4.	6359.	-4.
2239.	3.	6509.	-3.
2399.	3.	6719.	3.
2583.	2.	7088.	2.
2762.	2.	7420.	6.
2974.	3.	7620.	2.
3119.	3.	7861.	-11.
3322.	2.	8038.	-11.
3483.	0.	8283.	-8.
3653.	3.	8518.	-7.
3841.	5.	8765.	-5.
4084.	8.	9001.	-2.
4212.	13.	9180.	-8.
4474.	16.	9346.	-12.
4858.	18.	9606.	-12.
5318.	16.	9835.	-12.
5713.	17.	10061.	-8.
5898.	18.	10330.	-8.
5995.	20.	10570.	-9.
6005.	18.	10811.	-16.
6015.	15.	11127.	-17.
6025.	15.	11378.	-18.
6040.	15.	11608.	-19.
6060.	13.	11857.	-16.
6090.	13.		

PRESSURE HEAD DATA: S8T1
R=17.8 cm D=199.1 cm

TIME (min)	PH (cmH_2O)	TIME (min)	PH (cmH_2O)
713.	23.	6043.	18.
821.	25.	6062.	18.
955.	23.	6092.	23.
1144.	23.	6137.	20.
1316.	22.	6193.	12.
1504.	22.	6265.	6.
1680.	22.	6361.	3.
1868.	10.	6512.	1.
2075.	8.	6722.	8.
2243.	7.	7091.	5.
2405.	6.	7429.	6.
2586.	6.	7620.	-3.
2765.	6.	7864.	-9.
2977.	6.	8043.	-10.
3122.	6.	8291.	-8.
3325.	7.	8523.	-7.
3488.	7.	8769.	-5.
3658.	8.	9005.	-4.
3844.	8.	9183.	-6.
4215.	11.	9349.	-7.
4270.	31.	9610.	-9.
4285.	31.	9838.	-9.
4477.	31.	10064.	-10.
4861.	31.	10334.	-7.
5321.	30.	10573.	-7.
5715.	30.	10814.	-12.
5901.	33.	11131.	-17.
5997.	33.	11380.	-19.
6008.	25.	11610.	-18.
6018.	22.	11860.	-15.
6028.	21.		

PRESSURE HEAD DATA: S8T1
R=30.5 cm D=122.0 cm

TIME (min)	PH (cmH_2O)	TIME (min)	PH (cmH_2O)	TIME (min)	PH (cmH_2O)
0.	-80.	667.	-89.	6016.	-76.
3.	-80.	716.	-90.	6025.	-76.
8.	-80.	816.	-89.	6041.	-76.
13.	-80.	955.	-89.	6060.	-76.
18.	-80.	1141.	-88.	6091.	-76.
22.	-80.	1314.	-88.	6135.	-76.
27.	-80.	1501.	-89.	6192.	-76.
33.	-80.	1676.	-90.	6265.	-76.
44.	-80.	1862.	-90.	6360.	-76.
55.	-80.	2075.	-90.	6510.	-74.
68.	-80.	2240.	-89.	6720.	-73.
82.	-81.	2401.	-87.	7089.	-71.
110.	-81.	2584.	-86.	7425.	-69.
132.	-81.	2763.	-86.	7620.	-69.
140.	-81.	2975.	-86.	7862.	-69.
150.	-81.	3120.	-86.	8038.	-67.
165.	-83.	3323.	-86.	8286.	-65.
180.	-83.	3484.	-86.	8521.	-65.
195.	-83.	3655.	-85.	8767.	-64.
210.	-84.	3842.	-84.	9002.	-64.
240.	-85.	4081.	-84.	9181.	-64.
270.	-85.	4213.	-84.	9348.	-64.
300.	-85.	4475.	-84.	9607.	-63.
330.	-85.	4859.	-84.	9836.	-62.
360.	-86.	5319.	-81.	10063.	-62.
390.	-86.	5714.	-78.	10332.	-62.
420.	-88.	5899.	-77.	10571.	-62.
450.	-88.	5996.	-76.	10812.	-62.
480.	-88.	6006.	-76.	11129.	-63.
535.	-89.			11379.	-62.
595.	-89.			11609.	-62.
				11858.	-62.

PRESSURE HEAD DATA: S8T1
R=30.5 cm D=134.6 cm

TIME (min)	PH (cmH_2O)
0.	-47.
3.	-47.
8.	-47.
13.	-47.
18.	-47.
22.	-47.
27.	-47.
33.	-47.
44.	-47.
55.	-47.
68.	-47.
82.	-47.
110.	-47.
132.	-47.
140.	-47.
150.	-47.
165.	-47.
180.	-47.
195.	-46.
210.	-46.
240.	-46.
270.	-46.
300.	-45.
330.	-44.
360.	-44.
390.	-44.
420.	-44.
450.	-39.
480.	-40.
535.	-39.
595.	-36.
667.	-36.
716.	-36.
818.	-35.
955.	-35.
1141.	-35.
1314.	-37.
1501.	-37.
1676.	-36.
1862.	-35.
2075.	-36.
2240.	-37.
2401.	-39.
2584.	-40.
2763.	-40.
2975.	-40.
3120.	-40.
3323.	-39.
3484.	-38.
3655.	-39.
3842.	-39.
4031.	-37.
4213.	-37.
4475.	-30.
4859.	-24.
5319.	-24.
5714.	-24.
5899.	-24.
5996.	-23.
6006.	-22.
6016.	-21.
6025.	-21.
6041.	-21.
6060.	-21.
6091.	-20.
6135.	-21.
6192.	-27.
6265.	-27.
6360.	-30.
6510.	-34.
6720.	-34.
7089.	-33.
7425.	-27.
7620.	-29.
7862.	-40.
8038.	-39.
8286.	-39.
8521.	-36.
8767.	-34.
9002.	-31.
9181.	-32.
9348.	-41.
9607.	-40.
9836.	-39.
10063.	-37.
10332.	-36.
10571.	-37.
10812.	-44.
11129.	-45.
11379.	-46.
11609.	-45.
11858.	-44.

PRESSURE HEAD DATA: S8T1
R=30.5 cm D=48.9 cm

TIME (min)	PH (cmH_2O)	TIME (min)	PH (cmH_2O)
300.	-17.	5997.	-8.
330.	-13.	6006.	-10.
360.	-12.	6018.	-12.
390.	-12.	6028.	-13.
420.	-13.	6043.	-14.
450.	-12.	6062.	-16.
480.	-13.	6092.	-17.
535.	-12.	6137.	-24.
595.	-13.	6193.	-24.
667.	-14.	6265.	-27.
718.	-14.	6361.	-29.
821.	-16.	6512.	-30.
955.	-17.	6722.	-26.
1144.	-19.	7091.	-27.
1316.	-20.	7429.	-23.
1504.	-20.	7620.	-29.
1680.	-20.	7864.	-37.
1868.	-24.	8043.	-36.
2075.	-24.	8291.	-31.
2243.	-26.	8523.	-29.
2405.	-26.	8769.	-27.
2586.	-27.	9005.	-29.
2765.	-26.	9183.	-34.
2977.	-24.	9349.	-36.
3122.	-25.	9610.	-34.
3325.	-25.	9838.	-33.
3488.	-25.	10064.	-30.
3658.	-24.	10334.	-34.
3844.	-20.	10573.	-35.
4215.	-14.	10814.	-40.
4477.	-9.	11131.	-42.
4861.	-9.	11380.	-42.
5321.	-10.	11610.	-42.
5715.	-10.	11860.	-36.
5901.	-10.		

PRESSURE HEAD DATA: S8T1
R=30.5 cm D=170.2 cm

TIME (min)	PH (cmH_2O)
0.	-18.
3.	-17.
8.	-17.
13.	-14.
18.	-8.
22.	-4.
27.	1.
33.	5.
44.	11.
55.	15.
68.	16.
82.	16.
110.	17.
132.	18.
140.	20.
150.	20.
165.	18.
180.	20.
195.	18.
210.	20.
240.	20.
270.	20.
300.	18.
330.	17.
360.	16.
390.	16.
420.	16.
450.	16.
480.	16.
535.	15.
595.	13.
667.	12.
716.	12.
818.	11.
955.	10.
1141.	9.
1314.	6.
1501.	5.
1676.	6.
1862.	2.
2075.	-2.
2240.	-4.
2401.	-4.
2584.	-4.
2763.	-4.
2975.	0.
3120.	0.
3323.	-2.
3484.	-3.
3655.	-4.
3842.	1.
4081.	7.
4213.	9.
4475.	16.
4859.	15.
5319.	12.
5714.	12.
5899.	14.
5996.	16.
6006.	16.
6016.	16.
6025.	15.
6041.	17.
6060.	17.
6091.	16.
6135.	5.
6192.	5.
6265.	0.
6360.	-5.
6510.	-8.
6720.	-3.
7089.	-2.
7425.	3.
7620.	0.
7862.	-12.
8038.	-14.
8286.	-12.
8521.	-9.
8767.	-6.
9002.	-4.
9181.	-10.
9348.	-15.
9607.	-15.
9836.	-13.
10063.	-10.
10332.	-9.
10571.	-13.
10812.	-19.
11129.	-21.
11379.	-22.
11609.	-20.
11858.	-19.

PRESSURE HEAD DATA: S8T1
R=30.5 cm D=209.6 cm

TIME (min)	PH (cmH_2O)	TIME (min)	PH (cmH_2O)	TIME (min)	PH (cmH_2O)
0.	21.	717.	39.	6028.	33.
2.	21.	819.	40.	6042.	31.
5.	23.	955.	39.	6062.	29.
9.	23.	1142.	38.	6092.	31.
14.	24.	1315.	38.	6137.	31.
27.	25.	1502.	36.	6193.	23.
33.	30.	1678.	36.	6265.	19.
45.	33.	1865.	34.	6361.	15.
57.	33.	2075.	33.	6511.	14.
70.	33.	2241.	31.	6721.	24.
93.	33.	2403.	32.	7090.	18.
115.	33.	2585.	31.	7426.	13.
133.	36.	2764.	31.	7620.	8.
150.	36.	2976.	33.	7863.	2.
165.	38.	3121.	33.	8042.	1.
180.	38.	3325.	33.	8289.	2.
195.	39.	3485.	33.	8523.	3.
210.	38.	3657.	33.	8768.	4.
225.	39.	3843.	34.	9004.	5.
270.	39.	4086.	35.	9182.	5.
300.	39.	4215.	36.	9349.	4.
330.	39.	4477.	40.	9609.	2.
360.	39.	4860.	41.	9832.	2.
390.	40.	5320.	42.	10064.	1.
420.	39.	5714.	42.	10333.	2.
450.	40.	5900.	44.	10572.	3.
480.	40.	5997.	45.	10812.	2.
535.	39.	6008.	38.	11130.	-2.
595.	40.	6018.	35.	11380.	-4.
667.	39.			11610.	-4.
				11859.	-2.

PRESSURE HEAD DATA: S8T1
R= 30.5 cm D= 240.0 cm

TIME (min)	PH (cmH_2O)
0.	43.
2.	43.
5.	43.
9.	43.
14.	44.
27.	44.
33.	45.
45.	47.
57.	47.
70.	47.
93.	47.
115.	47.
133.	48.
150.	49.
165.	49.
180.	52.
195.	52.
210.	53.
225.	54.
270.	54.
300.	54.
330.	53.
360.	53.
390.	54.
420.	54.
450.	56.
480.	56.
535.	54.
595.	54.
667.	54.
717.	54.
819.	56.
955.	56.
1142.	56.
1315.	55.
1502.	56.
1678.	56.
1865.	56.
2075.	54.
2241.	53.

PRESSURE HEAD DATA: S8T1
R= 61.0 cm D= 122.0 cm

TIME (min)	PH (cmH_2O)
0.	97.
3.	94.
8.	84.
13.	84.
18.	78.
22.	78.
27.	72.
33.	66.
44.	53.
55.	47.
68.	40.
82.	22.
110.	13.
132.	3.
140.	-2.
150.	-6.
165.	-14.
180.	-20.
195.	-24.
210.	-29.
240.	-37.
270.	-46.
300.	-51.
330.	-59.
360.	-66.
390.	-70.
420.	-75.
450.	-81.
480.	-84.
535.	-90.
595.	-98.
667.	-101.
716.	-104.
818.	-107.
955.	-110.
1141.	-111.
1314.	-113.
1501.	-113.
1676.	-113.
1862.	-113.
2075.	-119.
2240.	-120.
2401.	-120.
2584.	-119.
2763.	-116.
2975.	-115.
3120.	-113.
3323.	-111.
3484.	-111.
3655.	-111.
3842.	-111.
4081.	-108.
4213.	-105.
4475.	-103.
4859.	-101.
5319.	-101.
5714.	-99.
5899.	-98.
5996.	-96.
6006.	-95.
6016.	-95.
6025.	-94.
6041.	-94.
6060.	-94.
6091.	-94.
6135.	-91.
6192.	-90.
6265.	-93.
6360.	-98.
6510.	-101.
6720.	-101.
7089.	-96.
7425.	-91.
7620.	-91.
7862.	-99.
8038.	-100.
8286.	-101.
8521.	-95.
8767.	-94.
9002.	-91.
9181.	-98.
9348.	-101.
9607.	-100.
9836.	-95.
10063.	-93.
10332.	-90.
10571.	-91.
10812.	-96.
11129.	-97.
11379.	-93.
11609.	-91.
11858.	-88.

PRESSURE HEAD DATA: S8T1
R= 61.0 cm D= 134.6 cm

TIME (min)	PH (cmH_2O)
0.	-66.
3.	-66.
8.	-67.
13.	-67.
18.	-69.
22.	-69.
27.	-67.
33.	-67.
44.	-67.
55.	-67.
68.	-67.
82.	-67.
110.	-67.
132.	-66.
140.	-62.
150.	-64.
165.	-62.
180.	-64.
195.	-64.
210.	-62.
240.	-55.
270.	-51.
300.	-46.
330.	-45.
360.	-41.
390.	-44.
420.	-45.
450.	-45.
480.	-45.
535.	-44.
595.	-42.
667.	-42.
716.	-42.
818.	-41.
955.	-40.
1141.	-39.
1314.	-40.
1501.	-40.
1676.	-36.
1862.	-40.
2075.	-45.
2240.	-46.
2401.	-45.
2584.	-45.
2763.	-45.
2975.	-42.
3120.	-44.
3323.	-45.
3484.	-44.
3655.	-45.
3842.	-44.
4081.	-40.
4213.	-39.
4475.	-34.
4859.	-31.
5319.	-32.
5714.	-31.
5899.	-29.
5996.	-22.
6006.	-23.
6016.	-21.
6025.	-22.
6041.	-22.
6060.	-20.
6091.	-22.
6135.	-21.
6192.	-32.
6265.	-37.
6360.	-44.
6510.	-47.
6720.	-46.
7089.	-45.
7425.	-31.
7620.	-42.
7862.	-56.
8038.	-59.
8286.	-57.
8521.	-56.
8767.	-51.
9002.	-50.
9181.	-53.
9348.	-63.
9607.	-64.
9836.	-61.
10063.	-59.
10332.	-54.
10571.	-53.
10812.	-69.
11129.	-69.
11379.	-67.
11609.	-60.
11858.	-56.

PRESSURE HEAD DATA: S8T1
R= 61.0 cm D= 170.2 cm

TIME (min)	PH (cmH_2O)
0.	-22.
2.	-22.
6.	-22.
11.	-22.
16.	-22.
25.	-21.
32.	-14.
42.	-11.
53.	-7.
65.	-3.
84.	-1.
105.	1.
130.	5.
140.	7.
150.	7.
165.	8.
180.	7.
195.	6.
210.	9.
240.	9.
270.	8.
300.	9.
330.	9.
360.	5.
390.	6.
420.	4.
450.	4.
480.	4.
535.	6.
595.	3.
667.	2.
715.	4.
817.	4.
955.	3.
1139.	2.
1312.	1.
1500.	1.
1675.	2.
1857.	-8.
2075.	-6.
2239.	-7.
2399.	-6.
2583.	-7.
2762.	-7.
2974.	-4.
3119.	-4.
3322.	-8.
3483.	-7.
3653.	-7.
3841.	-17.
4084.	-1.
4212.	0.
4474.	5.
4858.	9.
5318.	6.
5713.	6.
5898.	7.
5995.	12.
6005.	12.
6015.	9.
6025.	9.
6040.	9.
6060.	6.
6090.	4.
6135.	-1.
6191.	-9.
6265.	-9.
6359.	-12.
6509.	-14.
6719.	-9.
7088.	-12.
7420.	-2.
7620.	-16.
7861.	-33.
8038.	-27.
8283.	-23.
8518.	-23.
8765.	-19.
9001.	-20.
9180.	-24.
9346.	-28.
9606.	-27.
9835.	-26.
10061.	-25.
10330.	-23.
10570.	-25.
10811.	-30.
11127.	-30.
11378.	-31.
11608.	-26.
11857.	-29.

PRESSURE HEAD DATA: S8T1
R= 61.0 cm D= 209.6 cm

TIME (min)	PH (cmH_2O)	TIME (min)	PH (cmH_2O)	TIME (min)	PH (cmH_2O)
0.	15.	717.	31.	6028.	26.
2.	14.	819.	32.	6042.	23.
5.	15.	955.	31.	6062.	21.
9.	14.	1142.	31.	6092.	26.
14.	14.	1315.	31.	6137.	25.
27.	14.	1502.	30.	6193.	16.
33.	19.	1678.	30.	6265.	10.
45.	21.	1865.	27.	6361.	8.
57.	21.	2075.	26.	6511.	8.
70.	23.	2241.	25.	6721.	15.
93.	23.	2403.	25.	7090.	11.
115.	23.	2585.	25.	7426.	10.
133.	26.	2764.	25.	7620.	0.
150.	28.	2970.	26.	7863.	-1.
165.	28.	3121.	26.	8042.	-4.
180.	30.	3325.	26.	8289.	-4.
195.	29.	3485.	26.	8523.	-2.
210.	30.	3657.	27.	8768.	-2.
225.	29.	3843.	29.	9004.	-2.
270.	30.	4086.	43.	9182.	-2.
300.	30.	4215.	31.	9349.	-2.
330.	30.	4477.	35.	9609.	-2.
360.	30.	4860.	37.	9832.	-2.
390.	30.	5320.	38.	10064.	-2.
420.	30.	5714.	38.	10333.	-2.
450.	31.	5900.	39.	10572.	-1.
480.	31.	5997.	40.	10812.	-2.
535.	30.	6008.	31.	11130.	-5.
595.	30.	6018.	29.	11380.	-8.
667.	30.			11610.	-8.
				11859.	-6.

PRESSURE HEAD DATA: S8T1
R= 61.0 cm D= 240.0 cm

TIME (min)	PH (cmH_2O)	TIME (min)	PH (cmH_2O)
0.	49.	819.	61.
2.	49.	955.	61.
5.	49.	1142.	61.
9.	49.	1315.	61.
14.	49.	1502.	60.
27.	52.	1678.	59.
33.	53.	1865.	58.
45.	54.	2075.	57.
57.	54.	2241.	57.
70.	54.	6721.	34.
93.	54.	7090.	32.
115.	56.	7620.	17.
133.	56.	7863.	14.
150.	57.	8042.	14.
165.	58.	8289.	20.
180.	58.	8523.	20.
195.	58.	8768.	20.
210.	58.	9004.	22.
225.	58.	9182.	23.
270.	58.	9349.	20.
300.	59.	9609.	19.
330.	59.	9832.	18.
360.	59.	10064.	18.
390.	58.	10333.	20.
420.	59.	10572.	24.
450.	61.	10812.	19.
480.	61.	11130.	15.
535.	59.	11380.	13.
595.	61.	11610.	19.
667.	59.	11859.	18.
717.	61.		

PRESSURE HEAD DATA: S8T1
R= 91.0cm D=122.0 cm

TIME (min)	PH (cmH_2O)	TIME (min)	PH (cmH_2O)	TIME (min)	PH (cmH_2O)
0.	-59.	715.	-66.	6025.	-69.
2.	-57.	817.	-61.	6040.	-68.
6.	-57.	955.	-49.	6060.	-66.
11.	-56.	1139.	-39.	6090.	-66.
16.	-55.	1312.	-39.	6135.	-62.
25.	-55.	1500.	-63.	6191.	-40.
32.	-54.	1675.	-62.	6265.	-40.
42.	-55.	1857.	-34.	6359.	-42.
53.	-56.	2075.	-45.	6509.	-47.
65.	-57.	2239.	-52.	6719.	-59.
84.	-49.	2399.	-64.	7088.	-63.
105.	-39.	2583.	-69.	7420.	-56.
130.	-44.	2762.	-71.	7620.	-42.
140.	-45.	2974.	-73.	7861.	-45.
150.	-60.	3119.	-73.	8038.	-45.
165.	-52.	3322.	-66.	8283.	-55.
180.	-52.	3483.	-66.	8518.	-56.
195.	-51.	3653.	-66.	8765.	-59.
210.	-47.	3841.	-73.	9001.	-58.
240.	-41.	4084.	-74.	9180.	-59.
270.	-41.	4212.	-74.	9346.	-57.
300.	-39.	4474.	-79.	9606.	-57.
330.	-39.	4858.	-74.	9835.	-58.
360.	-37.	5318.	-73.	10061.	-58.
390.	-41.	5713.	-73.	10330.	-59.
420.	-44.	5898.	-72.	10570.	-57.
450.	-45.	5995.	-69.	10811.	-57.
480.	-50.	6005.	-69.	11127.	-56.
535.	-49.	6015.	-69.	11378.	-58.
595.	-59.			11608.	-59.
667.	-64.			11857.	-58.

PRESSURE HEAD DATA: S8T1
R=91.0 cm D=134.6 cm

TIME (min)	PH (cmH_2O)
0.	-65.
2.	-65.
6.	-65.
11.	-65.
16.	-65.
25.	-66.
32.	-66.
42.	-66.
53.	-69.
65.	-70.
84.	-74.
105.	-74.
130.	-74.
140.	-74.
150.	-72.
165.	-74.
180.	-74.
195.	-74.
210.	-75.
240.	-75.
270.	-76.
300.	-79.
330.	-76.
360.	-76.
390.	-76.
420.	-75.
450.	-75.
480.	-75.
535.	-75.
595.	-75.
667.	-75.
715.	-75.
817.	-74.
955.	-75.
1139.	-73.
1312.	51.

PRESSURE HEAD DATA: S8T1
R= 91.0 cm D= 170.2 cm

TIME (min)	PH (cmH_2O)
0.	-22.
2.	-21.
6.	-22.
11.	-22.
16.	-21.
25.	-21.
32.	-21.
42.	-21.
53.	-18.
65.	-13.
84.	-9.
105.	-5.
130.	0.
140.	-3.
150.	0.
165.	2.
180.	1.
195.	2.
210.	1.
240.	2.
270.	2.
330.	10.
360.	5.
390.	5.
420.	5.
450.	3.
480.	3.
535.	5.
595.	3.
667.	3.
715.	3.
817.	3.
955.	1.
1139.	1.
1312.	-2.

PRESSURE HEAD DATA: S8T1
R=91.0 cm D=177.0 cm

TIME (min)	PH (cmH_2O)
6722.	-7.
7091.	-13.
7429.	-7.
7620.	-15.
7864.	-22.
8043.	-21.
8291.	-19.
8523.	-19.
8769.	-18.
9005.	-18.
9183.	-22.
9349.	-24.
9610.	-24.
9838.	-23.
10064.	-22.
10334.	-20.
10573.	-27.
10814.	-26.
11131.	-27.
11380.	-28.
11610.	-26.
11860.	-24.

PRESSURE HEAD DATA: S8T1
R=91.0 cm D=209.5 cm

TIME (min)	PH (cmH_2O)	TIME (min)	PH (cmH_2O)	TIME (min)	PH (cmH_2O)
0.	10.	715.	33.	6015.	26.
2.	11.	817.	34.	6025.	25.
6.	11.	955.	33.	6040.	24.
11.	10.	1139.	34.	6060.	21.
16.	10.	1312.	33.	6090.	21.
25.	10.	1500.	24.	6135.	23.
32.	11.	1675.	25.	6191.	19.
42.	11.	1857.	23.	6265.	17.
53.	11.	2075.	22.	6359.	13.
65.	11.	2239.	20.	6509.	11.
84.	11.	2399.	20.	6719.	14.
105.	11.	2563.	19.	7088.	11.
130.	15.	2762.	19.	7420.	11.
140.	16.	2974.	19.	7620.	4.
150.	16.	3119.	19.	7861.	-3.
165.	21.	3322.	19.	8038.	-1.
180.	24.	3483.	20.	8283.	-3.
195.	25.	3653.	20.	8518.	-3.
210.	25.	3841.	21.	8765.	-3.
240.	25.	4084.	21.	9001.	-1.
270.	25.	4212.	21.	9180.	-4.
300.	25.	4474.	24.	9346.	-4.
330.	31.	4858.	25.	9606.	-4.
360.	31.	5318.	26.	9835.	-4.
390.	31.	5713.	26.	10061.	-3.
420.	31.	5898.	28.	10330.	-5.
450.	31.	5995.	28.	10570.	-4.
480.	33.	6005.	28.	10811.	-5.
535.	34.			11127.	-6.
595.	33.			11378.	-5.
667.	33.			11608.	-6.
				11857.	-7.

PRESSURE HEAD DATA: S8T1
R=91.0 cm D=238.8 cm

TIME (min)	PH (cmH_2O)
0.	47.
2.	47.
5.	47.
9.	47.
14.	47.
27.	51.
33.	51.
45.	51.
57.	51.
70.	51.
93.	51.
115.	51.
133.	51.
150.	52.
165.	52.
180.	52.
195.	52.
210.	52.
225.	51.
270.	51.
300.	51.
330.	51.
360.	52.
390.	52.
420.	52.
450.	57.
480.	56.
535.	54.
595.	54.
667.	54.
717.	56.
819.	56.
958.	56.
1142.	56.
1315.	56.
1502.	56.
1678.	55.
1865.	54.
2075.	53.
2241.	53.
6721.	32.
7090.	29.
7620.	8.
7863.	7.
8042.	7.
8289.	10.
8523.	10.
8768.	16.
9004.	16.
9182.	17.
9349.	17.
9609.	15.
9832.	15.
10064.	15.
10333.	16.
10572.	22.
10812.	17.
11130.	12.
11380.	10.
11610.	17.
11859.	17.

TOTAL HEAD DATA: S8T1
R=17.8 cm D=137.2 cm

TIME (min)	TH (cmH_2O)	TIME (min)	TH (cmH_2O)
1500.	-171.	6135.	-141.
1675.	-166.	6191.	-141.
1857.	-166.	6265.	-141.
2075.	-171.	6359.	-152.
2239.	-173.	6509.	-160.
2399.	-173.	6719.	-164.
2583.	-173.	7088.	-166.
2762.	-173.	7420.	-149.
2974.	-169.	7620.	-142.
3119.	-168.	7861.	-168.
3322.	-164.	8038.	-168.
3483.	-161.	8283.	-168.
3653.	-166.	8518.	-166.
3841.	-166.	8765.	-161.
4084.	-163.	9001.	-147.
4212.	-163.	9180.	-147.
4474.	-158.	9346.	-169.
4858.	-144.	9606.	-172.
5318.	-153.	9835.	-172.
5713.	-157.	10061.	-171.
5898.	-154.	10330.	-151.
5995.	-146.	10570.	-147.
6005.	-147.	10811.	-178.
6015.	-144.	11127.	-168.
6025.	-144.	11378.	-168.
6040.	-143.	11608.	-165.
6060.	-142.	11857.	-143.
6090.	-140.		

TOTAL HEAD DATA: S8T1
R= 17.8 cm D= 172.7 cm

TIME (min)	TH (cmH_2O)	TIME (min)	TH (cmH_2O)
1500.	-165.	6135.	-168.
1675.	-164.	6191.	-166.
1857.	-167.	6265.	-176.
2075.	-169.	6359.	-176.
2239.	-170.	6509.	-176.
2399.	-169.	6719.	-170.
2583.	-171.	7088.	-171.
2762.	-171.	7420.	-166.
2974.	-170.	7620.	-171.
3119.	-170.	7861.	-183.
3322.	-171.	8038.	-183.
3483.	-173.	8283.	-181.
3653.	-169.	8518.	-179.
3841.	-168.	8765.	-178.
4084.	-164.	9001.	-174.
4212.	-160.	9180.	-181.
4474.	-156.	9346.	-185.
4856.	-155.	9606.	-184.
5318.	-155.	9835.	-184.
5713.	-156.	10061.	-181.
5898.	-154.	10330.	-181.
5995.	-153.	10570.	-182.
6005.	-154.	10811.	-188.
6015.	-156.	11127.	-190.
6025.	-158.	11378.	-191.
6040.	-158.	11608.	-192.
6060.	-159.	11857.	-188.
6090.	-159.		

TOTAL HEAD DATA: S8T1
R= 17.8 cm D=199.1 cm

TIME (min)	TH (cmH_2O)
718.	-176.
821.	-174.
955.	-176.
1144.	-176.
1316.	-177.
1504.	-178.
1680.	-178.
1868.	-190.
2075.	-191.
2243.	-192.
2405.	-193.
2586.	-193.
2765.	-193.
2977.	-193.
3122.	-193.
3325.	-192.
3488.	-192.
3658.	-191.
3844.	-191.
4215.	-188.
4270.	-188.
4285.	-188.
4477.	-188.
4861.	-188.
5321.	-189.
5715.	-189.
5901.	-186.
5997.	-186.
6008.	-174.
6018.	-177.
6028.	-178.
6043.	-181.
6062.	-181.
6092.	-176.
6137.	-179.
6193.	-187.
6265.	-193.
6361.	-196.
6512.	-196.
6722.	-191.
7091.	-195.
7429.	-193.
7620.	-202.
7864.	-208.
8043.	-210.
8291.	-207.
8523.	-206.
8769.	-204.
9005.	-203.
9183.	-205.
9349.	-206.
9610.	-208.
9838.	-208.
10064.	-209.
10334.	-206.
10573.	-206.
10814.	-211.
11131.	-216.
11380.	-218.
11610.	-217.
11860.	-214.

TOTAL HEAD DATA: S8T1
R= 30.5cm D= 122.0cm

TIME (min)	TH (cmH_2O)
0.	-202.
3.	-202.
8.	-202.
13.	-202.
18.	-202.
22.	-202.
27.	-202.
33.	-202.
44.	-202.
55.	-202.
68.	-202.
82.	-203.
110.	-203.
132.	-203.
140.	-203.
150.	-203.
165.	-205.
180.	-205.
195.	-205.
210.	-206.
240.	-207.
270.	-207.
300.	-207.
330.	-207.
360.	-208.
390.	-208.
420.	-210.
450.	-210.
480.	-210.
535.	-211.
595.	-211.
667.	-211.
718.	-212.
818.	-211.
955.	-211.
1141.	-210.
1314.	-210.
1501.	-211.
1676.	-212.
1862.	-212.
2075.	-212.
2240.	-211.
2401.	-209.
2584.	-208.
2763.	-208.
2975.	-208.
3120.	-208.
3323.	-208.
3484.	-208.
3655.	-207.
3842.	-206.
4081.	-206.
4213.	-206.
4475.	-206.
4859.	-206.
5319.	-203.
5714.	-200.
5899.	-199.
5996.	-198.
6006.	-198.
6016.	-198.
6025.	-198.
6041.	-198.
6060.	-198.
6091.	-198.
6135.	-198.
6192.	-198.
6265.	-198.
6360.	-198.
6510.	-196.
6720.	-195.
7089.	-193.
7425.	-191.
7620.	-191.
7862.	-191.
8038.	-189.
8286.	-187.
8521.	-187.
8767.	-186.
9002.	-186.
9181.	-186.
9348.	-186.
9607.	-185.
9836.	-184.
10063.	-184.
10332.	-184.
10571.	-184.
10812.	-184.
11129.	-185.
11379.	-184.
11609.	-184.
11858.	-184.

TOTAL HEAD DATA: S8T1
R= 30.5 cm D= 134.6 cm

TIME (min)	TH (cmH_2O)
0.	-182.
3.	-182.
8.	-182.
13.	-182.
18.	-182.
22.	-182.
27.	-182.
33.	-182.
44.	-182.
55.	-182.
68.	-182.
82.	-182.
110.	-182.
132.	-182.
140.	-182.
150.	-182.
165.	-182.
180.	-182.
195.	-181.
210.	-181.
240.	-181.
270.	-181.
300.	-179.
330.	-178.
360.	-178.
390.	-178.
420.	-178.
450.	-173.
480.	-174.
535.	-173.
595.	-171.
667.	-171.
716.	-171.
818.	-169.
955.	-169.
1141.	-169.
1314.	-171.
1501.	-172.
1676.	-171.
1862.	-170.
2075.	-171.
2240.	-172.
2401.	-173.
2584.	-174.
2763.	-175.
2975.	-175.
3120.	-174.
3323.	-173.
3484.	-173.
3655.	-173.
3842.	-173.
4081.	-172.
4213.	-171.
4475.	-164.
4859.	-159.
5319.	-158.
5714.	-159.
5899.	-159.
5996.	-158.
6006.	-157.
6016.	-156.
6025.	-156.
6041.	-156.
6060.	-156.
6091.	-155.
6135.	-156.
6192.	-162.
6265.	-162.
6360.	-164.
6510.	-168.
6720.	-168.
7089.	-168.
7425.	-162.
7620.	-163.
7862.	-174.
8038.	-173.
8286.	-173.
8521.	-171.
8767.	-168.
9002.	-166.
9181.	-166.
9348.	-176.
9607.	-174.
9836.	-174.
10063.	-172.
10332.	-171.
10571.	-172.
10812.	-179.
11129.	-179.
11379.	-181.
11609.	-180.
11858.	-178.

TOTAL HEAD DATA: S8T1
R= 30.5cm D= 148.9cm

TIME (min)	TH (cmH_2O)
300.	-166.
330.	-162.
360.	-161.
390.	-161.
420.	-162.
450.	-161.
480.	-162.
535.	-161.
595.	-162.
667.	-163.
718.	-163.
821.	-164.
955.	-166.
1144.	-168.
1316.	-169.
1504.	-169.
1680.	-169.
1868.	-173.
2075.	-173.
2243.	-174.
2405.	-174.
2586.	-176.
2765.	-174.
2977.	-173.
3122.	-174.
3325.	-174.
3488.	-174.
3658.	-173.
3844.	-169.
4215.	-163.
4477.	-158.
4861.	-158.
5321.	-159.
5715.	-159.
5901.	-159.
5997.	-157.
6008.	-159.
6018.	-161.
6028.	-162.
6043.	-163.
6062.	-164.
6092.	-165.
6137.	-173.
6193.	-173.
6265.	-176.
6361.	-176.
6512.	-179.
6722.	-174.
7091.	-176.
7429.	-172.
7620.	-178.
7864.	-186.
8043.	-164.
8291.	-179.
8523.	-178.
8769.	-176.
9005.	-178.
9183.	-183.
9349.	-185.
9610.	-183.
9838.	-182.
10064.	-179.
10334.	-183.
10573.	-184.
10814.	-189.
11131.	-191.
11380.	-191.
11610.	-191.
11860.	-187.

TOTAL HEAD DATA: S8T1
R=30.5 cm D=170.2 cm

TIME (min)	TH (cmH_2O)
0.	-158.
3.	-187.
8.	-187.
13.	-184.
18.	-178.
22.	-174.
27.	-169.
33.	-166.
44.	-159.
55.	-156.
68.	-154.
82.	-154.
110.	-153.
132.	-152.
140.	-151.
150.	-151.
165.	-152.
180.	-151.
195.	-152.
210.	-151.
240.	-151.
270.	-151.
300.	-152.
330.	-153.
360.	-154.
390.	-154.
420.	-154.
450.	-154.
480.	-154.
535.	-156.
595.	-157.
667.	-158.
716.	-158.
818.	-159.
955.	-161.
1141.	-161.
1314.	-164.
1501.	-165.
1676.	-164.
1862.	-166.
2075.	-172.
2240.	-174.
2401.	-174.
2584.	-174.
2763.	-174.
2975.	-171.
3120.	-171.
3323.	-172.
3484.	-173.
3655.	-174.
3842.	-169.
4081.	-163.
4213.	-161.
4475.	-154.
4859.	-155.
5319.	-158.
5714.	-158.
5899.	-156.
5996.	-154.
6006.	-154.
6016.	-154.
6025.	-155.
6041.	-153.
6060.	-153.
6091.	-154.
6135.	-166.
6192.	-166.
6265.	-171.
6360.	-176.
6510.	-173.
6720.	-173.
7089.	-173.
7425.	-167.
7620.	-171.
7862.	-183.
8038.	-184.
8286.	-182.
8521.	-179.
8767.	-176.
9002.	-174.
9181.	-180.
9348.	-185.
9607.	-185.
9836.	-183.
10063.	-180.
10332.	-179.
10571.	-183.
10812.	-190.
11129.	-191.
11379.	-192.
11609.	-190.
11858.	-189.

TOTAL HEAD DATA: S8T1
R=30.5 cm D=209.6 cm

TIME (min)	TH (cmH_2O)
0.	-188.
2.	-188.
5.	-187.
9.	-187.
14.	-186.
27.	-184.
33.	-179.
45.	-177.
57.	-177.
70.	-177.
93.	-177.
115.	-177.
133.	-173.
150.	-173.
165.	-172.
180.	-172.
195.	-171.
210.	-172.
225.	-171.
270.	-171.
300.	-171.
330.	-171.
360.	-171.
390.	-169.
420.	-171.
450.	-169.
480.	-169.
535.	-171.
595.	-169.
667.	-171.
717.	-171.
819.	-170.
955.	-171.
1142.	-171.
1315.	-172.
1502.	-173.
1678.	-173.
1865.	-176.
2075.	-177.
2241.	-178.
2403.	-178.
2585.	-178.
2764.	-178.
2976.	-177.
3121.	-177.
3325.	-177.
3485.	-177.
3657.	-176.
3843.	-176.
4086.	-174.
4215.	-174.
4477.	-169.
4860.	-168.
5320.	-166.
5714.	-168.
5900.	-166.
5997.	-164.
6008.	-172.
6018.	-174.
6028.	-176.
6042.	-179.
6062.	-181.
6092.	-178.
6137.	-178.
6193.	-187.
6265.	-191.
6361.	-195.
6511.	-196.
6721.	-186.
7090.	-192.
7426.	-192.
7620.	-202.
7863.	-208.
8042.	-208.
8269.	-208.
8523.	-207.
8768.	-205.
9004.	-203.
9182.	-205.
9349.	-205.
9609.	-208.
9832.	-208.
10064.	-208.
10333.	-208.
10572.	-207.
10812.	-208.
11130.	-212.
11380.	-214.
11610.	-213.
11859.	-211.

TOTAL HEAD DATA: S8T1
R= 30.5 cm D= 240.0 cm

TIME (min)	TH (cmH_2O)
0.	-197.
2.	-197.
5.	-197.
9.	-197.
14.	-196.
27.	-196.
33.	-195.
45.	-193.
57.	-193.
70.	-193.
93.	-193.
115.	-193.
133.	-192.
150.	-191.
165.	-191.
180.	-188.
195.	-188.
210.	-187.
225.	-186.
270.	-186.
300.	-186.
330.	-187.
360.	-187.
390.	-186.
420.	-186.
450.	-184.
480.	-184.
535.	-186.
595.	-186.
667.	-186.
717.	-186.
819.	-184.
955.	-184.
1142.	-184.
1315.	-185.
1502.	-184.
1678.	-184.
1865.	-184.
2075.	-186.
2241.	-187.

TOTAL HEAD DATA: S8T1
R=61.0 cm D=122.0 cm

TIME (min)	TH (cmH_2O)
0.	-25.
3.	-28.
8.	-36.
13.	-38.
18.	-44.
22.	-44.
27.	-50.
33.	-56.
44.	-69.
55.	-75.
68.	-82.
82.	-100.
110.	-109.
132.	-119.
140.	-124.
150.	-128.
165.	-136.
180.	-142.
195.	-146.
210.	-151.
240.	-159.
270.	-168.
300.	-173.
330.	-181.
360.	-188.
390.	-192.
420.	-197.
450.	-203.
480.	-206.
535.	-212.
595.	-220.
667.	-223.
716.	-226.
818.	-229.
955.	-232.
1141.	-233.
1314.	-235.
1501.	-235.
1676.	-235.
1862.	-235.
2075.	-241.
2240.	-242.
2401.	-242.
2584.	-241.
2763.	-238.
2975.	-237.
3120.	-235.
3323.	-233.
3494.	-233.
3655.	-233.
3842.	-233.
4081.	-230.
4213.	-227.
4475.	-225.
4859.	-223.
5319.	-223.
5714.	-221.
5899.	-220.
5996.	-218.
6006.	-217.
6016.	-217.
6025.	-216.
6041.	-216.
6060.	-216.
6091.	-216.
6135.	-213.
6192.	-212.
6265.	-215.
6360.	-220.
6510.	-223.
6720.	-223.
7089.	-218.
7425.	-213.
7620.	-213.
7862.	-221.
8038.	-222.
8286.	-223.
8521.	-217.
8767.	-216.
9002.	-213.
9181.	-220.
9348.	-223.
9607.	-222.
9836.	-217.
10063.	-215.
10332.	-212.
10571.	-213.
10812.	-218.
11129.	-219.
11379.	-215.
11609.	-213.
11858.	-210.

TOTAL HEAD DATA: S8T1
R=61.0 cm D=134.6 cm

TIME (min)	TH (cmH_2O)
0.	-201.
3.	-201.
8.	-202.
13.	-202.
18.	-203.
22.	-203.
27.	-202.
33.	-202.
44.	-202.
55.	-202.
68.	-202.
82.	-202.
110.	-202.
132.	-201.
140.	-197.
150.	-196.
165.	-197.
180.	-198.
195.	-198.
210.	-197.
240.	-190.
270.	-186.
300.	-181.
330.	-179.
360.	-178.
390.	-178.
420.	-179.
450.	-179.
480.	-179.
535.	-178.
595.	-177.
667.	-177.
716.	-177.
818.	-176.
955.	-174.
1141.	-173.
1314.	-174.
1501.	-174.
1676.	-171.
1862.	-175.
2075.	-180.
2240.	-181.
2401.	-179.
2584.	-179.
2763.	-179.
2975.	-177.
3120.	-178.
3323.	-179.
3484.	-179.
3655.	-179.
3842.	-179.
4081.	-174.
4213.	-173.
4475.	-168.
4859.	-166.
5319.	-166.
5714.	-166.
5899.	-163.
5996.	-157.
6006.	-158.
6016.	-156.
6025.	-157.
6041.	-156.
6060.	-154.
6091.	-156.
6135.	-156.
6192.	-167.
6265.	-172.
6360.	-178.
6510.	-182.
6720.	-183.
7089.	-180.
7425.	-166.
7620.	-177.
7862.	-191.
8038.	-193.
8286.	-192.
8521.	-191.
8767.	-185.
9002.	-184.
9181.	-188.
9348.	-198.
9607.	-199.
9836.	-196.
10063.	-193.
10332.	-188.
10571.	-188.
10812.	-204.
11129.	-203.
11379.	-202.
11609.	-195.
11858.	-191.

TOTAL HEAD DATA: S8T1
R= 61.0cm D= 170.2cm

TIME (min)	TH (cmH_2O)
0.	-192.
2.	-192.
6.	-192.
11.	-192.
16.	-192.
25.	-191.
32.	-184.
42.	-181.
53.	-177.
65.	-173.
84.	-171.
105.	-169.
130.	-164.
140.	-163.
150.	-163.
165.	-162.
180.	-163.
195.	-162.
210.	-161.
240.	-161.
270.	-162.
300.	-161.
330.	-161.
360.	-164.
390.	-164.
420.	-166.
450.	-166.
480.	-166.
535.	-164.
595.	-167.
667.	-168.
715.	-166.
817.	-166.
955.	-167.
1139.	-168.
1312.	-169.
1500.	-169.
1675.	-168.
1857.	-178.
2075.	-176.
2239.	-177.
2399.	-176.
2583.	-177.
2762.	-177.
2974.	-174.
3119.	-174.
3322.	-178.
3483.	-177.
3653.	-177.
3841.	-187.
4084.	-171.
4212.	-170.
4474.	-165.
4858.	-164.
5318.	-164.
5713.	-164.
5898.	-163.
5995.	-158.
6005.	-158.
6015.	-161.
6025.	-161.
6040.	-161.
6060.	-164.
6090.	-166.
6135.	-171.
6191.	-179.
6265.	-179.
6359.	-182.
6509.	-184.
6719.	-179.
7088.	-182.
7420.	-172.
7620.	-186.
7861.	-203.
8038.	-197.
8283.	-193.
8518.	-193.
8765.	-189.
9001.	-190.
9180.	-194.
9346.	-196.
9606.	-197.
9835.	-196.
10061.	-195.
10330.	-193.
10570.	-195.
10811.	-200.
11127.	-200.
11378.	-201.
11608.	-196.
11857.	-199.

TOTAL HEAD DATA: S8T1
R=61.0 cm D=209.6 cm

TIME (min)	TH (cmH_2O)
0.	-195.
2.	-196.
5.	-195.
9.	-196.
14.	-196.
27.	-196.
33.	-191.
45.	-188.
57.	-188.
70.	-187.
93.	-187.
115.	-187.
133.	-183.
150.	-182.
165.	-182.
180.	-179.
195.	-181.
210.	-179.
225.	-181.
270.	-179.
300.	-179.
330.	-179.
360.	-179.
390.	-179.
420.	-179.
450.	-178.
480.	-178.
535.	-179.
595.	-179.
667.	-179.
717.	-178.
819.	-178.
955.	-176.
1142.	-178.
1315.	-176.
1502.	-180.
1678.	-180.
1865.	-183.
2075.	-184.
2241.	-184.
2403.	-184.
2585.	-184.
2764.	-184.
2976.	-183.
3121.	-183.
3325.	-183.
3485.	-183.
3657.	-183.
3843.	-181.
4086.	-167.
4215.	-178.
4477.	-175.
4860.	-173.
5320.	-172.
5714.	-172.
5900.	-171.
5997.	-169.
6008.	-179.
6018.	-181.
6028.	-184.
6042.	-186.
6062.	-188.
6092.	-188.
6137.	-184.
6193.	-194.
6265.	-200.
6361.	-202.
6511.	-202.
6721.	-195.
7090.	-199.
7426.	-200.
7620.	-210.
7863.	-213.
8042.	-213.
8289.	-213.
8523.	-212.
8768.	-212.
9004.	-211.
9182.	-211.
9349.	-212.
9609.	-212.
9832.	-212.
10064.	-212.
10333.	-212.
10572.	-211.
10812.	-212.
11130.	-215.
11380.	-217.
11610.	-217.
11859.	-216.

TOTAL HEAD DATA: S8T1
R=61.0 cm D=240.0 cm

TIME (min)	TH (cmH_2O)
0.	-191.
2.	-191.
5.	-191.
9.	-191.
14.	-191.
27.	-188.
33.	-187.
45.	-186.
57.	-186.
70.	-186.
93.	-186.
115.	-184.
133.	-184.
150.	-183.
165.	-182.
180.	-182.
195.	-182.
210.	-182.
225.	-182.
270.	-182.
300.	-181.
330.	-181.
360.	-181.
390.	-182.
420.	-181.
450.	-179.
480.	-179.
535.	-181.
595.	-179.
667.	-181.
717.	-179.
819.	-179.
955.	-179.
1142.	-179.
1315.	-179.
1502.	-180.
1678.	-181.
1865.	-182.
2075.	-183.
2241.	-183.
2403.	******
2764.	******
3121.	******
3485.	******
3843.	******
4215.	******
4860.	******
5714.	******
5997.	******
6018.	******
6042.	******
6092.	******
6193.	******
6361.	******
6721.	-206.
7090.	-208.
7620.	-223.
7863.	-226.
8042.	-226.
8289.	-220.
8523.	-220.
8768.	-220.
9004.	-218.
9182.	-217.
9349.	-220.
9609.	-221.
9832.	-222.
10064.	-222.
10333.	-220.
10572.	-216.
10812.	-221.
11130.	-225.
11380.	-227.
11610.	-221.
11859.	-222.

TOTAL HEAD DATA: S8T1
R= 91.0 cm D= 122.0 cm

TIME (min)	TH (cmH_2O)	TIME (min)	TH (cmH_2O)	TIME (min)	TH (cmH_2O)
0.	-181.	667.	-186.	6015.	-191.
2.	-179.	715.	-188.	6025.	-191.
6.	-179.	817.	-183.	6040.	-190.
11.	-178.	955.	-171.	6060.	-188.
16.	-177.	1139.	-161.	6090.	-188.
25.	-177.	1312.	-161.	6135.	-184.
32.	-176.	1500.	-165.	6191.	-162.
42.	-177.	1675.	-184.	6265.	-162.
53.	-178.	1857.	-156.	6359.	-164.
65.	-179.	2075.	-167.	6509.	-169.
84.	-171.	2239.	-174.	6719.	-181.
105.	-161.	2399.	-186.	7088.	-185.
130.	-166.	2583.	-191.	7420.	-178.
140.	-167.	2762.	-193.	7520.	-164.
150.	-182.	2974.	-195.	7861.	-167.
165.	-174.	3119.	-195.	8036.	-167.
180.	-174.	3322.	-188.	8283.	-177.
195.	-173.	3483.	-188.	8518.	-178.
210.	-169.	3653.	-188.	8765.	-181.
240.	-163.	3841.	-195.	9001.	-180.
270.	-163.	4084.	-196.	9180.	-181.
300.	-161.	4212.	-196.	9345.	-179.
330.	-161.	4474.	-201.	9606.	-179.
360.	-159.	4858.	-196.	9835.	-180.
390.	-163.	5318.	-195.	10061.	-180.
420.	-166.	5713.	-195.	10330.	-181.
450.	-167.	5898.	-194.	10570.	-179.
480.	-172.	5995.	-191.	10811.	-179.
535.	-171.	6005.	-191.	11127.	-180.
595.	-181.			11378.	-180.
				11608.	-181.
				11857.	-180.

TOTAL HEAD DATA: S8T1
R= 91.0 cm D= 134.6 cm

TIME (min)	TH (cmH_2O)
0.	-200.
2.	-200.
6.	-200.
11.	-200.
16.	-200.
25.	-201.
32.	-201.
42.	-201.
53.	-203.
65.	-205.
84.	-208.
105.	-208.
130.	-208.
140.	-206.
150.	-207.
165.	-208.
180.	-208.
195.	-208.
210.	-210.
240.	-210.
270.	-211.
300.	-213.
330.	-211.
360.	-211.
390.	-211.
420.	-210.
450.	-210.
480.	-210.
535.	-210.
595.	-210.
657.	-210.
715.	-210.
817.	-208.
955.	-210.
1139.	-208.
1312.	-84.

TOTAL HEAD DATA: S8T1
R= 91.0cm D= 170.2cm

TIME (min)	TH (cmH_2O)
0.	-192.
2.	-191.
6.	-192.
11.	-192.
16.	-191.
25.	-191.
32.	-191.
42.	-191.
53.	-188.
65.	-183.
84.	-179.
105.	-176.
130.	-171.
140.	-173.
150.	-171.
165.	-168.
180.	-169.
195.	-168.
210.	-169.
240.	-168.
270.	-168.
330.	-161.
360.	-166.
390.	-166.
420.	-166.
450.	-167.
480.	-167.
535.	-166.
595.	-167.
667.	-167.
715.	-167.
817.	-167.
955.	-169.
1139.	-169.
1312.	-173.

TOTAL HEAD DATA: S8T1
R= 91.0cm D= 177.0cm

TIME (min)	TH (cmH_2O)
6722.	-184.
7091.	-190.
7429.	-184.
7620.	-192.
7864.	-198.
8043.	-198.
8291.	-196.
8523.	-196.
8769.	-195.
9005.	-195.
9183.	-199.
9349.	-201.
9610.	-201.
9838.	-200.
10064.	-199.
10334.	-197.
10573.	-204.
10814.	-203.
11131.	-204.
11380.	-205.
11610.	-203.
11860.	-201.

TOTAL HEAD DATA: S8T1
R= 91.0 cm D= 209.5 cm

TIME (min)	TH (cmH_2O)
0.	-200.
2.	-198.
6.	-198.
11.	-200.
16.	-200.
25.	-200.
32.	-196.
42.	-198.
53.	-198.
65.	-198.
84.	-198.
105.	-196.
130.	-195.
140.	-193.
150.	-193.
165.	-188.
180.	-186.
195.	-184.
210.	-184.
240.	-184.
270.	-184.
300.	-184.
330.	-178.
360.	-178.
390.	-178.
420.	-178.
450.	-178.
480.	-177.
535.	-176.
595.	-177.
667.	-177.
715.	-177.
817.	-176.
955.	-177.
1139.	-176.
1312.	-177.
1500.	-186.
1675.	-184.
1857.	-187.
2075.	-188.
2239.	-190.
2399.	-190.
2583.	-190.
2762.	-191.
2974.	-191.
3119.	-191.
3322.	-190.
3483.	-190.
3653.	-190.
3841.	-189.
4084.	-189.
4212.	-188.
4474.	-186.
4858.	-184.
5316.	-183.
5713.	-183.
5898.	-182.
5995.	-182.
6005.	-182.
6015.	-184.
6025.	-184.
6040.	-186.
6060.	-188.
6090.	-188.
6135.	-187.
6191.	-191.
6265.	-193.
6359.	-196.
6509.	-198.
6719.	-195.
7088.	-198.
7420.	-198.
7620.	-206.
7861.	-212.
8038.	-211.
8283.	-212.
8518.	-212.
8765.	-212.
9001.	-211.
9180.	-213.
9346.	-213.
9606.	-213.
9835.	-214.
10061.	-213.
10330.	-215.
10570.	-214.
10811.	-215.
11127.	-215.
11378.	-215.
11608.	-216.
11857.	-216.

TOTAL HEAD DATA: S8T1
R= 91.0 cm D= 238.8 cm

TIME (min)	TH (cmH_2O)	TIME (min)	TH (cmH_2O)	TIME (min)	TH (cmH_2O)
0.	-192.	717.	-183.		
2.	-192.	819.	-181.		
5.	-192.	965.	-183.		
9.	-192.	1142.	-183.		
14.	-192.	1315.	-183.		
27.	-188.	1502.	-183.		
33.	-188.	1678.	-184.		
45.	-186.	1865.	-184.		
57.	-185.	2075.	-189.		
70.	-186.	2241.	-186.		
93.	-188.	6721.	-207.		
115.	-186.	7090.	-210.		
133.	-186.	7620.	-231.		
150.	-187.	7863.	-232.		
165.	-187.	8042.	-232.		
180.	-187.	8269.	-228.		
195.	-187.	8523.	-228.		
210.	-187.	8768.	-221.		
225.	-188.	9004.	-221.		
270.	-188.	9182.	-222.		
300.	-186.	9349.	-222.		
330.	-188.	9609.	-223.		
360.	-187.	9832.	-224.		
390.	-187.	10064.	-224.		
420.	-187.	10333.	-223.		
450.	-182.	10572.	-217.		
480.	-183.	10812.	-222.		
535.	-184.	11130.	-227.		
595.	-184.	11380.	-226.		
667.	-184.	11610.	-222.		
		11859.	-222.		

CORRECTED MOISTURE CONTENT DATA:S8T1
R= 30 cm

TIME (min)	DEPTH 30 (cm)	DEPTH 46 (cm)	DEPTH 61 (cm)	DEPTH 76 (cm)	DEPTH 91 (cm)	DEPTH 107 (cm)	DEPTH 114 (cm)	DEPTH 122 (cm)
	THETA							
0.0	0.0209	0.0416	0.0477	0.0547	0.0725	0.2545	0.3091	0.3177
3.0					0.0744	0.2549	0.3121	0.3195
9.0					0.0758	0.2538	0.3108	0.3272
14.0					0.0752	0.2566	0.3196	0.3239
20.0					0.0742	0.2520	0.3157	0.3195
26.0					0.0735	0.2590	0.3190	0.3208
38.0					0.0739	0.2550	0.3175	0.3175
51.0					0.0763	0.2527	0.3187	0.3187
60.0					0.0746	0.2555	0.3151	0.3151
107.0					0.0713	0.2538	0.3142	0.3142
138.0	0.0221	0.0326	0.0432	0.0505	0.0741	0.2550	0.3130	0.3130
186.0	0.0219	0.0351	0.0426	0.0531	0.0752	0.2555	0.3128	0.3128
226.0	0.0205	0.0323	0.0445	0.0529	0.0763	0.2604	0.3208	0.3253
294.0	0.0213	0.0354	0.0430	0.0530	0.0744	0.2561	0.3160	0.3272
321.0	0.0184	0.0355	0.0439	0.0559	0.0785	0.2547	0.3184	0.3258
372.0					0.0736	0.2567	0.3161	0.3249
393.0					0.0754	0.2584	0.3219	0.3257
472.0					0.0732	0.2569	0.3179	0.3227
567.0	0.0222	0.0344	0.0458	0.0539	0.0749	0.2582	0.3165	0.3253
604.0	0.0206	0.0337	0.0439	0.0529	0.0772	0.2557	0.3126	0.3292
738.0	0.0227	0.0343	0.0417	0.0512	0.0728	0.2555	0.3194	0.3208
799.0	0.0208	0.0329	0.0446	0.0559	0.0773	0.2576	0.3189	0.3263
977.0					0.0768	0.2569	0.3168	0.3229
1150.0					0.0777	0.2533	0.3157	0.3250
1334.0					0.0801	0.2595	0.3137	0.3241
1528.0					0.0793	0.2539	0.3222	0.3257
1678.0					0.0786	0.2592	0.3202	0.3299
1885.0					0.0799	0.2574	0.3142	0.3202
2054.0					0.0795	0.2613	0.3162	0.3231
2222.0					0.0810	0.2626	0.3195	0.3301
2441.0					0.0843	0.2617	0.3179	0.3240
2593.0					0.0841	0.2636	0.3186	0.3237
2807.0	0.0206	0.0352	0.0442	0.0534	0.0863	0.2642	0.3218	0.3221
2991.0					0.0841	0.2634	0.3163	0.3300
3184.0					0.0871	0.2673	0.3256	0.3227
3475.0					0.0893	0.2610	0.3135	0.3230
3684.0					0.0909	0.2663	0.3204	0.3244
3865.0					0.0913	0.2751	0.3218	0.3236
4093.0					0.0899	0.2731	0.3212	0.3248
4245.0	0.0238	0.0337	0.0462	0.0535	0.0930	0.2682	0.3199	0.3250
4526.0					0.0947	0.2715	0.3181	0.3223
4873.0					0.0957	0.2681	0.3232	0.3257
5333.0					0.0989	0.2704	0.3209	0.3237

CORRECTED MOISTURE CONTENT DATA:S8T1
R= 30 cm

TIME (min)	DEPTH 30 (cm)	DEPTH 46 (cm)	DEPTH 61 (cm)	DEPTH 76 (cm)	DEPTH 91 (cm)	DEPTH 107 (cm)	DEPTH 114 (cm)	DEPTH 122 (cm)
	----------	----------	----------	----------	THETA	----------	----------	----------
5692.0	0.0203	0.0341	0.0457	0.0568	0.0960	0.2796	0.3270	0.3243
5953.0					0.0977	0.2734	0.3221	0.3238
5998.0					0.0975	0.2759	0.3234	0.3309
6005.0					0.0987	0.2700	0.3217	0.3244
6013.0					0.0998	0.2740	0.3171	0.3265
6059.0					0.0990	0.2704	0.3257	0.3251
6068.0					0.0987	0.2717	0.3239	0.3247
6095.0					0.0981	0.2751	0.3213	0.3246
6140.0					0.0977	0.2655	0.3209	0.3256
6217.0					0.0963	0.2702	0.3195	0.3232
6265.0					0.1009	0.2741	0.3194	0.3223
6301.0	0.0230	0.0364	0.0436	0.0594	0.0976	0.2742	0.3169	0.3229
6495.0	0.0231	0.0349	0.0430	0.0593	0.0982	0.2748	0.3232	0.3253
6743.0	0.0208	0.0325	0.0461	0.0580	0.1019	0.2691	0.3193	0.3263
7086.0	0.0242	0.0343	0.0434	0.0609	0.1000	0.2675	0.3210	0.3274
7444.0					0.1009	0.2779	0.3204	0.3259
7611.0	0.0218	0.0331	0.0446	0.0582	0.0996	0.2777	0.3254	0.3212
7699.0	0.0224	0.0376	0.0441	0.0592	0.1026	0.2756	0.3171	0.3234
8052.0					0.1019	0.2669	0.3223	0.3200
8308.0					0.1028	0.2707	0.3213	0.3252
8523.0					0.1015	0.2719	0.3231	0.3286
8777.0					0.1015	0.2789	0.3237	0.3226
8996.0					0.1024	0.2745	0.3181	0.3247
9214.0	0.0222	0.0361	0.0449	0.0613	0.1030	0.2724	0.3215	0.3261
9359.0					0.1015	0.2763	0.3214	0.3188
10093.0					0.1033	0.2752	0.3257	0.3254
10579.0					0.1033	0.2731	0.3247	0.3241
11149.0					0.1036	0.2748	0.3199	0.3253
11385.0					0.1016	0.2707	0.3186	0.3216
11632.0	0.0216	0.0354	0.0452	0.0602	0.1007	0.2749	0.3231	0.3258
11867.0					0.1065	0.2749	0.3228	0.3238

CORRECTED MOISTURE CONTENT DATA:S8T1
R= 30 cm

TIME (min)	DEPTH 130 (cm)	DEPTH 137 (cm)	DEPTH 145 (cm)	DEPTH 152 (cm)	DEPTH 160 (cm)	DEPTH 168 (cm)	DEPTH 175 (cm)
	----------	----------	----------	THETA	----------	----------	----------
0.0	0.2799	0.2389	0.2154	0.2322	0.2692	0.3005	0.3301
3.0	0.2809	0.2351	0.2244	0.2303	0.2704	0.3028	0.3298
9.0	0.2796	0.2387	0.2213	0.2334	0.2723	0.2953	0.3264
14.0	0.2855	0.2407	0.2324	0.2585	0.2943	0.3124	0.3449
20.0	0.2820	0.2410	0.2383	0.2626	0.3002	0.3277	0.3498
28.0	0.2790	0.2508	0.2477	0.2873	0.3316	0.3568	0.3605
36.0	0.2871	0.2550	0.2610	0.2924	0.3343	0.3531	0.3631
51.0	0.2876	0.2590	0.2722	0.3026	0.3473	0.3562	0.3728
66.0	0.2832	0.2629	0.2729	0.3133	0.3520	0.3578	0.3728
107.0	0.2917	0.2684	0.2810	0.3133	0.3608	0.3715	0.3759
136.0	0.2915	0.2715	0.2856	0.3228	0.3647	0.3725	0.3734
180.0	0.2921	0.2752	0.2889	0.3252	0.3678	0.3725	0.3770
220.0	0.2959	0.2732	0.2896	0.3281	0.3629	0.3796	0.3767
294.0	0.2939	0.2796	0.2955	0.3239	0.3639	0.3685	0.3783
321.0	0.2971	0.2828	0.2999	0.3271	0.3673	0.3777	0.3823
372.0	0.2978	0.2764	0.2966	0.3259	0.3694	0.3773	0.3809
393.0	0.2994	0.2796	0.2965	0.3261	0.3642	0.3724	0.3817
472.0	0.2957	0.2817	0.3000	0.3249	0.3685	0.3716	0.3753
567.0	0.2984	0.2813	0.2994	0.3317	0.3725	0.3696	0.3814
604.0	0.2988	0.2822	0.3023	0.3302	0.3684	0.3787	0.3897
738.0	0.3038	0.2827	0.3014	0.3294	0.3722	0.3732	0.3846
799.0	0.2974	0.2784	0.3049	0.3276	0.3677	0.3740	0.3842
977.0	0.2965	0.2769	0.2983	0.3281	0.3669	0.3803	0.3899
1156.0	0.2958	0.2812	0.3011	0.3256	0.3666	0.3718	0.3885
1334.0	0.2980	0.2796	0.3016	0.3245	0.3684	0.3794	0.3926
1528.0	0.2984	0.2778	0.2960	0.3229	0.3637	0.3721	0.3852
1678.0	0.2962	0.2853	0.2988	0.3197	0.3619	0.3773	0.3896
1885.0	0.2942	0.2731	0.2939	0.3208	0.3598	0.3701	0.3841
2054.0	0.2932	0.2765	0.2984	0.3262	0.3631	0.3715	0.3912
2222.0	0.2883	0.2777	0.2912	0.3199	0.3624	0.3747	0.3870
2441.0	0.2965	0.2749	0.2892	0.3180	0.3547	0.3761	0.3842
2593.0	0.2940	0.2707	0.2938	0.3148	0.3559	0.3740	0.3885
2807.0	0.2945	0.2735	0.2906	0.3142	0.3564	0.3774	0.3857
2991.0	0.2948	0.2764	0.2907	0.3130	0.3555	0.3786	0.3889
3184.0	0.2946	0.2773	0.2896	0.3161	0.3517	0.3706	0.3886
3475.0	0.2934	0.2751	0.2876	0.3149	0.3598	0.3722	0.3916
3684.0	0.2939	0.2760	0.2923	0.3202	0.3585	0.3717	0.3945
3865.0	0.3130	0.2784	0.2881	0.3142	0.3516	0.3745	0.3913
4093.0	0.2930	0.2799	0.2939	0.3284	0.3530	0.3769	0.3913
4245.0	0.2988	0.2765	0.2978	0.3204	0.3577	0.3762	0.3917
4526.0	0.2971	0.2791	0.2995	0.3209	0.3575	0.3788	0.3884
4873.0	0.2945	0.2789	0.2962	0.3231	0.3646	0.3754	0.3951
5333.0	0.2986	0.2820	0.3005	0.3256	0.3572	0.3701	0.3881

CORRECTED MOISTURE CONTENT DATA:S8T1
R= 30 cm

TIME (min)	DEPTH 130 (cm)	DEPTH 137 (cm)	DEPTH 145 (cm)	DEPTH 152 (cm)	DEPTH 160 (cm)	DEPTH 168 (cm)	DEPTH 175 (cm)
	----------	----------	----------	THETA	----------	----------	----------
5092.0	0.3016	0.2841	0.3014	0.3222	0.3607	0.3780	0.3941
5953.0	0.2991	0.2836	0.3029	0.3243	0.3655	0.3803	0.3931
5998.0	0.2967	0.2831	0.3041	0.3272	0.3658	0.3769	0.3917
6005.0	0.3012	0.2883	0.2941	0.3301	0.3611	0.3796	0.3900
6013.0	0.2983	0.2871	0.2983	0.3192	0.3666	0.3783	0.3926
6059.0	0.2940	0.2791	0.2990	0.3224	0.3588	0.3719	0.3896
6068.0	0.2955	0.2804	0.2963	0.3179	0.3596	0.3803	0.3913
6095.0	0.2925	0.2768	0.2997	0.3212	0.3576	0.3779	0.3937
6140.0	0.2977	0.2756	0.2930	0.3143	0.3515	0.3814	0.3981
6217.0	0.2989	0.2707	0.2965	0.3172	0.3570	0.3728	0.3895
6265.0	0.2949	0.2721	0.2939	0.3181	0.3507	0.3729	0.3900
6381.0	0.2927	0.2737	0.2884	0.3140	0.3539	0.3738	0.3897
6495.0	0.2985	0.2749	0.2856	0.3116	0.3492	0.3669	0.3910
6743.0	0.2974	0.2764	0.2849	0.3118	0.3140	0.3636	0.3896
7086.0	0.2929	0.2711	0.2864	0.3056	0.3471	0.3653	0.3896
7444.0	0.2859	0.2718	0.2879	0.3064	0.3487	0.3700	0.3935
7611.0	0.2944	0.2728	0.2848	0.3048	0.3481	0.3666	0.3927
7899.0	0.2921	0.2715	0.2793	0.2956	0.3412	0.3605	0.3810
8052.0	0.2933	0.2656	0.2764	0.2973	0.3376	0.3500	0.3812
8308.0	0.2908	0.2669	0.2785	0.3014	0.3403	0.3545	0.3807
8523.0	0.2882	0.2699	0.2770	0.2955	0.3358	0.3504	0.3759
8777.0	0.2959	0.2685	0.2768	0.2994	0.3353	0.3529	0.3764
8996.0	0.2943	0.2709	0.2776	0.2923	0.3361	0.3542	0.3826
9214.0	0.2951	0.2695	0.2751	0.2958	0.3325	0.3527	0.3789
9359.0	0.2925	0.2680	0.2741	0.2915	0.3337	0.3533	0.3741
10093.0	0.2905	0.2636	0.2689	0.2905	0.3336	0.3542	0.3714
10579.0	0.2885	0.2637	0.2696	0.2895	0.3305	0.3514	0.3715
11149.0	0.2901	0.2602	0.2599	0.2847	0.3218	0.3425	0.3679
11385.0	0.2915	0.2600	0.2578	0.2812	0.3198	0.3385	0.3613
11632.0	0.2868	0.2601	0.2607	0.2812	0.3178	0.3346	0.3650
11867.0	0.2905	0.2614	0.2621	0.2790	0.3157	0.3435	0.3636

CORRECTED MOISTURE CONTENT DATA:S8T1
R= 60 cm

TIME (min)	DEPTH 30 (cm)	DEPTH 46 (cm)	DEPTH 61 (cm)	DEPTH 76 (cm)	DEPTH 91 (cm)	DEPTH 107 (cm)	DEPTH 114 (cm)	DEPTH 122 (cm)
	THETA							
0.0	0.0376	0.0301	0.0390	0.0566	0.1024	0.2576	0.2912	0.2888
78.0					0.1104	0.2581	0.2925	0.2829
98.0					0.1054	0.2558	0.2905	0.2859
156.0	0.0356	0.0330	0.0382	0.0544	0.1107	0.2541	0.2866	0.2741
196.0	0.0340	0.0335	0.0403	0.0559	0.1124	0.2608	0.2895	0.2807
242.0	0.0347	0.0325	0.0422	0.0554	0.1108	0.2587	0.2886	0.2846
309.0	0.0335	0.0325	0.0407	0.0558	0.1112	0.2557	0.2946	0.2787
332.0					0.1115	0.2563	0.2923	0.2827
380.0					0.1105	0.2561	0.2876	0.2806
416.0					0.1116	0.2610	0.2805	0.2661
492.0					0.1075	0.2563	0.2895	0.2820
554.0	0.0355	0.0338	0.0391	0.0566	0.1074	0.2595	0.2798	0.2653
613.0	0.0347	0.0305	0.0403	0.0572	0.1098	0.2548	0.2941	0.2804
728.0	0.0374	0.0320	0.0399	0.0556	0.1116	0.2540	0.2942	0.2863
789.0	0.0341	0.0325	0.0395	0.0538	0.1102	0.2599	0.2914	0.2831
966.0					0.1096	0.2588	0.2931	0.2830
1164.0					0.1110	0.2589	0.2934	0.2832
1342.0					0.1100	0.2601	0.2899	0.2860
1512.0					0.1092	0.2577	0.2944	0.2869
1690.0					0.1061	0.2608	0.2975	0.2858
1876.0					0.1102	0.2578	0.2945	0.2863
2038.0					0.1089	0.2546	0.2950	0.2857
2231.0					0.1081	0.2597	0.2953	0.2889
2433.0					0.1108	0.2554	0.2943	0.2885
2599.0					0.1087	0.2540	0.3012	0.2846
2798.0	0.0340	0.0326	0.0410	0.0567	0.1130	0.2548	0.2901	0.2920
2998.0					0.1156	0.2573	0.2936	0.2911
3178.0					0.1108	0.2613	0.2983	0.2890
3468.0					0.1136	0.2611	0.2922	0.2872
3675.0					0.1146	0.2622	0.2927	0.2872
3859.0					0.1149	0.2623	0.2990	0.2866
4104.0					0.1161	0.2600	0.2994	0.2887
4237.0	0.0359	0.0315	0.0410	0.0564	0.1159	0.2632	0.2945	0.2939
4532.0					0.1185	0.2645	0.2962	0.2916
4676.0					0.1151	0.2629	0.2999	0.2948
5339.0					0.1221	0.2624	0.2999	0.2915
5699.0	0.0344	0.0333	0.0393	0.0566	0.1217	0.2684	0.2997	0.3015
5960.0					0.1275	0.2762	0.3099	0.3017
6024.0	0.0344	0.0324	0.0391	0.0574	0.1247	0.2723	0.3091	0.3030
6034.0	0.0344	0.0300	0.0405	0.0559	0.1273	0.2710	0.3033	0.2970
6152.0	0.0347	0.0306	0.0403	0.0560	0.1241	0.2703	0.3086	0.2982
6275.0	0.0354	0.0330	0.0425	0.0574	0.1254	0.2729	0.3051	0.2991
6369.0	0.0339	0.0320	0.0403	0.0585	0.1245	0.2726	0.3112	0.3003

CORRECTED MOISTURE CONTENT DATA:S8T1
R=60 cm

TIME (min)	DEPTH 30 (cm) THETA	DEPTH 46 (cm) THETA	DEPTH 61 (cm) THETA	DEPTH 76 (cm) THETA	DEPTH 91 (cm) THETA	DEPTH 107 (cm) THETA	DEPTH 114 (cm) THETA	DEPTH 122 (cm) THETA
6505.0	0.0345	0.0357	0.0407	0.0549	0.1242	0.2700	0.3090	0.3035
6731.0	0.0353	0.0344	0.0407	0.0559	0.1212	0.2751	0.3071	0.3003
7097.0	0.0368	0.0320	0.0404	0.0581	0.1287	0.2773	0.3085	0.2999
7434.0	0.0341	0.0305	0.0413	0.0546	0.1343	0.2763	0.3085	0.2968
7621.0	0.0347	0.0322	0.0433	0.0568	0.1283	0.2803	0.3085	0.3003
7888.0	0.0361	0.0317	0.0410	0.0581	0.1319	0.2742	0.3074	0.2987
7939.0					0.1340	0.2805	0.3102	0.2985
8299.0					0.1338	0.2822	0.3095	0.2977
8531.0					0.1345	0.2810	0.3086	0.3019
8783.0					0.1343	0.2845	0.3088	0.3033
9003.0					0.1368	0.2855	0.3088	0.2989
9206.0	0.0350	0.0329	0.0401	0.0579	0.1394	0.2826	0.3136	0.2999
9365.0					0.1346	0.2790	0.3161	0.2971
10067.0					0.1411	0.2792	0.3114	0.3035
10585.0					0.1412	0.2837	0.3116	0.3034
11142.0					0.1405	0.2900	0.3125	0.3026
11392.0					0.1385	0.2899	0.3138	0.3018
11624.0	0.0364	0.0321	0.0379	0.0588	0.1420	0.2959	0.3117	0.3008
11875.0					0.1463	0.2861	0.3189	0.3012

CORRECTED MOISTURE CONTENT DATA:S8T1
R= 60 cm

TIME (min)	DEPTH 130 (cm)	DEPTH 137 (cm)	DEPTH 145 (cm)	DEPTH 152 (cm)	DEPTH 160 (cm)	DEPTH 168 (cm)	DEPTH 175 (cm)
	----------	----------	----------	THETA	----------	----------	----------
0.0	0.2652	0.2354	0.2161	0.2361	0.2429	0.2960	0.3364
78.0	0.2617	0.2361	0.2537	0.2398	0.2747	0.3132	0.3432
98.0	0.2615	0.2355	0.2374	0.2536	0.2749	0.3137	0.3483
156.0	0.2628	0.2411	0.2399	0.2502	0.2883	0.3215	0.3429
199.0	0.2631	0.2410	0.2406	0.2570	0.2887	0.3169	0.3478
242.0	0.2643	0.2406	0.2432	0.2592	0.2850	0.3194	0.3546
309.0	0.2631	0.2419	0.2450	0.2598	0.2867	0.3209	0.3551
332.0	0.2639	0.2421	0.2439	0.2604	0.2893	0.3225	0.3509
380.0	0.2632	0.2416	0.2403	0.2613	0.2870	0.3240	0.3510
416.0	0.2460	0.2413	0.2441	0.2665	0.2858	0.3217	0.3502
492.0	0.2651	0.2468	0.2460	0.2599	0.2903	0.3216	0.3520
554.0	0.2461	0.2448	0.2478	0.2654	0.2978	0.3226	0.3539
613.0	0.2660	0.2481	0.2524	0.2670	0.2949	0.3231	0.3523
728.0	0.2668	0.2514	0.2477	0.2595	0.2994	0.3261	0.3530
789.0	0.2665	0.2469	0.2478	0.2717	0.2985	0.3282	0.3579
968.0	0.2639	0.2464	0.2543	0.2712	0.2980	0.3318	0.3558
1164.0	0.2690	0.2526	0.2511	0.2704	0.3023	0.3332	0.3571
1342.0	0.2678	0.2510	0.2513	0.2809	0.3049	0.3337	0.3514
1512.0	0.2722	0.2535	0.2548	0.2764	0.3048	0.3368	0.3567
1690.0	0.2685	0.2508	0.2529	0.2768	0.3036	0.3328	0.3598
1870.0	0.2662	0.2549	0.2503	0.2790	0.3017	0.3327	0.3573
2038.0	0.2680	0.2497	0.2533	0.2772	0.3046	0.3313	0.3549
2231.0	0.2697	0.2518	0.2562	0.2754	0.2997	0.3313	0.3581
2433.0	0.2684	0.2540	0.2495	0.2758	0.3080	0.3350	0.3525
2599.0	0.2689	0.2537	0.2556	0.2754	0.3048	0.3388	0.3543
2798.0	0.2714	0.2527	0.2544	0.2829	0.3057	0.3392	0.3571
2998.0	0.2712	0.2478	0.2545	0.2817	0.3073	0.3389	0.3664
3178.0	0.2731	0.2492	0.2541	0.2819	0.3050	0.3350	0.3621
3468.0	0.2677	0.2525	0.2549	0.2784	0.3066	0.3341	0.3572
3675.0	0.2753	0.2499	0.2549	0.2799	0.3107	0.3387	0.3646
3859.0	0.2704	0.2539	0.2559	0.2805	0.3097	0.3407	0.3618
4104.0	0.2698	0.2537	0.2564	0.2795	0.3115	0.3392	0.3631
4237.0	0.2729	0.2572	0.2595	0.2855	0.3179	0.3422	0.3646
4532.0	0.2753	0.2584	0.2706	0.2924	0.3181	0.3452	0.3666
4676.0	0.2780	0.2592	0.2681	0.2906	0.3174	0.3447	0.3583
5339.0	0.2764	0.2585	0.2667	0.2963	0.3170	0.3458	0.3700
5699.0	0.2767	0.2575	0.2697	0.2948	0.3212	0.3475	0.3669
5960.0	0.2790	0.2607	0.2712	0.2934	0.3246	0.3507	0.3709
6024.0	0.2763	0.2566	0.2703	0.2915	0.3170	0.3480	0.3684
6034.0	0.2809	0.2600	0.2655	0.2938	0.3221	0.3486	0.3620
6152.0	0.2756	0.2588	0.2655	0.2917	0.3200	0.3435	0.3648
6275.0	0.2728	0.2552	0.2731	0.2862	0.3140	0.3417	0.3640
6369.0	0.2775	0.2544	0.2634	0.2797	0.3097	0.3437	0.3603

CORRECTED MOISTURE CONTENT DATA:S8T1
R= 60 cm

TIME (min)	DEPTH 130 (cm)	DEPTH 137 (cm)	DEPTH 145 (cm)	DEPTH 152 (cm)	DEPTH 160 (cm)	DEPTH 168 (cm)	DEPTH 175 (cm)
	THETA						
6505.0	0.2790	0.2585	0.2567	0.2822	0.3093	0.3400	0.3598
6731.0	0.2762	0.2514	0.2538	0.2771	0.3050	0.3329	0.3645
7097.0	0.2777	0.2505	0.2517	0.2781	0.3077	0.3349	0.3636
7434.0	0.2734	0.2519	0.2501	0.2807	0.3042	0.3359	0.3576
7621.0	0.2751	0.2530	0.2499	0.2758	0.3012	0.3278	0.3635
7888.0	0.2759	0.2478	0.2465	0.2670	0.2912	0.3313	0.3509
7939.0	0.2739	0.2505	0.2448	0.2678	0.2889	0.3247	0.3558
8299.0	0.2745	0.2448	0.2469	0.2614	0.2889	0.3215	0.3487
8531.0	0.2754	0.2471	0.2441	0.2650	0.2906	0.3243	0.3560
8783.0	0.2744	0.2494	0.2439	0.2597	0.2809	0.3185	0.3520
9003.0	0.2733	0.2490	0.2449	0.2589	0.2864	0.3215	0.3571
9206.0	0.2748	0.2463	0.2366	0.2606	0.2881	0.3144	0.3527
9365.0	0.2740	0.2449	0.2425	0.2609	0.2831	0.3168	0.3499
10097.0	0.2739	0.2450	0.2439	0.2567	0.2794	0.3192	0.3520
10585.0	0.2728	0.2476	0.2363	0.2528	0.2801	0.3171	0.3528
11142.0	0.2700	0.2417	0.2333	0.2450	0.2645	0.3046	0.3400
11392.0	0.2748	0.2399	0.2341	0.2403	0.2595	0.3007	0.3425
11624.0	0.2732	0.2385	0.2254	0.2405	0.2634	0.3015	0.3413
11675.0	0.2707	0.2398	0.2265	0.2397	0.2651	0.3059	0.3413

CORRECTED MOISTURE CONTENT DATA:S8T1
R=100 cm

TIME (min)	DEPTH 30 (cm)	DEPTH 46 (cm)	DEPTH 61 (cm)	DEPTH 76 (cm)	DEPTH 91 (cm)	DEPTH 107 (cm)	DEPTH 114 (cm)	DEPTH 122 (cm)
	THETA							
0.0	0.0268	0.0286	0.0379	0.0426	0.0632	0.2532	0.3241	0.3462
169.0	0.0274	0.0303	0.0370	0.0435	0.0611	0.2488	0.3260	0.3500
255.0	0.0269	0.0277	0.0378	0.0439	0.0636	0.2550	0.3333	0.3471
340.0	0.0262	0.0291	0.0382	0.0426	0.0645	0.2537	0.3291	0.3479
426.0	0.0271	0.0297	0.0367	0.0435	0.0637	0.2508	0.3305	0.3493
504.0	0.0244	0.0270	0.0364	0.0444	0.0609	0.2449	0.3325	0.3462
544.0	0.0246	0.0269	0.0373	0.0441	0.0643	0.2535	0.3270	0.3489
622.0	0.0264	0.0284	0.0362	0.0453	0.0622	0.2475	0.3305	0.3454
717.0	0.0264	0.0290	0.0380	0.0435	0.0618	0.2546	0.3359	0.3481
810.0	0.0265	0.0291	0.0369	0.0433	0.0623	0.2508	0.3330	0.3448
959.0					0.0617	0.2474	0.3293	0.3490
1171.0					0.0614	0.2539	0.3331	0.3422
1328.0					0.0641	0.2530	0.3358	0.3475
1503.0					0.0632	0.2531	0.3327	0.3471
1703.0					0.0647	0.2506	0.3302	0.3524
1867.0					0.0643	0.2486	0.3315	0.3409
2030.0					0.0644	0.2530	0.3360	0.3479
2241.0					0.0630	0.2509	0.3335	0.3398
2425.0					0.0628	0.2536	0.3305	0.3361
2606.0					0.0637	0.2488	0.3338	0.3395
2791.0	0.0257	0.0270	0.0360	0.0449	0.0629	0.2514	0.3281	0.3341
3191.0					0.0634	0.2467	0.3323	0.3348
3466.0					0.0639	0.2544	0.3335	0.3362
3607.0					0.0612	0.2458	0.3302	0.3498
3852.0					0.0656	0.2508	0.3319	0.3484
4108.0					0.0632	0.2527	0.3349	0.3466
4229.0	0.0242	0.0282	0.0357	0.0448	0.0637	0.2463	0.3311	0.3490
4538.0					0.0610	0.2470	0.3332	0.3501
4884.0					0.0629	0.2539	0.3271	0.3442
5345.0					0.0647	0.2534	0.3303	0.3484
5706.0	0.0265	0.0269	0.0343	0.0444	0.0657	0.2501	0.3287	0.3473
5966.0	0.0266	0.0289	0.0382	0.0446	0.0638	0.2569	0.3304	0.3484
6045.0	0.0270	0.0303	0.0345	0.0450	0.0623	0.2531	0.3290	0.3481
6167.0	0.0293	0.0289	0.0388	0.0445	0.0666	0.2565	0.3331	0.3443
6268.0	0.0249	0.0293	0.0369	0.0467	0.0653	0.2537	0.3266	0.3478
6356.0	0.0251	0.0283	0.0375	0.0451	0.0618	0.2530	0.3298	0.3498
6515.0	0.0267	0.0291	0.0371	0.0455	0.0640	0.2507	0.3314	0.3466
6719.0	0.0259	0.0294	0.0395	0.0433	0.0617	0.2503	0.3307	0.3462
7109.0	0.0259	0.0273	0.0367	0.0469	0.0631	0.2499	0.3345	0.3432
7424.0	0.0258	0.0300	0.0368	0.0440	0.0647	0.2520	0.3315	0.3464
7631.0	0.0239	0.0303	0.0390	0.0434	0.0661	0.2555	0.3279	0.3417
7879.0	0.0261	0.0280	0.0366	0.0451	0.0646	0.2536	0.3282	0.3477
7946.0	—	—	—	—	0.0633	0.2492	0.3307	0.3483

CORRECTED MOISTURE CONTENT DATA:S8T1
R= 100cm

TIME (min)	DEPTH 30 (cm)	DEPTH 46 (cm)	DEPTH 61 (cm)	DEPTH 76 (cm)	DEPTH 91 (cm)	DEPTH 107 (cm)	DEPTH 114 (cm)	DEPTH 122 (cm)
	----------	----------	----------	----------	THETA	----------	----------	----------
8292.0					0.0637	0.2512	0.3341	0.3450
8538.0					0.0633	0.2571	0.3315	0.3457
8790.0					0.0646	0.2486	0.3297	0.3514
9010.0					0.0643	0.2578	0.3316	0.3468
9198.0	0.0265	0.0280	0.0346	0.0441	0.0646	0.2527	0.3320	0.3442
9372.0					0.0648	0.2567	0.3301	0.3449
10081.0					0.0598	0.2532	0.3294	0.3491
10590.0					0.0651	0.2458	0.3303	0.3515
11135.0					0.0646	0.2507	0.3312	0.3517
11397.0					0.0642	0.2556	0.3277	0.3480
11010.0	0.0274	0.0290	0.0354	0.0439	0.0646	0.2547	0.3333	0.3505
11884.0					0.0668	0.2482	0.3287	0.3487

CORRECTED MOISTURE CONTENT DATA:S8T1
R=100 cm

TIME (min)	DEPTH 130 (cm)	DEPTH 137 (cm)	DEPTH 145 (cm)	DEPTH 152 (cm)	DEPTH 160 (cm)	DEPTH 168 (cm)
	THETA					
0.0	0.3345	0.2884	0.2393	0.2404	0.2771	0.2991
169.0	0.3346	0.2826	0.2396	0.2486	0.2825	0.3078
255.0	0.3360	0.2898	0.2440	0.2642	0.2866	0.3089
340.0	0.3330	0.2807	0.2507	0.2670	0.2911	0.3130
426.0	0.3380	0.2858	0.2551	0.2703	0.2966	0.3119
504.0	0.3335	0.2932	0.2552	0.2708	0.2946	0.3180
544.0	0.3349	0.2840	0.2553	0.2745	0.2969	0.3174
624.0	0.3342	0.2870	0.2555	0.2722	0.2942	0.3167
717.0	0.3336	0.2843	0.2543	0.2741	0.2952	0.3180
810.0	0.3335	0.2857	0.2595	0.2732	0.2951	0.3182
959.0	0.3369	0.2867	0.2552	0.2702	0.2975	0.3128
1171.0	0.3311	0.2876	0.2578	0.2713	0.2949	0.3166
1326.0	0.3321	0.2868	0.2441	0.2640	0.2992	0.3173
1503.0	0.3432	0.2871	0.2616	0.2703	0.2973	0.3214
1703.0	0.3336	0.2862	0.2590	0.2760	0.2921	0.3189
1867.0	0.3354	0.2854	0.2595	0.2732	0.2959	0.3181
2030.0	0.3332	0.2869	0.2633	0.2696	0.2934	0.3132
2241.0	0.3398	0.2905	0.2577	0.2738	0.2945	0.3197
2425.0	0.3361	0.2846	0.2592	0.2716	0.2934	0.3123
2606.0	0.3395	0.2871	0.2575	0.2685	0.2968	0.3156
2791.0	0.3341	0.2876	0.2582	0.2700	0.2969	0.3149
3191.0	0.3348	0.2872	0.2610	0.2701	0.2968	0.3122
3463.0	0.3362	0.2847	0.2605	0.2695	0.2927	0.3201
3607.0	0.3344	0.2887	0.2618	0.2724	0.2959	0.3156
3852.0	0.3320	0.2908	0.2565	0.2704	0.3013	0.3162
4108.0	0.3364	0.2901	0.2626	0.2730	0.2949	0.3177
4229.0	0.3356	0.2872	0.2613	0.2764	0.2993	0.3180
4538.0	0.3335	0.2890	0.2666	0.2824	0.3049	0.3148
4884.0	0.3406	0.2895	0.2673	0.2812	0.3033	0.3206
5345.0	0.3368	0.2884	0.2659	0.2867	0.3086	0.3221
5700.0	0.3327	0.2866	0.2645	0.2898	0.3079	0.3225
5966.0	0.3368	0.2938	0.2686	0.2856	0.3058	0.3290
6045.0	0.3360	0.2889	0.2634	0.2831	0.3122	0.3228
6167.0	0.3374	0.2940	0.2671	0.2840	0.3062	0.3267
6288.0	0.3345	0.2875	0.2606	0.2801	0.3023	0.3183
6358.0	0.3396	0.2893	0.2609	0.2787	0.2990	0.3016
6515.0	0.3355	0.2848	0.2616	0.2781	0.3013	0.3218
6719.0	0.3383	0.2878	0.2604	0.2806	0.3030	0.3167
7109.0	0.3341	0.2879	0.2606	0.2759	0.3022	0.3205
7424.0	0.3306	0.2877	0.2580	0.2717	0.2981	0.3230
7631.0	0.3355	0.2836	0.2567	0.2723	0.2931	0.3134
7879.0	0.3364	0.2873	0.2537	0.2688	0.2942	0.3164
7946.0	0.3377	0.2848	0.2506	0.2672	0.2898	0.3164

CORRECTED MOISTURE CONTENT DATA:S8T1
R= 100 cm

TIME (min)	DEPTH 130 (cm)	DEPTH 137 (cm)	DEPTH 145 (cm)	DEPTH 152 (cm)	DEPTH 160 (cm)	DEPTH 168 (cm)
	THETA					
8292.0	0.3359	0.2849	0.2578	0.2637	0.2964	0.3131
8538.0	0.3347	0.2818	0.2526	0.2615	0.2961	0.3155
8790.0	0.3386	0.2903	0.2495	0.2582	0.2914	0.3126
9010.0	0.3363	0.2861	0.2512	0.2633	0.2898	0.3224
9198.0	0.3322	0.2808	0.2506	0.2637	0.2902	0.3172
9372.0	0.3378	0.2883	0.2506	0.2620	0.2899	0.3175
10081.0	0.3325	0.2829	0.2512	0.2586	0.2952	0.3140
10590.0	0.3310	0.2850	0.2425	0.2586	0.2918	0.3106
11135.0	0.3350	0.2828	0.2424	0.2547	0.2852	0.3155
11397.0	0.3337	0.2830	0.2410	0.2574	0.2873	0.3062
11616.0	0.3365	0.2812	0.2496	0.2563	0.2951	0.3117
11884.0	0.3334	0.2840	0.2409	0.2517	0.2885	0.3146